UNIVERZITA KARLOVA V PRAZE, LÉKAŘSKÁ FAKULTA V PLZNI

ŠIKLŮV ÚSTAV PATOLOGIE

MOLEKULÁRNÍ GENETIKA NÁDORŮ UROGENITÁLNÍHO TRAKTU A JEJÍ VZTAH K BIOLOGICKÉMU CHOVÁNÍ

MUDr. KRISTÝNA PIVOVARČÍKOVÁ

Doktorská disertační práce

Plzeň 2017
Obor: Patologie
Školitel: prof. MUDr. Ondřej Hes, Ph.D.

Abstrakt

Disertační práce je komentovaným souborem sedmi v anglické literatuře publikovaných prací zabývajících se problematikou molekulární genetiky nádorů urogenitálního traktu. Při velkém množství současných poznatků v tomto odvětví a při širokém spektru urogenitálních lézí je pak tato dizertační práce blíže zaměřena zejména na současný pohled na renální neoplásie charakterizované predominantně papilárním typem růstu. Po obecném úvodu jsou blíže prezentovány jednotlivé renální neoplasie s papilární morfologií, specifikovány jsou jejich morfologické, imunohistochemické a molekulárně-genetické vlastnosti, komentována je jejich diferenciální diagnostika. Ve výsledcích jsou představeny recentně publikované novinky v morfologickém spektru těchto lézí, poznatky o heterogenitě výsledků molekulárně genetických metod u jednotlivých nádorových jednotek, zmíněna jsou úskalí běžné diagnostické praxe, komentován je též prognostický význam těchto lézí. Závěrem je zhodnocen a komentován klinický dopad a užití těchto poznatků v běžné praxi.

Abstract

The Ph.D. thesis is a collection of seven commented articles on the topic of molecular-genetic of urogenital tumors. The spectrum of urogenital lesions is very wide, there is lots of new insights in field of urogenital pathology. Therefore, presented Ph.D. thesis is focused only on small part of urogenital neoplasms - renal cell carcinomas characterized by papillary growing pattern. The introduction presents different entities with papillary morphology, there are specified basic morphological, immunohistochemical and molecular-genetic characteristic of these lesions, their differential diagnosis is commented. In the results, there are presented recently published studies dealing with newly described entities of renal neoplasias, heterogenity of molecular genetic studies in individual tumorous groups is established, prognostic significance is commented, typical pitfalls are introduced. In the conclusions, the limitations of the use molecular-genetic methods are discussed and clinical outcome and significance is evaluated.

Předmluva

Doktorská disertační práce je komentovaným souborem publikovaných prací zabývajících se problematikou molekulární genetiky nádorů urogenitálního traktu, na kterých se autorka podílela jako členka autorských kolektivů. Dizertační práce je pak blíže zaměřena na současný pohled na renální neoplásie charakterizované predominantně papilární architektonikou. Práce je psána z pohledu patologa, tedy oboru specializace autorky, čímž však autorka v žádném případě nechce upozaďovat ostatní odbornosti ani si přivlastňovat myšlenky a zásluhy spoluautorů. Představeno je celkem sedm prací v původním anglickém znění po předchozím úvodu v českém jazyce. Závěrem jsou komentovány limitace a eventuální dopady těchto studií.

Prohlášení

Prohlašuji, že jsem závěrečnou práci zpracovala samostatně a že jsem řádně uvedla a citovala všechny použité prameny a literaturu. Souhlasím s trvalým uložením elektronické verze mé práce v databázi UK LF Plzeň.
V Plzni, 4. listopadu 2017

Kristýna Pivovarčíková

Poděkování

Prof. MUDr. Ondřeji Hesovi, Ph.D. - svému školiteli, za nabídnutou příležitost, odborné vedení, prokazovanou trpělivost, ochotu a přátelský přístup.

Doc. MUDr. Ondřeji Daumovi, Ph.D. a MUDr. Mariánu Švajdlerovi, Ph.D. – za ochotu a pomoc ve specializačním výcviku.

Prof. MUDr. Michalu Michalovi – za podporu a poskytnuté zázemí.

Kolektivu Šiklova Ústavu Patologie a Bioptické laboratoře s.r.o. za poskytnuté zázemí.

Obsah

1 Úvod ... 8
1.1 Incidence nádorů ledvin ... 8
1.2 Klasifikace renálních neoplásií ... 8
1.3 Renální karcinomy asociované s papilární morfologií ... 8
1.3.1 Papilární renální karcinom ... 9
1.3.2 Karcinom ledviny asociovaný se syndromem familiární leiomyomatózy a karcinomem ledvin/fumarát hydratáza deficientní renální karcinom ... 13
1.3.3 Světlobuněčný papilární renální karcinom ... 14
1.3.4 Xp11.2 translokační renální karcinom ... 15
2 Cíle prací ... 17
3 Výsledky ... 18
3.1 "Mucin"-secreting papillary renal cell carcinoma: clinicopathological, immunohistochemical, and molecular genetic analysis of seven cases ... 18
3.2 Warthin-like papillary renal cell carcinoma: Clinicopathologic, morphologic, immunohistochemical and molecular genetic analysis of 11 cases ... 30
3.3 Biphasic squamoid alveolar renal cell carcinoma - A distinctive subtype of papillary renal cell carcinoma? ... 41
3.4 Solid papillary renal cell carcinoma: clinicopathologic, morphologic, and immunohistochemical analysis of 10 cases and review of the literature ... 55
3.5 Cystic and necrotic papillary renal cell carcinoma: prognosis, morphology, immunohistochemical, and molecular-genetic profile of 10 cases ... 63
3.6 Molecular-genetic analysis is essential for accurate classification of renal carcinoma resembling Xp11.2 translocation carcinoma ... 73
3.7 TFE3-fusion variant analysis defines specific clinicopathologic associations among Xp11 translocation cancers (letter to the editor) ... 85
4 Závěr ... 90
5 Seznam použité literatury ... 92
6 Publikace ... 99
6.1 Publikace autorky, které jsou podkladem dizertační práce ... 99
6.2 Další publikace autorky se vztahem k tématu dizertační práce ... 100
6.3 Publikace autorky bez vztahu k tématu dizertační práce ... 102
6.4 Prezentace na vědeckých konferencích ... 103

Seznam použitých zkratek

2SC	S-(2-sukcino)-cystein
aCGH	Array Comparative Genomic Hybridization (Komparativní genomová hybridizace na čipu)
AE1/AE3	Směs imunohistochemických protilátek detekující cytokeratiny
AMACR	Imunohistochemická protilátka detekující enzym α-methylacyl-CoA racemasu
BSARCC	Biphasic Squamoid Alveolar Renal Cell Carcinoma (Bifázický skvamoidně alveolární (papilární) renální karcinom)
CA-IX	Imunohistochemická protilátka detekující anhydrázu kyseliny uhličité *CA9*
CAM5.2	Imunohistochemická protilátka detekující cytokeratin *KRT8*
CCPRCC	Clear Cell Papillary Renal Cell Carcinoma (Světlobuněčný papilární renální karcinom)
CCRCC	Clear Cell Renal Cell Carcinoma (Světlobuněčný/konvenční renální karcinom)
CD10	Imunohistochemická protilátka detekující metaloendopeptidázu MME
CD117	Imunohistochemická protilátka detekující extracelulární část transmembránového tyrozin-kinázového receptoru c-Kit
CK7	Imunohistochemická protilátka detekující protein cytokeratinu *KRT7*
CK20	Imunohistochemická protilátka detekující protein cytokeratinu *KRT20*
EMA	Imunohistochemická protilátka detekující epiteliální membránový antigen
ESKD	End Stage Kidney Disease (Konečné stádium renálního onemocnění)
FH	Fumarat hydratase (Fumarát hydratáza)
FISH	Fluorescence In Situ Hybridization (Fluorescenční in-situ hybridizace)
HLRCC	Hereditary Leiomyomatosis and Renal Cell Carcinoma-Associated Renal Cell Carcinoma (Karcinom ledviny asociovaný se syndromem familiární leiomyomatózy a karcinomu ledvin)
HMB45	Imunohistochemická protilátka detekující antigen *PMEL*
HMWK	High molecular weight keratin - imunohistochemická protilátka detekující protein Cytokeratin 34 beta E12
ISUP	International Society of Urological Pathology (Mezinárodní Společnost Urogenitální Patologie)
LOH	Loss of Heterozygosity (Ztráta heterozygozity)
Melan A	Imunohistochemická protilátka detekující produkt genu *MELANA*
MMR	DNA mismatch repair (Korekce správného párování bází při replikaci DNA)
MTSCC	Mucinous Tubular and Spindle Cell Carcinoma (Mucinózní tubulární a vřetenobuněčný karcinom)
NOS	Not Otherwise Specified (Blíže nespecifikované)
OPRCC	Oncocytic Papillary Renal Cell Carcinoma (Onkocytický papilární renální karcinom)
OSCAR	Imunohistochemická protilátka detekující široké spektrum cytokeratinů
PAX8	Imunohistochemická protilátka detekující protein PAX8
PRCC	Papillary Renal Cell Carcinoma (Papilární renální karcinom)
PRCCM	"Mucin"-secreting Papillary Renal Cell Carcinoma ("Mucin"-secernující papilání renální karcinom)
RAT	Renal Angiomyoadenomatous Tumor (Renální angiomyomatózní tumor)
RO	Renal Oncocytoma (Renální onkocytom)
TNM	Systém klasifikace solidních nádorů

TFE3	Transkripční faktor TFE3
TTF-1	Imunohistochemická protilátka detekující thyroidální transkripční faktor 1
VHL	von Hippel-Lindau
WHO	World Health Organization (Světová Zdravotnická Organizace)
WT-1	Imunohistochemická protilátka detekující protein WT1
Xp11 TRCC	Xp11.2 Translocation Renal Cell Carcinoma (Xp11.2 translokační renální karcinom)

1 Úvod

1.1 Incidence nádorů ledvin

Česká republika je v celosvětovém měřítku zemí s nejvyšší incidencí renálního karcinomu. Četnost nádorů ledvin zde kolísá v rozmezí 1,5 – 2 % všech nádorů, přičemž úmrtnost na toto onemocnění dosahuje 1,5% ze všech onkologických onemocnění za rok (1).

Mezi dva nejčastějšími typy renálního karcinomu patří světlobuněčný renální karcinom (CCRCC) a papilární renální karcinom (PRCC), jejichž incidence představuje 65 - 70% (u CCRCC), resp. 18,5% (u PRCC) z celkového počtu renálních karcinomů (2).

1.2 Klasifikace renálních neoplásií

Klasifikace renálních neoplásií doznala v posledních 40 letech významných změn a i nadále se velmi dynamicky mění. V posledních letech bylo v anglické literatuře popsáno velké množství nových renálních nádorových jednotek, zároveň se začíná měnit i pohled a přístup k některým dlouhodobě uznávaným renálním neoplásiím.

Významným mezníkem v klasifikaci renálních neoplázií je rok 1997, kdy byla autory Kovacs a kol. představena tzv. Heidelbergská klasifikace renálních tumurů (The Heidelberg classification of renal cell tumors), první klasifikace integrující do diagnostiky renálních tumorů molekulárně genetické vlastnosti (3).

Současně platná WHO klasifikace renálních neoplásií (z roku 2016) vychází z Vancouverské klasifikace z roku 2013 (konsenzus Mezinárodní Společnosti Urogenitální Patologie/ISUP) (4). Obě tyto klasifikace jsou odrazem velkých pokroků na poli morfologie, imunohistochemie, cytogenetiky a molekulární patologie. Aktuální WHO klasifikace tak obsahuje několik desítek nádorových jednotek a čtyři tzv. provizorní jednotky (emerging/provisional new entities) (2).

1.3 Renální karcinomy asociované s papilární morfologií

Jedná se o jednotky s morfologicky obdobnými charakteristikami, avšak zcela odlišnými imunohistochemickými vlastnostmi, molekulárně-genetickým profilem a především klinicky rozdílným chováním. Rozlišení jednotlivých nádorových entit má tedy jednoznačný klinický význam.

Mezi renální karcinomy rostoucí pod obrazem papilární léze lze zařadit PRCC, renální karcinom asociovaný se syndromem familiární leiomyomatózy a karcinomem ledviny (HLRCC), světlobuněčný papilární renální karcinom (CCPRCC) a Xp11.2 translokační renální karcinom (Xp11 TRCC).

Ač se jedná o v současné WHO jasně vyhraněné a definované jednotky, diferenciálně diagnosticky mohou v běžné praxi působit obtíže, a to především na pracovištích s imunohistochemicky omezenými možnostmi, bez genetického zázemí. Diagnostika velké části těchto neoplásií tedy rozhodně patří do rukou zkušeného urogenitálního patologa a velkých laboratoří disponujícími výše jmenovanými diagnostickými modalitami.

1.3.1 Papilární renální karcinom

PRCC je druhým nejčastěji se vyskytujícím typem renálního karcinomu (2). Tradičně jsou v rámci této jednotky rozlišovány dvě podskupiny (na podkladě morfologických znaků) – PRCC typ 1 a PRCC typ 2 (5, 6).

Celkově je však PRCC velmi heterogenní jednotkou, v běžné klinické praxi se často setkáváme s PRCCs vyznačujícími se přesahující (smíšenou) morfologií, či s tumory zcela odlišnými, nezařaditelnými do žádné z těchto dvou kategorií. Tato tradičně uznávaná klasifikace se tedy postupně stala nedostatečnou a je evidentní, že spektrum PRCC je oproti výše zmiňovanému klasickému dělení ve skutečnosti mnohem širší. V posledních letech je publikováno stále větší množství prací, které obohacují spektrum PRCC, ať už se jedná o dobře známý onkocytický PRCC, či vzácnější léze jako PRCC s low-grade vřetenobuněčnými okrsky, "mucin"- secernující PRCC/PRCC s mucinózní sekrecí (PRCCM), Warthinovu tumoru podobný PRCC, PRCC se světlobuněčnými změnami, bifázický skvamoidně alveolární PRCC (BSARCC) či solidní PRCC (SPRCC).

PRCC typicky exprimuje cytokeratiny (AE1/AE3, CAM5.2, HMWK), membránový epiteliální antigen (EMA), AMARC, vimentin, CD10 (2). Variabilní je reaktivita pro CK7, kdy pozitivita CK7 je častější u PRCC typ 1, u PRCC typ 2 se pozitivita pohybuje okolo 50% případů (7).

Za typické molekulárně genetické znaky nacházané u PRCC jsou tradičně považovány trisomie/polysomie chromosomů 7 a 17 a ztráta gonosomu Y u mužských pacientů (2). Po pečlivé revizi dostupné literatury (8-13), na základě našich empirických zkušeností i velmi recentně vycházejících prací (14) však začíná být zřejmé, že toto všeobecně uznávané dogma je nepravdivé a zůstávající v platnosti snad pouze u PRCC typ 1 (8-13).

1.3.1.1 Papilární renální karcinom typ 1

PRCC typ 1 je tvořen neoplastickými buňkami s nízkým nukleárním gradem (Fuhrman grading system / ISUP), malým množstvím cytoplasmy, jádra jsou uspořádána do jedné řady (6).

PRCC typ 1 je napříč celým spektrem PRCC molekulárně-geneticky nejvíce uniformní subtyp PRCC. Papilárnímu renálnímu karcinomu typicky přisuzované molekulárně genetické znaky (trisomie/polysomie chromosomů 7 a 17 a ztráta gonosomu Y u mužů) jsou s největší frekvencí a pravidelností nacházeny právě u tohoto subtypu neoplásií. V literatuře se lze setkat i s dalšími, relativně často popisovanými chromozomálními numerickými aberacemi, jako je zisk chromosomů 3, 12, 16 a 20. Některé studie dále uvádějí kromě ztráty chromosomu Y ztráty i různých jiných chromosomů (1, 2, 4,5, 7, 8, 9, 10, 11, 14, 15, 16, 18, 19, 20, 21, and 22) (8-13).

Ač je PRCC typ 1 je oproti PRCC typ 2 všeobecně považován za tumor s lepší prognózou, dostupné studie s velkými počty pacientů ukazují, že na ledvinu omezený PRCC má bez ohledu na histologický subtyp nádoru postoperačně stejný onkologický výstup, a že superiorním nepříznivým prognostickým faktorem pro tzv. cancer-free survival je stage onemocnění vyšší než pT1 (15-17).

1.3.1.2 Papilární renální karcinom typ 2

Pro PRCC typ 2 je typických morfologickým znakem přítomnost tzv. nukleární pseudostratifikace, nádorové buňky mají hojnou eosinofilní cytoplasmu a vyšší nukleární grade (Fuhrman grading system / ISUP) (6). Evidentně se jedná o velmi spornou podjednotku a to jak morfologicky, klinicky, tak i molekulárně-geneticky. S vysokou pravděpodobností pak tato jednotka pod sebou zastřešuje skupinu zcela různých lézí.

Chromosomální numerický aberační status je o poznání méně konstantní než je tomu u PRCC typ 1, i přes to jsou však polysomie chromosomů 7 a 17 a ztráta gonosomu Y nejčastěji popisované chromosomální abnormality (avšak ve výrazně nižším procentu případů). Kromě těchto „typických" znaků je u PRCC typ 2 popsáno velké množství dalších chromosomálních aberací (s velkou variabilitou frekvence výskytu v různých studiích). Mezi častěji uváděné změny tak patří zisk chromosomů 12, 16 and 20, zcela v zanedbatelných procentech (jednotlivé případy) jsou v dostupné literatuře popsány zisky chromosomů 1, 2, 3, 4, 5, 6, 8, 9, 13, 18, 19 a 22. U PRCC typ 2 bylo popsáno i velké množství změn numerického chromosomálního statusu ve smyslu ztrát chromosomů, či jejich částí (chromosomy 1, 2, 3, 4, 5, 6, 7, 8, 9, 10, 12, 13, 14, 15, 17, 18, 19, 20, 21, 22 a X) (8-13).

1.3.1.3 Onkocytický papilární renální karcinom

Ve WHO 2016 si i tato, již dlouhou dobu známá, neoplásie našla své místo a je zde zmiňována jako odlišná morfologická varianta PRCC. Jedná se o lézi s typickou papilární architektonikou (fokálně však může být vyjádřeno i solidní uspořádání), papilární struktury jsou lemovány jednou vrstvou neoplastických buněk s hojnou granulární a výrazně eosinofilní cytoplasmou a nízkým nukleárním gradem (tzv. onkocytární buňky). Při vyšetření ultrastruktury je pak cytoplasma buněk napěchována četnými mitochondriemi (18).

Ani v této podskupině PRCC není numerický chomosomální status zcela homogenní, ačkoliv zisk chromosomů 7 a 17 zůstává dle dostupných studií stále nejčastěji detekovanou molekulárně genetickou změnou. Mezi další chromozomální aberace pak patří zisk chromosomů 3 a 11, ztráta chromosomu Y (v nekonstantním množství případů OPRCC) a ztráty chromosomů 1, 4, 11, 14 a gonosomu X (18-23).

Jedna z největších a velmi recentních studií (zahrnující 28 případů OPRCC) zaměřující se na numerický chromozomální status u OPRCC pak přinesla velmi zajímavé výsledky. Významná část OPRCC zahrnutých do této studie (43,5% OPRCC) vykazovala disomický status chromosomů 7 a 17, u části tumorů byla detekována delece chromosomu 14, delece 1p (locus 1p36) a některé případy měly ztrátu chromosomu Y. Všechny tyto jmenované změny jsou změnami typicky popisovanými u renálního onkocytomu (RO). Je tedy zřejmé, že OPRCC a RO mají z části překrývající se chromozomálně aberační patern, molekulárně genetické analýza má v diferenciální diagnostice těchto lézí jen velmi omezený význam (24).

Různé studie se rozcházejí v údajích o prognóze - v případech publikovaných v literatuře byl popsán jak spíše indolentní klinický průběh (18, 21), tak i agresivní chování (20, 24).

1.3.1.4 Papilármí renální karcinom s low-grade vřetenobuněčnými okrsky

Neoplásie popsaná v roce 2008 skupinou Arganiho jako PRCC napodobující mucinózní tubulární a vřetenobuněčný karcinom (MTSCC). Jedná se o nádory presentující se predominantně solidním typem růstu a přítomností low-grade vřetonobuněčných okrsků vytvářejících abortivní fascikly a větvící se tubuly. Jen fokálně mohou být zastiženy papilární růstové okrsky, které pokud jsou přítomny, tvoří minimální část neoplásie. Celkově tak nádor svou morfologií velmi připomíná MTSCC, s kterým má kromě překrývajícího se morfologického profilu i obdobný profil imunohistochemický (25).

U těchto tumorů byla prokázána přítomnost polysomie chromosomu 7 a 17 v 100% respektive 60% popsaných případů (25).

Follow-up data raritních případů PRCC s low-grade vřetenobuněčnými okrsky jsou velmi limitované, v literatuře dostupné údaje nedovolují bližší hodnocení jejich biologického chování (25).

1.3.1.5 "Mucin"-secernující papilání renální karcinom

První a pouze zcela okrajové zmínky o tumorech s papilární architektonikou a produkcí mucinózního materiálu se v literatuře objevily v 60. a následně 80. letech (26, 27).

Více se těmto tumorům ve svých pracích věnoval Val Bernal, který podrobně histologicky popsal podtyp PRCC s mucinózní produkcí, kterou rozlišil ve dvou formách - luminální/extracelulární a intracytoplasmatickou/intracelulární (přičemž obě formy produkce byly v jím popsaných případech zastiženy) a zároveň nastínil i histochemický profil nádorů (28, 29). Molekulárně genetické a imunohistochemické vlastnosti těchto tumorů byly podrobněji popsány až v roce 2016 na sérii sedmi případů (originální studie je součástí této disertační práce – viz výsledky).

Provedená studie demonstrovala zisk chromosomu 7 v 70% případů, zisk chromosomu 17 v 75% případů a ztrátu gonosomu Y ve 100% případů, jedná se však o velmi malou sérii s limitovaným množstvím případů vhodných pro molekulárně genetickou analýzu (4/7 případů) (30).

PRCCM je celkově velmi vzácná neoplásie, s frekvencí výskytu nižší než 0,5% z celkového počtu PRCC. V rámci dostupných dat bylo dokumentováno, že tyto léze mají metastatický potenciál.

1.3.1.6 Warthinovu tumoru podobný papilární renální karcinom

Tato podskupina PRCC má morfologicky velmi blízko k OPRCC. Jedná se o nádory predominantně s papilární architektonikou, onkocytární cytologií a denzním lymfoidním stromatem s tumor infiltrujícími lymfocyty. Varianta byla popsána velmi recentně, publikovaná práce je součástí disertační práce (viz výsledky).

Molekulárně genetická analýza prokázala široké spektrum chromosomálních změn, které v této skupině taktéž nejsou konstantním nálezem – některé případy byly zcela beze změn v numerickém chromosomálním statusu, jiné případy ukázaly necharakteristický zisk chromosomů 1, 2, 5, 7, 8, 12, 17, 21, či ztráty chromosomů 1, 3, 14, 15, 18, 22 a Y. Pouze u jediného z případů byla prokázána polysomie chomosomů 7 a 17 (31).

Jedná se o nádory s popsaným agresivním chováním a dokumentovaným letálním průběhem (31).

1.3.1.7 Papilární renální karcinom se světlobuněčnými změnami

Již z názvu je evidentní, že se jedná o subtyp PRCC s typickou papilární architektonikou, kde papilární struktury jsou lemovány buňkami se světlou cytoplasmou.

Různé studie představily malé série neoplásií s výše popsaným typickým morfologickým vzhledem, v rámci finální klasifikace pak tyto práce víceméně striktně následovaly výsledky molekulárně genetických analýz, tedy podstatná část nádorů zahrnutých v uvedených studiích byla nakonec klasifikována spíše jako CCRCC nežli PRCC.

Příkladem jsou práce autorů Fuzesi a kol. a Salama a kol., kteří popsali tři, respektive sedm tumorů morfologicky spadajících do této skupiny. Fuzesi detekoval ve všech třech případech ztrátu terminálního segmentu krátkého raménka chromosonu 3 (delece 3p – změna typická pro CCRCC) a ztrátu chromosomu 14 (32). Salamova skupina prokázala ztrátu heterozigozity 3p ve 100% analyzovaných případů, deleci chromosomů 7 a 17 v 4/6 respektive 6/6 případů (33). Na podkladě molekulárně genetických výsledků i přes jednoznačně vyjádřenou papilární morfologii byly tumory hodnoceny jako CCRCC, imunohistochemické vyšetření nebylo provedeno (32, 33).

Gobbo a kolektiv presentovali studii 14 neoplázií s papilárním typem růstu a variabilní proporcí světlobuněčných nádorových elementů, u nichž byla kromě molekulárně genetických vyšetření provedena i imunohistochemická barvení. Celkem devět případů zahrnutých ve studii bylo na podkladě morfologického nálezu, imunohistochemického profilu (AMACR pozitivita, CK7 reaktivita) a při presenci pro PRCC typického chromozomálně aberačního statusu (polysomie chromosomů 7 a/nebo 17, ztráta gonosomu Y v mužských případech) finálně klasifikováno jako PRCC se světlobuněčnými změnami (34). I v této práci byl tedy chromozomální status konečným a nejdůležitějším diagnostickým kritériem.

Ač se jedná o dlouhou dobu známou morfologickou variantu PRCC, studie blíže komentující typické znaky, přesně definující diagnostické modality a shrnující biologické chování nejsou v současné době v literatuře k dispozici.

1.3.1.8 Bifázický skvamoidně alveolární (papilární) renální karcinom

Petersson a kol. publikovali v roce 2012 tumor bifazického vzhledu, složený ze dvou morfologicky odlišných buněčných populací – velkých skvamoidních buněk s objemnou eosinofilní cytoplasmou a prominentními velkými vezikulárními jadérky a dále populací low-grade uniformních buněk s malým množstvím cytoplasmy a kulatými (jen mírně protáhlými) jádry. Dominantním nálezem byla přítomnost emperipolézy, která byla asociována s velkými skvamoidními buňkami. Nádorová jednotka dostala deskriptivní název, ukrývající v sobě základní morfologické charakteristiky - bifázický skvamoidně alveolární renální karcinom (BSARCC) (35).

Doposud největší publikovaná studie zabývající se touto jednotkou vyšla 4 roky po výše zmíněné úvodní práci a popsala 21 případů BSARCC, u nichž bylo na podkladě morfologického vzhledu, imunohistochemických vlastností a molekulárně genetického pozadí prokázáno, že se s největší pravděpodobností jedná o jednotku z morfologického spektra PRCC (původní rukopis je součástí disertační práce – viz výsledky) (36).

V posledním roce se BSARCC stal oblíbeným cílem velkého množství studií. Tyto prokazují, že BSARCC se může objevovat multifokálně, být asociován s jiným typem renálního karcinomu (37, 38), nádory se mohou vyskytovat v rodinném kontextu PRCC asociovaného s *MET* mutací (39) a přítomnost této vzácné morfologické varianty PRCC byla popsána i v ledvinném allograftu (40).

Provedené molekulárně genetické analýzy zaznamenaly kromě jiných abnormalit i zisk chromosomů 7 a 17 ve všech pro analýzu únosných případech (100%) a ztrátu gonosomu Y v 80% nádorů vzniklých mužů. Vysoké procentuální zastoupení těchto změn může být vysvětleno faktem, že některé z těchto tumorů kromě výše popsaných histologických znaků fokálně vykazovali morfologický vzhled typický pro PRCC typ 1 (36).

V rámci dlouhodobé dispenzarizace byl u některých z publikovaných případů detekován nepříznivý klinický průběh.

1.3.1.9 Solidní papilární renální karcinom

Originálně jednotka popsaná Renshawem a kol. v roce 1997 (41). Morfologickou charakteristikou tohoto typu PRCC je přítomnost těsně nahloučených malých komprimovaných tubulů a krátkých abortivních papil. Fokálně může být vyjádřena přítomnost klasických papilárních struktur, které pokud jsou zastiženy, nebývají příliš hojné. Neoplastické buňky jsou relativně monomorfní, s malým množstvím cytoplasmy a drobnými jádry (42).

I v rámci této podjednotky bylo uskutečněno několik molekulárně genetických studií. Tyto prokázaly polysomii chromosomů 7 a 17 a ztrátu chromosomu Y ve vysokém procentu analyzovaných případů (zisk chromosomu 7 v 78–100% publikovaných případů, zisk chromosomu 17 v 88-100% z publikovaných případů a ztrátu chromosomu Y u 100% analyzovaných případů) (43, 44).

Na základě publikovaných údajů se zdá, že tento podtyp PRCC má relativně příznivý klinický průběh (42).

1.3.2 Karcinom ledviny asociovaný se syndromem familiární leiomyomatózy a karcinomem ledvin/fumarát hydratáza deficientní renální karcinom

Jedná se o autosomálně dominantní nádorové onemocnění, které je definované molekulárně geneticky přítomností inaktivační mutace genu pro fumarát hydratasu (*FH*). Klinicky je syndrom charakterizován vrozenou predispozicí k tvorbě uterinních a kožních leiomyomů a vznikem velmi agresivních renálních karcinomů.

Syndrom byl komplexně popsán v roce 2001 skupinou Launonena u dvou finských rodin jako familiární predispozice k tvorbě uterinních leiomyomů a PRCC (45). WHO 2004 pak oficiálně uváděla existenci nádorového syndromu hereditární leiomyomatózy a renálního karcinomu, ale nikoliv jako samostatný podtyp renálního karcinomu, nýbrž jako předpokládaný hereditární protipól PRCC (46). S přibývajícími publikacemi začalo být evidentní, že morfologické spektrum renálních karcinomů vznikajících v rámci tohoto syndromu je oproti původnímu smýšlení mnohem širší. To vedlo i k celkové změně pohledu na klasifikaci těchto lézí a v ISUP Vancouverské klasifikaci renálních tumorů i v současné

WHO klasifikaci je na podkladě těchto zkušeností HLRCC uveden již jako samostatná nádorová jednotka (2, 4).

V souvislosti s tímto syndromem se v současné době užívají celkem dvě označení - renální karcinom asociovaný se syndromem hereditární leiomyomatózy a renálního karcinomu a fumarát hydratáza deficientní renální karcinom.

Jak už bylo řečeno výše, v prvních publikovaných pracích i ve WHO z roku 2004 je uváděno, že tumory svou morfologickou stavbou nejvíce a nejčastěji odpovídají PRCC typ 2 (45-47). Čím více postižených rodin a jedinců bylo v literatuře popsáno, tím jasněji se ukazovalo, že morfologické spektrum těchto tumorů je oproti původnímu smýšlení velmi široké. HLRCC tak zahrnuje tumory predominantně s papilární architektonikou, typicky smíšené s jiným růstovým typem (cystický, tubulární, tubulolopapilární, solidní) (48). Velká část tumorů v literatuře publikovaných jako HLRCC byla originálně klasifikována jako renální karcinomy blíže nespecifikované (dle WHO klasifikace tzv. renal cell carcinoma NOS) (49). Nejdůležitějším a možná i jediným parametrem v rekognici těchto neoplásií jsou typické nukleární charakteristiky, popisované jako velké jádro s prominentním eosinofilním jadérkem s perinukleolárním halo (48-50).

Pro nádory je typická a definující inaktivační mutace genu pro *FH* (2, 45). Tato mutace vede ke kompletní ztrátě či redukci aktivity enzymu fumarát hydratasy, která je za normálních okolností zodpovědná za konverzi fumarátu na malát během Krebsova cyklu (47, 51, 52). Z toho resultující zvýšené množství fumarátu vede k modifikaci buněčných enzymatických a látkových pochodů, kde jedním z důsledků je i zvýšená produkce S-(2-sukcino)-cysteinu (2SC). Akumulace 2SC vede k pozitivním výsledkům imunohistochemických barvení na 2SC (53, 54), naopak ztráta enzymatické aktivity FH resultuje v negativitu imunohistochemického barvení na FH. Na základě těchto poznatků je evidentní, že HLRCC se vyznačují imunohistochemickým profilem 2SC pozitivní, FH negativní, což lze relativně dobře využít i v diagnostické praxi (49, 53). I to však má své nemalé limitace, kvůli kterým není tento diagnostický algoritmus do reálné praxe lehce zaveditelný (imunohistochemická protilátka proti 2SC je nekomerční, vzhledem k raritě těchto lézí a tedy ne příliš častému užití protilátky je obtížná i interpretace výsledku vyšetření, taktéž přicházejí do popředí provozní otázky jako je expirační lhůta protilátky atd.). Definitivní diagnóza tedy musí být konfirmována molekulárně genetickým vyšetřením s průkazem mutace genu *FH*.

Klinicky se jedná o renální karcinomy asociované s velmi agresivním chováním, pokročilým stádiem onemocnění v době diagnózy, často končící letálně. Tumory se typicky objevují v mladém věku, v porovnání s jinými familiárně se vyskytujícím renálními karcinomy jsou solitární a unilaterální (45, 48, 50). U těchto tumorů je tedy doporučována brzká a kompletní chirurgická léčba a aktivní sledování pacientů z postižených rodin (50).

1.3.3 Světlobuněčný papilární renální karcinom

Pod touto jednotkou se ve WHO 2016 (2) ukrývají celkem dvě morfologicky velmi obdobné léze – renální angiomyoadematózní tumor (RAT) a vlastní CCPRCC.

V roce 2000 se ve formě kazuistiky v literatuře objevuje do té doby nepopsaná nádorová jednotka, která na podkladě morfologie dostává název RAT (55). CCPRCC pak byl poprvé popsán v roce 2006 jako nádor vznikající v terénu end-stage kidney disease (ESKD) (56), avšak pozdější práce prokázaly výskyt této neoplásie i v ledvině bez postižení ESKD

(57, 58). Různé studie se pak často zabývaly vztahem mezi RAT a CCPRCC a postupně bylo prokázáno, že morfologické, imunohistochemické a molekulárně genetické vlastnosti obou lézí jsou velmi obdobné a oba tumory jsou s největší pravděpodobností dva opačné konce jednoho morfologického spektra, kdy RAT se od CCPRCC liší pouze přítomností objemné hladkosvalové komponenty (57, 59).

Oba nádory se skládají z blandně vyhlížejících cylindrických neoplastických buněk s objemnou světlou cytoplasmou a jádrem s low-grade morfologií, lehce nadzdviženým od bazální membrány. Tumor roste pod obrazem papilární, tubulární či tubulopapilární léze, ve stromatu s jemnou sítí drobných kapilár.

Imunohistochemicky tyto nádory vykazují difúzní pozitivitu v CK7, HMWK a vimentinu, CA-IX je pozitivní v typické v tzv. cup-like (bazolaterální) distribuci. Naopak negativitní jsou nádorové buňky v racemáze (AMACR) a TFE3. Variabilní reaktivitu lze prokázat v CD10 (2, 57, 60).

CCPRCC byl dlouhou dobu považován za tumor bez molekulárně genetických aberací typických ať už pro CCRCC, či pro PRCC (60). Tumor tedy uniformně nevykazuje polysomii chromosomů 7 a 17 a ztrátu gonosomu Y u mužů. Avšak u ojedinělých v literatuře popsaných případů byly detekovány abnormality genu *VHL* (57, 58). Podle našeho názoru by léze s nejednoznačnou morfologií, ne příliš typickým imunohistochemickým profilem a se současně prokázanou abnormalitou *VHL* genu neměli být klasifikovány jako CCPRCC/RAT (59).

CCPRCC jsou tumory typicky s indolentním klinickým průběhem, převážná většina v literatuře publikovaných případů měla zcela benigní biologické chování (59).

1.3.4 Xp11.2 translokační renální karcinom

Xp11 TRCC je nádorovou jednotkou s velkým procentuálním zastoupením především u pediatrických renálních karcinomů. U populace dospělých pacientů je frekvence výskytu nejspíše výrazně podceňována, dostupná data uvádějí incidenci 1,6 – 4% z celkového počtu renálních karcinomů v této věkové kategorii (2). Z etiologických agens bývá popisována asociace této neoplastické entity s předchozí expozicí chemoterapii (61).

První ucelené práce popisující Xp11 TRCC se začínají v literatuře objevovat od roku 2001 (62). Na podkladě těchto prací se Xp11 TRCC stal v roce 2004 samostatnou jednotkou WHO klasifikace renálních neoplásií (46). V poslední WHO klasifikaci (z roku 2016) tato jednotka zůstává, avšak již nikoliv jako samostatná kategorie. Xp11 TRCC se stal společně s v klasifikaci nově zahrnutým t(6,11) translokačním renálním karcinomem součástí větší souhrnné kategorie tzv. MiT rodiny translokačních renálních karcinomů (2).

Xp11 TRCC je renální neoplásií, kde přítomnost translokace transkripčního faktoru TFE3 (se širokým spektrem genů partnerských za vzniku různých fúzních genů) je charakteristikou tuto nádorovou jednotku definující. Spektrum popsaných fúzních partnerů genu *TFE3* je opravdu široké. Mezi známé fúzní partnery patří geny *ASPSCR1* (také nazýván *ASPL*), *PRCC*, *NONO* (také nazýván *p54nrb*), *SFPQ1* (nazýván též *PSF*), *CLTC*, *PARP14*, *LUC7L3*, *KHSRP*, *DVL2*, *RBM10* (63). Recentně vychází množství velmi zajímavých prací věnujících se specificky průkazu různých fúzních genů a s nimi asociovaným morfologickým paternem tumorů (64-66).

Pro nádory je typická velká variabilita morfologického vzhledu, klasicky je však popisována papilární architektonika, buňky s jasnou a eosinofilní objemnou cytoplasmou, psammomatózní tělíska, hyalinní globule, krevní lakuny.

Imunohistochemický profil není konstantní, nádory obyčejně neexprimují cytokeratinové markery, jsou pozitivní v PAX8, někdy jsou reaktivní v průkazu melanomových markerů (Melan A, HMB45), část nádorů je cathepsin K pozitivní. Imunohistochemický průkaz proteinu TFE3 (jaderná reaktivita) je problematický, nevykazuje konstantní pozitivitu (ovlivněn fixací materiálu) a je tedy nutno k jeho interpretaci přistupovat obezřetně a finální diagnózu konfirmovat molekulárně genetickým vyšetřením zlomu TFE3 pomocí vyšetření FISH s break apart sondou (originální práce zabývající se problematikou je součástí disertační práce – viz výsledky).

Xp11 TRCC má prognózu obdobnou CCRCC (67).

2 Cíle prací

1. Specifikovat neobvyklé, raritní či doposud nepopsané varianty PRCC (morfologicky, imunohistochemicky, molekulárně geneticky), stanovit diagnostické algoritmy a upřesnit diferenciální diagnostiku.

2. Stanovit prognostický význam přítomnosti nekrózy a cystických změn u PRCC typ 1.

3. Určit význam molekulárně genetického vyšetření (FISH) u lézí suspektních z diagnózy Xp11 TRCC, posoudit význam imunohistochemického vyšetření TFE3.

4. Zhodnotit a rozšířit morfologické spektrum Xp11 TRCC s fúzním partnerem *NONO-TFE3*.

3 Výsledky

Výsledky dizertační práce jsou prezentovány sedmi původními pracemi uvedenými níže.

3.1 "Mucin"-secreting papillary renal cell carcinoma: clinicopathological, immunohistochemical, and molecular genetic analysis of seven cases

Produkce mucínu a mucínu podobného materiálu není všeobecně považována za znak typický pro PRCC a tato produkce pak bývá spíše spojována s jinými typy RCC (např. MTSCC).

Z Plzeňského registru nádorů, čítajícího 1311 PRCC, bylo zpětně vyhledáno a opětovně hodnoceno 7 nádorů diagnostikovaných jako PRCC, u kterých byla zaznamenána extracelulární a/nebo intracelulární produkce mucinózního/mucínu podobného materiálu. Tyto případy byly analyzovány morfologicky, histochemicky, imunohistochemicky a za pomoci molekulárně genetických metod (FISH, arrayCGH).

Klinická data byla dostupná u šesti ze sedmi případů (5 mužů, 1 žena, věkové rozmezí pacientů 61-78 let). Údaje o dispenzarizaci byly k dispozici u čtyř pacientů (v trvání 2-4 roky), u jednoho pacienta vedlo onemocnění k smrti následkem generalizace procesu. Velikost tumorů se pohybovala v rozmezí 3-5 cm (průměr 3,8 cm). U všech případů morfologicky dominovala papilární architektonika. Mucinózní/mucínu podobný materiál byl zaznamenán u jednoho případu pouze extracelulárně, pouze intracelulární produkce byla prokázána ve třech případech a intra- i extracelulární produkce mucinózního materiálu byla přítomna ve třech v této studii analyzovaných případech. Všechny nádory vykazovaly pozitivitu v imunohistochemickém průkazu racemázy (AMACR), vimentinu, cytokeratinu OSCAR, pouze u čtyř případů byla zaznamenána pozitivita cytokeratinu CK7. Barvení mucikarmínem bylo pozitivní u všech sedmi případů, barvení PAS prokázalo pozitivitu mucinózní produkce v šesti případech a barvení alciánovou modří bylo pozitivní u třech případů. Pět případů vykazovalo reaktivitu v imunohistochemickém průkazu MUC1. MUC2, MUC4 a MUC6 byly negativní ve všech případech. Pouze u čtyř případů dovolila kvalita materiálu provedení molekulárně genetického vyšetření. U dvou případů byla prokázána polysomie chromosomů 7 a 17, u jednoho případu pouze polysomie chromosomu 17. Ztráta heterozigozity 3p (LOH3p) společně s polysomií chromosomů 7 a 17 detekovalo molekulárně genetické vyšetření v jednom z případů. U žádného z tumorů nebyla zaznamenána abnormalita genu *VHL, FH* či translokace genu *TFE3*.

Na základě této studie lze konstatovat, že PRCC s mucinózní sekrecí je vzácná varianta PRCC, jistě zasluhující další studie. Mucinózní materiál obsažený v těchto tumorech vykazuje pozitivitu speciálního histochemického barvení mucikarmínem, avšak jiná konvenční histochemická a imunohistochemická barvení používaná pro mucinózní materiál nejsou u těchto nádorů konstantní ve své pozitivitě. Molekulárně genetický profil PRCCM je relativně konzistentní s molekulárně genetickým profilem klasicky považovaným za typický pro PRCC, avšak jeden z nádorů vykazoval molekulárně genetické znaky typické jak pro PRCC tak pro CCRCC. Je evidentní, že PRCC s mucinózní sekrecí má metastatický potenciál a zaslouží si být odlišen jako samostatná varianta PRCC.

Virchows Arch (2016) 469:71–80
DOI 10.1007/s00428-016-1936-7

ORIGINAL ARTICLE

“Mucin”-secreting papillary renal cell carcinoma: clinicopathological, immunohistochemical, and molecular genetic analysis of seven cases

Kristyna Pivovarcikova [1] & Kvetoslava Peckova [1] & Petr Martinek [1] & Delia Perez Montiel [2] & Kristyna Kalusova [3] & Tomas Pitra [3] & Milan Hora [3] & Faruk Skenderi [4] & Monika Ulamec [5] & Ondrej Daum [1] & Pavla Rotterova [1] & Ondrej Ondic [1] & Magdalena Dubova [1] & Romuald Curik [1] & Ana Dunatov [6] & Tomas Svoboda [7] & Michal Michal [1] & Ondrej Hes [1,8]

Received: 28 December 2015 / Revised: 9 March 2016 / Accepted: 28 March 2016 / Published online: 12 April 2016

Abstract Mucin and mucin-like material are features of mucinous tubular and spindle renal cell carcinoma (MTS RCC) but are rarely seen in papillary renal cell carcinoma (PRCC). We reviewed 1311 PRCC and identified 7 tumors containing extracellular and/or intracellular mucinous/mucin-like material (labeled as PRCCM). We analyzed these using morphological, histochemical, immunohistochemical, and molecular genetic methods (arrayCGH, FISH). Clinical data were available for six of the seven patients (five males and one female, age range 61–78 years). Follow-up was available for four patients (2–4 years); one patient died of widespread metastases. Tumor size ranged from 3 to 5 cm (mean 3.8). Of all cases, histological architecture showed a predominantly papillary pattern. Mucin or mucin-like was extracellular in one, intracellular in three, and both intra/extracellular in three cases. All tumors were positive for AMACR, vimentin, and OSCAR, while CK7 was positive in four. Mucicarmine stain was positive in all cases, PAS in six and Alcian blue in three cases. Five tumors were positive for MUC 1, but none were positive for MUC 2, MUC 4, or MUC 6. In only four cases, genetic analysis could be performed. Gain of chromosomes 7 and 17 was found in two cases; gain of 17 only was found in one case. Loss of heterozygosity of 3p was found in one case together with polysomy of chromosomes 7 and 17. No abnormalities of VHL, fumarate dehydrogenase, and TFE3 genes were detected. We conclude that PRCCM is a rare but challenging subtype of RCC that deserves to be further studied. In all the tumors, the mucin-like material was found in those stained with mucicarmin, but other conventional and immunohistochemical stains did not reveal consistent features of a single mucin. The molecular-genetic profile of these tumors was most consistent with that of typical papillary RCC, although one case had mixed genetic features of papillary and clear RCC. PRCCM has metastatic potential, as evidenced by one case with widespread metastases. It remains to be determined whether PRCCM represents a unique tumor subtype, deserving to be distinguished from other subtypes of PRCC.

* Ondrej Hes
hes@medima.cz

[1] Department of Pathology, Medical Faculty, Charles University and Charles University Hospital Plzen, Alej Svobody 80, 304 60 Pilsen, Czech Republic

[2] Department of Pathology, Instituto Nacional de Cancerologia, Mexico City, Mexico

[3] Department of Urology, Medical Faculty, Charles University and Charles University Hospital Plzen, Prague, Czech Republic

[4] Department of Pathology, University Hospital Sarajevo, Sarajevo, Bosna and Hercegovina

[5] Pathology Department, Clinical Hospital Center, Sestre milosrdnice, Zagreb, Croatia

[6] Department of Pathology, University Hospital Split, Split, Croatia

[7] Department of Oncology, Medical Faculty, Charles University and Charles University Hospital Plzen, Prague, Czech Republic

[8] Biomedical Centre, Faculty of Medicine in Plzen, Charles University in Prague, Plzen, Czech Republic

Keywords Kidney . Papillary renal cell carcinoma . Mucin . Mucin-like secretion . Immunohistochemistry . Array CGH . FISH

Introduction

Interstitial mucin is an almost constant feature of mucinous tubular and spindle RCC (MTS RCC) [1]. Other renal cell

tumors with mucin production, including mucinous papillary renal cell carcinoma (PRCC), renal papillary adenoma (RPA), renal oncocytoma (RO), and clear cell RCC (CCRCC), are rare, and most of them have been reported in the literature as case reports or a short series of cases. Mucin deposits in MPRCC, RPA, and CCRCC have been described as intracytoplasmic and intraluminal [2–5]. In RO, mucin was described in the lumen of scattered tubules but not intracytoplasmic [6].

Mucicarmine, an empirical stain for mucin and mucin-like material, has been occasionally used by pathologists to exclude renal origin in case of a papillary carcinoma with unknown primary [7]. However, rare cases of mucicarmine-positive papillary renal cell carcinomas have been reported. We therefore decided to determine how common mucicarmine-positive PRCC are and whether or not they represent a distinct clinicopathological entity. To this end, we reviewed 1311 PRCC in our files and identified 7 cases that were mucicarmine positive. This paper presents characteristics of these tumors.

Material and methods

Ten renal tumors matching keywords “unclassified, papillary, mucin, renal cell carcinoma” were retrieved out of 1311 PRCC from the Plzen Tumor Registry. All cases were reviewed by two pathologists (KPi, OH), who compared the features with the index cases. Finally, 7 cases were selected. There were 1–13 blocks available for each case; 1–2 representative blocks of each case were selected for immunohistochemical and molecular genetic study.

Tissue for light microscopy had been fixed in 4 % formaldehyde and embedded in paraffin using routine procedures. Tissue sections (4 μm) were cut and stained with hematoxylin and eosin (H&E). As special staining techniques for mucin, we used mucicarmine, Periodic Acid-Schiff (PAS), and Alcian blue at pH 2.5.

Immunohistochemical staining was performed using primary antibodies against the following antigens: racemase/AMACR (13H4, monoclonal, DAKO, Glostrup, Denmark, 1:200), carbonic anhydrase IX (rhCA9, 303123, monoclonal, RD Systems, Abingdon, GB, 1:100), vimentin VM (D9, monoclonal, NeoMarkers, Westinghouse, CA, 1:1000), MUC 1 (Ma695, monoclonal, Leica, Newcastle, UK, 1:200), MUC 5 AC (CLH2, monoclonal, Leica, 1:400), MUC 2 (Ccp58, monoclonal, Novocastra,Newcastle upon Tyne, UK, 1:400), MUCIN 4 (8G7, monoclonal, Santa Cruz Biotechnology, Dallas, TX, 1:50), MUC 6 (CLH5, monoclonal, Novocastra, 1:300), OSCAR (OSCAR, 1:500, Covance, Herts, UK, 1:500), PAX-8 (polyclonal rabbit, Cell Marque, Rocklin, CA, 1:25), CDX2 (CDX2-88, monoclonal, BioGenex, San Ramon, CA, 1:150), cytokeratin 7 (OV-TL12/30, monoclonal, DakoCytomation, Carpenteria, CA, 1:200), cytokeratin 20 (Ks20.8, monoclonal, DakoCytomation, 1:100), and cytokeratin (AE1-AE3, monoclonal, BioGenex, 1:1000). Bound antibodies were visualized using a supersensitive streptavidin-biotin-peroxidase complex (Biogenex). Appropriate positive controls were employed.

DNA extraction

DNA from macro-dissected formalin-fixed paraffin-embedded (FFPE) tissue was extracted using a QIAsymphony DNA Mini Kit (Qiagen, Hilden, Germany) on an automated system (QIAsymphony SP, Qiagen) according to the manufacturer’s supplementary protocol for FFPE samples (purification of genomic DNA from FFPE tissue using the QIAamp DNA FFPE Tissue Kit and Deparaffinization Solution). Samples were then purified using Qiaquick kit (Qiagen) and eluted in EB buffer. Concentration and purity of isolated DNA was measured using NanoDrop ND-1000 (NanoDrop Technologies Inc., Wilmington, DE, USA). DNA integrity was examined by amplification of control genes in multiplex PCR [8].

Array comparative genomic hybridization

CytoChip Focus Constitutional (BlueGnome Ltd., Cambridge, UK) array was used for array comparative genomic hybridization (aCGH) analysis. It uses BAC technology and covers 143 regions of known significance with 1 Mb spacing across a genome. Probes are spotted in triplicate. First, 400 ng of DNA was labeled using a Fluorescent Labeling System (BlueGnome Ltd., Cambridge, UK). The procedure included Cy3 labeling of a test sample and Cy5 labeling of a reference sample. Commercially produced reference of the opposite sex was used when no reference sample was available (MegaPool Reference DNA Male/Female, Kreatech Diagnostics, Amsterdam, Netherlands). The labeled reference and the test sample were mixed, dried, and hybridized overnight at 47 °C using Arrayit hybridization cassette (Arrayit Corporation, California, U.S.A.). Post-hybridization washing was done using SSC buffers with increasing stringency. Dried microarrays were scanned with InnoScan 900 (Innopsys, France) at a resolution of 5 μm. Scanned images were analyzed and quantified by BlueFuse Multi software (BlueGnome Ltd., Cambridge, UK). The software uses Bayesian algorithms to generate intensity values for each Cy5 and Cy3 labeled spot on the array according an appropriate gal file. Cutoff values for log 2 ratio are preset to −0.3 for loss and to 0.3 for gain by BlueFuse software. All genomic coordinates were based on the March 2009 assembly of the reference genome GRCh37.

Fluorescent in situ hybridization (FISH)

FFPE tissue sections (4 μm) were placed onto a positively charged glass slide. The target area, corresponding to what was marked on a H&E stained slide, was circled with a diamond pen. The section was routinely deparaffinized, incubated in the 1× Target Retrieval Citrate Solution (DAKO, Glostrup, Denmark; pH 6 for 40 min at 95 °C) then cooled in the same solution (20 min at room temp). The slide was washed in deionized water and digested in protease solution with Pepsin (0.5 mg/ml in 0.01 M HCl; Sigma Aldrich, St. Louis, MO, USA) at 37 °C for 15 min. The slide was then immersed in deionized water for 5 min, dehydrated in a series of ethanol solutions (70, 85, and 96 %, 2 min each), and air-dried. Fluorescent in situ hybridization (FISH) probes CEP 7 Spectrum Orange (D7Z1), CEP 17Spectrum Orange, CEP X (DXZ1) Spectrum Green/CEP Y (DYZ3), and Spectrum Orange (Vysis/Abbott Molecular, Des Plaines, Illinois) were mixed with water and hybridization buffers according to the manufacturer's protocol. The slide was incubated in a ThermoBrite instrument (StatSpin/Iris Sample Processing, Westwood, Massachusetts) with codenaturation (85 °C for 8 min) and hybridization (37 °C for 16 h). Post-hybridization wash was performed in 2× SSC/0.3 % NP-40 solution (72 °C for 2 min). The section was counterstained with DAPI I (Vysis) and stored in the dark at −20 °C until examined. FISH signals were assessed using an Olympus BX51 fluorescence microscope. Scoring of aneuploidy was performed by counting the number of fluorescent signals in 100 randomly selected, non-overlapping tumor cell nuclei. The slide was independently enumerated by two observers (PG, TV). Cutoff values were set for each probe as shown in previous study [9].

Results

Clinical data were available for six of the seven cases (Table 1). These included five males and one female, age range 61 to 78 years (median 74 years, mean 71.17 years). Tumor size ranged from 3 to 5 cm in the greatest dimension (median 3.5 cm, mean 3.8 cm). One tumor was found in the left kidney and two in the right kidney; no information about laterality was available for four cases. On gross section, the tumors were yellowish to gray-white to grayish-brown, with visible hemorrhages in two cases.

Follow-up was available for four patients (range 2 to 4 years, mean 2.75 years, median 2.5 years). One patient died of disease 4 years after diagnosis despite treatment (sunitinib). One patient died of colorectal adenocarcinoma 2 years after diagnosis. Two patients are alive and well without signs of recurrence or metastasis, although for one patient, only basic and limited information was available. Other patients were lost to follow-up.

Histological findings

The histopathological features are summarized in Table 2. All seven cases showed at histological examination a papillary pattern architecture (Fig. 1). In two cases, a prominent tubulopapillary component (cases 4 and 5) was noted (Fig. 2). Cases 2 and 3 contained smaller areas with a solid pattern. Bluish to eosinophilic mucin-like material was present to a variable extent in all cases (Fig. 3a, b). This was only extracellular in one case; in three cases, it was only intracellular; and in three cases, it was present both intracellularly and extracellularly in H&E-stained sections.

Extracellular material presented as a bluish to eosinophilic deposit of mucin-like material in the interstitium between tumor cells or within papillary stalks. Intracellular material presented as a mucin-like substance in the cytoplasm as larger or smaller clear vacuoles. Some of these cells had the features of signet-ring cells (Fig. 4a, b) and they were present in five cases. In all cases, mucin-like material was positive for mucicarmine (Fig. 5), and in six cases, it was PAS positive (Fig. 6). In three cases, the cells were reactive with Alcian blue, and this was designated as PAS and Alcian blue co-staining. The intracellular mucin-like material was positive either for mucicarmine or for PAS in two of the cases containing cells with signet-ring

Table 1 Basic clinicopathological data

Case	Sex	Age (years)	Size (cm)	Site	Stage	Color	Follow-up
1	F	78	3 × 2 × 1.5NA pT1a (TNM09)			NA	NA
2	M	77	3 × 3.5 × 1.5 and 2 × 1.5 × 1 Right pT1a (TNM09)			Ochroid	2 years, AW
3	M	76	3.5 × 2.5 × 3Right pT1 (TNM09)			Yellowish	Dead of disease 4 years after dg.
4	M	63	Diameter 5NA NA			NA	NA
5	NA	NA	NA	NA	NA	NA	NA
6	M	61	3 × 3.7 × 4	NA	NA	Gray-white	3 years, A, no information about health condition
7	M	72	NA	Left	NA	Grayish-brown	Dead 2 years after dg.—other malignant disease

M male, F female, NA not available, AW alive and well, A alive

Histopathological features	Case	Papillary	Tubulopapillary	Solid	NOS1	NOS22
		11				
Type grade (ISUP)						
		22			42	333
Heamorrhage		−+			+−	−++
Siderophages						
Foamy		−−			+−	−++
Giant macrophages cells		−+			++	+++
Signet-ring		−−			+−	−++
Hibernoma-like						
Psammomamorphology changes		−−			+−	−−−
bodies		−−			+−	−−+
		+−			+−	+++
Intracellularmucin-likesecretion		++			+−	+++
Extracellularmucin-likesecretion		−				
		+ (10 %)			+ (intraluminal) + (papillary stroma)	
		+ (20 %)			−− + (papillary stroma)	
		−			+ (intraluminal)	
		−	−		−	
					−	
					−+ (80 %)	
		−−				+−−
		++			++	+++
		12			34	567

Table 2

+ = present, − = absent, NOS not otherwise specified

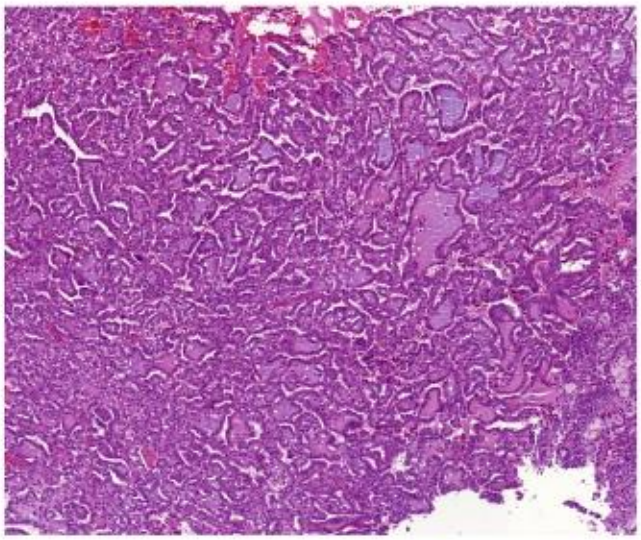

Fig. 1 All 7 cases were arranged in papillary pattern

morphology. In three of the cases, cells with signet-ring morphology did not react with mucicarmine nor PAS. Four tumors contained hemorrhagic areas. Foamy macrophages were found in six cases. Hemosiderophages were observed in three cases and in two cases (cases 3 and 7) clear cell-like areas, containing cells with foamy cytoplasm and microvacuolated appearance resembling macrophages or hibernoma cells (Fig. 7). These tumors both contained also giant multinucleated neoplastic cells.

In addition to these morphological features, we found a focus with epithelial cells in pseudorosette formation in case 3, numerous extracellular eosinophilic globules, and larger pools of eosinophilic material in case 5 and in case 6 abundant giant multinucleated cells and foamy macrophages.

Nuclear grades according to the “Fuhrman (ISUP) nucleolar” grading system was 4 (one case), 3 (three cases), and 2 (three cases). No relationship or direct connection with renal pelvis or calyces was seen.

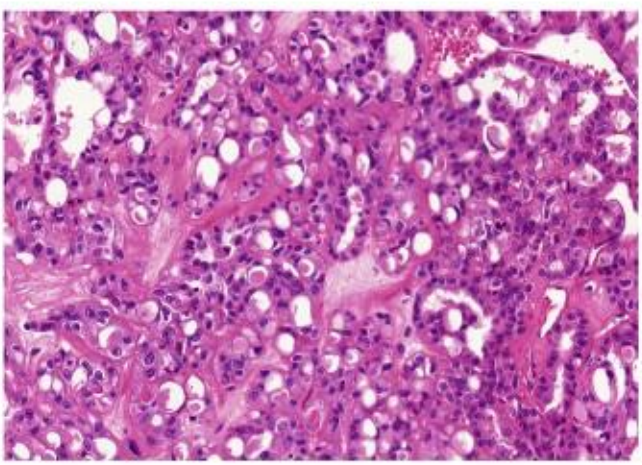

Fig. 2 Focus of tubulopapillary architecture was noted in 2 cases

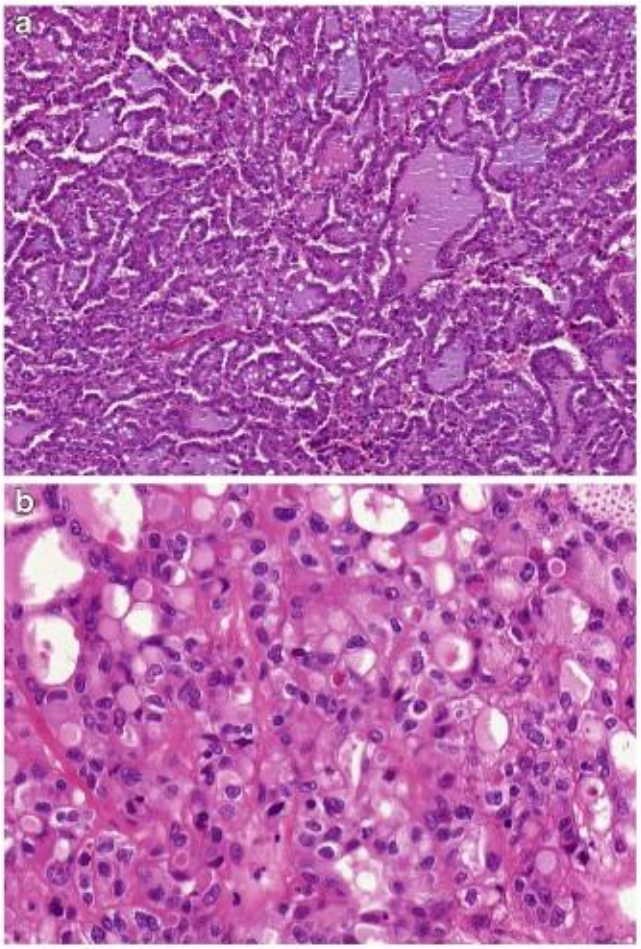

Fig. 3 Bluish to eosinophilic mucin-like secretion was variably present in all cases in the intersticium (a) or in intracellular vacuoles (b)

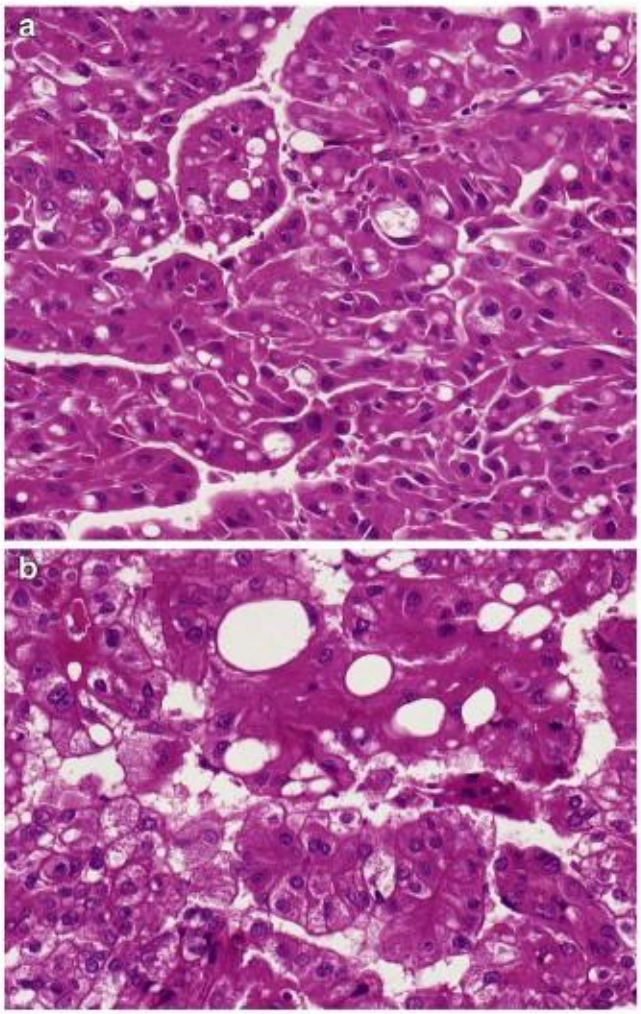

Fig. 4 As intracellular production was considered presence of the same material within cytoplasm in form of larger or smaller vacuoles. Some such cells reached the shape and characteristics of signet-ring cells (a+b)

Immunohistochemical analysis

Results of immunohistochemical examination are summarized in Table 3. All tumors were positive for AMACR, vimentin, and OSCAR. Keratin AE1-AE3 was diffusely positive in five tumors. CK 7 was diffusely positive in three (Fig. 8), focally in one case, and was negative in three cases. CK 20 was focally moderately positive in one tumor (CK 7 was negative in this case). Carbonic anhydrase IX was focally moderately positive in one case. PAX 8 was positive in six tumors, five strongly and diffuse, one focally. All tumors were negative for CDX2.

Mucin-like deposits were examined using a panel of antibodies against different MUC antigens (Table 4). MUC 1 was diffusely strongly positive in two cases and focally in three cases (two strongly and one moderately) (Fig. 9). None of the tumors were reactive for MUC 2, MUC 4, and MUC 6. Two cases were weakly positive for MUC 5 AC.

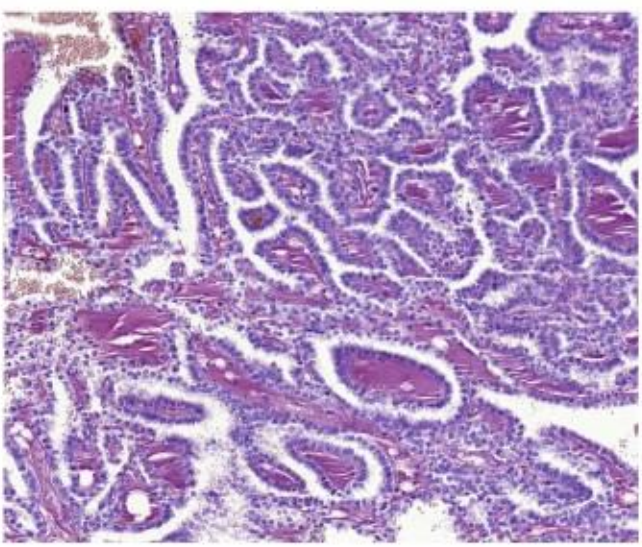

Fig. 5 Interstitial mucin-like material was positive for mucicarmin

Molecular genetic analysis

Results of molecular genetic analyses are summarized in Table 5. Array CGH analysis was performed on one case (case

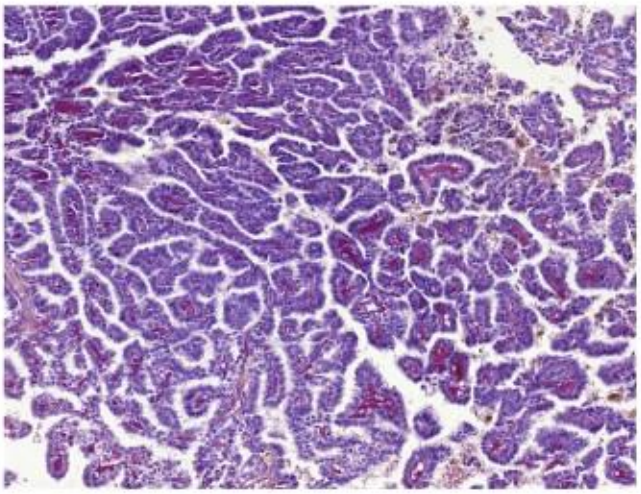

Fig. 6 The same interstitial deposition was positive for PAS

2), which showed gain of chromosomes 7, 16, and 17 and loss of chromosome Y. FISH was performed on four cases. Polysomy of chromosomes 7 and 17 was found in two cases. In one case, polysomy of only chromosome 17 was present. One case (case 1) was disomic for both chromosomes 7 and 17. Loss of heterozygosity (LOH) of chromosome 3p was assessed in five cases and was positive in one case (case 5), which also showed polysomy of chromosomes 7 and 17. In none of the six cases analyzed were mutations found in the VHL gene. We found no methylation of VHL gene promoter in the six cases analyzed.

Discussion

RCC with mucin or mucin-like secretion was initially published in 1963 by Foster and Levine [10], who reported Mayer's mucicarmine positive material in 2 out of 71 renal cell carcinomas. Their description unfortunately does not allow any conclusion as to the histological type according to current classifications [11]. Grignon et al. [12] described an RCC with luminal and cytoplasmic presence of mucin, reactive with Mayer's mucicarmine and Alcian blue. The documentation allows to conclude that this tumor was a papillary RCC with mucin/mucin-like secretion [12].

The term "mucin" encompasses a large family of glycoproteins expressed by many normal and neoplastic cell types. Two main classes are distinguished: membrane-bound and secreted or gel forming [13]. Mucin can be stained empirically with mucicarmine, historically regarded as highly sensitive [14]. Recent studies correlating the results of mucicarmine staining with immunohistochemical staining for various antigens specific for individual mucin subtypes are lacking. Staining with PAS and Alcian blue might be more sensitive as they cover both neutral and acidic mucins, produced by epithelial or mesenchymal cells. However, these stains lack specificity as they also bind to other substances such as glycosylated proteins.

Of the MUC family, only MUC1 is expressed in normal epithelial cells of the kidney. MUC2, a secreted gel-forming mucin, is typically secreted by goblet cells of the gastrointestinal and respiratory tract [15]. MUC4 is a transmembrane glycoprotein, which provides a protective layer of mucus to epithelial cells of the intestine, airways, and mammary ducts [16]. MUC5AC is found mainly in the mucosal layer of the stomach, while MUC6 is located principally in gastric pyloric glands [17]. MUC 1 is expressed in convoluted distal tubules and in collecting ducts in normal renal tissue, with a polar apical distribution [18–20]. Leroy et al. reported that MUC1 is expressed in 54 % of PRCC. They found that MUC1 is predominantly expressed in type 1 PRCC and only rarely in type 2 PRCC [21].

The most frequent type of renal cell carcinoma with mucin production is MTS RCC, which is composed of tubules, many of which are elongated and merge into cord-like structures with transitions into spindle cells. Weakly basophilic mucin is present at least focally in most tumors [22], located mostly in the interstitium, and a proper term for such a finding would be myxoid rather than mucinous. Fine et al. mapped the histologic spectrum of MTS RCC and documented cases of MTS RCC without conspicuous extracellular mucin in H&E-stained sections [23]. However, scant mucinous material within cellular areas has been reported in these "mucin-poor" MTS RCC [24].

Our cases were completely different from MTS RCC. Tumors from our series lacked typical dual architecture; tubules lined by cuboidal cells were not encountered nor a spindle cell component with characteristic myxoid changes in the stroma. Immunohistochemical staining does not distinguish between PRCC and MTS RCC because of an overlapping

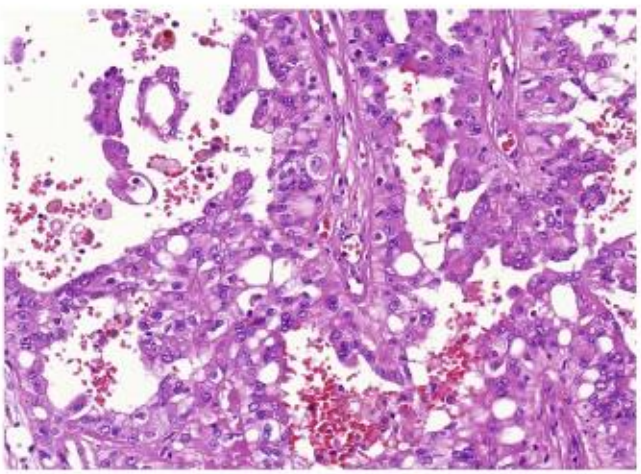

Fig. 7 Focally, cells had foamy cytoplasm and microvacuolated appearance resembling macrophages or hibernoma cells

Table 3 Immunohistochemical examination

Case	AMACR	CANH9	VIM	OSCAR	AE1/3	PAX8	CK7	CK20	CDX2
1	+++	−	+++	+++	++	+++	++	−	−
2	+++	++ Foc.	+++	+++	++	+++	+++	−	−
3	+++	−	+++	+++	++	+++	+++ Foc.	−	−
4	++	−	+++	+++	+++	+++	+++	−	−
5	+++	−	+++	+++	+++	+++	−	−	−
6	++	−	+++	+	−	++ Foc.	−	−	−
7	+++	−	++	+	−	−	−	++ Foc.	−

Foc. = < 50 % cells staining, − = negative, + = weak positivity, ++ = moderate positivity, +++ = strong positivity, AMACR racemase, CANH9 carbonic anhydrase, AE1/3 cytokeratin AE1-AE3, vim vimentin

marker profile. However, a molecular genetic profile might help to differentiate between these entities. We have documented gain of chromosomes 7, 16, and 17 and loss of chromosome Yusing array CGH analysis, confirmed subsequently by FISH. The pattern of these numerical chromosomal aberrations is not compatible with that of MTS RCC, which shows disomy of chromosomes 7 and 17 and chromosomal loss, notably of chromosomes 1, 4, 6, 8, 9, 13, 14, 15, and 22, regardless of grade [23].

Mucin production has been described in three primary papillary RCCs, which showed eosinophilic cuboidal to columnar cells and extensive luminal or intracytoplasmic acid mucin deposition, including sulphomucins as indicated by mucicarmine, Alcian blue (at pH 2.5), and high-iron diamine staining. Furthermore, foam cells (in two cases), hemosiderin, and siderophages (in two cases), calcification (in one case), and an incomplete fibrous capsule were described [2] [3]. Mucin production has also been reported in four papillary adenomas. Mucin was of acid type, as indicated by mucicarmine, Alcian blue (at pH 2.5), and Mowry's colloidal iron staining, intracellular in numerous scattered tumor cells in two cases, focal luminal in one case, and mixed intracellular and luminal in another case [4].

In this study, all tumors were classified as PRCC. Morphological and immunohistochemical features were mostly compatible with type 1 PRCC; however, some morphologic variability was noted [25]. All tumors expressed AMACR, vimentin, and OSCAR while four cases expressed CK 7. Architecture was predominantly papillary, even in CK 7-negative tumors. CK 7-negative PRCC has been reported notably by Langner et al. who described variable CK 7 reactivity in renal cell carcinoma subtypes, including PRCC [9]. Morphology and marker expression pattern (coexpression of AMACR, vimentin, and CK 7-among others) of our case 1 was typical of PRCC. However, for PRCC disomy of chromosomes 7, 17, and Y is unusual. Case 5 showed polysomy of chromosomes 7 and 17, supernumerary chromosome X, and LOH3p, compatible with both PRCC and clear cell RCC but morphology was consistent with PRCC. The marker expression pattern (CK 7 and carbonic anhydrase IX both negative) in this case was unusual for PRCC. We used morphology as ultimate criterion and considered the case as PRCC. Two more cases were not entirely typical of PRCC (cases 6 and 7) because they were negative for CK 7. Genetic analysis could not be performed on case 7 due to low quality of DNA. In case 6, status of the VHL gene (mutations, LOH3p, and methylation status) was normal but it showed loss of chromosome Y, which fits with PRCC. However, analysis of chromosomes 7 and 17 failed because of low-quality DNA.

We introduced the term "mucin-like" instead of "mucinous" because of the results of immunohistochemical staining for MUC antigens. The MUC antigens most commonly expressed in human mucinous carcinomas are MUC1, MUC2, MUC4, MUC5AC, and MUC6. Lack of expression of these antigens raises questions as to specificity of traditional stains (mucicarmine, PAS, Alcian blue) used to detect mucin. Reports on mucin deposits in tumors based only on traditional stains should be interpreted with caution when the results are not corroborated by immunohistochemistry. In all our cases, in H&E-stained sections, mucin-like material was present. Mucin-like material was

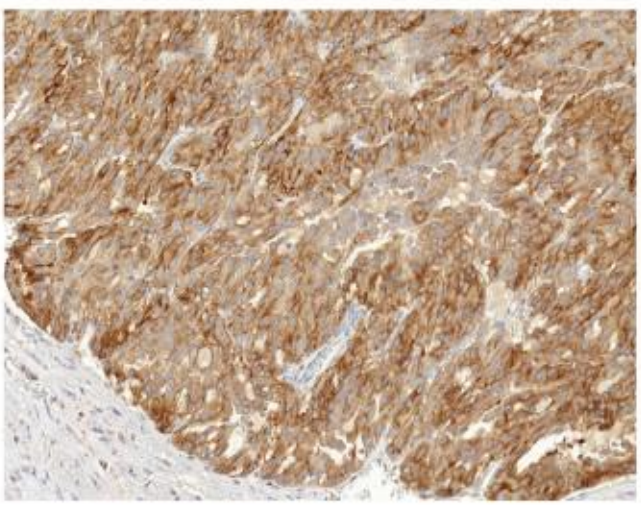

Fig. 8 CK 7 was diffusely positive in three cases

Table 4 Mucin staining

Case	Mucicarmine	Periodic Acid Schiff	Alcian blue	MUC1	MUC2	MUC4	MUC5AC	MUC6
1	+	++	−	+++ Foc.	−	−	−	−
2	+++ Foc.	+	+	+++ Foc.	−	−	+	−
3	+ Foc.	++	−	++ Foc.	−	−	−	−
4	+	−	+	+++	−	−	−	−
5	+	++	+	+++	−	−	+ Foc.	−
6	+ Foc.	+ Foc.	−	−	−	−	−	−
7	+ Foc.	+ Foc.	−	−	−	−	−	−

Foc. = < 50 % cells staining, − = negative, + = weak positivity, ++ = moderate positivity, +++ = strong positivity

intracytoplasmic in six cases, extracellular (intraluminal or in the stroma) in four cases. The interstitial myxoid changes were exclusively found in the core of papillae. Areas with diffuse myxoid changes which are seen in MTS RCC were absent. In five cases, we found cells with signet-ring morphology. Signet-ring cells are tumor cells with intracytoplasmic mucin that displaces the nucleus and their presence favors a diagnosis of signet-ring cell carcinoma regardless of site [26]. In two of our cases, mucicarmine or PAS-positive cells with signet-ring morphology were found which we considered as signet-ring cells. In three other cases, the cells with signet-ring morphology were negative for mucicarmine and PAS.

In the differential diagnosis of MTS RCC, several entities should be considered.

1. Hereditary leiomyomatosis renal cell carcinoma syndrome-associated renal cell carcinoma (HLRCC) arises in patients with a germline mutation in the fumarate hydratase (FH) gene. These tumors often have a papillary architecture but can be tubulopapillary, cribriform, or solid [22]. Even though the morphology of our tumors was not entirely compatible with HLRCC, we tested four cases for FH gene mutation but all of them showed a wild type FH gene.
2. Val-Bernal described a case of RO, composed of typical oncocytes in a predominantly tubular pattern and scattered tubules containing basophilic mucin (positive with Alcian blue at pH 2.5 and Mayer's mucicarmin), in the lumen but not intracytoplasmic. Immunohistochemistry was not reported. Tumor cells did not show gain of chromosomes 7 and 17 [6]. Our cases differed from RO in terms of morphology and marker profile, being mostly papillary and with expression of different markers. Chromosomal analysis with polysomy of chromosomes 7 and 17 supports our diagnosis of RCC. An oncocytic variant of PRCC has been reported but with morphologic characteristics different from our cases.
3. Val-Bernal also reported extracellular mucin within alveoli in CCRCC but only occasionally in the cytoplasm of neoplastic cells [24]. The mucin stained with Mayer's mucicarmine, Alcian blue-PAS (at pH 2.5), and Mowry's colloidal iron. Staining with Alcian blue at pH 0.4 indicated the presence of strongly acidic sulphated mucosubstances [5]. Our cases showed characteristic papillary architecture without clear cell elements. The marker profile was typical of PRCC only in four cases, with coexpression of vimentin and AMACR even in CK 7-negative tumors. Moreover, VHL was not mutated and its promoter not methylated. LOH of 3p was observed in one out of five analyzable cases. The latter case showed polysomy of chromosomes 7 and 17 and an unusual XXY pattern of sex chromosomes.

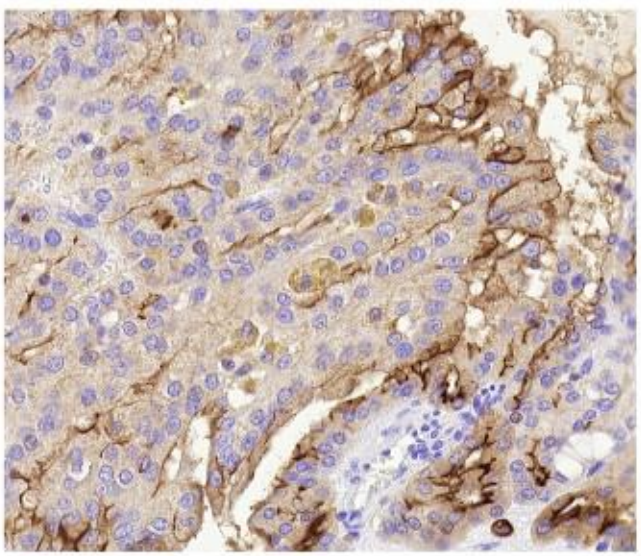

Fig. 9 MUC 1 was diffusely strongly positive in two cases and focally in three cases

Mucin/mucin-like secretion along with papillary architecture is more common in urothelial carcinomas (UC). Primary adenocarcinoma, UC with signet-ring cells, UC with gland-like lumina, and colonic types (villous

Table 5 Results of molecular genetic analyses

Case	Array CGH	LOH3p	TFE3F	TFEBF	VHL	VHLM	FISH 7	FISH16	FISH17	FISH Y	FH
1	NA	−	−	NA	−	−	D	−	D	XY	−
2	+7, +16, +17, −Y	−	−	NA	−	−	P	P	P	−Y	−
3	NA	NP	−	NA	−	−	NA	NA	NA	−Y	NA
4	NA	−	−	−	−	−	D	NA	P	−Y	−
5	NA	+	NA	NA	−	−	P	NA	P	XXY	NA
6	NA	−	NA	NA	−	−	NA	NA	NA	−Y	−
7	NA	NA	NA	NA	NA	NA	NA	NA	NA	NA	NA

− = negative, + = positive, NA not analyzable, NP not performed, −Y loss of chromosome Y, VHL VHL mutation, VHLM VHL methylation, FH fumarate hydratase gene mutation, P polysomy, D disomy

adenomas, villous carcinomas) are not extremely rare subtypes, and several reports have been published of such tumors in the whole urinary tract [27] [28]. Morphology of UC can be polymorphic and histochemical features and marker profile may vary. Glandular differentiation is observed in less than 10 % of urothelial carcinomas, usually in the form of small tubular or gland-like spaces in conventional urothelial carcinoma [29] [30]. Less frequently, foci similar to colonic-type adenocarcinoma can be found in otherwise typical UC and, rarely, a signet-ring cell or a mucinous component [31]. Primary adenocarcinoma is extremely rare in the renal pelvis, while at approximately 2 % of primary epithelial malignancies in the urinary bladder [6,8]. This entity includes primary bladder adenocarcinoma (non-urachal adenocarcinoma) and urachal carcinoma. Primary bladder adenocarcinoma develops in transitional epithelium through gradual changes (intestinal metaplasia) initiated by chronic inflammation [32]. Urachal carcinoma is less common than non-urachal adenocarcinoma of the bladder and arises from urachal remnants [10] [33]. Colonic-type villous adenoma and adenocarcinoma of the urinary tract are rare. Villous adenoma is characterized by papillary structures covered by columnar mucinous epithelium, as in colonic villous adenoma. Often an infiltrating adenocarcinoma coexists, which emphasizes the need to adequate sampling of any lesion diagnosed by biopsy as villous adenoma [28]. Our cases were located in the renal cortex or paracortex, without any connection with pelvic-calyceal system. No signs of urothelial differentiation were found, marker pattern was also unlike UC. One case was focally positive for CK 20 but not for CK 7.

The patient of case 7 died of metastatic colorectal carcinoma. In this case, the architecture of renal tumor was papillary, without tubules or dirty necrosis. Although the renal tumor was focally positive for CK 20, it also expressed vimentin and AMACR, which would be extremely unusual for metastasis of colorectal adenocarcinoma.

Conclusions

1. PRCCs with mucin/mucin-like secretion are rare (<0.5 % of all PRCC), and defining their morphology, immunohistochemical, and molecular genetic profile remains a challenge.
2. Mucicarmine-positive secretion does not rule out a diagnosis of PRCC.
3. A genuine mucin nature of the secreted material still needs to be confirmed by immunohistochemical analysis. Whether what is secreted in these PRCC cases is mucin or mucin-like remains to be clarified.
4. In the differential diagnosis of RCC with mucin/mucin-like secretion, in addition to tumors originating in renal parenchyma, also, lesions of urothelial origin should be considered, as they are more often mucicarmine positive.
5. PRCCs with mucin/mucin-like secretion have metastatic potential.

Acknowledgments The authors thank Dr. Ivan Damjanov for his help with the editing of our paper and for the constructive discussion.

Compliance with ethical standards The study was approved by local Ethics Committee (Medical Teaching Hospital and Medical School of Charles University in Plzen).

Funding The study was supported by the Charles University Research Fund (project number P36), by the project CZ.1.05/2.1.00/03.0076 from European Regional Development Fund, and by SVV 260283.

Conflict of interest The authors declare no conflict of interest.

References

1. Hes O, Hora M, Perez-Montiel DM, Suster S, Curik R, Sokol L, Ondic O, Mikulastik J, Betlach J, Peychl L, Hrabal P, Kodet R, Straka L, Ferak I, Vrabec V, Michal M (2002) Spindle and cuboidal renal cell carcinoma, a tumour having frequent association with nephrolithiasis: report of 11 cases including a case with hybrid conventional renal cell carcinoma/spindle and cuboidal renal cell carcinoma components. Histopathology 41:549–555

2. Val-Bernal JF, Gomez-Roman JJ, Vallina T, Villoria F, Mayorga M, Garcia-Arranz P (1999) Papillary (chromophil) renal cell carcinoma with mucinous secretion. Pathol Res Pract 195:11–17
3. Val-Bernal JF, Mayorga M, Garcia-Arranz P, Gomez-Roman JJ (1998) Mucin secretion in papillary (chromophil) renal cell carcinoma. Am J Surg Pathol 22:1037–1040
4. Val-Bernal JF, Pinto J, Gomez-Roman JJ, Mayorga M, Villoria F (2001) Papillary adenoma of the kidney with mucinous secretion. Histol Histopathol 16:387–392
5. Val-Bernal JF, Salcedo W, Val D, Parra A, Garijo MF (2013) Mucin-secreting clear cell renal cell carcinoma. A rare variant of conventional renal cell carcinoma. Ann Diagn Pathol 17:226–229
6. Val-Bernal JF, Val D, Garijo MF (2011) Mucin-producing renal oncocytoma. An undescribed variant of oncocytoma. Pathol Res Pract 207:271–274
7. A Renshaw, Fine needle aspiration of the kidney, In: Bostwick D, Cheng L. (eds) Urologic Surgical Pathology (2st ed), (2008) 196–213.
8. van Dongen JJ, Langerak AW, Bruggemann M, Evans PA, Hummel M, Lavender FL, Delabesse E, Davi F, Schuuring E, Garcia-Sanz R, van Krieken JH, Droese J, Gonzalez D, Bastard C, White HE, Spaargaren M, Gonzalez M, Parreira A, Smith JL, Morgan GJ, Kneba M, Macintyre EA (2003) Design and standardization of PCR primers and protocols for detection of clonal immunoglobulin and T-cell receptor gene recombinations in suspect lymphoproliferations: report of the BIOMED-2 Concerted Action BMH4-CT98–3936. Leukemia 17:2257–2317
9. Sperga M, Martinek P, Vanecek T, Grossmann P, Bauleth K, Perez-Montiel D, Alvarado-Cabrero I, Nevidovska K, Lietuvietis V, Hora M, Michal M, Petersson F, Kuroda N, Suster S, Branzovsky J, Hes O (2013) Chromophobe renal cell carcinoma–chromosomal aberration variability and its relation to Paner grading system: an array CGH and FISH analysis of 37 cases. Virchows Archiv: Int J Pathol 463:563–573
10. Gopalan A, Sharp DS, Fine SW, Tickoo SK, Herr HW, Reuter VE, Olgac S (2009) Urachal carcinoma: a clinicopathologic analysis of 24 cases with outcome correlation. Am J Surg Pathol 33:659–668
11. Foster EA, Levine AJ (1963) Mucin production in metastatic carcinomas. Cancer 16:506–509
12. Grignon DJ, Ro JY, Ayala AG (1988) Primary mucin-secreting adenocarcinoma of the kidney. Archiv Pathol Laboratory Med 112:847–849
13. Fowler J, Vinall L, Swallow D (2001) Polymorphism of the human muc genes. Front Biosci J Virtual Library 6:D1207–D1215
14. Lauren PA, Sorvari TE (1969) The histochemical specificity of mucicarmine staining in the identification of epithelial mucosubstances. Acta Histochem 34:263–272
15. Gum JR Jr, Hicks JW, Toribara NW, Siddiki B, Kim YS (1994) Molecular cloning of human intestinal mucin (MUC2) cDNA. Identification of the amino terminus and overall sequence similarity to prepro-von Willebrand factor. J Biol Chem 269:2440–2446
16. Jonckheere N, Van Seuningen I (2010) The membrane-bound mucins: from cell signalling to transcriptional regulation and expression in epithelial cancers. Biochimie 92:1–11
17. Ho SB, Shekels LL, Toribara NW, Kim YS, Lyftogt C, Cherwitz DL, Niehans GA (1995) Mucin gene expression in normal, preneoplastic, and neoplastic human gastric epithelium. Cancer Res 55:2681–2690
18. Cao Y, Karsten U, Zerban H, Bannasch P (2000) Expression of MUC1, Thomsen-Friedenreich-related antigens, and cytokeratin 19 in human renal cell carcinomas and tubular clear cell lesions. Virchows Archiv Int J Pathol 436:119–126
19. Kraus S, Abel PD, Nachtmann C, Linsenmann HJ, Weidner W, Stamp GW, Chaudhary KS, Mitchell SE, Franke FE, el Lalani N (2002) MUC1 mucin and trefoil factor 1 protein expression in renal cell carcinoma: correlation with prognosis. Human Pathol 33:60–67.
20. Leroy X, Copin MC, Devisme L, Buisine MP, Aubert JP, Gosselin B, Porchet N (2002) Expression of human mucin genes in normal kidney and renal cell carcinoma. Histopathology 40:450–457
21. Leroy X, Zini L, Leteurtre E, Zerimech F, Porchet N, Aubert JP, Gosselin B, Copin MC (2002) Morphologic subtyping of papillary renal cell carcinoma: correlation with prognosis and differential expression of MUC1 between the two subtypes. Modern Pathol Off J United States Canadian Acad Pathol Inc 15:1126–1130
22. Srigley JR, Delahunt B, Eble JN, Egevad L, Epstein JI, Grignon D, Hes O, Moch H, Montironi R, Tickoo SK, Zhou M, Argani P, Panel IRT (2013) The International Society of Urological Pathology (ISUP) Vancouver Classification of renal Neoplasia. Am J Surg Pathol 37:1469–1489
23. Peckova K, Martinek P, Sperga M, Montiel DP, Daum O, Rotterova P, Kalusova K, Hora M, Pivovarcikova K, Rychly B, Vranic S, Davidson W, Vodicka J, Dubova M, Michal M, Hes O (2015) Mucinous spindle and tubular renal cell carcinoma: analysis of chromosomal aberration pattern of low-grade, high-grade, and overlapping morphologic variant with papillary renal cell carcinoma. Ann Diagn Pathol 19:226–231
24. Fine SW, Argani P, DeMarzo AM, Delahunt B, Sebo TJ, Reuter VE, Epstein JI (2006) Expanding the histologic spectrum of mucinous tubular and spindle cell carcinoma of the kidney. Am J Surg Pathol 30:1554–1560
25. Delahunt B, Eble JN (1997) Papillary renal cell carcinoma: a clinicopathologic and immunohistochemical study of 105 tumors. Modern Pathol Off J United States and Canadian Acad Pathol Inc 10:537–544
26. Sung CO, Seo JW, Kim KM, Do IG, Kim SW, Park CK (2008) Clinical significance of signet-ring cells in colorectal mucinous adenocarcinoma. Modern Pathol Off J United States and Canadian Acad Pathol Inc 21:1533–1541
27. Alvarado-Cabrero D, Perez-Montiel O (2008) Hes, Multicystic urothelial carcinoma of the bladder with gland-like lumina and with signet-ring cells. A case report. Diagn Pathol 3:36
28. Seibel JL, Prasad S, Weiss RE, Bancila E, Epstein JI (2002) Villous adenoma of the urinary tract: a lesion frequently associated with malignancy. Hum Pathol 33:236–241
29. Lopez-Beltran L (2006) Cheng, histologic variants of urothelial carcinoma: differential diagnosis and clinical implications. Hum Pathol 37:1371–1388
30. Black PC, Brown GA, Dinney CP (2009) The impact of variant histology on the outcome of bladder cancer treated with curative intent. Urol Oncol 27:3–7
31. Amin MB (2009) Histological variants of urothelial carcinoma: diagnostic, therapeutic and prognostic implications. Modern Pathol Off J United States and Canadian Acad Pathol Inc 22(Suppl 2):S96–S118
32. Thomas DG, Ward AM, Williams JL (1971) A study of 52 cases of adenocarcinoma of the bladder. Br J Urol 43:4–15
33. Paner GP, Barkan GA, Mehta V, Sirintrapun SJ, Tsuzuki T, Sebo TJ, Jimenez RE (2012) Urachal carcinomas of the nonglandular type: salient features and considerations in pathologic diagnosis. Am J Surg Pathol 36:432–442

3.2 Warthin-like papillary renal cell carcinoma: Clinicopathologic, morphologic, immunohistochemical and molecular genetic analysis of 11 cases

Poslední WHO klasifikace renálních neoplásií (z roku 2016) již oproti dřívějším poznatkům oficiálně připouští onkocytický PRCC jako možnou novou variantu PRCC. Morfologicky se tyto nádory vyznačují papilárním uspořádáním, kde papily jsou lemovány jednou vrstvou eosinofilních buněk s lineárně uspořádanými "onkocytoma-like" jadérky.

V této práci bylo 11 onkocytických PRCC s prominentním lymfocytárním infiltrátem, připomínajícím svým morfologickým vzhledem Warthinův tumor slinné žlázy, posuzováno klinickopatologicky, morfologicky, imunohistochemicky a molekulárně-geneticky. Predominantně se jednalo o tumory mužů (8/11, 73%), průměrný věk pacientů se pohyboval v rozmezí 14-76 let (průměr 59 let), maximální rozměr tumoru byl v rozmezí 1-22 cm (průměr 7 cm). Všechny tumory se vyznačovaly vzhledem typickým pro onkocytický PRCC, s predominantně papilárním typem růstu (papilární struktury představovaly více než 60% z celkového objemu nádoru), u všech nádorů byl přítomen nápadný denzní lymfocytární stromální infiltrát, u 8/11 neoplásií byla fokálně zastižena přítomnost pseudostratifikace. Přítomnost tubulární či solidní komponenty byla zaznamenána u pěti, respektive tří případů zahrnutých do této studie. V nádorech zastižená populace tumor infiltrujících lymfocytů (TILs) byla tvořena B- i T-lymfocyty. Nádorové struktury vykazovaly uniformní pozitivitu v imunohistochemickém průkazu AMACR, PAX8, MIA, vimentinu a cytokeratinu OSCAR. Naopak negativní byla většina nádorů v imunohistochemickém barvení CA-IX, CD117, CK20 a TTF-1. Imunohistochemické vyšetření MMR proteinů (status DNA mismatch repair proteinů) prokázalo zachovanou expresi MLH1 a PMS2 u všech tumorů, ztráta exprese MSH2 a MSH6 byla zastižena v jednom případě. Numerický status chromosomů prokázal variace v 5 případech (od ztráty jediného chromosomu až po komplexní genomovou alteraci). Pouze u jediného případu byla prokázána polysomie chromosomů 7 a 17 (mimo jiné aberace přítomné u tohoto případu). Ve čtyřech případech nebyly za pomoci molekulárně genetických metod detekovány žádné numerické chromozomální aberace. Data o průběhu další dispenzarizace byla dostupná u devíti pacientů (v délce trvání 1-132 měsíců, průměr 47,6 měsíce). Tři pacienti zemřeli na následky generalizace, u šesti pacientů bylo zaznamenáno metastatické chování, prozatím bez letální progrese.

Warthin-like PRCC je subtypem PRCC morfologicky velmi blízkým onkocytickému PRCC, od kterého se liší přítomností denzního lymfoidního stromatu. Numerický chromozomální status je u těchto nádorů velmi různorodý, pouze u jednoho z nádorů byl prokázán zisk chromosomů 7 a 17 (tedy numerický chromosomální status typicky přisuzovaný PRCC). Warthin-like PRCC je nádor s agresivním chováním a letálním potenciálem, kdy u 3/9 pacientů zahrnutých v této studii byla generalizace tohoto onemocnění příčinou smrti.

Annals of Diagnostic Pathology 27 (2017) 48–56

Contents lists available at ScienceDirect

Annals of Diagnostic Pathology

Warthin-like papillary renal cell carcinoma: Clinicopathologic, morphologic, immunohistochemical and molecular genetic analysis of 11 cases☆

Faruk Skenderi [a], Monika Ulamec [b], Tomas Vanecek [c], Petr Martinek [c], Reza Alaghehbandan [d], Maria Pane Foix [e], Iva Babankova [f], Delia Perez Montiel [g], Isabel Alvarado-Cabrero [h], Marian Svajdler [c], Pavol Dubinský [i], Dana Cempirkova [j], Michal Pavlovsky [k], Semir Vranic [a], Ondrej Daum [c], Ondrej Ondic [c], Kristyna Pivovarcikova [c], Kvetoslava Michalova [c], Milan Hora [l], Pavla Rotterova [m], Adela Stehlikova [c], Martin Dusek [c], Michal Michal [c], Ondrej Hes [c,□]

[a] Department of Pathology, University of Sarajevo Clinical Center, Sarajevo, Bosnia and Herzegovina
[b] "Ljudevit Jurak" Pathology Department, Clinical Hospital Center "Sestre milosrdnice", Zagreb, Croatia
[c] Department of Pathology, Charles University, Medical Faculty and Charles University Hospital Plzen, Czech Republic
[d] Department of Pathology, University of British Columbia, Royal Columbian Hospital, Vancouver, BC, Canada
[e] Department of Pathology, Bellvitge University Hospital, Barcelona, Spain
[f] Department of Pathology, Masaryk's Oncologic Institute, University Hospital Brno, Czech Republic
[g] Department of Pathology, Instituto Nacional de Cancerologia, Mexico City, Mexico
[h] Department of Pathology, Centro Medico, Mexico City, Mexico
[i] Department of Radiation Oncology, Oncology Institute, Kosice, Slovakia
[j] Department Pathology, Regional Hospital Jindrichuv Hradec, Czech Republic
[k] Department Pathology, Regional Hospital Most, Czech Republic
[l] Department of Urology, Charles University, Medical Faculty and Charles University Hospital Plzen, Czech Republic
[m] Biopticka Laboratory, Pilsen, Czech Republic

article info

Keywords:
Kidney
Oncocytic papillary renal cell carcinoma
Warthin's tumor
Warthin-like
Lymphoid stroma
Immunohistochemistry
Chromosomal aberration pattern

abstract

Oncocytic papillary renal cell carcinoma (PRCC) is a distinct subtype of PRCC, listed as a possible new variant of PRCC in the 2016 WHO classification. It is composed of papillae aligned by large single-layered eosinophilic cells showing linearly arranged oncocytoma-like nuclei.

We analyzed clinicopathologic, morphologic, immunohistochemical and molecular-genetic characteristics of 11 oncocytic PRCCs with prominent tumor lymphocytic infiltrate, morphologically resembling Warthin's tumor.

The patients were predominantly males (8/11, 73%), with an average age of 59 years (range 14–76), and a mean tumor size of 7 cm (range 1–22 cm). Tumors had the features of oncocytic PRCCs with focal pseudostratification in 8/11 cases and showed dense stromal inflammatory infiltration in all cases. Papillary growth pattern was predominant, comprising more than 60% of tumor volume. Tubular and solid components were present in 5 and 3 cases, respectively. Uniform immunohistochemical positivity was found for AMACR, PAX-8, MIA, vimentin, and OSCAR. Tumors were mostly negative for carboanhydrase 9, CD117, CK20, and TTF-1. Immunohistochemical stains for DNA mismatch repair proteins MLH1 and PMS2 were retained in all cases, while MSH2 and MSH6 were negative in 1 case. Tumor infiltrating lymphocytes (TILs) consisted of both B and T cells. Chromosomal copy number variation analysis showed great variability in 5 cases, ranging from a loss of one single chromosome to complex genome rearrangements. Only one case showed gains of chromosomes 7 and 17, among other aberrations. In 4 cases no numerical imbalance was found. Follow up data was available for 9 patients (median 47.6 months, range 1–132). In 6 patients no lethal progression was noted, while 3 died of disease.

In conclusion, Warthin-like PRCC is morphologically very close to oncocytic PRCC, from which it differs by the presence of dense lymphoid stroma. Chromosomal numerical aberration pattern of these tumors is variable;

☆ The study was supported by the Charles University Research Fund (project number P36) and by the grant of Ministry of Health of the Czech Republic - Conceptual Development of Research Organization (Faculty Hospital in Pilsen – FN Pl, 00669806).
□ Corresponding author at: Department of Pathology, Charles University, Medical Faculty and Charles University Hospital Plzen, Alej Svobody 80, 304 60 Pilsen, Czech Republic.
E-mail address: hes@medima.cz (O. Hes).

http://dx.doi.org/10.1016/j.anndiagpath.2017.01.005

only one case showed gains of chromosomes 7 and 17. Warthin-like PRCC is a potentially aggressive tumor since a lethal outcome was recorded in 3/9 cases.

1. Introduction

Renal cell carcinoma (RCC) is a highly heterogeneous group of tumors, consisting of at least 14 subtypes recognized in the latest WHO classification, and several additional tentatively distinct variants [1-3]. The subgroup of papillary renal cell carcinoma (PRCC) is further divided into type 1 and 2. Recently, a number of studies have described a small series of morphologically distinctive PRCCs, such as oncocytic, solid, biphasic squamoid alveolar, “mucin”-secreting, or clear cell types, not belonging to any of the two main types [4-9]. These tumors may be associated with foci of type 2-resembling areas and are thus often designated as such, which may contribute to the molecular-genetic heterogeneity of PRCC type 2 tumors [10]. Some of these tumors are even designated as unclassified [11]. Even though the tumor stage remains the best determinant for the survival of patients after nephron sparing surgery within the PRCC group [12], the histological variants of PRCC are important to recognize. This is due to the fact that the papillary morphology is also seen in other RCC subtypes, and thus the treatment and outcome may significantly differ in patients with variant tumors as compared with those who have two classical forms of PRCC.

Oncocytic PRCC [4,13,14] is mentioned in the 2016 WHO classification as a tumor that has a papillary architecture, and is composed of large cells with finely granular eosinophilic cytoplasm, mostly single-layered, and linearly aligned oncocytoma-like nuclei [3]. Such morphology, with addition of a prominent lymphocytic infiltrate in stroma, may commonly be seen in the papillary cystadenoma lymphomatosum (Warthin's tumor) of the salivary glands. To the best of our knowledge, carcinomas resembling benign Warthin's tumor have been described in salivary glands [15] and thyroid [16], but not in the kidney. Tumor infiltrating lymphocytes (TILs) may have prognostic value and that with the advent of novel immune mediated therapies [17], tumors with TILs could be considered for potential immunotherapy in the future. Of note, lymphoid infiltrates are frequently found in tumors of other organs associated with Lynch syndrome. However, a potential link between this hereditary syndrome and lymphoid infiltrates in some renal tumors has not been explored.

The aim of this study was to analyze the clinicopathologic, morphologic, immunohistochemical and molecular-genetic characteristics of 11 oncocytic PRCCs with prominent lymphoid stroma (Warthin-like papillary renal cell carcinoma - WPRCC), morphologically reminiscent of Warthin's tumor.

2. Materials and methods

2.1. Case selection and routine microscopy

There were 1147 in-house and consultation cases of PRCC in Plzen Tumor Registry. We searched the database for keywords “oncocytic, papillary, kidney, lymphoid stroma”, and reviewed 147 tumors. We subsequently selected 11 cases with predominant oncocytic cytology and abundant intratumoral lymphocytic infiltrate. All the cases were reviewed by three pathologists (FS, MU, OH). There were 1–10 tissue blocks available for each case, and 1–2 representative blocks were selected for immunohistochemical and molecular–genetic studies. Clinical, gross and follow-up data were collected by review of the institutional medical records and by contacting the consulting pathologists.

Tissue for light microscopy was fixed in 4% formaldehyde, embedded in paraffin using routine procedures. 5 μm thin sections were cut and stained with hematoxylin and eosin. Special stain technique for evaluation of mucin was performed using mucicarmine, periodic acid - Schiff (PAS) and alcian blue at pH 2.5. We evaluated percentages of papillary, tubular, cystic, and solid architectural patterns, abundance of TIL with reference to index case, nuclear grade according to the guidelines of ISUP (International Society of Urologic Pathology), nuclear pseudostratification, single versus multiple cell layers forming papillae, presence of foamy macrophages, and microscopic necrosis.

2.2. Immunohistochemistry

Immunohistochemical study was performed using primary antibodies recognizing following antigens: racemase/AMACR (13H4, monoclonal, Dako, Glostrup, Denmark, 1:200), carbonic anhydrase IX (rhCA9, monoclonal, RD systems, Abingdon, GB, 1:100), vimentin (D9, monoclonal, NeoMarkers, Westinghouse, CA, 1:1000), OSCAR (OSCAR, monoclonal, Covance-SpinChem, San Diego, CA, 1:500), PAX-8 (polyclonal, Cell Marque, Rocklin, CA, 1:25), cytokeratin 7 (OV-TL12/30, monoclonal, Dako, 1:200), cytokeratin 20 (M7019, monoclonal, Dako, 1:100), cytokeratins (AE1-AE3, monoclonal, BioGenex, San Ramon, CA, 1:1000), CD117 (CD117, polyclonal; Dako, Glostrup, Denmark; RTU), EMA (E29, monoclonal; DakoCytomation, Carpinteria, CA; 1:1000), CD10 (56C6, monoclonal; Novocastra, Newcastle upon Tyne, UK; 1:50), TTF-1 (SPT24, monoclonal; Novocastra, 1:400), anti-mitochondrial antigen (MIA, monoclonal; BioGenex; 1:100), CD3 (monoclonal, LN10, Novocastra, 1:50), CD5 (monoclonal, 4C7, Novocastra, 1:50), CD20 (monoclonal, L26, DakoCytomation, RTU), MSH2 (monoclonal, G219-1129, Cell Marque, RTU), MSH6 (monoclonal, 44, Ventana, Manheim, Germany, RTU), PMS2 (monoclonal, EPR 3947, Cell Marque, RTU), MLH1 (monoclonal, G168-728, Cell Marque, RTU). The primary antibodies were visualized using the supersensitive streptavidin-biotin-peroxidase complex (BioGenex). Appropriate positive controls were employed for all assays. Immunohistochemical staining was recorded negative if no staining, or less than 5% of staining was observed; as weak (+) for staining of up to 25% of tumor cells; moderate (++) for staining 25–50% of tumor cells; and strong (+++) for staining in more than 50% of tumor cells.

2.3. DNA extraction

DNA was extracted using the QIAsymphony DSP DNA Mini Kit on automated extraction system QIAsymphony SP (QIAGEN, Hilden, Germany) according to the manufacturer's supplementary protocol for FFPE samples. Concentration and purity of isolated DNA were measured using the NanoDrop ND-1000 (NanoDrop Technologies, Inc., Wilmington, DE, USA). DNA integrity was examined by multiplex PCR amplification of five fragments of lengths ranging from 100 to 600 base pairs (bp) [18].

2.4. Low pass whole genome analysis

All samples were tested for copy number variations (CNV) in all chromosomes using low pass whole genome sequencing on Ion Torrent PGM platform using kits and software from Life Technologies (Thermo Fisher Scientific, Waltham, MA USA). The extracted DNA (100 ng) was enzymatically fragmented using a shear enzyme mix contained in Ion Xpress Plus Fragment Library Kit. Samples with DNA integrity control result of 600 bp were sheared 10 min, and samples with lower integrity were sheared 5 min. Sequencing adapters were ligated and the sequencing library was size-selected for 200 bp. Final libraries were

Table 1
Clinicopathological data on Warthin-like papillary renal cell carcinoma.

Case No.	Age	Sex	Size (cm)	TNM stage	Follow-up (months)
Case 1	48	M	1.0[a]	–	DUD 1 months, autopsy, no generalization
Case 2	64	M	6.0	pT3	DOD 9 m, generalization, retroperitoneal lymph nodes, liver, lung, bones
Case 3	69	F	3.0	pT1	AW 12
Case 4	76	M	22[b]	pT3	DOD 12
Case 5	45	M	2.8	pT1	AW 108, then LFU
Case 6	64	M	14.5	pT2	LFU
Case 7	14	M	12.5	pT2	DOD 36
Case 8	NA	M	NA	NA	LFU
Case 9	59	M	2.5	pT1	AW 108
Case 10	74	F	4.2	pT1	AW 132
Case 11	75	F	1.5	pT1	AW 10

DUD = death of unrelated disease.
DOD = death of disease.
AW = alive and well.
LFU = lost to follow up.
NA = not available.
[a]Associated with renal oncocytoma 3.0 cm.
[b]Sarcomatoid component.

pooled and templating and enrichment steps were performed using Hi-Q Template OT2 200 Kit. Sequencing was performed on a 316v2 chip using Hi-Q Sequencing kit according to manufacturer's protocols aiming to obtain minimum of 100 000 reads per sample. Signal processing, mapping and quality control was performed with Torrent Suite v.5.0. CNVs were called and visualized using Ion Reporter v5.2 using low-pass whole-genome aneuploidy workflow. The Median of the Absolute values of all Pairwise Differences (MAPD) score filter was set to 0.3. The called CNVs passing the confidence filter (≥ 1) were annotated using ISCN cytogenetic coordinates and sequence positions using Hg19 genome assembly and reported in the Table 4. The aneuploidies of gonosomes were adjusted manually regarding the sex of the patient. For each sample several detected CNVs were confirmed by FISH using enumeration probes as described elsewhere [19].

2.5. Mutation analysis of MLH1, MSH2 and MSH6 genes

Mutation analysis of the MLH1, MSH2 and MSH6 genes was performed using PCR and Sanger sequencing as previously described in Kacerovska et al. 2016 [20]. Whole coding sequences (including exon-intron junctions) of the MLH1, MSH2 and MSH6 genes were obtained and compared to the appropriate reference sequences.

2.6. Microsatellite instability (MSI) analysis

Five mononucleotide markers (BAT-25, BAT-26, NR-21, NR-24, and MONO-27) were analyzed using the “MSI Analysis System” kit (Promega, Madison, WI) according to the manufacturer's instructions. The PCR products were separated by capillary electrophoresis using ABI 3130XL Genetic Analyzer (Applied Biosystems), and the output data were analyzed with GeneMapper software (Applied Biosystems).

2.7. MLH1 promoter methylation analysis

To perform methylation analysis, the bisulfite conversion (“EZ DNA Methylation-Gold Kit;” Zymo Research, Burlington, ON, Canada) was followed by the methylation-specific PCR targeting the MLH1 promoter according to Chan et al. [21].

2.8. BRAF V600E mutation analysis

Presence of the BRAF V600E mutation status was tested using the real-time PCR kit Cobas® 4800 BRAF V600 Mutation Test (Roche; Mannheim, Germany) according to the manufacturer's instructions.

3. Results

3.1. Clinicopathologic data

Clinical and pathologic data were available for 10 of 11 cases and are summarized in Tables 1 and 2. The patients were predominantly males (73%) with male to female ratio of 3:1. Average age was 59 years (range 14–76). One half of all tumors were at pT1 stage. The mean size of tumors was 7 cm (range 1–22 cm).

Table 2
Morphological data on Warthin-like papillary renal cell carcinoma.

Case No.	ISUP grade	Foamy macrophages	Architectural pattern[a]	TIL abundance[b]	Cell layers	Nuclear pseudostr.[c]	Necrosis
Case 1	2	+	P	++	SI	+	−
Case 2	2	−	S/P/T	+++	MU	−	+++
Case 3	2	−	P/T	+++	SI	+	+
Case 4	4	−	P	+++	SI	+	+
Case 5	3	−	P	++	SI	+++	−
Case 6	2	−	T	++	SI	+	−
Case 7	3	−	P/T	++	SI	++	−
Case 8	2	+	S/P	++	MU	−	−
Case 9	3	−	P/S	+++	SI	+	+
Case 10	2	+	S/TA	++	SI	+	−
Case 11	2	−	P	+++	SI	−	−

SI – single cell layer; MU – multiple cell layers.
[a]Architectural pattern: P-papillary, S-solid, T-tubular.
[b]TIL - tumor infiltrating lymphocytes: abundance was assessed both on HE and CD3, CD5, and CD20 stained slides, in reference to index case which was designated as +++.
[c]Nuclear pseudostratification was assessed as negative (−), sparse (+), moderate (++), prominent (+++), in reference to index case.

Fig. 1. On cross section the tumors were mostly brown to grey, compact, and well-circumscribed.

In cases when gross description was available (8 of 11 cases), the tumors were brown to grey, compact, and well-circumscribed (Fig. 1). Grossly visible necroses or hemorrhages were not reported.

Follow up information was available for 9/11 patients. Follow up period ranged from 1 to 132 months (median range 47.6 months). In 6 patients, there were no records about aggressive behavior or disease progression. However, 3 patients died of disease 9–36 months after resection. Metastatic spreading was documented to lymph nodes, liver, lung and bones. Sarcomatoid tumor differentiation was present in one case with a lethal outcome.

3.2. Morphologic characteristics

Basic morphologic characteristics are summarized in Table 2. Most of the tumors showed papillary growth pattern in more than 60% of tumor volume (Fig. 2). However, tubular and solid/compressed papillary components were also present in smaller volume percentages, in the majority of the cases (Fig. 3). The tumors were composed of medium to large eosinophilic cells, most of them had visible nucleoli at high

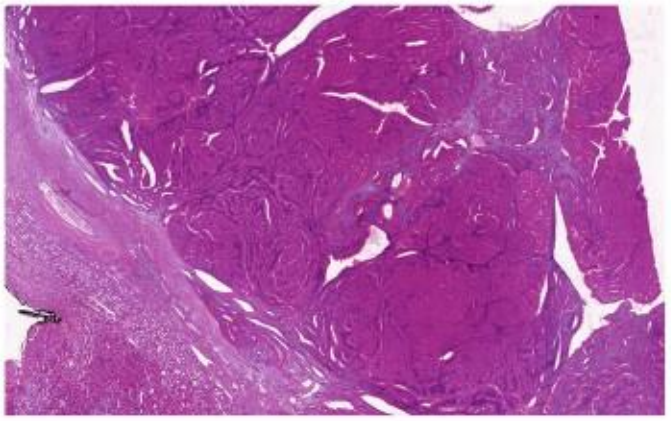

Fig. 3. Tubular and solid components. These were also present in smaller volume percentages in the majority of cases.

magnification, corresponding to ISUP grade 2 (Fig. 4). Two cases were ISUP grade 3 and one was grade 4. Nuclear pseudostratification was present in 8/11 (Fig. 5A), however it was not prominent in the majority of cases (Fig. 5B). Foamy macrophages were seen in 3/11 cases (Fig. 6 and Table 2). Prominent feature in all cases was moderate to strong stromal inflammatory infiltration, predominantly composed of lymphocytes (Fig. 7A and B). The stroma was mostly loose, located within papillary tufts and also in some cases within areas with tubulocystic architecture. Desmoplastic stroma was not seen in any of the cases. Necrotic foci were present in 4/11 cases.

One WPRCC contained in addition to the papillary architecture, oncocytic cells and dense lymphoid stroma, a large component showing nondescript spindle cell sarcomatoid differentiation. Clinically, this tumor had an aggressive course and caused patient's death.

3.3. Immunohistochemical examinations

The results of the immunohistochemistry evaluation are summarized in Table 3. Briefly, the tumor cells were positive for PAX-8 (11/11, 100%), MIA (11/11, 100%) (Fig. 8A and B), vimentin (10/11, 91%) and OSCAR (11/11, 100%); variable for AMACR (10/11, 91%), CK7 (5/11, 54%) (Fig. 9 A + B), EMA (5/11, 45%), CD10 (7/11, 63%), and AE1/3 (4/11, 36%); mostly negative for carboanhydrase 9 (0/11, 0%), CD117

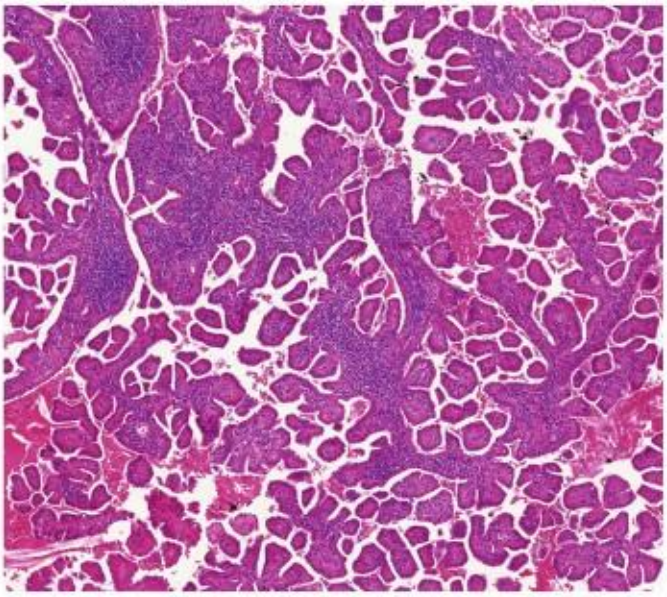

Fig. 2. Papillary growth pattern. It was seen in more than 60% of tumor volume in most tumors.

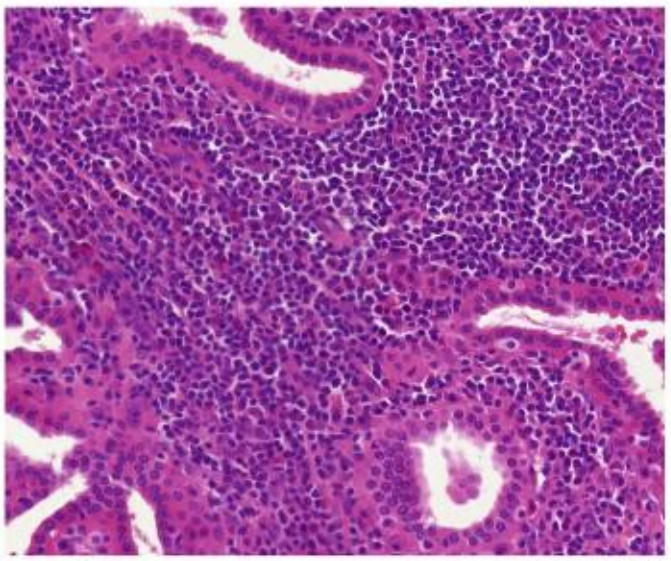

Fig. 4. Medium to large eosinophilic cells. Most of these cells had visible nucleoli at high magnification and corresponded to ISUP grade 2.

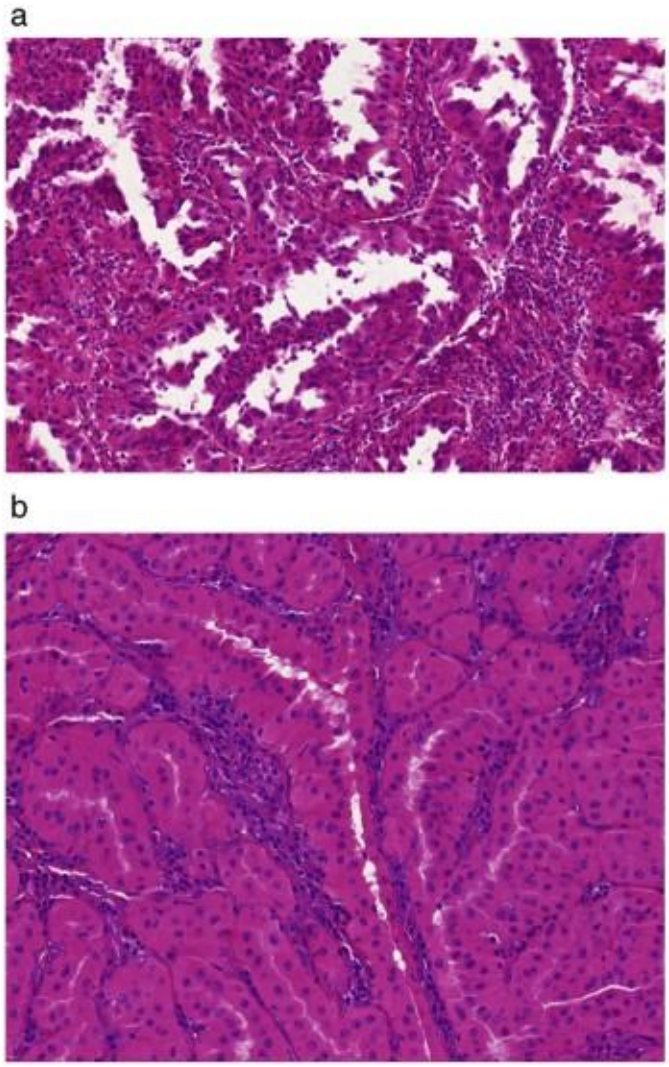

Fig. 5. Nuclear pseudostratification. It was present in 8/11 (A), however it was not prominent in the majority of cases (B).

(0/11, 0%), CK20 (1/11, 9%) and TTF-1 (0/11, 0%). DNA mismatch repair proteins (MLH1, MSH2, MSH6, PMS2) were retained in all cases except one case that exhibited a loss of MSH2 and MSH6 proteins (case no. 4).

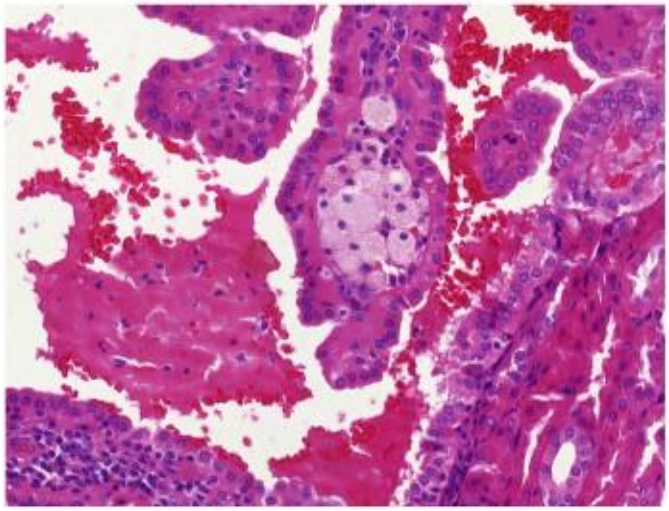

Fig. 6. Foamy macrophages. These cells were seen in 3/11 cases.

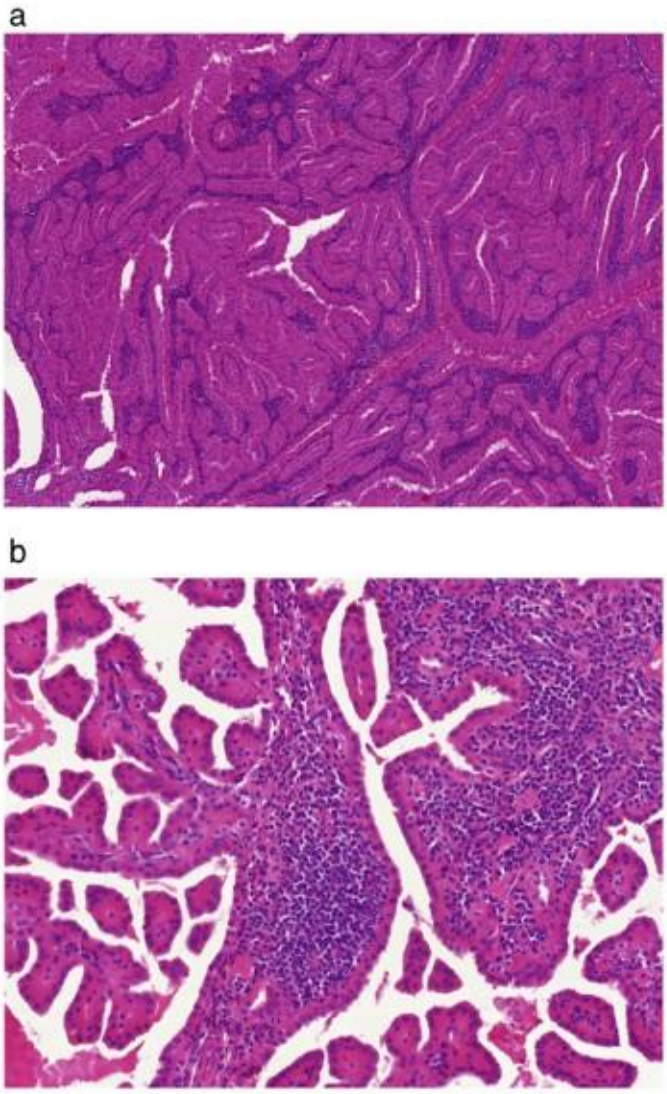

Fig. 7. A + B: lymphoid infiltration of the stroma. Moderate to strong stromal lymphoid infiltration was seen in all tumors.

TILs consisted of both B and T cells, mostly CD5 and CD3 positive, while in two cases CD20 positive lymphocytes were predominant.

3.4. Molecular genetic analysis

Nine cases produced good quality libraries and were successfully sequenced, while the remaining two samples were not analyzable. No CNV were found in four samples. The remaining five samples showed great variability in detected CNV ranging from loss of one chromosome to complex genome rearrangements including gains and losses of various parts of chromosomes as summarized in Table 4 and visualized in Fig. 10. Only one of the cases showed gain of chromosomes 7 and 17 (among the other aberrations). The range and quality of every detected CNV is summarized in Table 5.

Analyses of MMS and BRAF V600E were performed in one case (case 4), due to the loss of immunohistochemical reactivity with MSH2 and MSH6.

In the DNA purified from FFPE sample no microsatellite instability (MSI), no aberrant methylation of MLH1 promoter and no mutations in MLH1, MSH2 and MSH6 genes were found. Also BRAF V600E mutation was absent.

Table 3
Immunohistochemistry profile of Warthin-like papillary renal cell carcinoma.

Case No.	AMACR	PAX-8	Vimentin	MIA	CD10	CD117	CANH9	CK7	CK20	OSCAR	AE1/AE3	EMA	TTF-1	MSH2	MSH6	MLH1	PMS2
Case 1	+++	+++	+++	+++	+	−	−	−	−	+++	−	−	−	+++	+++	+++	+++
Case 2	−	+++	+++	+++	±	−	−	++	−	+++	+++	∓	−	+++	+++	+++	+++
Case 3	+++	+++	+++	+++	++	−	−	+++	−	+++	+++	+++	−	+++	+	+++	+++
Case 4	++	+++	−	+++	++	−	−	+	−	+++	−	+++	−	−	−	+++	+++
Case 5	+++	+++	++	+++	+++	−	−	−	−	+++	−	−	−	+++	+	+++	+++
Case 6	+++	++	+++	+++	++	−	−	−	−	+++	−	−	−	+++	++	+++	+++
Case 7	+++	+++	+++	+++	−	−	−	−	−	+	−	++	−	+++	+++	+++	+++
Case 8	+++	+++	+++	+++	++	−	−	+	−	+++	−	+	−	+++	+++	+++	+++
Case 9	+++	+++	+++	+++	++	−	−	−	+++	+++	−	−	−	+++	+	+++	+++
Case 10	+++	+++	+++	+++	−	−	−	+	−	+	+	−	−	+++	+++	+++	+++
Case 11	++	+++	+++	+++	−	−	−	+++	−	+++	+++	+++	−	+++	+++	+++	+++
	10/11 (91%)	11/11 (100%)	10/11 (91%)	11/11 (100%)	7/11 (63%)	0/11 (0%)	0/11 (0%)	6/11 (54%)	1/11 (9%)	11/11 (100%)	4/11 (36%)	5/11 (45%)	0/11 (0%)	10/11 (91%)	10/11 (91%)	11/11 (100%)	11/11 (100%)

Intensity and percentage of positive tumor cells were scored as: negative (−) if no staining or less than 5% staining was observed; weakly positive (+), if focal positivity seen in up to 25% of tumor cells; moderate (++), if positivity observed in 25–50% of tumor cells; diffuse (+++), if more than 50% of tumor cells positive. AMACR – alpha-methylacyl-CoA racemase; CANH9 – carboanhydrase 9; MIA – antimitochondrial antigen; MSH2, MSH6, PMS2, MLH1 – DNA mismatch repair enzymes/proteins.

4. Discussion

There are ongoing debates over the PRCC classification. Traditionally these carcinomas have been classified morphologically as type 1 and type 2. However, many cases of PRCC show only a part of the diagnostic criteria or overlapping morphology between both of the types. Results of immunohistochemical analyses are also more compact for type 1 PRCC and rather variable for type 2 PRCC [2]. Recent large multicentric studies from The Cancer Genome Atlas group and Marsaud et al. reported the genetic profile of large number of PRCCs and found that type 1 and type 2 are genetically distinct entities, but type 2 tumors may further be genetically subdivided into three groups [10,11].

Herein we report the clinicopathologic, morphological, immunohistochemical and molecular genetic profile of a distinct variant of renal carcinoma, showing predominantly papillary architecture, oncocytic cytology, and abundant tumor infiltrating lymphocytes, resembling benign Warthin's tumors of the parotid gland.

A series of so-called oncocytic PRCC (OPRCC) and several case reports of these tumors were previously published [4,13,22-25]. All of the studies reported similar morphological characteristics of the tumors, which are arranged mostly in papillary, but also tubular and solid architecture, with deeply eosinophilic cells, arranged in a single layer or in multiple layers, in some cases with pseudostratification. Nuclei are described mostly as bland and round, however, tumors with a nuclear grade 3 were also reported. Necrosis is recorded rarely. Foamy macrophages were occasionally present [13,25].

Our cohort of WPRCC was composed of tumors with similar morphology, however there were some substantial differences. The most striking feature was the presence of dense lymphocytic infiltration of the stroma within core of the papillae or stroma interspersed among tubular component. OPRCC are described mostly as tumors without pseudostratification [25,26], however this feature is mentioned in some papers [4,25]. In WPRCC series nuclear pseudostratification was detected in 8 cases, whereas in 2 cases was prominent and in 6 cases focal.

An interesting finding in our study was that of 10 cases with available follow-up data, 3 had an aggressive clinical course. Furthermore, one tumor with characteristic morphology (papillary architecture, oncocytic cells and dense lymphoid stroma) was associated with sarcomatoid differentiation. Remaining 2 aggressive cases were graded as grade 2 and 3 according ISUP grading system. Of note, the tumor with grade 2 was staged as pT3 according to the TNM 2009.

Immunohistochemical profile of OPRCCs has been reported in several studies [4,13,27]. In the current study, we found the immunoprofile of WPRCC almost identical to previously reported immunoprofile of OPRCC. However, vimentin was diffusely positive in 91% of cases in the current study, while it was variable in the OPRCC. WPRCCs were diffusely positive for AMACR, PAX-8, vimentin, MIA, and OSCAR, variably for cytokeratin AE1/AE3, CK7, CD10, EMA. Tumors were negative for carboanhydrase 9, CD117, CK20 and TTF-1.

Copy number variation analysis was successful in 9/11 cases. No numerical chromosomal aberrations were found in 4 tumors. The remaining 5 cases revealed variable chromosomal gains and losses. Such CNV variability is known in chromophobe RCC, in which, besides frequently encountered multiple loses, variable CNV pattern has been documented [19,28,29]. Only 1 of these 5 cases showed, among other chromosomal abnormalities, a polysomy of chromosomes 7 and 17, which is believed to be characteristic for PRCC. Given significant morphologic and genetic heterogeneity of the PRCC, even within type 2 category, these results are not too surprising. Recent large study from The Cancer Genome Atlas group identified genomic profile of PRCC, concluding that type 1 and 2 PRCC are distinctly different entities, and that type 2 PRCC is a heterogeneous disease with multiple distinct subgroups [10]. These results were also supported by previous studies comprising fewer cases [4,11,13,30,31].

The role of TILs is currently investigated by numerous research groups. Present data suggest that specific TIL phenotypes may have prognostic, predictive, or therapeutic value, however, this is yet to be clarified [17,32]. TIL and peritumoral lymphocytes are commonly found in carcinomas associated with Lynch syndrome (LS). LS is a hereditary cancer syndrome caused by mutations in DNA mismatch repair (MMR) proteins, resulting in deficient DNA repair machinery, eventually leading to a hypermutational phenotype and development of neoplasms in other organs. It is believed that renal cell carcinoma (in contrast to urothelial carcinoma of the renal pelvis) is not associated with LS. To find out whether WPRCC with its TILs could be associated with LS, we analyzed immunoreactivity of four MMR proteins, namely the MSH2, MSH6, PMS2, and MLH1. Except one case, we found in all tumors moderate to strong nuclear expression of investigated proteins, both in the tumor tissue and adjacent normal kidney tissue. In case with lost of MSH2 and MSH6 staining, microsatellite instability (MSI) and methylation of MLH1 promoter analyses, as well as mutations analysis in MLH1, MSH2 and MSH6 genes and BRAF V600E mutation were performed, which showed no abnormalities. Our results suggest no relationship between TILs in WPRCC and Lynch syndrome, and possibly, exclude the involvement of investigated MMR genes in tumorigenesis of WPRCC. The expression of MMR proteins was previously evaluated in clear cell RCC [33,34], but this is a first report of such in this unusual variant of PRCC.

Diagnostic features of WPRCC are not highly specific, and that several entities should be considered in the differential diagnosis. The most important one is a metastasis. Oncocytic variant of papillary thyroid

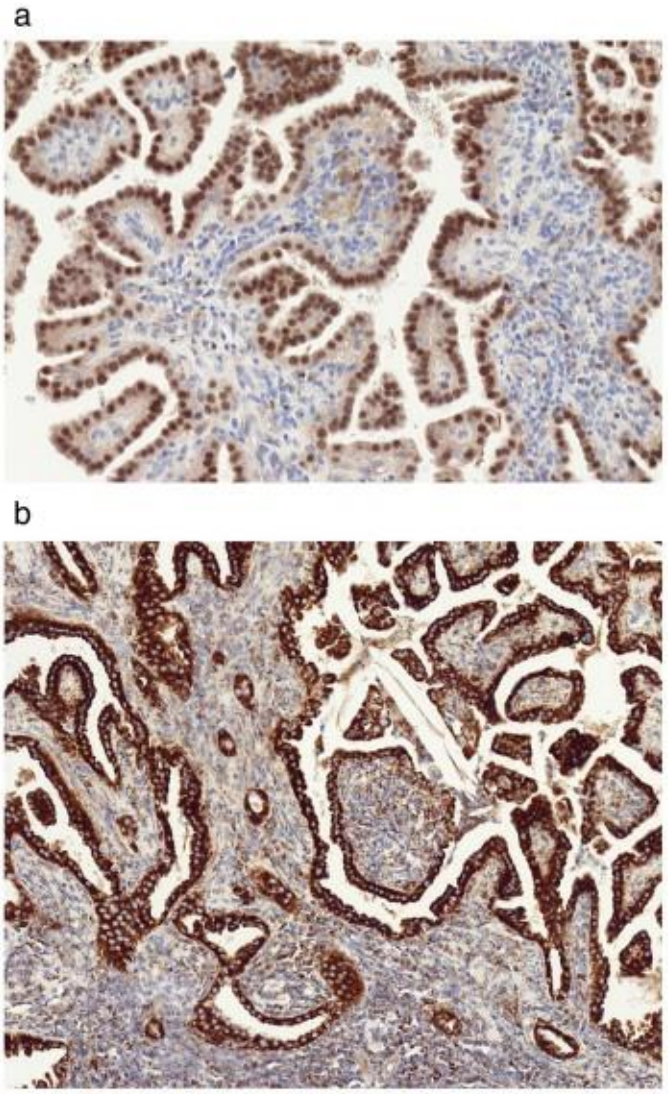

Fig. 8. Immunohistochemistry for PAX8 (A) and antimitochondrial antigen (B)·These immunostainings were positive in n all cases.

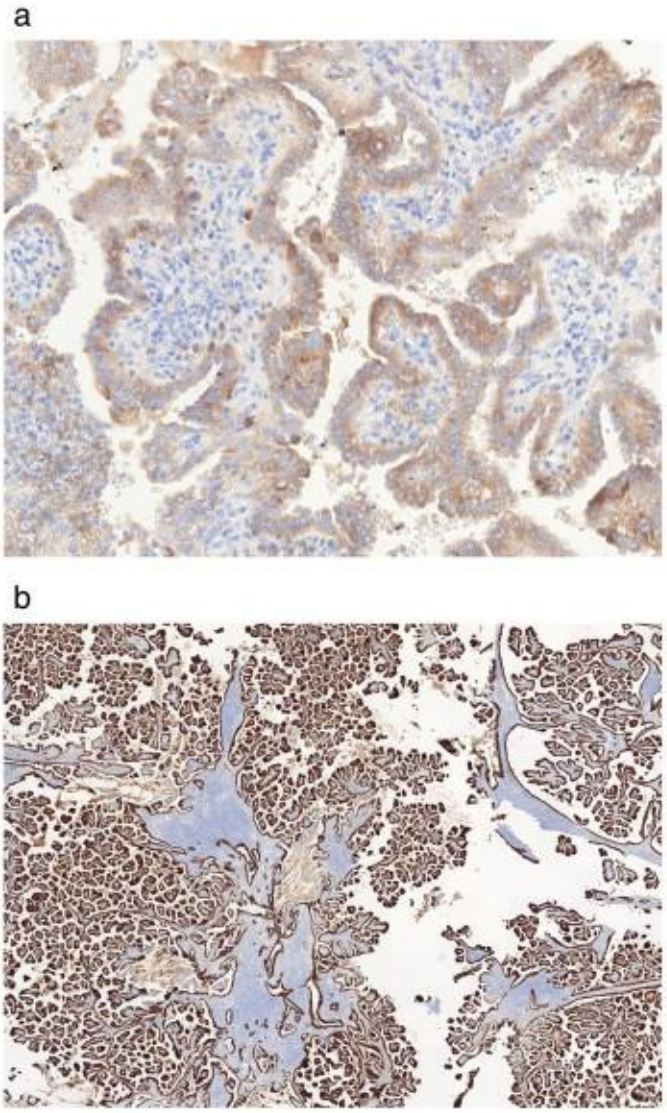

Fig. 9. Immunohistochemistry for AMACR (A) and CK 7 (B). All but one case (case 2) were positive for AMACR, 6 cases were immunoreactive for CK 7.

carcinoma with lymphocytic stroma (Warthin-like variant) is a rare tumor, generally reported to have a favorable prognosis but it may show aggressive clinical behavior [35]. The possibility of a renal metastasis of such a tumor was excluded in our series both clinically and by the fact that TTF-1 was negative in all tumors.

All eosinophilic subtypes of RCC may be considered in the differential diagnosis of Warthin-like PRCC. Oncocytoma and chromophobe RCC may rarely present with architecture mimicking PRCC, however true papillae are not part of the morphologic spectrum of these tumors [2]. Lymphocytic infiltrate in these tumors would be a highly unusual morphologic feature as well.

Another morphologically similar, but much more aggressive entity to be excluded is hereditary leiomyomatosis and renal cell carcinoma (HLRCC)-associated RCC/fumarate hydratase-deficient RCC [2,36,37]. This tumor can be papillary/tubulocystic, composed of eosinophilic cells with high grade nuclei and prominent deep red nucleoli. These tumors are characterized by mutation of the fumarate hydratase gene (FH). Oncocytic characteristics of cell population in these tumors are not mentioned in the literature. In contrast to HLRCC-associated RCC, we were not able to find typical large nuclei with red nucleoli and perinucleolar halo resembling cytomegalovirus inclusions. Moreover prominent TILs are not described in kidney tumors related to hereditary leiomyomatosis [37]. MiT family translocation carcinomas (namely spectrum of Xp11.2 RCC) may also be considered in the differential diagnosis, as they have papillary growth pattern, and may show areas composed of eosinophilic

Table 4
Summary of copy number variations of chromosomes.

Case No.	Gains	Loses
Case 1	None	None
Case 2	5	1, 3, Y
Case 3	None	None
Case 4	None	None
Case 5	NA	NA
Case 6	None	None
Case 7	None	1, 14, 18, 22
Case 8	1, 2, 5, 21	1, 3, 14, 15, Y
Case 9	7, 8, 12, 17	None
Case 10	None	x
Case 11	NA	NA

NA – not analyzable.

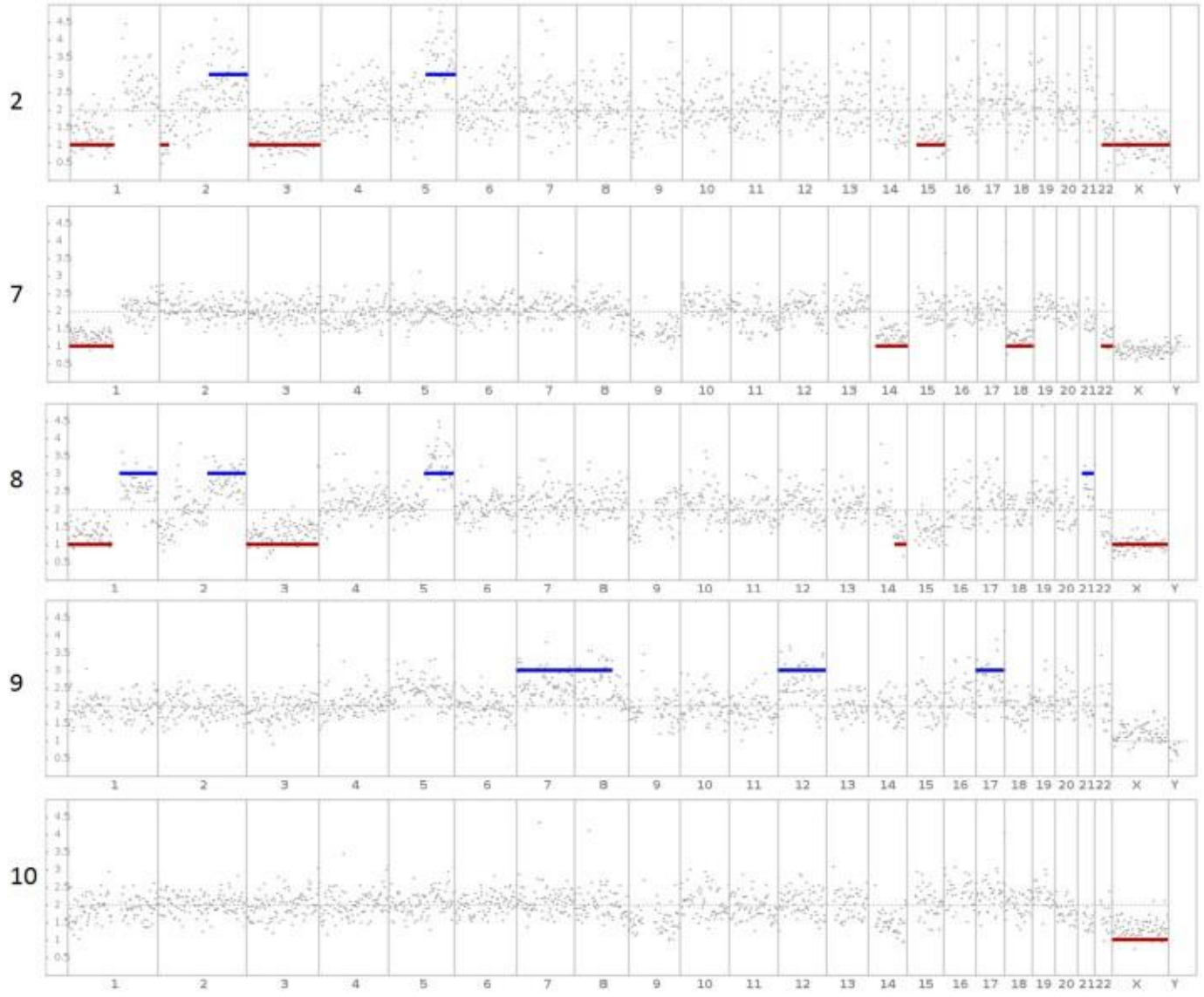

Fig. 10. Chromosome aberration patterns. CNV ranged from loss of one chromosome to complex genome rearrangements including gains and losses of various parts of chromosomes.

cells. Our cases were uniformly composed of oncocytic cells and did not show hyaline bodies, typical microcalcifications and areas with larger pale/clear cells [2].

Tubulocystic RCC may also be considered in the differential diagnosis, mainly because some of our cases did not display CNV. However, our cases differed from tubulocystic RCC by predominantly papillary architecture. No single case from our series showed a predominant tubulocystic growth pattern [38-40].

Succinate dehydrogenase-deficient RCC (SC-RCC) can be in the differential diagnosis as it includes tumors composed of vacuolated eosinophilic to clear cells with inconspicuous nucleoli, usually with a solid growth pattern, but rarely/less frequently showing a tubular or even papillary pattern. This tumor is characterized by the presence of cells with bubbly appearing eosinophilic cytoplasm. In addition to morphological differences, SC-RCC has different imunohistochemical and molecular hallmarks [2,41].

RCC in acquired cystic disease of the kidney (ACDK) is observed exclusively in patients with end-stage renal disease. All our patients had normal renal function, no one was dialyzed or had transplant kidney. Histologically, a variety of RCC types can be found in ACDK patients, including RCC with papillary and tubulopapillary architectures. The tumor cells always have acidophilic cytoplasm with oncocytic features and prominent nucleoli [2]. The presence of mostly abundant oxalate crystalloids is considered to be a typical morphologic feature. We were not able to find oxalate crystals in our cases.

In summary, we analyzed a cohort of PRCCs with oncocytic morphology and dense lymphoid stroma. While the immunohistochemical profile was consistent with PRCC, molecular genetic analysis revealed variable chromosomal abnormalities, indicating that they do not belong to neither type 1, nor type 2 PRCC. Nevertheless, due to the mophological resemblance to the OPRCC, we believe that WPRCC can be considered as part of the spectrum of this variant of papillary renal cell carcinoma group. Since 3/11 cases of WPRCC appeared to have metastatic potential, additional cases need to be studied to elucidate the true malignant potential of these tumors.

Conflict of interest

All authors declare no conflict of interest.

Table 5
Details of detected copy number variations.

Case No.	chr No.	ISCN	Hg19	Copies	Confidence
2	1	1p36.33p11.2	521368-120697156	1	10.02
	2	2p25.3p23.3	10000-25207815	1	1.50
	2	2q22.1q37.3	137858809-243102476	3	2.66
	3	3p26.3q29	60000-197962430	1	27.37
	5	5q21.1q35.3	99536286-180905260	3	13.43
	15	15q11.2q26.3	23564853-102521392	1	8.91
	22	22q11.1q13.33	16847850-50364777	1	5.59
	X	Xp22.33q28	2699520-154931044	1	57.92
7	1	1p36.33p11.2	521368-120697156	1	23.06
	14	14q11.1q32.33	19020000-107289540	1	11.64
	18	18p11.32q23	10000-78017248	1	12.69
	22	22q11.1q13.33	16847850-50364777	1	2.65
8	1	1p36.33p11.2	521368-120697156	1	12.12
	1	1q21.1q44	144810724-248908210	3	4.95
	2	2q22.1q37.3	139830771-243102476	3	14.84
	3	3p26.3q29	60000-197962430	1	24.09
	5	5q21.1q35.3	101498825-180905260	3	35.77
	14	14q24.3q32.33	75191525-107289540	1	1.22
	21	21q11.2q22.3	14338129-48119895	3	2.39
	X	Xp22.33q28	2699520-154931044	1	104.37
9	7	7p22.3q36.3	282484-159128663	3	11.13
	8	8p23.3q22.2	10000-100736467	3	5.95
	12	12p13.33q24.33	145739-133841895	3	8.85
	17	17p13.3q25.3	396626-81195210	3	6.32
10	X	Xp22.33q28	2699520-154931044	1	20.43

chr = chromosome, ISCN = International System for Human Cytogenetic Nomenclature.

Acknowledgement

We would like to thank our friend Ivan Damjanov, MD, PhD (University of Kansas), for all his critical and constructive comments and his assistance with editing of the manuscript.

References

[1] Kuroda N, Hess O, Zhou M. New and emerging renal tumour entities. Diagn Histopathol 2016;22:47–56.
[2] Moch H, Cubilla AL, Humphrey PA, Reuter VE, Ulbright TM. The 2016 WHO classification of tumours of the urinary system and male genital organs-part a: renal, penile, and testicular tumours. Eur Urol 2016;70:93–105.
[3] Moch H, Humphrey PA, Ulbright TM, Reuter VE. WHO classification of tumours of the urinary system and male genital organs. 4th ed. Lyon: IARC; 2016.
[4] Hes O, Brunelli M, Michal M, Cossu Rocca P, Hora M, Chilosi M, et al. Oncocytic papillary renal cell carcinoma: a clinicopathologic, immunohistochemical, ultrastructural, and interphase cytogenetic study of 12 cases. Ann Diagn Pathol 2006;10:133–9.
[5] Hes O, Condom Mundo E, Peckova K, Lopez JI, Martinek P, Vanecek T, et al. Biphasic squamoid alveolar renal cell carcinoma: a distinctive subtype of papillary renal cell carcinoma? Am J Surg Pathol 2016;40:664–75.
[6] Ulamec M, Skenderi F, Trpkov K, Kruslin B, Vranic S, Bulimbasic S, et al. Solid papillary renal cell carcinoma: clinicopathologic, morphologic, and immunohistochemical analysis of 10 cases and review of the literature. Ann Diagn Pathol 2016;23:51–7.
[7] Pivovarcikova K, Peckova K, Martinek P, Montiel DP, Kalusova K, Pitra T, et al. "Mucin"-secreting papillary renal cell carcinoma: clinicopathological, immunohistochemical, and molecular genetic analysis of seven cases. Virchows Arch 2016;469:71–80.
[8] Klatte T, Said JW, Seligson DB, Rao PN, de Martino M, Shuch B, et al. Pathological, immunohistochemical and cytogenetic features of papillary renal cell carcinoma with clear cell features. J Urol 2011;185:30–5.
[9] Ross H, Martignoni G, Argani P. Renal cell carcinoma with clear cell and papillary features. Arch Pathol Lab Med 2012;136:391–9.
[10] Cancer Genome Atlas Research N, Linehan WM, Spellman PT, Ricketts CJ, Creighton CJ, Fei SS, et al. Comprehensive molecular characterization of papillary renal-cell carcinoma. N Engl J Med 2016;374:135–45.
[11] Marsaud A, Dadone B, Ambrosetti D, Baudoin C, Chamorey E, Rouleau E, et al. Dismantling papillary renal cell carcinoma classification: the heterogeneity of genetic profiles suggests several independent diseases. Genes Chromosomes Cancer 2015;54:369–82.
[12] Bigot P, Bernhard JC, Gill IS, Vuong NS, Verhoest G, Flamand V, et al. The subclassification of papillary renal cell carcinoma does not affect oncological outcomes after nephron sparing surgery. World J Urol 2016;34:347–52.
[13] Xia QY, Rao Q, Shen Q, Shi SS, Li L, Liu B, et al. Oncocytic papillary renal cell carcinoma: a clinicopathological study emphasizing distinct morphology, extended immunohistochemical profile and cytogenetic features. Int J Clin Exp Pathol 2013;6:1392–9.
[14] Lefevre M, Couturier J, Sibony M, Bazille C, Boyer K, Callard P, et al. Adult papillary renal tumor with oncocytic cells: clinicopathologic, immunohistochemical, and cytogenetic features of 10 cases. Am J Surg Pathol 2005;29:1576–81.
[15] Ishibashi K, Ito Y, Masaki A, Fujii K, Beppu S, Sakakibara T, et al. Warthin-like mucoepidermoid carcinoma: a combined study of fluorescence in situ hybridization and whole-slide imaging. Am J Surg Pathol 2015;39:1479–87.
[16] Yeo MK, Bae JS, Lee S, Kim MH, Lim DJ, Lee YS, et al. The Warthin-like variant of papillary thyroid carcinoma: a comparison with classic type in the patients with coexisting Hashimoto's thyroiditis. Int J Endocrinol 2015;2015:456027.
[17] Festino L, Botti G, Lorigan P, Masucci GV, Hipp JD, Horak CE, et al. Cancer treatment with anti-PD-1/PD-L1 agents: is PD-L1 expression a biomarker for patient selection? Drugs 2016;76:925–45.
[18] van Dongen JJ, Langerak AW, Bruggemann M, Evans PA, Hummel M, Lavender FL, et al. Design and standardization of PCR primers and protocols for detection of clonal immunoglobulin and T-cell receptor gene recombinations in suspect lymphoproliferations: report of the BIOMED-2 concerted action BMH4-CT98-3936. Leukemia 2003;17:2257–317.
[19] Sperga M, Martinek P, Vanecek T, Grossmann P, Bauleth K, Perez-Montiel D, et al. Chromophobe renal cell carcinomas—chromosomal aberration variability and its relation to Paner grading system: an array CGH and FISH analysis of 37 cases. Virchows Archiv 2013;463:563–73.
[20] Kacerovska D, Drlik L, Slezakova L, Michal M, Stehlik J, Sedivcova M, et al. Cutaneous sebaceous lesions in a patient with MUTYH-associated polyposis mimicking Muir-Torre syndrome. Am J Dermatopathol 2016;38:915–23.
[21] Chan AO, Broaddus RR, Houlihan PS, Issa JP, Hamilton SR, Rashid A. CpG island methylation in aberrant crypt foci of the colorectum. Am J Pathol 2002;160:1823–30.
[22] Matsuoka T, Ichikawa C, Fukunaga A, Yano T, Sugino Y, Okada T, et al. Two cases of oncocytic papillary renal cell carcinoma. Hinyokika kiyo Acta Urol Jpn 2016;62:187–91.
[23] Masuzawa N, Kishimoto M, Nishimura A, Shichiri Y, Yanagisawa A. Oncocytic renal cell carcinoma having papillotubular growth: rare morphological variant of papillary renal cell carcinoma. Pathol Int 2008;58:300–5.
[24] Mai KT, Kohler DM, Robertson SJ, Belanger EC, Marginean EC. Oncocytic papillary renal cell carcinoma with solid architecture: mimic of renal oncocytoma. Pathol Int 2008;58:164–8.
[25] Kunju LP, Wojno K, Wolf Jr JS, Cheng L, Shah RB. Papillary renal cell carcinoma with oncocytic cells and nonoverlapping low grade nuclei: expanding the morphologic spectrum with emphasis on clinicopathologic, immunohistochemical and molecular features. Hum Pathol 2008;39:96–101.
[26] Kim JY. Oncocytic papillary renal cell carcinoma in the background of renal adenomatosis: a case report. Int J Surg Pathol 2016.
[27] Han G, Yu W, Chu J, Liu Y, Jiang Y, Li Y, et al. Oncocytic papillary renal cell carcinoma: a clinicopathological and genetic analysis and indolent clinical course in 14 cases. Pathol Res Pract 2017;213:1–6.
[28] Krill-Burger JM, Lyons MA, Kelly LA, Sciulli CM, Petrosko P, Chandran UR, et al. Renal cell neoplasms contain shared tumor type-specific copy number variations. Am J Pathol 2012;180:2427–39.
[29] Brunelli M, Eble JN, Zhang S, Martignoni G, Delahunt B, Cheng L. Eosinophilic and classic chromophobe renal cell carcinomas have similar frequent losses of multiple chromosomes from among chromosomes 1, 2, 6, 10, and 17, and this pattern of genetic abnormality is not present in renal oncocytoma. Mod Pathol 2005;18:161–9.
[30] Durinck S, Stawiski EW, Pavia-Jimenez A, Modrusan Z, Kapur P, Jaiswal BS, et al. Spectrum of diverse genomic alterations define non-clear cell renal carcinoma subtypes. Nat Genet 2015;47:13–21.
[31] Kovac M, Navas C, Horswell S, Salm M, Bardella C, Rowan A, et al. Recurrent chromosomal gains and heterogeneous driver mutations characterise papillary renal cancer evolution. Nat Commun 2015;6:6336.
[32] Massari F, Santoni M, Ciccarese C, Santini D, Alfieri S, Martignoni G, et al. PD-1 blockade therapy in renal cell carcinoma: current studies and future promises. Cancer Treat Rev 2015;41:114–21.
[33] Yoo KH, Won KY, Lim SJ, Park YK, Chang SG. Deficiency of MSH2 expression is associated with clear cell renal cell carcinoma. Oncol Lett 2014;8:2135–9.
[34] Petersson F, Sima R, Sperga M, Kazakov DV, Michal M, Hora M, et al. Lymphocyte-rich renal cell carcinoma: an unusual histomorphologic manifestation of a tumor that is not part of lynch syndrome. Appl Immunohistochem Mol Morphol 2011;19:519–27.
[35] Gross M, Eliashar R, Ben-Yaakov A, Weinberger JM, Maly B. Clinicopathologic features and outcome of the oncocytic variant of papillary thyroid carcinoma. Ann Otol Rhinol Laryngol 2009;118:374–81.
[36] Smith SC, Trpkov K, Chen YB, Mehra R, Sirohi D, Ohe C, et al. Tubulocystic carcinoma of the kidney with poorly differentiated foci: a frequent morphologic pattern of fumarate hydratase-deficient renal cell carcinoma. Am J Surg Pathol 2016;40:1457–72.
[37] Trpkov K, Hes O, Agaimy A, Bonert M, Martinek P, Magi-Galluzzi C, et al. Fumarate hydratase-deficient renal cell carcinoma is strongly correlated with fumarate hydratase mutation and hereditary leiomyomatosis and renal cell carcinoma syndrome. Am J Surg Pathol 2016;40:865–75.
[38] Tran T, Jones CL, Williamson SR, Eble JN, Grignon DJ, Zhang S, et al. Tubulocystic renal cell carcinoma is an entity that is immunohistochemically and genetically distinct from papillary renal cell carcinoma. Histopathology 2016;68:850–7.
[39] Ulamec M, Skenderi F, Zhou M, Kruslin B, Martinek P, Grossmann P, et al. Molecular genetic alterations in renal cell carcinomas with tubulocystic pattern: tubulocystic renal cell carcinoma, tubulocystic renal cell carcinoma with heterogenous component and familial leiomyomatosis-associated renal cell carcinoma. clinicopathologic and molecular genetic analysis of 15 cases. Appl Immunohistochem Mol Morphol 2016;24:521–30.
[40] Banerjee I, Yadav SS, Tomar V, Yadav S, Talreja S. Tubulocystic renal cell carcinoma: a great imitator. Rev Urol 2016;18:118–21.
[41] Kuroda N, Yorita K, Nagasaki M, Harada Y, Ohe C, Jeruc J, et al. Review of succinate dehydrogenase-deficient renal cell carcinoma with focus on clinical and pathobiological aspects. Pol J Pathol 2016;67:3–7.

3.3 Biphasic squamoid alveolar renal cell carcinoma - A distinctive subtype of papillary renal cell carcinoma?

Bifázický skvamoidní a alveolární renální karcinom (BSARCC) je v literatuře relativně recentně popsanou renální neoplázií.

V rámci této multiinstitucionální studie je prezentováno celkem 21 případů BSARCC, které byly analyzovány morfologicky, za použití imunohistochemie a molekulárně genetických metod (arrayCGH a FISH). V 11 případech se jednalo o tumory u mužů, ve zbylých 10 případech byly postiženy ženy. Věkové rozmezí pacientů se pohybovalo mezi 53 a 79 lety, rozptyl velikosti nádorů byl mezi 1,5 a 16 cm. Údaje o dispenzarizaci byly k dispozici u 14 pacientů (délka dispenzarizace činila 1-96 měsíců), z toho u pěti pacientů byla dokumentována přítomnost metastatického onemocnění. Morfologicky všechny nádory obsahovaly dvě různé populace buněk uspořádané do odlišných organoidních struktur: malé buňky s low-grade morfologií a malým množstvím cytoplasmy vytvářely alveolární struktury, větší skvamoidní buňky s objemnější cytoplasmou a vezikulárním jadérkem tvořily kompaktní okrsky/hnízda (okrsky větších skvamoidních buněk tvořily od 10% do 80% z celkového objemu tumorů). U devíti nádorů byl dále zastižen i přechod výše popsaných solidních a alveolárních okrsků do papilární komponenty. Ve všech 21 případech byla histologicky zachycena přítomnost emperipoézy. Všechny případy reagovaly pozitivně v imunohistochemickém průkazu CK7, EMA, vimentinu a cyklinu D1 (přičemž pozitivita cyklinu D1 byla exklusivně omezena pouze na okrsky velkých skvamoidních buněk). Různé spektrum chromozomálních numerických aberací bylo detekováno v analyzovatelných případech (11/21 případů), včetně polysomie chromosomů 7 a 17 (tedy molekulárně genetických znaků manifestujících příslušnost BSARCC k PRCC).

Na podkladě morfologie, imunohistochemického a molekulárně genetického profilu těchto lézí je evidentní, že BSARCC je zvláštní morfologickou variantou PRCC s morfologickým spektrem sahajícím od renálního karcinomu s typickou papilární architektonikou a velkými skvamoidními buňkami až k tumorům s plně vyjádřenou morfologií typickou pro BSARCC popsanou výše. Přítomnost emperipoézy je pak pro tyto nádory konstantním znakem. U některých z případů bylo popsáno agresivní chování, avšak prognóza této nádorové entity nemůže být s definitivní jistou hodnocena z velmi omezeného množství doposud publikovaných dat.

Biphasic Squamoid Alveolar Renal Cell Carcinoma

A Distinctive Subtype of Papillary Renal Cell Carcinoma?

Ondrej Hes, MD, PhD,* Enric Condom Mundo, MD, PhD,wz Kvetoslava Peckova, MD,* Jose I. Lopez, MD,y Petr Martinek, PhD,* Tomas Vanecek, PhD,* Giovanni Falconieri, MD,8 Abbas Agaimy, MD,z Whitney Davidson, MD,# Fredrik Petersson, MD, PhD,** Stela Bulimbasic, MD, PhD,ww Ivan Damjanov, MD, PhD,# Mireya Jimeno, MD,zz Monika Ulamec, MD, PhD,yy Miroslav Podhola, MD, PhD,88 Maris Sperga, MD,zz Maria Pane Foix, MD,wz Ksenya Shelekhova, MD, PhD,## Kristyna Kalusova, MD,*** Milan Hora, MD, PhD,*** Pavla Rotterova, MD, PhD,* Ondrej Daum, MD, PhD,* Kristyna Pivovarcikova, MD,* and Michal Michal, MD*

Abstract: Biphasic squamoid alveolar renal cell carcinoma (BSARCC) has been recently described as a distinct neoplasm. Twenty-one cases from 12 institutions were analyzed using routine histology, immunohistochemistry, array comparative genomic hybridization (aCGH) and fluorescence in situ hybridization. Tumors were removed from 11 male and 10 female patients, whose age ranged from 53 to 79 years. The size of tumors ranged from 1.5 to 16 cm. Follow-up information was available for 14 patients (range, 1 to 96 mo), and metastatic spread was found in 5 cases. All tumors comprised 2 cell populations arranged in organoid structures: small, low-grade neoplastic cells with scant cytoplasm usually lining the inside of alveolar structures, and larger squamoid cells with more prominent cytoplasm and larger vesicular nuclei arranged in compact nests. In 9/21 tumors there was a visible transition from such solid and alveolar areas into papillary components. Areas composed of large squamoid cells comprised 10% to 80% of total tumor volume. Emperipolesis was present in all (21/21) tumors. Immunohistochemically, all cases were positive for cytokeratin 7, EMA, vimentin, and cyclin D1. aCGH (confirmed by fluorescence in situ hybridization) in 5 analyzable cases revealed multiple numerical chromosomal changes including gains of chromosomes 7 and 17 in all cases. These changes were further disclosed in 6 additional cases, which were unsuitable for aCGH. We conclude that tumors show a morphologic spectrum ranging from RCC with papillary architecture and large squamoid cells to fully developed BSARCC. Emperipolesis in squamoid cells was a constant finding. All BSARCCs expressed CK7, EMA, vimentin, and cyclin D1. Antibody to cyclin D1 showed a unique and previously not recognized pattern of immunohistochemical staining. Multiple chromosomal aberrations were identified in all analyzable cases including gains of chromosomes 7 and 17, indicating that they are akin to papillary RCC. Some BSARCCs were clinically aggressive, but their prognosis could not be predicted from currently available data. Present microscopic, immunohistochemical, and molecular genetic data strongly support the view that BSARCC is a distinctive and peculiar morphologic variant of papillary RCC.

From the Departments of *Pathology; ***Urology, Charles University, Medical Faculty and Charles University Hospital Plzen; 88Department of Pathology, Charles University, Medical Faculty and Charles University Hospital Hradec Kralove, Czech Republic; wDepartment of Pathology, Bellvitge University Hospital, Bellvitge Biomedical Research Institute (IDIBELL); zDepartment of Pathology and Experimental Therapeutics, University of Barcelona School of Medicine; zzDepartment of Pathology, Consorci Sanitari Integral, Barcelona; yDepartment of Pathology, Cruces University Hospital, Biocruces Research Institute, University of the Basque Country, Barakaldo, Spain; 8Department of Pathology, University of Trieste, Trieste, Italy; zDepartment of Pathology, University Hospital Erlangen, Erlangen, Germany; #Department of Pathology, The University of Kansas School of Medicine, Kansas City, KS; **Department of Pathology, National University Health System, Singapore, Singapore; wwDepartment of Pathology, Clinical Hospital Center Zagreb; yy"Ljudevit Jurak" Pathology Department, Clinical Hospital Center "Sestre milosrdnice", Zagreb, Croatia; zzDepartment of Pathology, East University, Riga, Latvia; and ##Department of Pathology, Petrov's Research Institute of Oncology, St Petersburg, Russia.

Conflicts of Interest and Source of Funding: Supported by the Charles University Research Fund (project number P36) and by the project CZ.1.05/2.1.00/03.0076 from European Regional Development Fund (O.H.). The authors have disclosed that they have no significant relationships with, or financial interest in, any commercial companies pertaining to this article.

Correspondence: Ondrej Hes, MD, PhD, Department of Pathology, Charles University, Medical Faculty and Charles University Hospital Plzen, Alej Svobody 80, 304 60 Pilsen, Czech Republic (e-mail: hes@medima.cz).

Key Words: kidney, biphasic squamoid alveolar renal cell carcinoma, papillary renal cell carcinoma, immunohistochemistry, aCGH, FISH

(Am J Surg Pathol 2016;40:664–675)

Three years ago we reported 2 renal cell carcinomas (RCCs) that we thought had unique and previously unrecognized histopathologic features.[1] We named that neoplasm descriptively as a biphasic alveolo-squamoid renal cell carcinoma (BSARCC). Unique to this tumor

were organoid structures composed of centrally located solid nests of large squamoid cells surrounded in an alveolar manner by smaller cuboidal and flattened cells reminiscent of dilated tubules or cysts. The squamoid cells had vesicular large nuclei, which were surrounded by eosinophilic cytoplasm with distinct cell borders. The alveolar cells were smaller and mostly cuboidal displaying a high nuclear to cytoplasmic ratio.[1] The clinicopathologic significance of these histopathologic data was not addressed, and thus we decided to assemble a much larger number of similar cases.

In the present paper we present 20 additional cases of this tumor type, providing evidence that BSARCCs are histogenetically closely related to papillary RCC (PRCC). Clinical follow-up shows that some of these cases had an adverse outcome. We hope that our study will stimulate other uropathologists to review their databases and further contribute to the characterization of BSARCC as a clinicopathologic entity.

MATERIALS AND METHODS

A search algorithm including the keywords "unclassified, squamoid, squamous, glomeruloid" was used to identify renal tumors from the Plzen Tumor Registry and multiple other institutional archives and consult files of the other authors. All cases were reviewed by 3 pathologists (O.H., K.Pe., M.M.) and compared with the index case to identify matching features. One or more hematoxylin and eosin–stained slides were available for review in all cases (1 to 23 slides/case). Altogether 21 cases were identified from a total of 18,500 cases. Three cases have already been published previously and were included into the present study (cases 7, 14, and 15). These cases are marked by the sign y in Table 1.[1,2]

Light Microscopy

Tissue for light microscopy had been fixed in 4% formaldehyde and embedded in paraffin using routine procedures. Sections of 5 mm thickness were cut and stained with hematoxylin and eosin.

Immunohistochemistry

A relatively broad panel of antibodies was used for complex analysis of tumors with apparently dual population. All staining analyses were performed in 1 institution (University Hospital Plzen). The immunohistochemical study was performed using a Ventana Benchmark XT automated stainer (Ventana Medical System Inc., Tucson, AZ).

The following primary antibodies were used: epithelial membrane antigen (EMA) (E29, monoclonal; DakoCytomation, Carpinteria, CA; 1:1000), cytokeratins (AE1-AE3, monoclonal; BioGenex, San Ramon, CA; 1:1000), CK5/6 (D5/16B4, monoclonal; DakoCytomation; 1:100), CD10 (56C6; Novocastra, Burlingame, CA; 1:20), cytokeratin 7 (OV-TL12/30, monoclonal;

TABLE 1. Basic Clinicopathologic Data

Case	Sex	Age	Size (cm)	Side	Follow-up (mo)	Squamoid Area-extend in %	Emperipolesis
1	M	65	10 Â9.5Â 7	R	24, AWD*	10	Yes
2	M	57	6Â5Â 4	UN	ND	20	Yes
3	F	60	10.5	L	29, DOD	20	Yes
4	F	53	3.2	R	1, DUNw	10	Yes
5	F	70	UN	UN	UN	40	Yes
6	M	66	3.5	R	6, AWD, then NDz	10	Yes
7y	F	54	3	R	72, AW, then ND	100 (minimal papillary focus)	Yes
8	F	54	1.9 Â1.4Â 2	R	24, AW	40	Yes
9	M	63	3.5	UN	UN	60	Yes
10	M	57	3	UN	ND	45	Yes
11	F	79	4.5	UN	ND	30	Yes
12	F	70	2.9 Â1.7Â 1.5	R	18, AW	30	Yes
13	F	62	2.8 Â1.9Â 2	L	13, AW8	35	Yes
14y	M	55	2	R	48, AW, then DUNz	30	Yes
15y	F	54	2.2	R	96, AW, then DUN#	20	Yes
16	M	46	1.5	R	UN	40	Yes
17	M	60	2	R	24, AW	40	Yes
18	M	78	16.0	L	45, DOD**	45	Yes
19	M	53	3.0	R	6, AWDz	5	Yes
20	M	65	5	UN	ND	30	Yes
21	F	72	6	L	3, AW	40	Yes

*pT3, pN2: lymph nodes paracaval (TNM 09).
wDead of hemorrhagic shock 3 weeks after surgery, 18 years on hemodialysis.
z6 months after nephrectomy, multiple bilateral lung metastases, lymph node metastases.
yPreviously published cases.[1,2]
8Ductal invasive carcinoma of breast treated 1 year before nephrectomy.
zDead of small cell carcinoma of the lung.
#Dead of cholangiogenic carcinoma of the liver.
**Metastases in mediastinal lymph nodes.
AW indicates alive and well; AWD, alive with disease; DOD, dead of disease; DUN, dead of unrelated condition; F, female; L, left; M, male; ND, not documented; R, right; UN, unknown.

FIGURE 1. Grossly, tumors are solid.

FIGURE 3. Some tumors were solid, firm with whitish color.

DakoCytomation; 1:200), cytokeratin 20 (M7019, monoclonal; DakoCytomation; 1:100), racemase/AMACR (P504S, monoclonal; Zeta, Sierra Madre, CA; 1:50), vimentin (D9, monoclonal; NeoMarkers, Westinghouse, CA; 1:1000), parvalbumin (PA-235, monoclonal; Sigma Aldrich, St Luis, MO; 1:500), Ki-67 (MIB1, monoclonal; Dako, Glostrup, Denmark; 1:1000), c-kit (CD117, polyclonal, Dako, Glostrup, Denmark, 1:300), CD10 (monoclonal, Sp67; Ventana, RTU), E-cadherin (12H6, monoclonal; Zymed, San Francisco, CA; 1:200), carbonic anhydrase IX (rhCA9, monoclonal; RD systems, Abingdon, GB; 1:100), p63 (4A4, monoclonal; Ventana, Tucson, AZ, RTU), p53 (DO-7, monoclonal; DakoCytomation; 1:30), antimelanosome (HMB45, monoclonal; DakoCytomation; 1:200), TFE3 (polyclonal; Abcam; 1:100), cathepsin K (3F9, monoclonal; Abcam; 1:100), WT1 (GF-H2, monoclonal; DakoCytomation; 1:150), TTF-1 (SPT24, monoclonal; Novocastra, Newcastle, UK; 1:400), antibody against cyclin D1-M 30 (M30 monoclonal; Lobome, Enzo Life Sciences, Ann Arbor, MI; 1:100), bcl-2 (monoclonal, 124; Cell Marque, Rocklin, CA; 1:100), cyclin D1 (SP4-R, monoclonal; Cell Marque; 1:100), (SP4-R, monoclonal; Ventana, RTU), (polyclonal; NeoMarkers, Fremont, CA; 1:100), and PAX-8 (polyclonal; Cell Marque; 1: 25). The primary antibodies were visualized using the supersensitive streptavidin-biotin-peroxidase complex (BioGenex). Appropriate positive controls were used.

FIGURE 2. Color ranges from whitish to tan/brown. Tan color of the gross section seen on a formalin-fixed tissue/specimen.

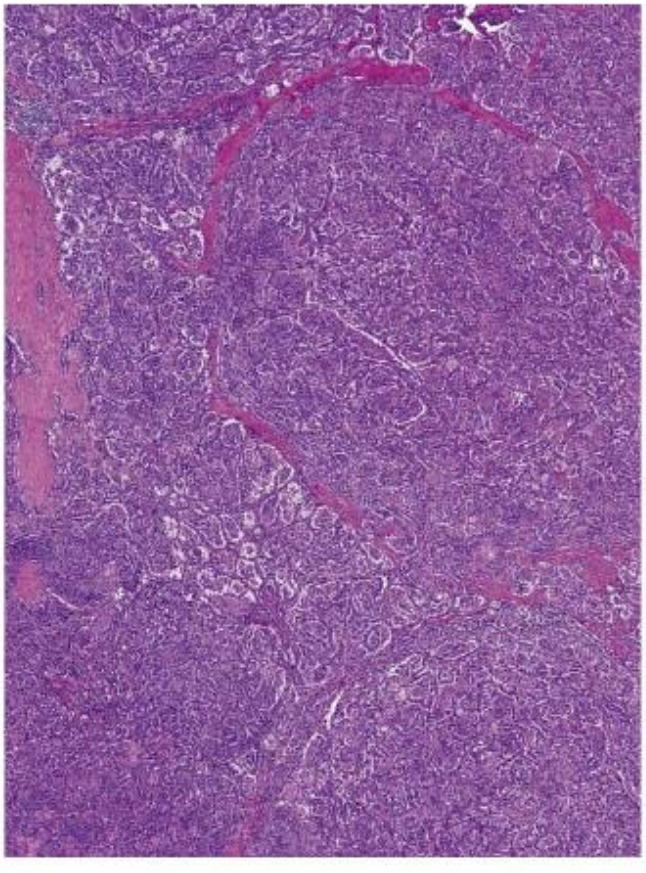

FIGURE 4. Well-developed BSARCC in which squamoid cells forming the majority of the tumors mass.

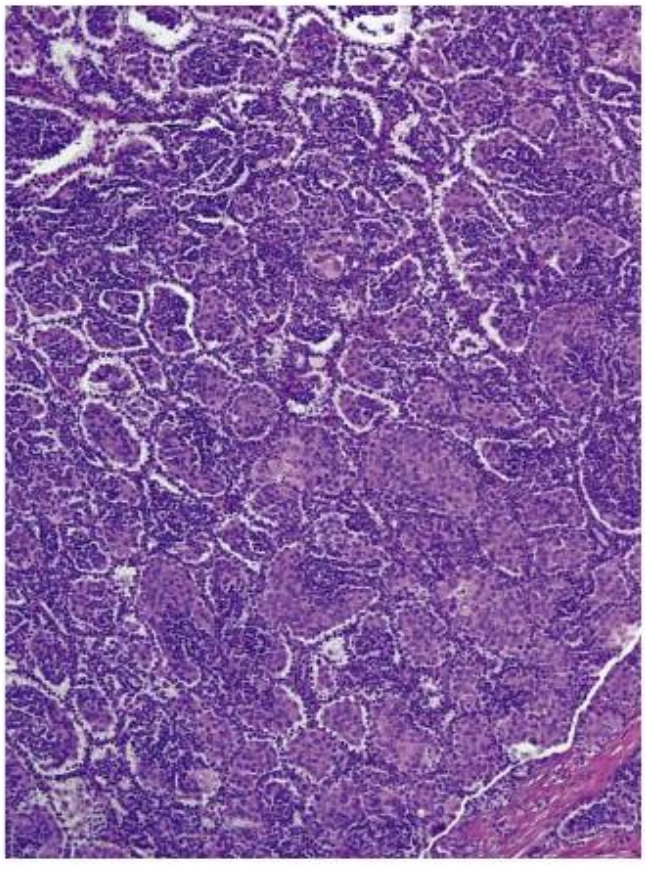

FIGURE 5. Solid-alveolar pattern of BSARCC is clearly seen.

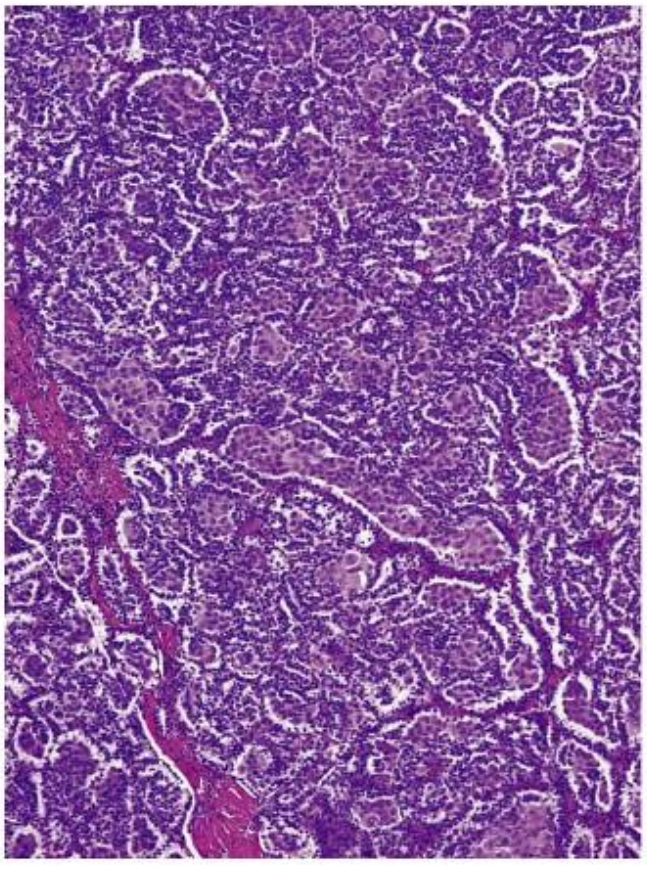

FIGURE 6. Squamoid areas surrounded by smaller cells with scant cytoplasm.

DNA Extraction

DNA from macrodissected formalin-fixed paraffin-embedded (FFPE) tissue was extracted using a QIAsymphony DNA Mini Kit (Qiagen, Hilden, Germany) on automated system (QIAsymphony SP, Qiagen) according to the manufacturer's supplementary protocol for FFPE samples (purification of genomic DNA from FFPE tissue using the QIAamp DNA FFPE Tissue Kit and Deparaffinization Solution). Samples were then purified using Qiaquick kit (Qiagen) and eluted in EB buffer (Qiagen). Concentration and purity of isolated DNA was measured using NanoDrop ND-1000 (NanoDrop Technologies Inc., Wilmington, DE). DNA integrity was examined by amplification of control genes in a multiplex polymerase chain reaction.[3]

Array Comparative Genomic Hybridization

Five cases (no 3, 9, 12, 13, 14) were suitable for analysis using array comparative genomic hybridization (aCGH).

CytoChip Focus Constitutional (BlueGnome Ltd, Cambridge, UK) array was used for aCGH analysis. It uses BAC technology and covers 143 regions of known significance with 1 Mb spacing across a genome. Probes are spotted in triplicates. First, 400 ng of DNA was labeled using the Fluorescent Labeling System (BlueGnome Ltd). The procedure included Cy3 labeling of a test sample and Cy5 labeling of a reference sample. Commercially produced reference of opposite sex was used in cases in which no reference sample was available (MegaPool Reference DNA Male/Female, Kreatech Diagnostics, Amsterdam, Netherlands). The labeled reference and the test sample were mixed, dried, and hybridized overnight at 471C using Arrayit hybridization cassette (Arrayit Corporation, CA). Posthybridization washing was done using SSC buffers with increasing stringency. Dried microarray was scanned with InnoScan 900 (Innopsys, France) at a resolution of 5 mm. Scanned image was analyzed and quantified by BlueFuse Multi software (BlueGnome Ltd). The software uses Bayesian algorithms to generate intensity values for each Cy5 and Cy3 labeled spot on the array according an appropriate.gal file. Cutoff values for log 2 ratio are preset to À 0.3 for loss and to 0.3 for gain by BlueFuse software.

Fluorescence In Situ Hybridization

Eleven cases were suitable for fluorescence in situ hybridization (FISH) analysis. A 4-mm-thick FFPE tissue section was placed onto a positively charged slide. The target area was circled with a diamond pen according to the corresponding hematoxylin and eosin–stained slide. The slide was routinely deparaffinized, incubated in the Â 1 Target Retrieval Solution Citrate pH 6 (Dako) for 40 minutes at 951C, then cooled for 20 minutes at room

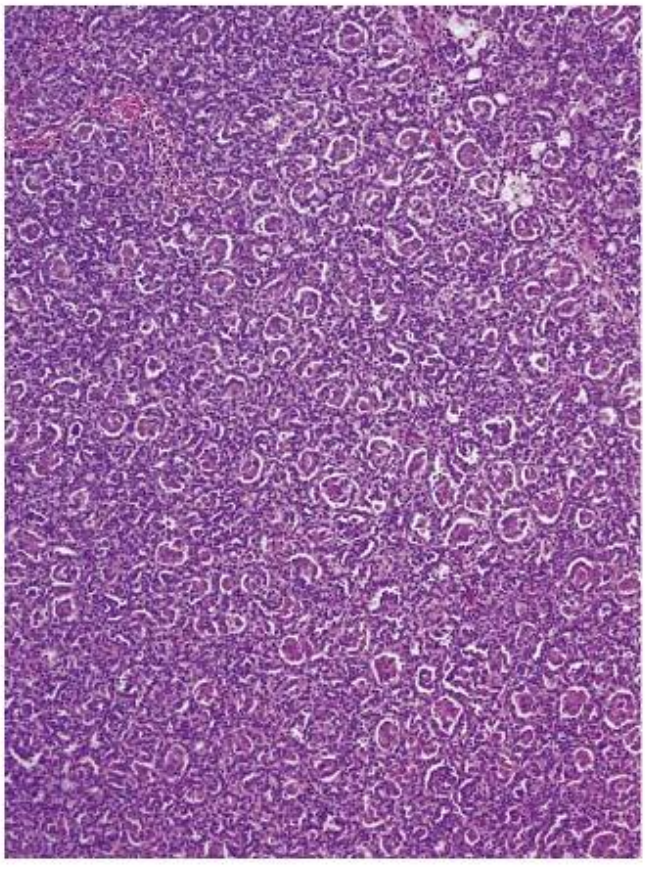

FIGURE 7. Scanning, low-power magnification shows RCC with papillary architecture comprising areas composed of large squamoid cells.

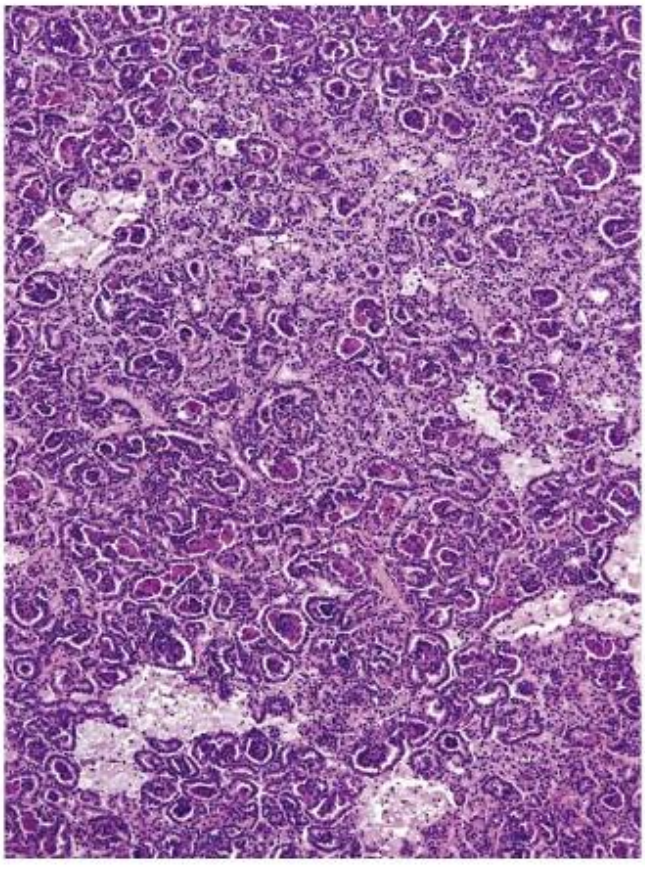

FIGURE 8. In some areas, foci of foam cells are present.

temperature in the same solution. The slide was washed in deionized water and digested in protease solution with pepsin (0.5 mg/mL) (Sigma Aldrich) in 0.01 M HCl at 371C for 15 minutes. The slide was then immersed in deionized water for 5 minutes, dehydrated in a series of ethanol solutions (70%, 85%, and 96% for 2 min each) and air-dried. FISH probes CEP 7 Spectrum Orange (D7Z1), CEP 17 Spectrum Orange, CEP X (DXZ1) Spectrum Green/CEP Y (DYZ3) Spectrum Orange (Vysis/Abbott Molecular, Des Plaines, IL) were mixed with water and hybridization buffers according to manufacturer's protocol. The slide was incubated in a ThermoBrite instrument (StatSpin/Iris Sample Processing, Westwood, MA) with codenaturation at 851C for 8 minutes and hybridization at 371C for 16 hours. Posthybridization wash was performed in 2Â SSC/0.3% NP-40 solution at 721C for 2 minutes. The slide was counterstained with DAPI I (Vysis) and stored in the dark at À 201C until examined. FISH signals were assessed using an Olympus BX51 fluorescence microscope. Scoring of aneuploidy was performed by counting the number of fluorescent signals in 100 randomly selected, nonoverlapping tumor cell nuclei. The slide was independently enumerated by 2 observers (P.M., T.V.). Cutoff values were set for each probe as shown in previous study.[4]

RESULTS

The clinicopathologic features of 21 cases of BSARCC are summarized in Table 1. Eleven of the patients were male and 10 were female; their ages ranged from 53 to 79 years (mean, 61.57 y). Tumor size ranged from 1.5 to 16 cm in greatest dimension (mean, 4.63 cm; median, 3.1 cm). All cases were solitary lesions. Follow-up data were available for 14/21 patients, with follow-up period ranging from 1 to 96 months (mean, 29.21 mo; median, 24 mo); metastatic spread was confirmed in 5 cases.

Three patients were alive with disease (lymph node involvement and bilateral lung metastases) after periods ranging from 6 to 24 months. However, 1 patient from this group (lung and lymph node metastases) was lost to follow-up 6 months after nephrectomy. Two patients died of widespread metastatic disease 29 and 45 months status post nephrectomy. Six patients were alive and well 3 to 72 months after diagnosis, whereas another 3 patients were without evidence of disease at 1, 48, and 96 months after surgery but died of unrelated diseases or conditions.

On gross examination the tumors were described as solid with color varying from whitish to tan or light brown (Figs. 1–3). Small areas of hemorrhage were reported in 4 cases with grossly visible necrotic foci noted in a single case.

All tumors were composed of a distinctly dual cell population. The first contained relatively uniform, small, low-grade neoplastic cells with scant cytoplasm. Such

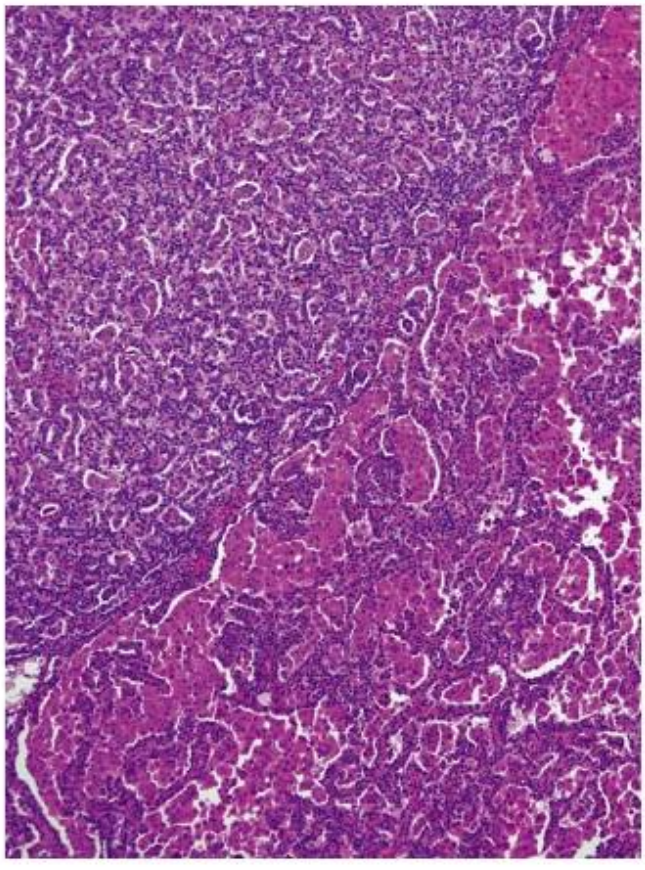

FIGURE 9. Transition between areas composed nearly exclusively of large squamoid cells and an area of more typical PRCC.

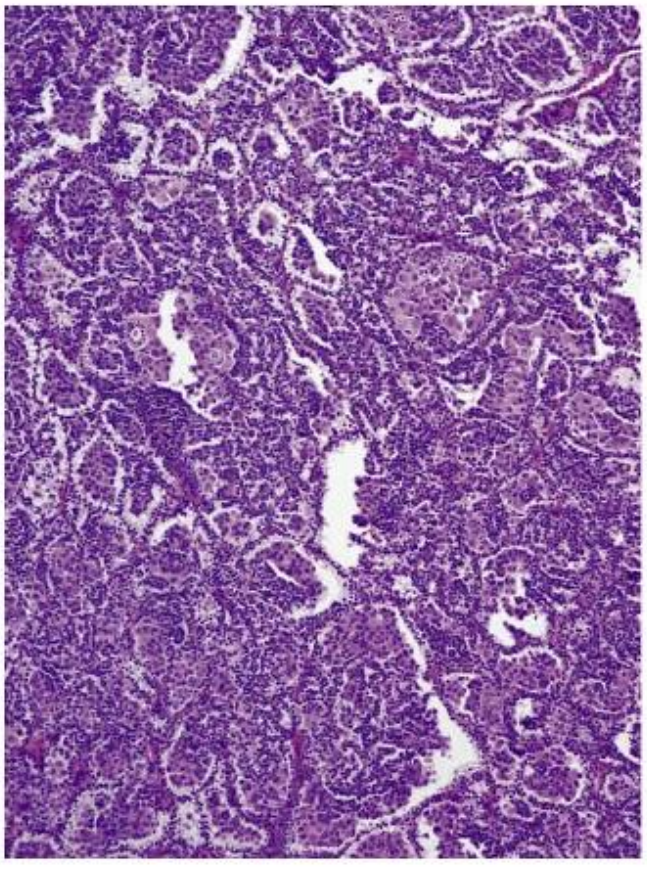

FIGURE 10. Emperipolesis was present in 21/21 tumors. This was found in large cells within squamoid areas. Scanning low-power magnification showing numerous foci of emperipolesis within squamoid areas.

small cells with scant cytoplasm had mostly round slightly elongated nuclei, resembling those of normal lymphocytes. These cells were arranged in rows forming alveolar-like structures, reminiscent of dilated tubules, microcystic structures, or Bowman capsular spaces. Alveolar spaces were often attached to the vascular septa contributing to their walls. Alveolar cells were separated by a slit space from the solid nests composed of larger squamoid cell, which formed the second cell population of all tumors. This second population was made up of large cells containing voluminous pink cytoplasm and large nuclei with prominent nucleoli. These eosinophilic cells were arranged in solid islands, forming the centers of alveolar structures and often revealing retraction artifacts, most likely related to the biphasic cell populations that were so closely intermixed. A retraction from the walls of the alveoli formed by smaller cells with scant cytoplasm may be seen in Figures 4–6. Neither the keratin pearls nor the intercellular bridges observed in true squamous epithelium were noted in any case. Large squamoid cells formed between 5% and 100% of the total tumor volume. Small foci of necrosis were identified on histologic examination in 3/21 cases, and a larger necrotic area was seen in just 1 case. Rare psammoma bodies were present in 7 tumors.

A visible transition from areas with a papillary pattern containing groups of large squamoid cells (Figs. 7, 8) to a fully developed solid-alveolar pattern was seen in 9 tumors (Fig. 9). These former areas were characterized by the presence of well-developed papillae and tubules all lined by mostly cuboidal low-grade epithelial cells with round nuclei. Focally, tubulopapillary formations with glomeruloid morphology were also noted.

Of particular note was the presence of emperipolesis, a highly unusual phenomenon among renal cell tumors. It was easily identified in all 21 cases. Emperipolesis was present only in large squamoid cells and was a very prominent feature within solid squamoid islands in some cases (Figs. 10–12). In fact, it was a conspicuous morphologic feature in a majority of the cases.

One case (case 3) included metastatic neoplastic tissue from multiple foci on the peritoneal surface and omentum. The metastatic deposits showed a mostly solid-alveolar pattern with large squamoid cells (Fig. 13), rare psammoma bodies (Fig. 14), and absent emperipolesis.

Immunohistochemical data are summarized in Table 2. One of the cases were not available for immunohistochemical examination. All analyzable tumors were positive for CK7 (Fig. 15), EMA, and vimentin in

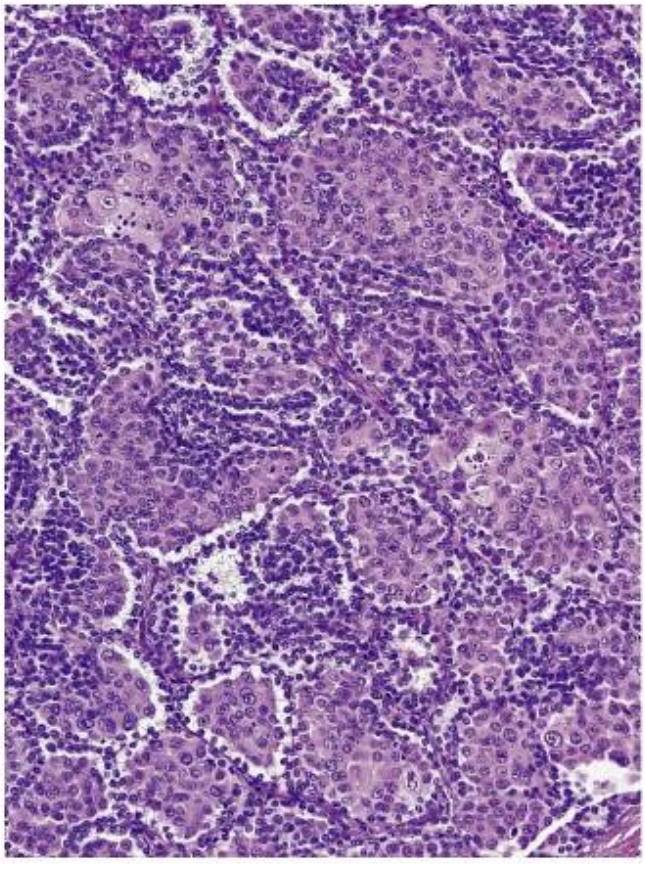

FIGURE 11. High-power magnification of squamoid cells with emperipolesis.

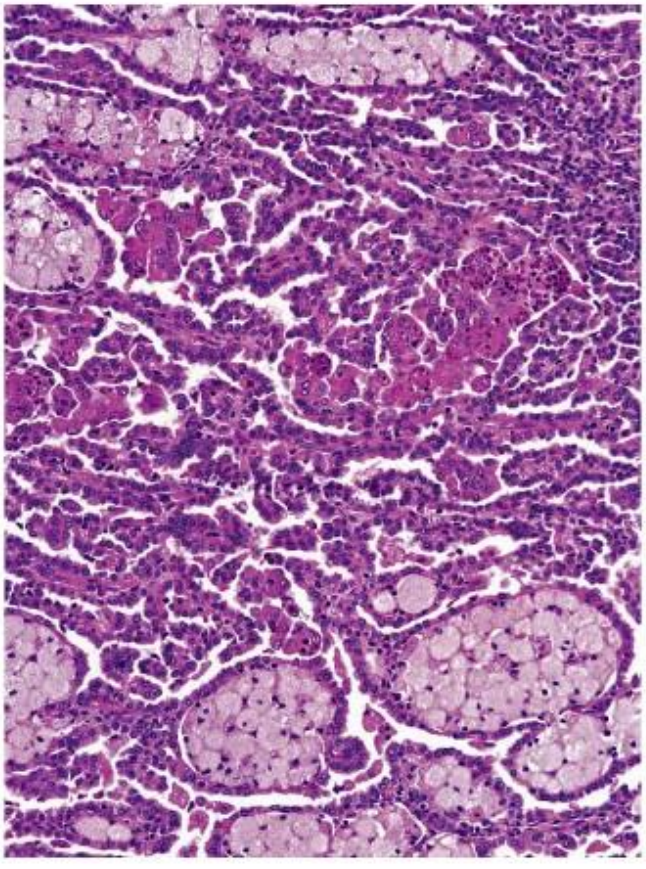

FIGURE 12. Similar to Figure 10. Emperipolesis in squamoid cells seen with foam cell macrophages intermingled among large squamoid cells.

both types of neoplastic cells. Nineteen of 21 cases were positive for cytokeratin AE1-AE3, and racemase (AMACR). All large squamoid cells expressed cyclin D1. There were no major differences among all 3 different antibodies against cyclin D1 (2 monoclonal and 1 polyclonal) (Figs. 16, 17). Large squamoid cells weakly expressed M30. All tumors were completely negative for TTF1, TFE 3, HMB45, and parvalbumin. Nineteen of 21 tumors were negative for CK 20, and 17/21 were negative for CD117 with documented positivity being focal, weak, and within the small-cell component.

Molecular-Genetic Data

Complete results of molecular genetic analyses, that is, aCGH and FISH, are summarized in Table 3. All analyzed samples (11/21) showed gains of chromosomes 7 and 17 (Fig. 18). Four of 5 analyzed male samples showed loss of chromosome Y. Additional gains of chromosome 20 were found in 3 of 5 analyzable cases using aCGH. Further chromosomal numerical changes including gain of chromosomes 16 and 12, loss of chromosome 21, and a loss of Xp22.33 were found in a single case.

DISCUSSION

Two cases of the so-called biphasic alveolo-squamoid renal carcinoma were reported in 2013.[1] Subsequently, 3 additional cases of the same tumor type were published in an abstract form in 2014.[1,2] The described tumors were composed of a distinctly dual cell population in which the larger tumor cells displayed squamoid features and formed round well-demarcated solid alveolar areas that, in large part, were surrounded by smaller neoplastic cells. Since publication of the above-mentioned paper, we have collected 20 additional cases from 12 institutions worldwide. In case 1 from Petersson et al's[1] paper, there was a very small, inconspicuous focus of papillary formation within the tumor. However, there were no other distinctive features to suggest the diagnosis of PRCC. Still we thought that the link of BSARCC and PRCC deserves to be explored.

PRCC is the second most frequently diagnosed RCC and is usually defined as a tumor derived from renal tubular epithelium with either papillary or tubule-papillary architecture. PRCC has traditionally been divided into 2 types. Type 1 PRCCs are mostly papillary, wherein the papillae are covered by cells with nuclei arranged in a single cell layer. The cells are relatively uniform with scant, pale, or basophilic cytoplasm and round nuclei. Type 2 is more polymorphic. Pseudostratification of nuclei is the key feature distinguishing type 2 from type 1 PRCC. PRCC type 2 usually has a higher nuclear grade, and cytoplasm is frequently eosinophilic.[5–7] A so-called

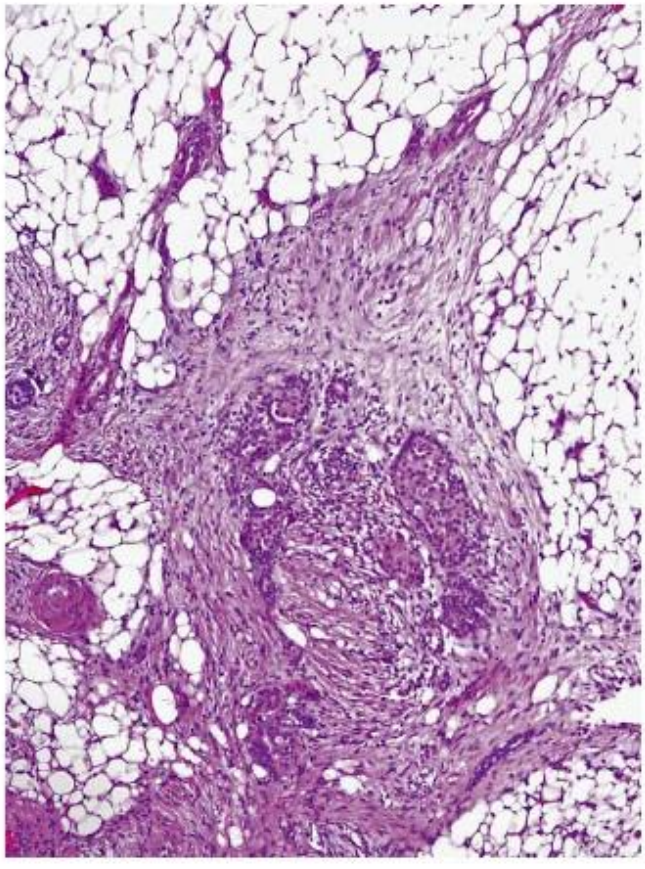

FIGURE 13. The metastatic deposits displayed a mostly solid alveolar pattern with large squamoid cells.

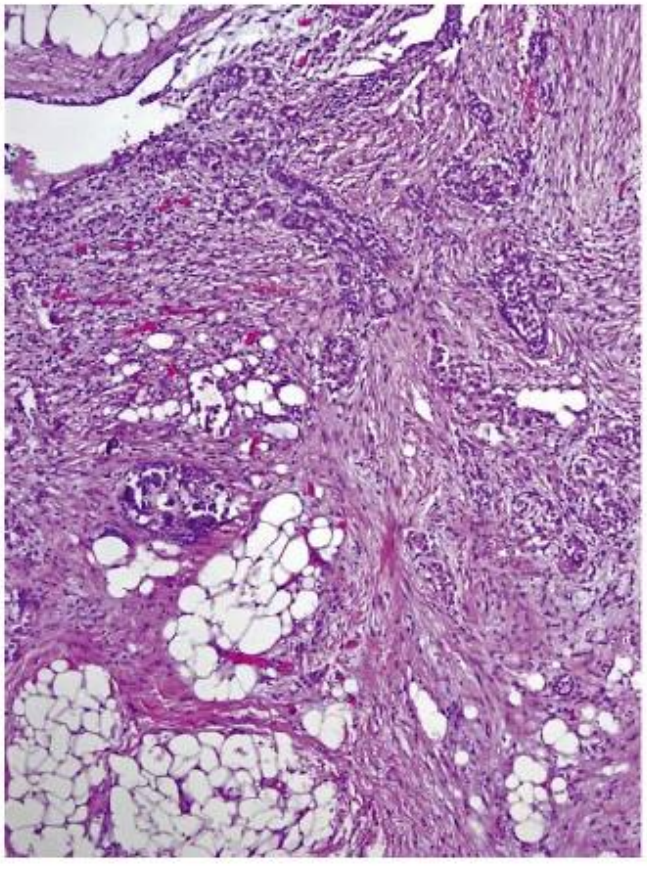

FIGURE 14. Rare psammoma bodies were present in metastases.

oncocytic variant of PRCC has also been described in the literature. These tumors are composed of cells with eosinophilic oncocytic cytoplasm, usually without pseudostratification of nuclei.[7–9] Some PRCCs are not easy to characterize as type 1, type 2, or oncocytic, and in such cases the diagnosis of PRCC, not otherwise specified, is usually established.

The fact that 10/21 cases of BSARCC exhibited components of classical PRCC suggests that BSARCC may be closely related to PRCC, or it may be a variant thereof with a peculiar and unusual morphology. The identified papillary component in these tumors was mostly compatible with type 1 PRCC according to Delahunt classification[5]; most papillae were covered by a single layer of smaller cells that had regular nuclei and scant cytoplasm.

In some areas the compression of papillae leads to the formation of tubulopapillary structures. Groups of larger, more pleomorphic cells with eosinophilic cytoplasm were found with such a pattern in the background. These larger cells displayed the same squamoid features seen in classical BSARCC and were immunohistochemically positive for cyclin D1. These transitional areas were either intermingled with areas exhibiting a more prominent biphasic pattern and with large areas of squamoid cells showing prominent emperipolesis or the transition between both patterns was in some cases more abrupt.

PRCC with large eosinophilic cells like the cases reported herein has been described in the literature previously. It is shown in Sternberg's Diagnostic Pathology textbook (page 1982, figure 42.20).[10] The same type of PRCC is illustrated for example in the paper written by Mantoan Padilha et al.[11] We believe that so-called PRCC with formation of glomeruloids could be an early stage and BSARCC late stage of 1 neoplastic lesion and that we can consider such morphology as opposite ends of the same morphologic spectrum.

FISH analysis showed gains of chromosomes 7 and 17 in all 11 analyzable cases. Loss of chromosome Y was detected in 4 of 5 male cases, which is in line with patterns found in PRCC.[12,13] aCGH revealed some additional chromosomal changes, the most frequent being gain of chromosome 20. Case 2, which has been presented by Petersson et al[1] revealed a different chromosomal aberration pattern (losses on chromosomes 2, 5, 6, 9, 12, 15,16, 17, 18, and 22, including biallelic loss of the CDKN2A locus, and gains on chromosomes 1, 5, 11, 12, and 13). This case, after careful reevaluation of all available blocks and materials, was excluded from the current study and was rediagnosed as unclassified RCC. Hence, the pattern of chromosomal numerical aberrations was very uniform in all analyzable cases in our current study and was fully compatible with a diagnosis of PRCC.[7,14]

TABLE 2. Results of Immunohistochemical Examinations

Case	CANH	MIB1/hpf	TTF1	WT1	Cath	TFE3	HMB45	p53	p63	AE1/3	EMA	CK7
1	+	2-3 SC 5-6 LC	À	À	À	À	À	À	À	À	+++	+ foc
2	À	0-1 SC 3-4 LC	À	À	À	À	À	À	À	+++	++	++
3	À	0-1 SC 4-6 LC	À	À	À	À	À	+ LC	À	+++ foc	+++ foc	+++
4	+	0-1	À	À	À	À	À	À	À	+++	+++ foc	+++
5	NP	NP	NP	NP	NP	NP	NP	NP	NP	NP	NP	NP
6	++	0-1 SC 2-3 LC	À	À	À	À	À	À	À	+++	+++	+++
7	+	0-2	À	À	À	À	À	++ LC	À	+++	+++	+++
8	++	0-1	À	+ foc.	À	À	À	À	À	+++ foc	+++	+++
9	++	0-1	À	À	À	À	À	À	À	+++ foc	+++	+++
10	++	0 SC 1-2 LC	À	À	À	À	À	À	À	+++	+++	+++
11	++	0 SC 1-2 LC	À	À	À	À	À	À	À	+++	+++	+++
12	À	0-1	À	À	À	À	À	À	À	+++	+++	+++
13	À	0 SC 3-6 LC	À	À	À	À	À	À	À	+++ foc	+++	+++
14	À	0-1	À	À	À	À	À	À	À	+++	+++	+++
15	À	0-1	À	À	À	À	À	À	À	+++	+++	+++
16	++LC	1-2 SC 4-7 LC	À	+ foc.	À	À	À	+	+ foc	+++	+++	+++
17	À	0-1	À	À	++ foc	À	À	+ foc	À	+++	+++	+++
18	À	0-1 SC 5-7 LC	À	À	À	À	À	+ LC	À	+++	+++	+++
19	À	0–1	À	À	À	À	À	À	À	+++	+++	++
20	À	0-1	À	À	À	À	À	+foc	À	+++	+++	+++
21	À	0-1 SC, 2-3 LC	À	À	À	À	À	À	À	++	+++	++

+++ indicates strong positivity; ++, intermediate positivity; +, weak positivity; À , negative; AE1/3, AE1-AE3; CANH, carbonic anhydrase 9; cath, cathepsin K; E-cadh, E-cadherin; foc, focal; hpf, high-power field (Â400); LC, large cells (squamoid); NP, not performed; parval, parvalbumin; SC, small cells; vim, vimentin.

Like in previous reports, we were not able to identify definitive morphologic proof of full squamous differentiation by light microscopy (intercellular bridges and/or keratin pearl formation) in any case.[1] Immunohistochemically, the absence of nuclear expression of p63 and only focal positivity with CK5/6 in 3/21 cases is in line with the light microscopic impression of “squamoid” rather than true squamous differentiation.

The presence of emperipolesis within the large squamoid cells is a very interesting phenomenon. Emperipolesis is defined as the presence of a non-neoplastic cell within the cytoplasm of another cell. An example of an entity featuring prominent emperipolesis is Rosai Dorfman disease.[15] Although the presence of emperipolesis is well recognized in several different tumorous entities, it is a highly unusual finding within RCCs. Emperipolesis was noted in all 21 cases and was a very prominent feature in some tumors. Staining with cyclin D1 proved helpful in revealing cells with emperipolesis, and such positivity was found exclusively in the large squamoid cell areas. Interestingly, cyclin D1 immunostaining has also proven helpful in disclosing cells with emperipolesis in cases of myxoinflammatory fibroblastic sarcomas.[16] Cyclin D1/PRAD 1, a cell cycle-related gene mapped to chromosome 11q13, has been found to be amplified in some breast cancers, certain squamous cell carcinomas of the head and neck and esophagus, several different lymphomas, etc.[17] Expression of cyclin D1 in RCCs has only recently been studied; Leroy et al[18] described overexpression of cyclin D1 in clear cell PRCC. Lima et al[19] looked at the prognostic significance of cyclin D1 expression in RCCs and concluded that high expression is associated with favorable prognosis. In addition, cyclin D1 has been used as part of the immunohistochemical panel for distinguishing between chromophobe RCC (CHRCC), clear cell RCC, and renal oncocytoma.[20] It seems that cyclin D1 positivity is one of the characteristic features of BSARCC; however, expression of cyclin D1 is not a specific diagnostic marker for BSARCC.

Differential Diagnosis

Squamoid differentiation described in all the 21 tumors of this series is one of the defining morphologic features of BSARCC. Generally speaking, squamous differentiation in RCC occurs extremely rarely. If ever found it should raise the possibility that particular tumor might be of urothelial origin. There have been several reports describing urothelial carcinoma within the kidney displaying squamous or squamoid features and even typical morphology of squamous carcinoma.[21–26] The present tumors differ, however, from such urothelial carcinomas: they were located inside the kidney parenchyma, and none of them was related to the urothelium of the renal pelvis or calices. No urothelial carcinoma in situ or urothelial dysplasia was detected in any of the current 21 cases. Thus we have excluded the possibility that the squamoid differentiation in BSARCC was related to squamous metaplasia of the urothelium.

Further evidence supporting the above interpretation was derived from the immunohistochemical data. Coexpression of CK7 and CK20 was noted within some large cells of the squamoid component in 1 case (case 7), but the small cells were completely negative for CK20. The vast majority of analyzable tumors were negative for CK20 in both cell components. Finally, we are not aware of any urothelial lesions with such a distinctly biphasic population of neoplastic cells in an organoid arrangement as seen in these renal tumors. Moreover, the cases with well-preserved

TABLE 2. (continued)

CyclinD1	CK20	CK5/6	CD10	AMACR	E-cadh	vim	Parval	CD117	M30	bcl2	PAX8
+++	ÀÀ		+++	++	À+++ foc À			À	++	foc.	++
+++	ÀÀ		À	+++	À++À			À	++	À	+
+++	ÀÀ		+ foc	+++	+ foc.+++À			À	++	À	+ dif
+++	ÀÀ		À	+++	+ foc.+++ foc À			À	+++	À	À
NP	NPNP		NP	NP	NPNPNP			NP	NP	NP	NP
+++	ÀÀ		À	+++	À+++À			À	+++	À	À
+++	++foc LC ++		À	+++	À+++À			À	+++	+SC	++
+++	ÀÀ		À	+++	++ foc.+++À			À	+++	À	+ dif.
+++	À++		À	+++	+++ foc.+++À			À	+	À	À
+++À	ÀÀ		À	À	+ foc.+++À			À	+++	À	+ dif.
+++	ÀÀ		À	+++	À+++À			À	++ foc.	+	+
+++	À++		À	+++	++ foc.+++ foc À			À	+++	À	+ foc.
+++	ÀÀ		À	+++	+++ foc.+++			À	+++	+++	++
+++	ÀÀ		À	+++	+ foc.+++À			À	++ foc.	+ dif.	+ dif
+++	ÀÀ		À	+++	+ foc.+++À			+	+++	À	+++
+++	ÀÀ		+foc ++	+++	+++++À			++ foc SC	+++	+foc.	++ foc
+++	ÀÀ		À	+++	++ foc+++À			+ foc SC	+++	+	+++
+++	ÀÀ		++ foc	+++	++ SC+++ LC +++À			À	++ dif	À	+
+++	ÀÀ		À	++	ÀSC+ LC+++À			À	+++ dif.	À	À
+++	ÀÀ		À	+++	À+++À			À	Foc +	+ foc	++
+++	ÀÀ		À	++	foc.++++À			À	À	À	++

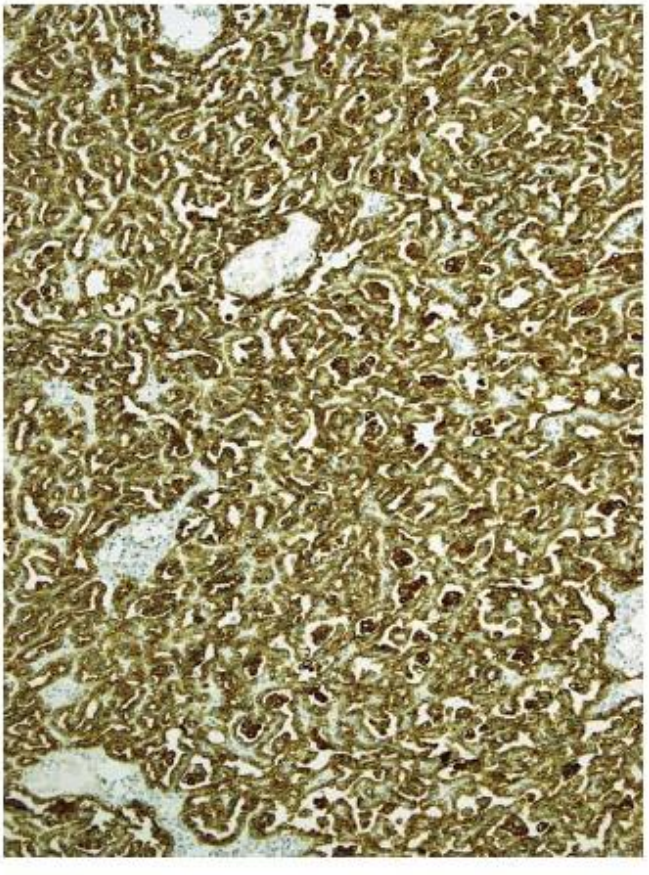

FIGURE 15. All tumors were positive for cytokeratin 7.

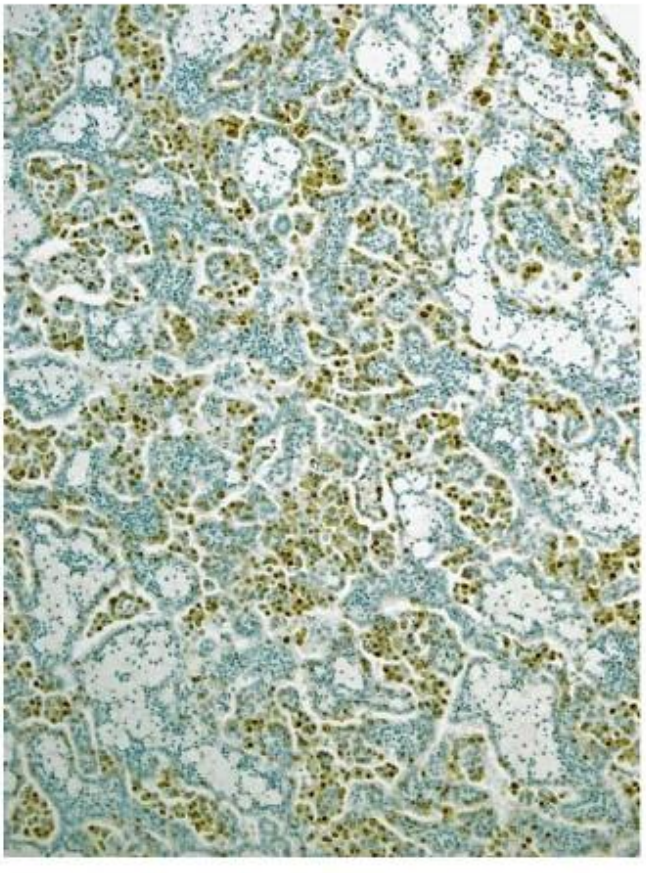

FIGURE 16. All large, squamoid cells expressed cyclin D1, reacting with both monoclonal antibodies (DAB-positive cells are brown).

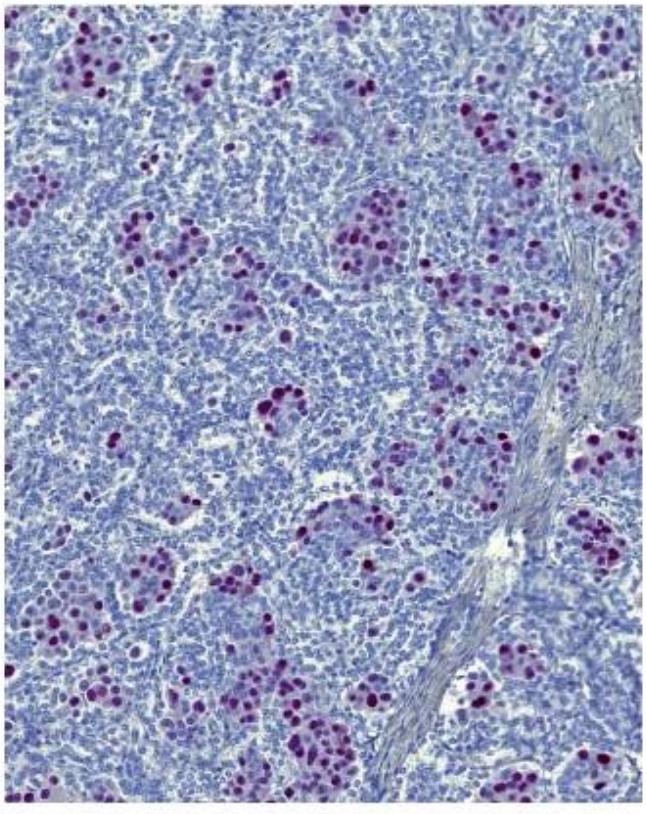

FIGURE 17. Squamoid cells were also positive with polyclonal antibody against cyclin D1 (alkaline phosphatase–positive cells are red).

DNA submitted to aCGH showed gains of chromosomes 7 and 17, which is suggestive of a connection to PRCC rather than urothelial carcinoma.

TABLE 3. Results of aCGH and FISH Analysis

Case	Sex	aCGH Result	CEP 7	CEP 17	CEP XY
1	M	NA	NA	NA	NA
2	M	NA	NA	NA	NA
3	F	+7, +17, +20, À 21	P	P	XX
4	F	NA	P	P	XX
5	F	NA	NA	NA	NA
6	M	NA	NA	NA	NA
7	F	NA	P	P	XX
8	F	+7, +16, +17	P	P	XX
9	M	NA	NA	NA	NA
10	M	+7, +17, ÀXp22.33, X-	P	P	X-
11	F	+7, +12, +17, +20	P	P	XX
12	F	+7, +17, +20	P	P	XX
13	F	NA	NA	NA	NA
14	M	NA	NA	NA	NA
15	F	NA	NA	NA	XX
16	M	NA	P	P	X-
17	M	NA	NA	NA	NA
18	M	NA	P	P	XY
19	M	NA	P	P	X-
20	M	NA	P	P	X-
21	F	NA	NA	NA	NA

CEP indicates centromeric probe; F, female; M, male; NA, not analyzable; P, polysomy; X-, loss of chromosome Y.

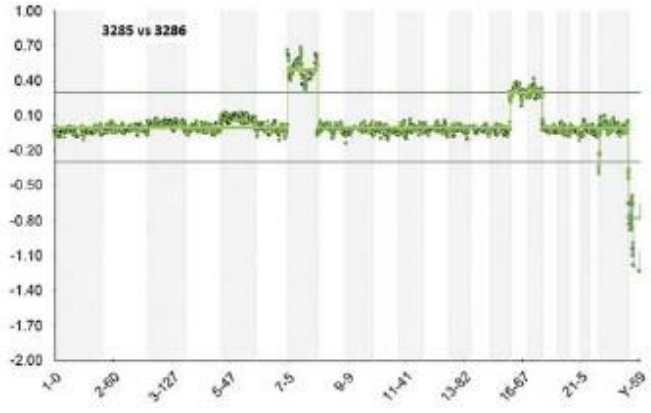

FIGURE 18. Gains of chromosomes 7 and 17 and losses of chromosomes 21 (variable) and Y were detected by aCGH analysis.

Squamous differentiation has been reported in RCC, but it seems to be a very rare phenomenon. Practically all RCCs with such morphology reported in the literature were CHRCCs with sarcomatoid transformation.[27–29] The cases presented here differ from CHRCC not only by morphology but also by their immunohistochemical and chromosomal profiles. There are 2 main variants of CHRCC that have been recognized: classical and eosinophilic.[30] Microscopically, these tumors are described as mostly solid or solid alveolar. However, the morphologic spectrum has been expanded to include microcystic, oncocytoma-like, adenomatoid, and tumors with neuroendocrine differentiation, and papillary arrangements.[31–37] There were no leaf-like cells or small eosinophilic cells present within the included tumors, and we were not able to identify raisinoid nuclei with perinuclear clearing typical of CHRCC. The sarcomatoid transformation seen in some CHRCCs has not been seen in our cases. The immunohistochemical profile of these cases differed from that of CHRCC. In this respect it is most important to note that CD117 was negative in 17/21 cases, and vimentin was positive in all analysable cases, which excludes the diagnosis of CHRCC. CD117 was only weakly positive within a small cell population of the 2 cases not counted above. CHRCCs are usually further characterized by multiple chromosomal losses of chromosomes 1, 2, 6, 10, 13, 17, and 21 in both classic and eosinophilic CHRCC.[30] Other studies also report numerical gains of chromosomes 4, 7, 15, 19, and 20,[4,38,39] but the significance of these findings is still a topic of discussion. The molecular genetic findings in all analyzed cases in this paper are completely different from the profiles identified in CHRCCs.

From the available clinical data, it is evident that BSARCC has metastatic potential. The morphology of the metastatic neoplasms did not differ significantly from that of the primary tumors, and it could be possible, albeit difficult, to recognize this unique pattern within a metastatic lesion even without information about the morphology of the primary tumor.

REFERENCES

1. Petersson F, Bulimbasic S, Hes O, et al. Biphasic alveolosquamoid renal carcinoma: a histomorphological, immunohistochemical, molecular genetic, and ultrastructural study of a distinctive morphologic variant of renal cell carcinoma. Ann Diagn Pathol. 2012;16:459–469.
2. Coromias Cishek A, Gonzalez M, Caamano V, et al. Biphasic alveolo-squamoid renal cell carcinoma (BASRC): light and immunohistochemical study of 3 cases. Virchows Arch. 2014;465(suppl 1): S157.
3. Van Dongen JJ, Langerak AW, Bruggemann M, et al. Design and standardization of PCR primers and protocols for detection of clonal immunoglobulin and T-cell receptor gene recombinations in suspect lymphoproliferations: report of the BIOMED-2 Concerted Action BMH4-CT98-3936. Leukemia. 2003;17:2257–2317.
4. Sperga M, Martinek P, Vanecek T, et al. Chromophobe renal cell carcinoma—chromosomal aberration variability and its relation to Paner grading system: an array CGH and FISH analysis of 37 cases. Virchows Arch. 2013;463:563–573.
5. Delahunt B, Eble JN. Papillary renal cell carcinoma: a clinicopathologic and immunohistochemical study of 105 tumors. Mod Pathol. 1997;10:537–544.
6. Delahunt B, Eble JN, McCredie MR, et al. Morphologic typing of papillary renal cell carcinoma: comparison of growth kinetics and patient survival in 66 cases. Hum Pathol. 2001;32:590–595.
7. Srigley JR, Delahunt B, Eble JN, et al. The International Society of Urological Pathology (ISUP) Vancouver Classification of Renal Neoplasia. Am J Surg Pathol. 2013;37:1469–1489.
8. Lefevre M, Couturier J, Sibony M, et al. Adult papillary renal tumor with oncocytic cells: clinicopathologic, immunohistochemical, and cytogenetic features of 10 cases. Am J Surg Pathol. 2005;29: 1576–1581.
9. Hes O, Brunelli M, Michal M, et al. Oncocytic papillary renal cell carcinoma: a clinicopathologic, immunohistochemical, ultrastructural, and interphase cytogenetic study of 12 cases. Ann Diagn Pathol. 2006;10:133–139.
10. Mills SE, Greenson JK, Hornick JL, et al, eds. Sternberg's Diagnostic Surgical Pathology, 6 ed. Philadelphia: Wolters Kluwer; 2015:2703.
11. Mantoan Padilha M, Billis A, Allende D, et al. Metanephric adenoma and solid variant of papillary renal cell carcinoma: common and distinctive features. Histopathology. 2013;62:941–953.
12. Kovacs G, Fuzesi L, Emanual A, et al. Cytogenetics of papillary renal cell tumors. Genes Chromosomes Cancer. 1991;3:249–255.
13. Jiang F, Richter J, Schraml P, et al. Chromosomal imbalances in papillary renal cell carcinoma: genetic differences between histological subtypes. Am J Pathol. 1998;153:1467–1473.
14. Eble JN, Sauter G, Epstein JI, et al. WHO Classification of Tumours Tumours of the Urinary System and Male Genital Organs Pathology and Genetics. Lyon: IARC Press; 2004:359.
15. Foucar E, Rosai J, Dorfman R. Sinus histiocytosis with massive lymphadenopathy (Rosai-Dorfman disease): review of the entity. Semin Diagn Pathol. 1990;7:19–73.
16. Michal M, Kazakov DV, Hadravsky L, et al. High-grade myxoinflammatory fibroblastic sarcoma: a report of 23 cases. Ann Diagn Pathol. 2015;19:157–163.
17. Zhang SY, Caamano J, Cooper F, et al. Immunohistochemistry of cyclin D1 in human breast cancer. Am J Clin Pathol. 1994;102: 695–698.
18. Leroy X, Camparo P, Gnemmi V, et al. Clear cell papillary renal cell carcinoma is an indolent and low-grade neoplasm with overexpression of cyclin-D1. Histopathology. 2014;64:1032–1036.
19. Lima MS, Pereira RA, Costa RS, et al. The prognostic value of cyclin D1 in renal cell carcinoma. Int Urol Nephrol. 2014;46: 905–913.
20. Zhao W, Tian B, Wu C, et al. DOG1, cyclin D1, CK7, CD117 and vimentin are useful immunohistochemical markers in distinguishing chromophobe renal cell carcinoma from clear cell renal cell carcinoma and renal oncocytoma. Pathol Res Pract. 2015;211: 303–307.
21. Mardi K, Kaushal V, Sharma V. Rare coexistence of keratinizing squamous cell carcinoma with xanthogranulomatous pyelonephritis in the same kidney: report of two cases. J Cancer Res Ther. 2010;6: 339–341.
22. Bhaijee F. Squamous cell carcinoma of the renal pelvis. Ann Diagn Pathol. 2012;16:124–127.
23. Zainuddin MA, Hong TY. Primary renal adenosquamous carcinoma. Urol Ann. 2010;2:122–124.
24. Terada T. Synchronous squamous cell carcinoma of the kidney, squamous cell carcinoma of the ureter, and sarcomatoid carcinoma of the urinary bladder: a case report. Pathol Res Pract. 2010; 206:379–383.
25. Holmang S, Lele SM, Johansson SL. Squamous cell carcinoma of the renal pelvis and ureter: incidence, symptoms, treatment and outcome. J Urol. 2007;178:51–56.
26. Perez-Montiel D, Wakely PE, Hes O, et al. High-grade urothelial carcinoma of the renal pelvis: clinicopathologic study of 108 cases with emphasis on unusual morphologic variants. Mod Pathol. 2006; 19:494–503.
27. Mete O, Kilicaslan I, Ozcan F, et al. Sarcomatoid chromophobe renal cell carcinoma with squamous differentiation. Pathology. 2007; 39:598–599.
28. Viswanathan S, Desai SB, Prabhu SR, et al. Squamous differentiation in a sarcomatoid chromophobe renal cell carcinoma: an unusual case report with review of the literature. Arch Pathol Lab Med. 2008;132:1672–1674.
29. Husain AEBJ, Trpkov K. Composite chromophobe renal cell carcinoma with sarcomatoid differentiation containing osteosarcoma, chondrosarcoma, squamous metaplasia and associated collecting duct carcinoma: a case report. Anal Quant Cytopathol Histopathol. 2014;36:235–240.
30. Brunelli M, Eble JN, Zhang S, et al. Eosinophilic and classic chromophobe renal cell carcinomas have similar frequent losses of multiple chromosomes from among chromosomes 1, 2, 6, 10, and 17, and this pattern of genetic abnormality is not present in renal oncocytoma. Mod Pathol. 2005;18:161–169.
31. Hes O, Vanecek T, Perez-Montiel DM, et al. Chromophobe renal cell carcinoma with microcystic and adenomatous arrangement and pigmentation—a diagnostic pitfall. Morphological, immunohistochemical, ultrastructural and molecular genetic report of 20 cases. Virchows Arch. 2005;446:383–393.
32. Dundr P, Pesl M, Povysil C, et al. Pigmented microcystic chromophobe renal cell carcinoma. Pathol Res Pract. 2007;203: 593–597.
33. Parada DD, Pena KB. Chromophobe renal cell carcinoma with neuroendocrine differentiation. APMIS. 2008;116:859–865.
34. Kuroda N, Tamura M, Hes O, et al. Chromophobe renal cell carcinoma with neuroendocrine differentiation and sarcomatoid change. Pathol Int. 2011;61:552–554.
35. Kuroda N, Liyama T, Moriki T, et al. Chromophobe renal cell carcinoma with focal papillary configuration, nuclear basaloid arrangement and stromal osseous metaplasia containing fatty bone marrow element. Histopathology. 2005;46:712–713.
36. Ohe C, Kuroda N, Keiko M, et al. Chromophobe renal cell carcinoma with neuroendocrine differentiation/morphology: a clinicopathological and genetic study of three cases. Hum Pathol. 2014;1:31–39.
37. Kuroda N, Tanaka A, Yamaguchi T, et al. Chromophobe renal cell carcinoma, oncocytic variant: a proposal of a new variant giving a critical diagnostic pitfall in diagnosing renal oncocytic tumors. Med Mol Morphol. 2013;46:49–55.
38. Vieira J, Henrique R, Ribeiro FR, et al. Feasibility of differential diagnosis of kidney tumors by comparative genomic hybridization of fine needle aspiration biopsies. Genes Chromosomes Cancer. 2010; 49:935–947.
39. Tan MH, Wong CF, Tan HL, et al. Genomic expression and single-nucleotide polymorphism profiling discriminates chromophobe renal cell carcinoma and oncocytoma. BMC Cancer. 2010;10:196.

3.4 Solid papillary renal cell carcinoma: clinicopathologic, morphologic, and immunohistochemical analysis of 10 cases and review of the literature

Solidní PRCC je v literatuře jen zřídka popisovaným subtypem PRCC, který nezapadá do tradičně uznávaného konceptu dělení PRCC na typ 1 a typ 2. Tyto nádory sestávají z monomorfních epiteliálních buněk s malým množstvím cytoplasmy a malými jádry. Nádorové buňky jsou uspořádány do drobných komprimovaných tubulů a krátkých abortivních papil, což dává tumoru charakteristický solidní vzhled (s/bez přítomnosti pravých papilárních struktur, které pokud jsou v nádoru přítomny, nejsou četné). Tyto neoplasie vykazují imunohistochemické (pozitivita imunohistochemických barvení CK7, EMA, AMACR) i molekulárně genetické znaky (polysomie/trisomie chromosomů 7 a 17, ztráta chromosomu Y u mužů) typicky přisuzované „konvenčnímu" PRCC. V literatuře pak bylo doposud popsáno celkem 53 případů solidních PRCC, s predominancí postižení mužů a věkovým rozmezím pacientů 17-82 let. Z literatury je též evidentní, že tyto nádory mají příznivý klinický průběh.

Z archivu Plzeňského registru nádorů, čítajícího 1311 nádorů klasifikovaných jako PRCC, bylo vyhledáno 10 nádorů, kompatibilních s diagnózou solidního PRCC. Ve všech případech se jednalo o nádory mužů, věkové rozmezí pacientů 34-70 let. Téměř u všech nádorů byl stage onemocnění pT1 dle TMN 2009 (pouze jeden případ byl ve stádiu pT3). Velikost tumorů se pohybovala v rozmezí 1,4-5,5 cm (průměr 3,32 cm). V rámci dispenzarizace, follow-up byl dostupný u všech 10 pacientů (v délce trvání 3-13 let). Osm pacientů bylo po úvodní chirurgické léčbě dlouhodobě bez známek recidivy či generalizace onemocnění, u jednoho pacienta byla diagnostikována rekurence tumoru a jeden pacient po úvodní oboustranné nefrektomii pro četné drobné PRCCs zemřel do tří let od stanovení diagnózy (na generalizaci onemocnění). Makroskopicky byly tumory dobře ohraničené, bělavožluté, s lehce granulárním povrchem. Mikroskopicky byla dominantním histologickým znakem přítomnost solidní architektoniky, avšak při detailní morfologické analýze byly kromě „opravdových" solidních okrsků zastiženy i okrsky s komprimovanými, krátkými abortivními papilami a komprimované tubuly (tyto okrsky do sebe vzájemně přecházely). Přítomnost „pravých" papil byla relativně raritním nálezem. Všechny nádory byly silně difúzně pozitivní v imunohistochemickém barvení CK7 a naopak negativní v průkazu WT-1.

Solidní PRCC je vzácným nádorem (s incidencí výskytu onemocnění méně než 1% všech RCC). Imunohistochemický a molekulárně genetický profil lézí je kompatibilní s profilem typicky přisuzovaným „konvenčnímu" PRCC. Diferenciálně diagnosticky mají tyto nádory svým morfologickým vzhledem relativně blízko k metanefrickému adenomu a epiteloidnímu nefroblastomu, méně pak k MTSCC a OPRCC.

Annals of Diagnostic Pathology 23 (2016) 51–57

Contents lists available at ScienceDirect

Annals of Diagnostic Pathology

Solid papillary renal cell carcinoma: clinicopathologic, morphologic, and immunohistochemical analysis of 10 cases and review of the literature

Monika Ulamec [a,b], Faruk Skenderi [c], Kiril Trpkov [d], Bozo Kruslin [a,b], Semir Vranic [c], Stela Bulimbasic [b,e], Sandra Trivunic [f], Delia Perez Montiel [g], Kvetoslava Peckova [h], Kristyna Pivovarcikova [h], Ondrej Ondic [h], Ondrej Daum [h], Pavla Rotterova [h], Martin Dusek [h], Milan Hora [i], Michal Michal [h], Ondrej Hes [h,□]

[a] Ljudevit Jurak Pathology Department, Clinical Hospital Center Sestre milosrdnice, Zagreb, Croatia
[b] Pathology Department, Medical University, Medical Faculty Zagreb, Croatia
[c] Department of Pathology, Clinical Centre of the University of Sarajevo, Sarajevo, Bosnia and Herzegovina
[d] Department of Pathology, Calgary Laboratory Services and University of Calgary, Calgary, AB, Canada
[e] Department of Pathology, Clinical Hospital Center Zagreb, Zagreb, Croatia
[f] Department of Pathology, Medical Faculty, University of Novi Sad, Serbia
[g] Department of Pathology, Institute Nacional de Cancerologia, Mexico City, Mexico
[h] Department of Pathology, Charles University, Medical Faculty and Charles University Hospital Plzen, Czech Republic
[i] Department of Urolology, Charles University, Medical Faculty and Charles University Hospital Plzen, Czech Republic

article info

Keywords:
Kidney
Solid
Papillary renal cell carcinoma
Review
Differential diagnosis

abstract

Solid papillary renal cell carcinoma is rarely reported in the literature, and its tumor characteristics are not entirely compatible with the concept of 2 histological subtypes of papillary renal cell carcinoma (PRCC). Tumor is composed mostly of small compressed tubules and short abortive papillae giving solid appearance of monomorphic epithelial cells with scanty cytoplasm and small nuclei, sometimes mimicking spindle cells, without or with sparse true papillae. It shows immunohistochemical (+ CK7, + EMA, + AMACR) and genetic hallmarks (polysomy/trisomy 7/17, loss of Y) of conventional PRCC. About 53 cases have been described in the literature, with male predominance and age ranging from 17 to 82 years. By available follow-up data, solid PRCC has a favorable clinical course. We describe 10 cases compatible with the diagnosis of solid PRCC. All patients were males age range was from 34 to 70 years, and all but one were pT1 according to TNM 2009. On follow-up, 9 patients were without evidence of disease, and 1 had recurrent tumor. Size of the tumor ranged from 1.4 to 5.5 cm (mean, 3.32 cm). Tumors were well-circumscribed whitish to yellow masses with granular surface. Although solid architecture was a prominent morphologic feature, detailed analysis revealed that the tumors were composed of compressed short abortive papillae and compressed tubules admixed with true solid areas. Well-formed papillae were exceptionally present. All 10 cases were strongly and diffusely positive for CK7 and negative for WT-1. In conclusion, solid PRCC is a rare tumor with an incidence of less than 1% of all renal tumors. In majority of the cases, tumors were composed of tightly compressed tubular structures and short abortive papillae that render a solid morphologic appearance. Immunohistochemical and molecular features do not differ from conventional PRCC. Metanephric adenoma; epithelioid nephroblastoma; and, rarely, mucinous tubular and spindle cell carcinoma and oncocytic variant of PRCC should be considered in the differential diagnosis.

1. Introduction

Papillary renal cell carcinoma (PRCC) was first formally recognized as a specific entity in the Heidelberg classification, and then it was accepted in the 2004 World Health Organization (WHO) classification [1–2]. It was described as a malignant renal tumor with characteristic papillary or tubulopapillary architecture and with specific immunohistochemical and cytogenetic profile. PRCC is the second most common renal cell carcinoma (RCC) subtype occurring in up to 18.5% of all RCCs [3–5]. The description of PRCC dates back to 1974 in the study of Mancilla-Jimenez et al [6]. The authors reported in detail the ultrasonographic, macroscopic, and microscopic features of PRCC and recognized 2 consistent histologic patterns, namely, the papillae lined either by a single row of cells with scant cytoplasm or cells with pseudostratifed nuclei and abundant eosinophilic cytoplasm. Besides these 2 patterns,

Disclosure of conflict of interest: All authors declare no conflict of interest
The study was supported by the Charles University Research Fund (project number P36) and by project CZ.1.05/2.1.00/03.0076 from the European Regional Development Fund.
□ Corresponding author at: Department of Pathology, Charles University, Medical Faculty and Charles University Hospital Plzen, Alej Svobody 80, 304 60 Pilsen, Czech Republic.
E-mail address: hes@medima.cz (O. Hes).

http://dx.doi.org/10.1016/j.anndiagpath.2016.04.008
1092-9134/

Table 1
Clinicopathological features and follow-up of solid PRCC

Case	Age (y)	Sex	Size (cm)	Follow-up
1	49	M	5.5	NED-8 y
2	70	M	1.5	DOC-3 y[a]
3	37	M	3.5	NED
4	66	M	2.5	NA
5	60	M	4.5	NED
6	54	M	2.8	NED-5 y
7	63	M	4	NED
8	34	M	2.5	NED-13 y
9	52	M	1.4	NED-9.5 y
10	48	M	5	AWD-8 y[b]

NED, no evidence of desease; DOC, dead for other reasons; NA, not available; AWD, alive with desease.
[a] Bilateral nephrectomy for PRCCs; dead for metastatic prostate cancer 3 years later; MSCT during follow-up diagnostics showed nephrectomy area without tumor.
[b] Only T3N0Mx tumor, recidivant tumor after 8 years, placed in the prior nephrectomy area.

they also reported papillary tumors with clear cells and other morphological features. PRCCs were later characterized in more details in several studies [7–9]. In 2004, the WHO classification adopted 2 types of PRCC: type 1, with papillae lined by a single cell layer of cuboidal cells with scant cytoplasm, and type 2, in which papillae are lined by large eosinophilic cells with pseudostratified nuclei [2]. Although less frequently encountered, several additional patterns were subsequently reported in the literature, including oncocytic [10–11], PRCC with clear cells [12], and solid PRCC. Solid variant of PRCC is composed of monomorphic epithelial cells with scant cytoplasm and small nuclei, arranged in tightly packed, ill-defined tubules or papillae and solid sheets [3,13–18]. It closely resembles metanephric adenoma (MA) and may share similar morphologic features with epitheloid nephroblastoma or mucinous tubular and spindle cell carcinoma (MTSC).

In this study, we describe a series of 10 cases collected from multiple institutions, and we discuss the diagnostic pitfalls and the differential diagnosis of the solid form of PRCC.

2. Material and methods

Ten cases compatible with the diagnosis of solid PRCC were retrieved out of 1311 papillary RCCs (including institutional, consultation, and archive cases) in the Pilsen Tumor Registry. Pathologic examination of all available hematoxylin and eosin–stained sections from each case (range, 1-18 slides) was performed by at least 3 pathologists (MU, FS, and OH). Cases were reevaluated, and solid, tubular, and papillary components were accessed as percentage of the tumor. Tissue for light microscopy was fixed in 4% formaldehyde and embedded in paraffin using routine procedures. Three-micrometer thin sections were cut and stained with hematoxylin and eosin to evaluate the architecture of the tumors. Basal membranes were highlighted by periodic acid Schiff (PAS) stain.

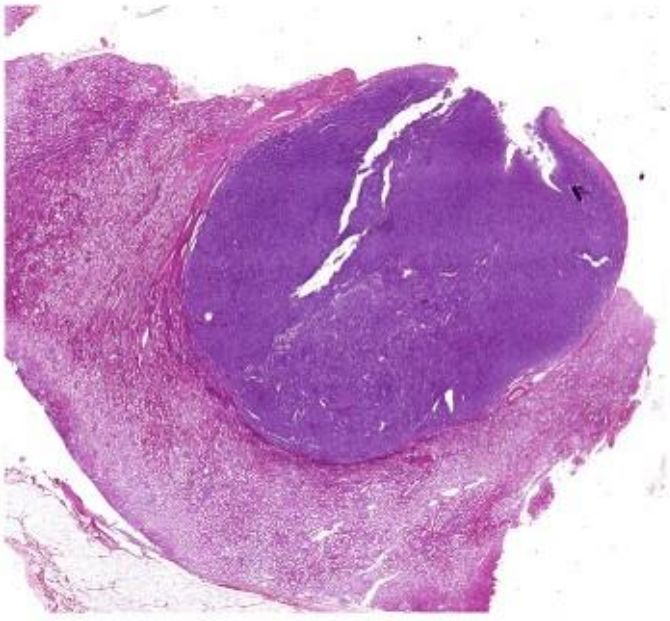

Fig. 1. Using scanning magnification, most of the tumors appeared completely solid.

The immunohistochemical study was performed using a Ventana Benchmark XT automated stainer (Ventana Medical System, Inc, Tucson, AZ).

The following primary antibodies were used in the immunohistochemical study: racemase/AMACR (13H4, monoclonal, DAKO, Glostrup, Denmark, 1:200), cytokeratin 7 (OV-TL12/30, monoclonal, DakoCytomation, Carpenteria CA, 1:200), epithelial membrane antigen (EMA) (E29, monoclonal, DakoCytomation, 1:1000), CD10 (monoclonal, Sp67, Ventana, RTU), CD34 (QBEnd-10, monoclonal, Dako, 1:100), CD57(NK 1, Leica Biosystems, Newcastle upon Tyne, UK, 1:200), WT1 (GF-H2, monoclonal, DakoCytomation, 1:150), Ki-67 (MIB1, monoclonal, Dako, 1:1000). Appropriate positive and negative controls were used. Immunostains were scored as 1+ (focal in small clusters of individual cells), 2+ (up to 50% positive cells), and 3+ (diffuse strong positivity in more than 50% of cells).

3. Results

The clinicopathologic data are summarized in Table 1. The age of the patients ranged from 34 to 70 years (mean age, 53.30); all patients were male. Size of the tumor in the largest diameter ranged from 1.4 to 5.5 cm (mean, 3.32 cm). Most of the cases were pT1 stage (TNM 09); 1 tumor was pT3. Most of the patients (8/10) were alive and well without signs of metastatic disease or relapse within follow-up period of 3-13 years. One patient was faced with recurrent tumor 8 years after resection. One patient had bilateral nephrectomy due to multiple small PRCCs and died of metastatic prostate cancer 3 years later.

Table 2
Gross and microscopic features of solid PRCC

Patient	Gross description	True solid (%)	Compressed tubuli (%)	Compressed abortive papillae; occasional glomeruloid formations (%)	True papillae (%)	Capsule	ISUP grade
1	Yellow well-circumscribed nodule	10	40	50	0	+	1
2	Yellow well-circumscribed nodule, bilateral papillary RCCs	20	70	10	0	+	1
3	Gray well-circumscribed nodule	5	80	10	5	+	2
4	Yellow well-circumscribed nodule	80	10	5	5	+	1
5	Gray well-circumscribed nodule	20	30	50	0	−	1
6	Yellow well-circumscribed nodule	5	10	80	5	+	1
7	Yellow well-circumscribed nodule	20	70	10	0	+	1
8	Yellow well-circumscribed nodule	10	50	40	0	−/+	1
9	Yellow well-circumscribed nodule	30	10	60	0	+	1
10	Yellow well-circumscribed nodule, necrotic −50%	60	20	20	0	+	2

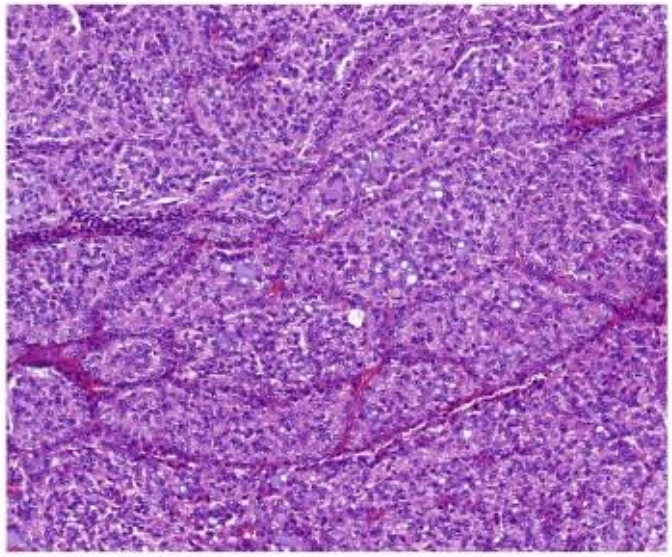

Fig. 2. Only 2 cases from our series were mostly arranged in solid-alveolar pattern.

Morphologic features are summarized in Table 2. Macroscopically, tumors were well-circumscribed yellow to white homogeneous nodules, sometimes with fine-granulated surface. One tumor showed necrotic area in up to 50% of the tumor.

Nine tumors were encapsulated. Using scanning magnification, most of the tumors appeared completely solid (Fig. 1), but on closer examination, true solid areas comprised 5% to 80% of the tumor. On high power and using PAS staining, only 2 tumors were mostly solid (60% and 80% of the tumors, respectively, comprised solid areas) (Fig. 2). Four tumors were composed mostly of compressed tubules (between 50% and 80% of the 2 tumors) (Fig. 3A and B), whereas the remaining 4 were composed mostly of compressed abortive papillae with occasional glomeruloid formations (between 50% and 80% of these contained compressed abortive papillae) (Fig. 4). True papillae with fibrovascular cores were found in 3 cases in up to 5% of the tumor. Tumor cells had scant cytoplasm and small, round to elongated nuclei with occasional nuclear grooves (International Society of Urological Pathology [ISUP] nucleolar grade was 1 or 2) (Fig. 5). In all but 1 case, the cells with scant but eosinophilic cytoplasm were also focally found. Small foci of tubules with cells showing sparse but clear cytoplasm were found in 2 cases.

The immunohistochemistry results are summarized in Table 3. All 10 cases were strongly and diffusely positive for CK7 (Fig. 6) and negative for WT-1. AMACR was diffusely positive in 9 cases (Fig. 7). EMA was positive diffusely in 8 cases and focally in 2. Vimentin was diffusely positive in 6 cases, and 4 were positive focally (less than 50% of cells). CD10 was focally positive in 4 cases. CD57 showed weak and focal positivity in 1 case. Proliferation activity was less than 2% in all tumors using Ki-67 labeling.

4. Discussion and review of the literature

4.1. Clinical and pathological characteristics

So-called solid PRCC, as a part of the morphologic PRCC spectrum, has been described for the first time by Renshaw et al [13]. The incidence was less than 1% of all renal tumors [3], and this estimation corresponds with the proportion of solid PRCCs in this series. In our study, the incidence was actually 0.76% of all PRCCs in the Pilsen Tumor Registry.

In toto, about 53 cases have been described in the literature with tumors showing distinctive solid PRCC features. The data from the English literature are summarized in Table 4. There is a male predominance, with a male to female ratio of 3.5:1. Age at time of diagnosis was from 17 to 82 years. The follow-up data are however limited, and it seems that solid PRCC has favorable clinical course. Most cases were classified as pT1 tumors, with nuclear grade up to 2, according to Fuhrman grading system [3,13–19]. In our study, the age range was from 34 to 70 years (mean age, 53.3), and all patients were male. The largest tumor size ranged from 1.4 to 5.5 cm (mean, 3.3 cm), which is similar to the previously published data. Nine of our cases were pT1 stage (TNM 09). One case was pT3 and demonstrated infiltration through the renal capsule with invasion into the perirenal fat. This patient had recurrent tumor after 8 years. Seven of the 10 cases were without evidence of disease during the follow-up from 3 to 13 years. One patient had multiple small PRCCs and died of metastatic prostate cancer 3 years later.

In the previous studies, the tumors were well-circumscribed, solid, homogeneous, and nodular masses, grayish white in color and located in the renal cortex. Hemorrhage and necrosis in the central areas were also described, as well as presence of multifocal tumors [13,16–17]. In this study, the tumors represented well-circumscribed solid nodules, mostly yellow in color and often showing finely granular cut surface. In 1 case, multifocal, bilateral PRCCs were found, together with the solid PRCC. Abundant necrosis was found in only 1 case.

Solid PRCC is typically composed of cells with scant cytoplasm and small, round to elongated nuclei, cytologically resembling type 1 PRCC. The cells are organized in solid sheets or tubular structures that are tightly packed, sometimes mimicking spindle cells, with no true papillae and lacking fibrovascular stalks. Some tumors may exhibit completely

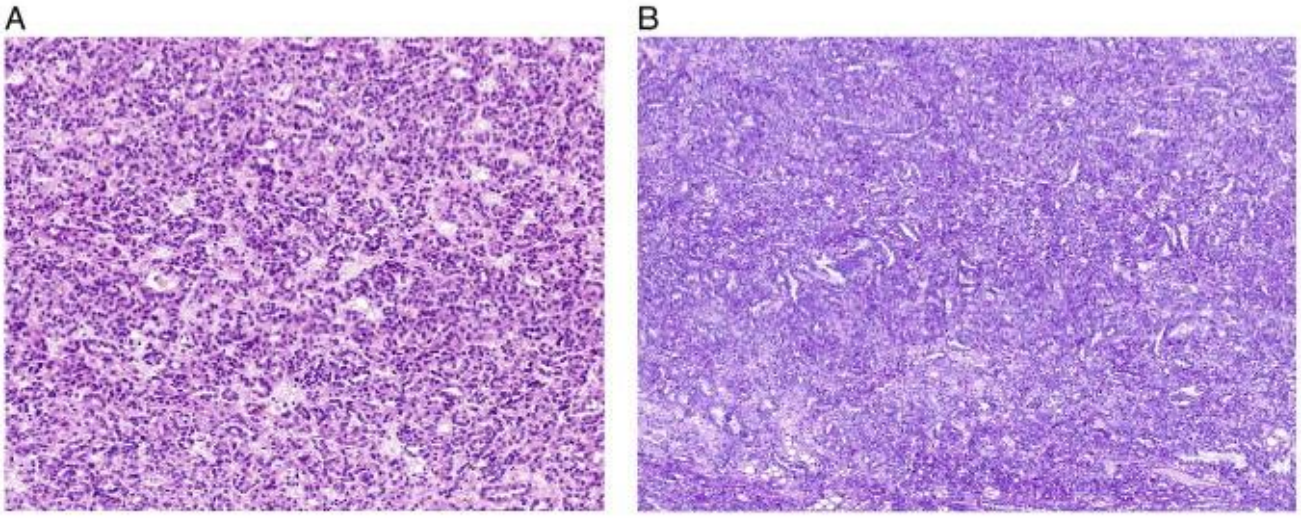

Fig. 3. (A) Four tumors were composed of small tubules. (B) Predominantly tubular architecture highlighted by PAS staining.

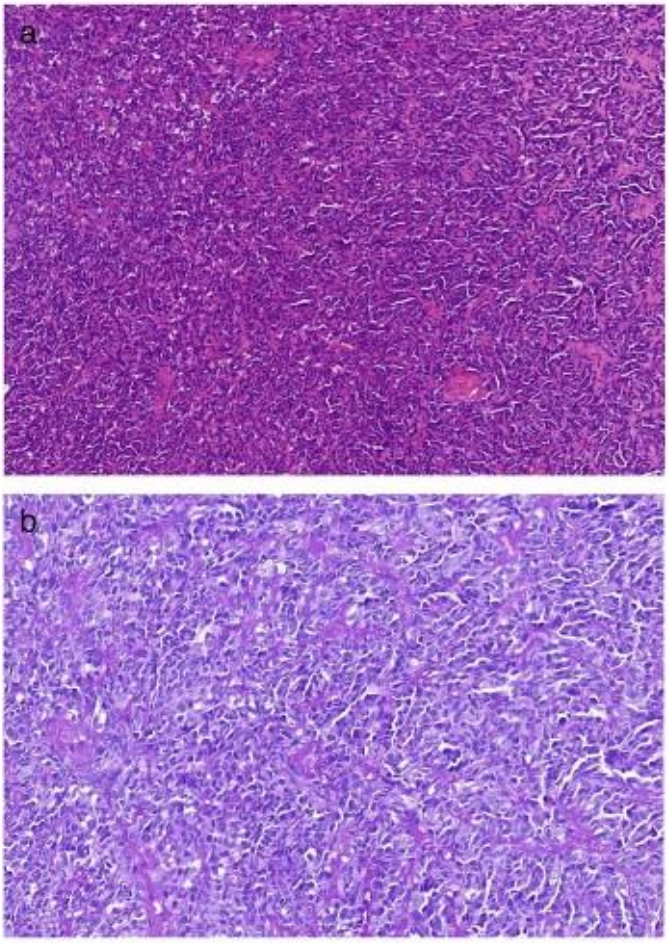

Fig. 4. (A-B) Four tumors in our series were composed of short compressed abortive papillae (hematoxylin and eosin = A, PAS = B).

solid morphology and distinct micronodules, with the cells showing eosinophilic cytoplasm. Abortive papillae are also frequently found.

In the current study, true solid areas comprised 5%-80% of the individual tumors; on high power and PAS stain, only 2 tumors had more than 50% solid pattern, without any visible tubules or papillae. Areas of compressed, tightly packed tubular structures and abortive papillae comprised the rest of the tumors, usually mimicking solid areas and rarely showing focal spindle cell appearance. Four tumors were mostly composed of compressed and abortive papillae, and 4 were composed

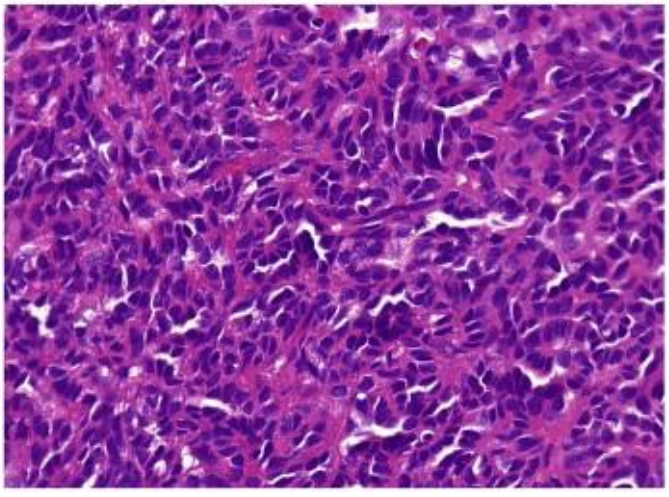

Fig. 5. Tumor cells had scant cytoplasm and small, round to elongated nuclei.

Table 3
Immunohistochemical staining results in solid PRCC

Patient	CK7	AMACR	EMA	WT-1	CD57	CD10	Vim	Ki-67
1	+++	+++	+++	−	+	−	+	≤1%
2	+++	+++	+++	−	−	+	+++	≤1%
3	+++	+++	+	−	−	−	++	≤1%
4	+++	+++	+++	−	−	++	++	≤1%
5	+++	+++	++	−	−	−	+++	≤1%
6	+++	+++	+++	−	−	−	+++	≤1%
7	+++	−	+++	−	−	−	+++	≤1%
8	+++	+++	+++	−	−	−	+++	≤1%
9	+++	+++	+++	−	−	+	+++	≤1%
10	+++	+++	+++	−	−	++	+	≤2%

+: focal positivity, in small clusters or single cells; ++: up to 50% of positive cells; +++: diffuse, strong positivity, more than 50% of positive cells. Vim, vimentin.

mostly of compressed tubules. True papillae with fibrovascular cores were found in 3 cases and formed up to 5% of the tumor volume.

The amount of cytoplasm in the neoplastic cells may be variable. In most of the cases, the cells had scant cytoplasm and appeared basophilic, but cells having more abundant cytoplasm and low-grade nuclear features were also noted. The spindle cell–like component was usually low grade with slightly elongated nuclei, moderate pleomorphism, finely dispersed chromatin, and distinct nucleoli. These cells were different from true sarcomatoid morphology and resembled the cells of mucinous tubular and spindle cell RCC. Mitoses were rarely found [3,13–19]. Cantley et al [16] described a case of a young male patient with renal tumor showing sarcomatoid RCC, with an epithelial component identical to the solid PRCC. In some cases, foamy macrophages and psammoma bodies were found in the stroma of the tumor [17]. Occasionally, isolated foam cells and psammoma bodies were also present in our cases, but mitotic figures were not found. Most of the neoplastic cells had scant cytoplasm and small, round to elongated nuclei, with ISUP nucleolar grade 1 and 2. In all cases, there were low-grade nuclei, except in 1 case in which cells showed scant eosinophilic cytoplasm.

Although small solid areas in conventional PRCC are compatible with the diagnosis of PRCC, specific criteria for the diagnosis of solid PRCC are not provided in the recent renal tumor classifications [5]. In published studies, however, variable percentages of solid architecture, compressed papillae, or tubules were used to define this entity. Some authors proposed that solid PRCC should not contain true papillae, whereas others suggested that true papillae could comprise up to 20% [3,16–17].

4.2. Immunohistochemical profile and genetics

PRCC usually stains positive for cytokeratin AE1/AE3, CAM5.2, high–molecular weight cytokeratins, CK7, EMA, vimentin, CD10, AMACR, and RCC [2,4–5,7–9]. Of note, CK7 positivity can be variable, and it is not a

Fig. 6. All 10 cases were strongly and diffusely positive for CK7.

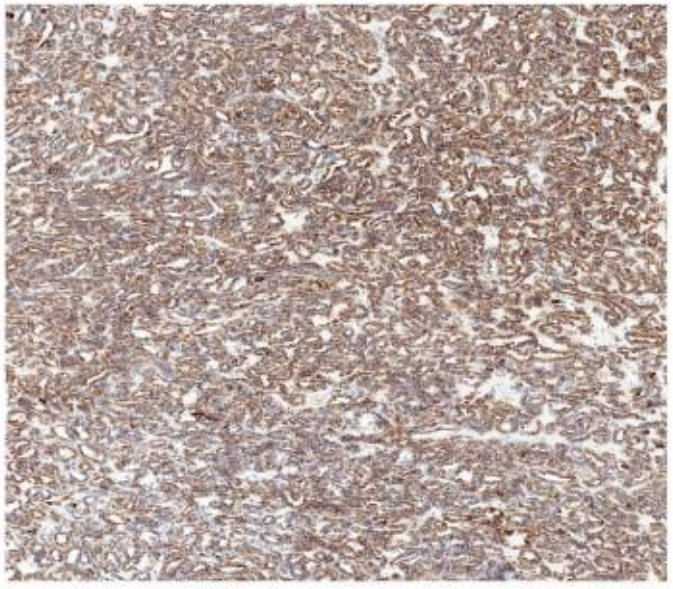

Fig. 7. Racemase (AMACR) was diffusely positive in 9 cases.

constant feature of PRCC; however, CK7 is frequently expressed in PRCC type 1. Solid PRCC shows immunoprofile similar to “conventional type” of PRCC, with strong, diffuse positivity for EMA, CK7, and AMACR and usually focal positivity for CD10 [3,13–19]. According to some studies, vimentin may be also focally positive.

In our experience, all10 evaluated cases were strongly and diffusely positive for CK7 and negative for WT-1. CK7 may in fact highlight the collapsed tubular architecture. AMACR was diffusely positive in 9 and EMA in 7 cases. CD10 was focally positive in 4 cases. CD57 showed weak and individual cell positivity in 9 cases. Proliferation activity, evaluated by Ki-67, was between 1% and 2% in all tumors.

4.3. Molecular genetic profile

Trisomy and tetrasomy of chromosome 7 and trisomy of 17, as well as loss of Y, are nearly pathognomic for PRCC. According to the published data, this also applies to solid PRCC [3,13–19]. According to WHO 2016, however, a wide variety of other chromosomal aberrations can be seen in PRCC, including trisomy 8, 12, 16, and 20 and loss of 1p, 4q, 6q, 7, 9p, 13q, Xp, and Xq, as well as amplification of 8q and overexpression of MYC. Thirteen percent of sporadic PRCCs demonstrate MET mutations. Loss of heterozygosity of VHL and FHIT can also be found. Type 1 PRCC shows gains of 7p and 17p, whereas LOH of 1p, 3p, 5q, 6, 8, 9p, 10, 11, 15, 18, and 22 was found in PRCC type 2. Allelic imbalance of 9q13 has been shown to be of prognostic significance in PRCC [5]. Renshaw et al [13] described cytogenetic changes in 1 case of solid PRCC, which demonstrated a karyotype of 45XXX, +X, +3, +5, +12, −14, +16, +17, −18, +20, and −21.

4.4. Pitfalls and differential diagnosis

Several entities should be considered in the differential diagnosis of solid PRCC, such as MA, epithelioid nephroblastoma, MTSC, and solid oncocytic PRCC (Table 5).

Metanephric adenoma of the kidney is a benign tumor usually found in younger patients, predominantly in women. It accounts for 0.2%-0.7% of adult renal epithelial neoplasms. It is sharply demarcated without a distinct pseudocapsule and consists of bland, small blue cells forming small, tightly packed tubular structures and acini but infrequently may also show more solid growth. Some tubules are typically elongated and branching. Both PRCC and MA may contain glomeruloid bodies with abortive papillae, tightly packed tubules, or solid tumor cell sheets. Psammoma bodies can be present in both MA and solid PRCC [20–22].

MA typically shows CK7 −, AMACR −, WT1 +, and CD57 + immunoprofile and does not exhibit the chromosomal changes typical of PRCC [20–25]. In fact, MA with polysomy 7 and 17 or loss of Y described in the literature most likely represents solid PRCC [20]. According to more recent data, BRAF V600E mutations were identified in nearly 90% of MAs, but similar BRAF exon 15 mutations are extremely rare in other renal tumors, including PRCCs. Immunohistochemistry for detection of BRAF V600E mutations was also validated, and it can be used as an additional tool in the differential diagnostic process [26]. According to the study of Yakirevich et al [27], majority of MAs are positive for kidney-specific catherin, whereas PRCCs and nephroblastomas are negative.

Table 4
Literature data

	Renshaw et al	Ngan et al	Argani et al	Zhang et al	Mantoan Padilha et al	Kinney et al	Cantley et al
No. cases	6[a]	1	5	2	23	15	1
Age	35-82	36	17-68	50-51	30-80	69-83	31
Sex (M/F)	4/2	1/0	1/0	2/0	15/8	11/?	1/0
Size (cm)	1-12	–	2.1-5.2	2-8	0.9-10	1.9-2	4.5
Nuclear grade 1/2/3/4	2/2/2/0	–	0/5/0/0	0/1/1/0	–	–	–
pTNM	2 T1, 4 T2	–	4T1a, 1T1b	1T1a, 1 T2	11T1a, 9T1b, 3 T2	–	T1b
Follow-up (mo)	2-108	–	Up to 8	8, 14	–	–	24
Follow-up	1 AWD (6 mo) 4 NED	–	5 NED	2 NED	–	–	NED
No. cases	6[a]	1	5	2	23	15	1
Papillae/solid encount	4-S	S	2-S[b]	2-T	10 S	–	T[c]
	2-T		3-T[b]		13 T		
	6+		5+		23+		
	–		–		23+		
	6+		–		21+		
	–		–		23−		
CK7	–	1+	5+ (focal)	2+	–	14+	1+
AMACAR	–	–	–	2+	23−	15+	–
EMA	–	1+	–	2+	16+ (focal)	–	1+
Vimentin	2	1−	5	2+	14	–	1+
CD10	3	–	3	1 (focal)	15	–	–
WT-1	–	–	–	–	–	15−	1−
CD57		–		–		14−; 1+	1−
Trisomy 7		–		2		8	1
Trisomy 17		–		2		8	–
Y loss		–		2		11	–

S, predominantly solid with small micronodules and abortive papillae; T, mostly tubular pattern and compressed tubules; –, no data; AWD, alive with disease; NED, no evidence of disease; M, male; F, female.
[a] Three were multifocal.
[b] Tumors with spindle cell foci.
[c] Foci with high-grade nuclei, with spindle cells.

Table 5
Differential diagnosis of solid PRCC

Characteristics	S PRCC	MA	EN	MTSC	OPRCC
Age (y)	17-83, average 54	Children, young adults, 5-83, average 49	Mostly children up to 6; in adult 21-67, average 32	32-79, average 56	40-82, average 67
Sex (M/F ratio)	M (3.5/1)	F (1/9)	Equal	F (1/1.5)	M (5/1)
Fibrous pseudocapsule	+	−	+	+	+
Multifocality	+	−	+	−	+
Cytology					
Cells with eosinophilic cytoplasm	+[a]	−	−	+[a]	+ (abundant)
Cells with scant cytoplasm	+	+	+	+	−
Nuclei	Low gr	Low gr	Low-high gr	Low gr	Low-high gr
True solid areas	+	+	+	+	+
Spindle cells with low-grade features	+	−	−	+	−
Compressed tubuli	+	+	+	+	+
Compressed abortive papillae (glomeruloid)	+	+	+	−	−
Real papillae with fibrovasc. CORE	+ (sparse)	+ (sparse)	−	−	+
Visible tubuli on LPF	+ (sparse)	+	+	+	+
Mucinous stroma	−	−	−	+	−
AE1/3	+	−	−	+	+
CK7	+	−	−	+	+
EMA	+	−	−	+	+
AMACAR	−	+	−	−	−
WT-1	+	−	+	−	−
CD57	−	+	+	−	−
Trisomy 7	Y	N	N	N	Y
Trisomy 17	Y	N	N	N	Y
Loss of Y	Y	N	N	N	Y

Y, yes; N, no; LPF, low-power field; SPRCC, solid PRCC; EN, epithelioid nephroblastoma; OPRCC, oncocytic PRCC; gr, grade; MA, metanephric adenoma; MTSC, mucinous tubulary and spindle cell carcinoma.
[a]Not so abundant cytoplasm as in oncocytic PRCC.

In a recently published study, 21 MAs and 23 solid PRCCs shared similar morphologic features. Eleven solid PRCCs lacked papillae completely but showed typical immunoprofile and genetic aberrations of PRCCs [3]. Some of these cases with solid and glomeruloid structures were composed of larger eosinophilic cells and resembled a renal tumor described by Petersson et al [28], provisionally named biphasic alveolosquamoid renal carcinoma. This entity was further analyzed in a larger cohort and was recently recognized as a subtype of PRCC. Therefore, a solid-alveolar morphology of this newly described PRCC variant should also be considered in the differential diagnosis of solid PRCC. However, it appears that there is little difference in the clinical management and the prognosis of this entity [29]. It is also worth mentioning that the diagnostic criteria for malignant MA described in the literature were never generally accepted, and likely all malignant MAs represent examples of extremely well-differentiated epithelioid nephroblastomas [20].

Nephroblastoma is very rare in adult patients, but adult nephroblastomas generally do not differ from their pediatric counterpart. Pure epithelioid nephroblastoma is exceptionally rarely seen in adult patients. However, this tumor type should also be considered in the differential diagnosis of solid PRCC. The morphology typically shows tubulopapillar and solid patterns; the cells are small and uniform with scant cytoplasm, and there are absent or very rare mitotic figures [18–19,30–32]. Kinney et al [18] analyzed 37 tumors originally diagnosed as MA, 13 solid PRCCs, and 20 epithelial-predominant nephroblastomas using immunohistochemistry and fluorescence in situ hybridization for trisomy of chromosomes 7 and 17 and loss of Y. All epithelial-predominant nephroblastomas were diffusely positive for WT-1, and only 1 was focally positive for CK7. All tumors showed disomy of chromosomes 7, 17, and Y present [18].

Another renal tumor which frequently shows solid architecture is MTSC. It is characterized by elongated and compressed tubules or cordlike formations of uniform, cuboidal cells with eosinophilic, focally vacuolated cytoplasm and distinct cell spindling, and usually demonstrates low-grade nuclei. The stroma is typically myxoid and contains variable amount of extracellular mucin. Focal clusters of foamy macrophages may also be seen. In cases with limited myxoid stroma (so-called mucin-poor variant) and limited presence of well-formed papillae, it may be difficult to distinguish MTSC from solid PRCC [33–34]. In rare examples of MTSC, the cells form solid and compact areas with minimal amount of interstitial mucin. Such cases can truly mimic solid PRCC, but in well-sampled tumors, more typical areas of MTSC are usually found. Both solid PRCC and MTSC can have tubular structures, papillary architecture, spindle cell appearance, psammoma bodies, foamy macrophages, and interstitial mucin and demonstrate positive staining for vimentin, CK7, CK19, EMA, AMACR, CD10, and RCC [15,17].

There are several studies that consider the issue of MTSC in the differential diagnosis of solid PRCC, raising the possibility that MTSC represents a subtype of PRCC [33–37]. Peckova et al [38] analyzed 54 MTSCs using array comparative genomic hybridization and divided the MTSCs into 3 categories: low grade, high grade, and MTSC overlapping with PRCC. They showed multiple chromosomal losses and no gains in low- and high-grade MTSC groups, supporting the concept that MTSC represents a distinct type of RCC. However, the group showing overlapping features with PRCC demonstrated more heterogeneous status, with frequent gains of chromosomes 7 and/or 17, suggesting that this MTSC subgroup should be considered in the spectrum of PRCC [38].

An oncocytic variant of PRCC different from PRCC type 1 and 2 was also reported, composed of papillae lined by single or rarely pseudostratified layers of cells with granular, deeply eosinophilic cytoplasm and round regular nuclei. In the new 2016 WHO classification of renal tumors, the oncocytic PRCC is considered as a possible new variant of PRCC [5]. This type of PRCC can also show solid pattern in up to 90% of the tumor. The immunoprofile and the genotype are compatible with PRCC [10–11,39–41]. Despite the solid architecture, oncocytic PRCC can be differentiated from solid PRCC mostly by histology. The oncocytic cells of oncocytic PRCC are eosinophilic and contain voluminous cytoplasm and differ from the smaller epithelial cells of solid PRCC which contain scanty cytoplasm.

5. Conclusion

In conclusion, solid PRCC is a rare tumor with an incidence less than 1% of all renal tumors. In the majority of cases, it is composed of solid areas and compressed tubular structures or short abortive papillae that result in a solid appearance. The immunohistochemical and molecular genetic features do not differ from conventional PRCC. Metanephric

adenoma, epithelioid nephroblastoma, and less often MTSC and an oncocytic variant of PRCC should all be considered in the differential diagnosis of solid PRCC.

References

[1] Kovacs G, Akhtar M, Beckwith BJ, Bugert P, Cooper CS, Delahunt B, et al. The Heidelberg classification of renal cell tumours. J Pathol 1997;183(2):131–3.
[2] Eble JN, Sauter G, Epstein JI, Sesterhenn IA, editors. Tumours of the urinary system andmale genital organs. World Health Organization classification of tumours. Press LI; 2004. p. 27–9.
[3] Mantoan Padilha M, Billis A, Allende D, Zhou M, Magi-Galluzzi C. Metanephric adenoma and solid variant of papillary renal cell carcinoma: common and distinctive features. Histopathology 2013;62(6):941–53.
[4] Klatte T, Said JW, Seligson DB, Rao PN, de Martino M, Shuch B, et al. Pathological, immunohistochemical and cytogenetic features of papillary renal cell carcinoma with clear cell features. J Urol 2011;185(1):30–5.
[5] Moch H, Humphrey PA, Ulbright TM, Reuter VE, editors. WHO classification of tumours of the urinary system and male genital organs. 4th ed. Lyon: IARC; 2016.
[6] Mancilla-Jimenez R, Stanley RJ, Blath RA. Papillary renal cell carcinoma: a clinical, radiologic, and pathologic study of 34 cases. Cancer 1976;38(6):2469–80.
[7] Delahunt B, Eble JN. Papillary renal cell carcinoma: a clinicopathologic and immunohistochemical study of 105 tumors. Mod Pathol 1997;10(6):537–44.
[8] Amin MB, Corless CL, Renshaw AA, Tickoo SK, Kubus JK, Schultz DS. Papillary (chromophil) renal cell carcinoma (PRCC): evaluation of conventional pathologic prognostic parameters in 62 cases. Am J Surg Pathol 1997;21:621–35.
[9] Delahunt B, Eble JN, McCredie MR, Bethwaite PB, Stewart JH, Bilous AM. Morphologic typing of papillary renal cell carcinoma: comparison of growth kinetics and patient survival in 66 cases. Hum Pathol 2001;32(6):590–5.
[10] Lefevre M, Couturier J, Sibony M, Bazille C, Boyer K, Callard P, et al. Adult papillary renal tumor with oncocytic cells: clinicopathologic, immunohistochemical, and cytogenetic features of 10 cases. Am J Surg Pathol 2005;29(12):1576–81.
[11] Hes O, Brunelli M, Michal M, Cossu Rocca P, Hora M, Chilosi M, et al. Oncocytic papillary renal cell carcinoma: a clinicopathologic, immunohistochemical, ultrastructural, and interphase cytogenetic study of 12 cases. Ann Diagn Pathol 2006;10(3):133–9.
[12] Gobbo S, Eble JN, Maclennan GT, Grignon DJ, Shah RB, Zhang S, et al. Renal cell carcinomas with papillary architecture and clear cell components: the utility of immunohistochemical and cytogenetical analyses in differential diagnosis. Am J Surg Pathol 2008;32(12):1780–6.
[13] Renshaw AA, Zhang H, Corless CL, Fletcher JA, Pins MR. Solid variants of papillary (chromophil) renal cell carcinoma: clinicopathologic and genetic features. Am J Surg Pathol 1997;21(10):1203–9.
[14] Ngan KW, Ng KF, Chuang CK. Solid variant of papillary renal cell carcinoma. Chang Gung Med J 2001;24(9):582–6.
[15] Argani P, Netto GJ, Parwani AV. Papillary renal cell carcinoma with low-grade spindle cell foci: a mimic of mucinous tubular and spindle cell carcinoma. Am J Surg Pathol 2008;32(9):1353–9.
[16] Cantley R, Gattuso P, Cimbaluk D. Solid variant of papillary renal cell carcinoma with spindle cell and tubular components. Arch Pathol Lab Med 2010;134(8):1210–4.
[17] Zhang Y, Yong X, Wu Q, Wang X, Zhang Q, Wu S, et al. Mucinous tubular and spindle cell carcinoma and solid variant papillary renal cell carcinoma: a clinicopathologic comparative analysis of four cases with similar molecular genetics datum. Diagn Pathol 2014;9:194.
[18] Kinney SN, Eble JN, Hes O, Williamson SR, Grignon DJ, Wang M, et al. Metanephric adenoma: the utility of immunohistochemical and cytogenetic analyses in differential diagnosis, including solid variant papillary renal cell carcinoma and epithelial-predominant nephroblastoma. Mod Pathol 2015 Sep;28(9):1236–48.
[19] Chen L, Deng FM, Melamed J, Zhou M. Differential diagnosis of renal tumors with tubulopapillary architecture in children and young adults: a case report and review of literature. Am J Clin Exp Urol 2014;2(3):266–72.
[20] Arroyo MR, Green DM, Perlman EJ, Beckwith JB, Argani P. The spectrum of metanephric adenofibroma and related lesions: clinicopathologic study of 25 cases from the National Wilms Tumor Study Group Pathology Center. Am J Surg Pathol 2001;25(4):433–44.
[21] Gatalica Z, Grujic S, Kovatich A, Petersen RO. Metanephric adenoma: histology, immunophenotype, cytogenetics, ultrastructure. Mod Pathol 1996;9(3):329–33.
[22] Jones EC, Pins M, Dickersin GR, Young RH. Metanephric adenoma of the kidney. A clinicopathological, immunohistochemical, flow cytometric, cytogenetic, and electron microscopic study of seven cases. Am J Surg Pathol 1995;19(6):615–26.
[23] Brown JA, Anderl KL, Borell TJ, Qian J, Bostwick DG, Jenkins RB. Simultaneous chromosome 7 and 17 gain and sex chromosome loss provide evidence that renal metanephric adenoma is related to papillary renal cell carcinoma. J Urol 1997;158(2):370–4.
[24] Brunelli M, Eble JN, Zhang S, Martignoni G, Cheng L. Metanephric adenoma lacks the gains of chromosomes 7 and 17 and loss of Y that are typical of papillary renal cell carcinoma and papillary adenoma. Mod Pathol 2003;16(10):1060–3.
[25] Obulareddy SJ, Xin J, Truskinovsky AM, Anderson JK, Franklin MJ, Dudek AZ. Metanephric adenoma of the kidney: an unusual diagnostic challenge. Rare Tumors 2010;2(2), e38.
[26] Udager AM, Pan J, Magers MJ, Palapattu GS, Morgan TM, Montgomery JS, et al. Molecular and immunohistochemical characterization reveals novel BRAF mutations in metanephric adenoma. Am J Surg Pathol 2015;39(4):549–57.
[27] Yakirevich E, Magi-Galluzzi C, Grada Z, Lu S, Resnick MB, Mangray S. Cadherin 17 is a sensitive and specific marker for metanephric adenoma. Am J Surg Pathol 2015;39(4):479–86.
[28] Petersson F, Bulimbasic S, Hes O, Slavik P, Martinek P, Michal M, et al. Biphasic alveolosquamoid renal carcinoma: a histomorphological, immunohistochemical, molecular genetic, and ultrastructural study of a distinctive morphologic variant of renal cell carcinoma. Ann Diagn Pathol 2012;16(6):459–69.
[29] Hes O, Condom Mundo E, Peckova K, Lopez JI, Martinek P, Vanecek T, et al. Biphasic Squamoid alveolar renal cell carcinoma: a distinctive subtype of papillary renal cell carcinoma? Am J Surg Pathol 2016;40(5):664–75.
[30] Huser J, Grignon DJ, Ro JY, Ayala AG, Shannon RL, Papadopoulos NJ. Adult Wilms' tumor: a clinicopathologic study of 11 cases. Mod Pathol 1990;3(3):321–6.
[31] Muir TE, Cheville JC, Lager DJ. Metanephric adenoma, nephrogenic rests, and Wilms' tumor: a histologic and immunophenotypic comparison. Am J Surg Pathol 2001;25(10):1290–6.
[32] Reinhard H, Aliani S, Ruebe C, Stockle M, Leuschner I, Graf N. Wilms' tumor in adults: results of the Society of Pediatric Oncology (SIOP) 93-01/Society for Pediatric Oncology and Hematology (GPOH) study. J Clin Oncol 2004;22(22):4500–6.
[33] Fine SW, Argani P, DeMarzo AM, Delahunt B, Sebo TJ, Reuter VE, et al. Expanding the histologic spectrum of mucinous tubular and spindle cell carcinoma of the kidney. Am J Surg Pathol 2006;30(12):1554–60.
[34] Paner GP, Srigley JR, Radhakrishnan A, Cohen C, Skinnider BF, Tickoo SK, et al. Immunohistochemical analysis of mucinous tubular and spindle cell carcinoma and papillary renal cell carcinoma of the kidney: significant immunophenotypic overlap warrants diagnostic caution. Am J Surg Pathol 2006;30(1):13–9.
[35] Alexiev BA, Burke AP, Drachenberg CB, Richards SM, Zou YS. Mucinous tubular and spindle cell carcinoma of the kidney with prominent papillary component, a non-classic morphologic variant. A histologic, immunohistochemical, electron microscopic and fluorescence in situ hybridization study. Pathol Res Pract 2014;210(7):454–8.
[36] Cossu-Rocca P, Eble JN, Delahunt B, Zhang S, Martignoni G, Brunelli M, et al. Renal mucinous tubular and spindle carcinoma lacks the gains of chromosomes 7 and 17 and losses of chromosome Y that are prevalent in papillary renal cell carcinoma. Mod Pathol 2006;19(4):488–93.
[37] Shen SS, Ro JY, Tamboli P, Truong LD, Zhai Q, Jung SJ, et al. Mucinous tubular and spindle cell carcinoma of kidney is probably a variant of papillary renal cell carcinoma with spindle cell features. Ann Diagn Pathol 2007;11(1):13–21.
[38] Peckova K, Martinek P, Sperga M, Montiel DP, Daum O, Rotterova P, et al. Mucinous spindle and tubular renal cell carcinoma: analysis of chromosomal aberration pattern of low-grade, high-grade, and overlapping morphologic variant with papillary renal cell carcinoma. Ann Diagn Pathol 2015;19(4):226–31.
[39] Allory Y, Ouazana D, Boucher E, Thiounn N, Vieillefond A. Papillary renal cell carcinoma. Prognostic value of morphological subtypes in a clinicopathologic study of 43 cases. Virchows Arch 2003;442(4):336–42.
[40] Kunju LP, Wojno K, Wolf Jr JS, Cheng L, Shah RB. Papillary renal cell carcinoma with oncocytic cells and nonoverlapping low grade nuclei: expanding the morphologic spectrum with emphasis on clinicopathologic, immunohistochemical and molecular features. Hum Pathol 2008 Jan;39(1):96–101.
[41] Mai KT, Kohler DM, Robertson SJ, Belanger EC, Marginean EC. Oncocytic papillary renal cell carcinoma with solid architecture: mimic of renal oncocytoma. Pathol Int 2008;58(3):164–8.

3.5 Cystic and necrotic papillary renal cell carcinoma: prognosis, morphology, immunohistochemical, and molecular-genetic profile of 10 cases

Prognostický dopad přítomnosti nekrózy v PRCC není jednoznačně stanoven a v literatuře publikovaná data se značně rozcházejí. Ve zcela obecné rovině je obyčejně přítomnost nádorové nekrózy považována za špatný prognostický ukazatel. V této práci je představeno celkem 10 jasně cystických a extensivně nekrotických nádorů, které při dlouhodobé dispenzarizaci vykazovaly biologicky jednoznačně příznivé chování.

Deset případů morfologicky uniformních PRCC typu 1 bylo vybráno z více než 19 500 renálních tumorů v Plzeňském registru nádorů. Nádory byly vyšetřeny morfologicky, finální diagnóza byla podpořena imunohistochemickým barvením a molekulárně-genetickou analýzou. V osmi případech se jednalo o tumory mužů, ve dvou případech byly postiženy ženy, věk pacientů se pohyboval v rozmezí 32-85 let (průměrný věk 62,6 let). Nádory měřily 6-14 cm (průměrná velikost 9,4 cm). Dispenzarizační data byla dostupná v sedmi případech, s délkou trvání od 0,5 do 14 let (průměr 4 roky). Všechny tumory byly makroskopicky sférického tvaru, cystické, ohraničené pomocí tlusté fibrózní kapsuly, vyplněné hemoragickým/nekrotickým obsahem. Pouze velmi limitované množství vitální nádorové tkáně bylo mikroskopicky zastiženo jako tenký lem vystýlající vnitřní povrch stěny cysty, přičemž tyto nádorové hmoty byly konzistentní s diagnózou PRCC typ 1. Ve všech případech byly nádorové buňky pozitivní v imunohistochemickém průkazu racemázy (AMACR), cytokeratinu OSCAR, CAM 5.2, HIF-2 a vimentinu. Polysomie chromosomů 7 a 17 byla detekována u pěti z celkem osmi pro molekulárně genetickou analýzu vhodných případů. Dva případy vykazovali normální (disomický) statut chromosomů 7 a 17 a u jednoho tumoru byla zastižena pouze polysomie chromosomu 17. Ztráta gonosomu Y byla detekována v pěti případech, z toho v jednom případě se jednalo o tumor s disomickým statusem chromosomů 7 a 17. Molekulárně genetické vyšetření neprokázalo abnormalitu *VHL* genu v žádném z vyšetřovaných případů.

Na základě výše popsaných poznatků lze říci, že PRCC typ 1 se může prezentovat jako objemná a rozsáhle hemoragicky/nekroticky změněná cystická léze s tlustým fibroleiomyomatózním pouzdrem. Většina případů vykazuje chromozomální numerické aberace „typické“ pro PRCC. Všechny tumory se prezentovaly neagresivním klinickým průběhem. Přítomnost kolikvační nekrózy tedy nemusí být nutně považována za špatný prognostický znak a to zejména u rozsáhle cysticky změněných PRCC typu 1 s jednokomorovou cystickou dutinou vyplněnou nekrotickým/hemoragickým materiálem.

Annals of Diagnostic Pathology 26 (2017) 23–30

Contents lists available at ScienceDirect

Annals of Diagnostic Pathology

Cystic and necrotic papillary renal cell carcinoma: prognosis, morphology, immunohistochemical, and molecular-genetic profile of 10 cases☆,☆☆

Kvetoslava Peckova, MD [a], Petr Martinek, PhD [a], Kristyna Pivovarcikova, MD [a], Tomas Vanecek, PhD [a], Reza Alaghehbandan, MD [b], Kristyna Prochazkova, MD [c], Delia Perez Montiel, MD [d], Milan Hora, MD, PhD [c], Faruk Skenderi, MD [e], Monika Ulamec, MD, PhD [f], Pavla Rotterova, MD, PhD [g], Ondrej Daum, MD, PhD [a], Jiri Ferda, MD, PhD [h], Whitney Davidson, BS [i], Ondrej Ondic, MD [a], Magdalena Dubova, MD [a], Michal Michal, MD [a], Ondrej Hes, MD, PhD [a,]

[a] Department of Pathology, Charles University, Medical Faculty and Charles University Hospital Plzen, Czech Republic
[b] Department of Pathology, University of British Columbia, Royal Columbian Hospital, Vancouver, Canada
[c] Department of Urology, Charles University, Medical Faculty and Charles University Hospital Plzen, Czech Republic
[d] Department of Pathology, Instituto Nacional de Cancerologia, Mexico City, Mexico
[e] Department of Pathology, University Clinical Center, Sarajevo, Bosnia and Herzegovina
[f] "Ljudevit Jurak" Pathology Department, Clinical Hospital Center "Sestre milosrdnice,", Zagreb, Croatia
[g] Biopticka Laborator, Plzen, Czech Republic
[h] Department of Radiodiology, Charles University, Medical Faculty and Charles University Hospital Plzen, Czech Republic
[i] Department of Pathology, The University of Kansas School of Medicine, Kansas City, KS

article info

Keywords:
Kidney
Papillary renal cell carcinoma
Cystic
Necrosis
Necrotics
Molecular genetics

abstract

Conflicting data have been published on the prognostic significance of tumor necrosis in papillary renal cell carcinoma (PRCC). Although the presence of necrosis is generally considered an adverse prognostic feature in PRCC, we report a cohort of 10 morphologically distinct cystic and extensively necrotic PRCC with favorable biological behavior. Ten cases of type 1 PRCC with a uniform morphologic pattern were selected from the 19 500 renal tumors, of which 1311 were PRCCs in our registry. We focused on precise morphologic diagnosis supported by immunohistochemical and molecular-genetic analysis. Patients included 8 men and 2 women with an age range of 32-85 years (mean, 62.6 years). Tumor size ranged from 6 to 14 cm (mean, 9.4 cm). Follow-up data were available in 7 patients, ranging from 0.5 to 14 years (mean, 4 years). All tumors were spherical, cystic, and circumscribed by a thick fibrous capsule, filled with hemorrhagic/necrotic contents. Limited viable neoplastic tissue was present only as a thin rim in the inner surface of the cyst wall, consistent with type 1 PRCC. All cases were positive for AMACR, OSCAR, CAM 5.2, HIF-2, and vimentin. Chromosome 7 and 17 polysomy was found in 5 of 9 analyzable cases, 2 cases demonstrated chromosome 7 and 17 disomy, and 1 case showed only chromosome 17 polysomy. Loss of chromosome Y was found in 5 cases, including 1 case with disomic chromosomes 7 and 17. No VHL gene abnormalities were found. Papillary renal cell carcinoma type 1 can present as a large hemorrhagic/necrotic unicystic lesion with a thick fibroleiomyomatous capsule. Most cases showed a chromosomal numerical aberration pattern characteristic of PRCC. All tumors followed a nonaggressive clinical course. Large liquefactive necrosis should not necessarily be considered an adverse prognostic feature, particularly in a subset of type 1 PRCC with unilocular cysts filled with necrotic/hemorrhagic material.

1. Introduction

Papillary renal cell carcinoma (PRCC) accounts for 15% to 20% of renal carcinomas and is a heterogeneous disease with histologic subtypes and variations in clinical behavior and outcome. It is traditionally subclassified as type 1, which is a distinct entity (morphologically, immunohistochemically, and genetically), and type 2, which is composed of more heterogeneous group of diseases [1]. Grossly, PRCCs are usually well circumscribed and may contain foci of necrosis and

☆ Disclosure of Conflict of Interest: All authors declare no conflict of interest.
☆☆ The study was supported by the Charles University Research Fund (Project No. P36), by the Ministry of Health of the Czech Republic—Conceptual Development of Research Organization (Faculty Hospital in Pilsen, 00669806), and by SVV 260283.
Corresponding author at: Department of Pathology, Charles University, Medical Faculty and Charles University Hospital Plzen, Alej Svobody 80, 304 60 Pilsen, Czech Republic.
E-mail address: hes@medima.cz (O. Hes).

http://dx.doi.org/10.1016/j.anndiagpath.2016.10.007
1092-9134/

hemorrhage. Nonetheless, unilocular cystic tumors within type 1 PRCC are rather uncommon.

We describe a cohort of PRCC, morphologically consistent with type 1 according to the Delahunt classification, which were large unilocular cystic tumors surrounded by thick-wall fibrous capsule and filled with hemorrhagic/necrotic contents, demonstrating long-term favorable clinical outcome [1,2]. The purpose of this study was to describe a unique subpopulation of type 1 PRCC with an unusual gross and histologic presentation (cystic lesion with necrotic content) to enhance our understating of the prognostic significance of tumor necrosis (TN) in these tumors.

2. Materials and methods

This study design was approved by local ethical committee (Charles University, Medical School Plzen).

Of 19 500 renal tumors and tumor-like lesions (including 1311 PRCCs) in the institutional and consultation files of the Sikl's Department of Pathology at Charles' University, Plzen, Czech Republic, 10 cases of cystic and largely necrotic type 1 PRCC were retrieved. The tissue had been fixed in neutral formalin, embedded in paraffin, 3- to 4-μm-thick sections were cut and stained with hematoxylin and eosin.

All tumors were large cystic lesions encapsulated by a thick, mostly fibrotic tissue. In 2 cases, the tumor capsule was histologically composed of so-called phenomenon inflammatory pseudotumor, for which one of them has already been reported [3]. Cysts were filled with sanguinolent necrotic material, whereas viable neoplastic structures were identified only in the inner surface of the cyst wall. Cases were further examined by immunohistochemistry and analyzed by molecular-genetic methods.

2.1. Immunohistochemistry

The immunohistochemical study was performed using a Ventana Benchmark XT automated stainer (Ventana Medical System, Inc, Tucson, AZ). The following primary antibodies were used: cytokeratin AE1/3 VM (AE1/AE3/PCK26, monoclonal; Ventana-Roche, Mannheim, Germany, RTU), wide-spectrum keratin (OSCAR, monoclonal, 1:2000; Covance, Princetown, NJ), cytokeratin (CAM 5,2 monoclonal, 1:200; Becton-Dickinson, San Jose, CA), racemase/AMACR (P504S, monoclonal, 1:50; Zeta, Sierra Madre, CA), vimentin (D9, monoclonal, 1:1000; Neomarkers, Westinghouse, CA), carbonic anhydrase IX (rhCA9, monoclonal, 1:100; RD Systems, Abingdon, GB), CD31 (JC70A, monoclonal, 1:50; DakoCytomation, Glostrup, Denmark), CD34 (QBEnd-10, monoclonal, 1:100; DakoCytomation), c-kit (CD 117, polyclonal; DakoCytomation, RTU), cathepsin K (monoclonal, 3F9, 1:100; Abcam, Cambridge, UK), PAX-8 (polyclonal rabbit, 1:25; Cell Marque–Medac/RNDr. A. Manthey, Rocklin, CA), TFE3 (polyclonal, 1:100; Abcam), HIF-1α (ESEE122, 0.5:150; Abcam), HIF-2α (ep190b, 1:30; Abcam), and phospho-mTOR (Ser2448, 1:80; Cell Signaling Technology, Danvers, MA). Appropriate positive and negative controls were used.

2.2. Molecular-genetic study

2.2.1. Fluorescence in situ hybridization methods

Four-micrometer-thick section was placed onto a positively charged slide. Hematoxylin and eosin–stained slide was examined for the cell counting area determination.

The unstained slide was routinely deparaffinized and incubated in the 1× Target Retrieval Solution Citrate pH 6 (Dako, Glostrup, Denmark) for 40 minutes at 95°C and subsequently cooled for 20 minutes at room temperature in the same solution. The slide was washed in deionized water for 5 minutes and digested in protease solution with Pepsin (0.5 mg/mL; Sigma-Aldrich, St Louis, MO) in 0.01 M HCl at 37°C for 20 minutes. The slide was then placed into deionized water for 5 minutes, dehydrated in a series of ethanol solution (70%, 85%, and 96% for 2 minutes each), and air-dried. Probes for aneuploidy detection of chromosomes 7 and 17 (Vysis/Abbott Molecular, Des Plaines, IL; see Table 1) were mixed with water and LSI/WCP (Locus-Specific Identifier/Whole Chromosome Painting) Hybridization buffer (Vysis) in a 1:2:7 ratio. An appropriate amount of probe mix was applied on the specimen, covered with a glass coverslip and sealed with a rubber cement. The slide was incubated in the ThermoBrite instrument (StatSpin/Iris Sample Processing, Westwood, MA) with co-denaturation parameters 85°C for 8 minutes and hybridization parameters 37°C for 16 hours. Rubber-cemented coverslip was then removed and the slide was placed in a posthybridization wash solution (2× SSC/0.3% NP-40) at 72°C for 2 minutes. The slide was air-dried in the dark, counterstained with DAPI (Vysis), coverslipped and immediately examined.

2.2.2. Fluorescence in situ hybridization interpretation

The section was examined with an Olympus BX51 fluorescence microscope (Olympus Corporation, Tokyo, Japan) using a ×100 objective and filter sets Triple Band Pass (DAPI/SpectrumGreen/SpectrumOrange) and Single Band Pass (SpectrumGreen/SpectrumOrange). Scoring of aneuploidy was performed by counting the number of fluorescent signals in 100 randomly selected nonoverlapping tumor cell nuclei. The slide was independently enumerated by 2 observers (OH and PG). Monosomy and polysomy for studied chromosomes were defined as the presence of one signal per cell in greater than 45% and 3 and more signals in greater than 10% (mean + 3 SD in normal nonneoplastic control tissues), respectively.

2.2.3. DNA extraction and bisulfite DNA conversion

DNA for molecular-genetic investigation was extracted from formalin-fixed, paraffin-embedded tissue. Several 5-μm-thick sections were placed on the slides. Hematoxylin and eosin–stained slides were examined for identification of neoplastic tissue. Subsequently, neoplastic tumor and nonneoplastic tissue from unstained slides were scraped and DNA was isolated by the NucleoSpin Tissue Kit (Macherey-Nagel, Düren, Germany).

Bisulfite conversion of DNA was carried out using EZ DNA Methylation–Gold Kit (DNA input 500 ng; Zymo Research, Orange, CA).

All procedures were performed according to the manufacturer's protocols.

2.3. VHL gene analysis

Mutation analysis of exons 1, 2, and 3 of the VHL gene was performed using polymerase chain reaction (PCR) and direct sequencing. Polymerase chain reaction was carried out using primers shown in Table 2. The reaction conditions were as follows: 12.5 μL of HotStar Taq PCR Master Mix (Qiagen, Hilden, Germany), 10 pmol of each primer, 100 ng of template DNA, and distilled water up to 25 μL. The amplification program consisted of denaturation at 95°C for 15 minutes and then 40 cycles of denaturation at 95°C for 1 minute, annealing at 55°C for 1 minute, and extension at 72°C for 1.5 minute for all amplicons. The program was finished by 72°C incubation for 7 minutes.

The PCR products were checked on 2% agarose gel electrophoresis.

Successfully amplified PCR products were purified with magnetic particles Agencourt AMPure (Agencourt Bioscince Corporation, A Beckman Coulter Company, Beverly, MA), both side sequenced using Big Dye Terminator Sequencing kit (Applied Biosystems, Foster City, CA) and purified with magnetic particles Agencourt CleanSEQ (Agencourt Bioscince Corporation) all according to the manufacturer's protocol, and subsequently run on an automated sequencer ABI Prism 3130xl (Applied Biosystems) at a constant voltage of 13.2 kV for 20 minutes. All samples were analyzed in duplicates. Analyses of positive samples were repeated.

Table 1
Clinicopathologic data

Case	Age (y)	Sex	Size (cm)	Follow-up (y)	Follow-up (clinical information)
1	40	M	6 × 5.5 × 3.5	0.5	Open resection; pT1b. AW, without recurrency
2	67	F	6.5 × 5.5 × 5.5	2	Right kidney resection; pT1b; duplicate malignancy-brest cancer. AW, without recurrency
3	67	M	9 × 7.5 × 4	NA	NA
4	37	M	NA	NA	NA
5	65	F	9×7×6	4	AW
6	83	M	14 × 11.5 × 7	0.5	Nephrectomy with appendectomy; pT2. Epidermoid lung carcinoma. Died in 2008 of lung carcinoma. No autopsy
7	69	M	9 × 11 × 11	14	Nephrectomy with appendectomy; AW, without progression
8	85	M	9.5 × 7.5 × 5	NA	NA
9	32	M	NA	4	Marsupialization of “renal cyst”; pT2. Died in 2007 of hepatic failure. No autopsy
10	81	M	10 × 8 × 4	3	Nephrectomy. Died 3 y later of unknown causes. Suspect malignant tumor diagnosed from needle biopsy.

Abbreviations: AW, alive and well; F, female; M, male; NA, not available.

2.3.1. Analysis of VHL promoter methylation

Detection of promoter methylation was carried out via methylation-specific PCR as described by Herman et al [4]. Briefly, 100 ng of DNA or 2 μL of converted DNA was added to reaction consisted of 12.5 μL of HotStar Taq PCR Master Mix (Qiagen), 10 pmol of forward and reverse primer (Table 3), and distilled water up to 25 μL. The amplification program comprised denaturation at 95°C for 14 minutes and then 40 cycles of denaturation at 95°C for 1 minute, annealing at 60°C for 1 minute, and extension at 72°C for 1 minute. The program was finished by incubation at 72°C for 7 minutes.

The PCR products were checked on 2% agarose gel electrophoresis.

A patient with known VHL mutation and fully methylated HeLa cell DNA were used as a positive control for VHL mutation analysis and promoter methylation analysis, respectively. As a negative control, randomly selected healthy donor blood was used.

3. Results

3.1. Clinical features

Clinicopathologic data of the patients under study are summarized in Table 1. Of 10 patients, 8 were men and 2 were women, with age ranging from 32 to 85 years (mean, 62.6 years; median, 67 years). The tumor size ranged from 6 to 14 cm (mean, 9.4 cm; median, 9.3 cm). Follow-up data were available for 7 patients and ranged from 5 months to 14 years (mean, 4 years; median, 3 years). Three patients died of conditions unrelated to renal tumor progression (ie, lung cancer and hepatic failure). The remaining 7 patients were alive and well without disease progression or metastasis at the time of study.

3.2. Gross and microscopic findings

Grossly, tumors were large, with size up to 14 cm in greatest dimension (case 6). The tumors grew expansively, were well demarcated, and did not invade into adjacent structures (Fig. 1A + B). All tumors presented as unilocular cystic mass encapsulated by thick whitish fibrous tissue. The inner surface of the capsule was mainly covered by a very thin layer of brownish friable tissue, and the whole cyst was usually filled with hemorrhagic and necrotic material (Fig. 2). No grossly identifiable neoplastic tissue was noted within the entire tumor.

Microscopically, all cases showed similar basophilic morphologic appearance with low-grade nuclear features consistent with type 1 PRCC. In most cases, there was only very limited amount of viable neoplastic tissue present lining the inner surface the cyst (Fig. 3A + B). This residual viable neoplastic tissue focally formed short papillae/tubulopapillary structures mostly lined by a single-cuboidal or low-columnar epithelial cells with scant cytoplasm and relatively uniform nuclei (Fig. 4A + B). Occasionally, more complex papillary structures were encountered. Histologic grade 2 was found in 8 cases, 3 in 2 cases (International Society of Urological Pathology [ISUP] nucleolar grading).

All tumors were well circumscribed, with a prominent fibrous capsule showing a thickness up to 2 cm. In 2 cases (cases 9 and 10), the capsule wall comprised rather cellular tissue composed mostly of fibroblasts with focally dense lymphocytic infiltration. Such a phenomenon was morphologically consistent with the diagnosis of inflammatory pseudotumor (Fig. 5A + B). Cysts were filled with hemorrhagic and necrotic material.

3.3. Immunohistochemistry

The immunohistochemical findings are summarized in Table 2. All of the examined tumors were diffusely positive for AMACR, OSCAR, CAM 5.2, anti–HIF-2 and vimentin (Fig. 6). CD117 and anti HIF-1 were weakly positive. MIA was diffusely positive in 9/10 cases, and in one case (case 8) the positivity was focal. 7 of 10 tumors diffusely reacted with PAX 8, and the remaining 3 cases were focally positive. There was no expression of CANH and TFE3 in any case. Expression of CD34, CD31, mTor, Cathepsin K, and AE1-AE3 was variable. ALK-1 was negative both in pseudocapsules and in the neoplastic tissue in all cases.

3.4. Molecular-genetic findings

Findings of molecular-genetic analyses are summarized in Table 3. Tumors were analyzed for chromosomal copy number variation using array comparative genomic hybridization (aCGH) and fluorescence in

Table 2
Immunohistochemical findings

Case	CD117	CD31	CD34	Cath	AMACR	OSCAR	Vim	AE 1/3	CAM 5.2	MIA	TFE 3	CANH	PAX 8	Anti–HIF-1	Anti–HIF-2	mTOR	ALK 1[a]
1	+	−	−	−	+++	+++	+++	foc +++	++	+++	−	−	+++	+	+++	foc +++	−
2	+	+	+	−	+++	+++	+++	foc ++	++	+++	−	−	++	+	+++	foc +++	−
3	+	+	+	−	+++	+++	+++	foc +++	++	+++	−	−	++	+	+++	foc +++	−
4	+	+	−	−	+++	+++	+++	+++	+++	+++	−	−	+++	++	+++	foc +++	−
5	+	+	+	−	+++	+++	+++	foc +++	+++	+++	−	−	+++	+	+++	+	−
6	+	+	−	−	+++	+++	+++	+++	++	+++	−	−	++	++	+++	−	−
7	+	−	−	−	+++	+++	+++	foc +++	++	+++	−	−	foc +++	+	+++	foc +++	−
8	+	+	+	+	+++	+++	+++	+++	++	foc +++	−	−	foc +++	++	+++	foc +++	−
9	+	+	+	−	+++	+++	+++	+++	++	+++	−	−	foc +++	++	+++	foc ++	−
10	+	+	+	+	+++	+++	+++	foc ++	++	+++	−	−	+++	+	+++	+	−

Abbreviations: Cath, cathepsin K; foc, focally; Vim, vimentin; −, negative; +, weakly positive; ++, moderately positive; +++, strongly positive.
[a]Assessed in the capsule only.

Table 3
Molecular-genetic analyses

Case	Sex	aCGH	CEP 7	CEP 17	CEP XY	LOH 3p	VHL	VHLM
1	M	+9,+12,+20,−Y	D	D	X-	Neg	Neg	Neg
2	F	+12,+13,+16,+17,−21	D	P	XX	Neg	Neg	Neg
3	M	No changes	NA	NA	NA	Neg	Neg	Neg
4	M	NP	P	P	X-	NA	NA	Neg
5	F	NP	NP	NP	NP	NP	NP	NP
6	M	+7,+17	P	P	X-	Neg	Neg	Neg
7	M	+(7pter-7q22.1),+17,−Y	P	P	X-	NA	Neg	Neg
8	M	No changes	D	D	XY	Neg	Neg	Neg
9	M	+2,+3,+7,+12,+16,+17,+20,+21,+22	P	P	XY	Neg	Neg	Neg
10	M	NP	P	P	X-	NA	Neg	Neg

situ hybridization. Seven cases were analyzable by aCGH. Chromosome 7 and 17 polysomy was found in 5 cases (Fig. 7). No chromosomal numerical aberrations were found in 2 cases. In case 1, both chromosomes 7 and 17 were disomic with loss of chromosome Y detected by aCGH and subsequently confirmed by fluorescence in situ hybridization. Polysomies of chromosomes 9, 12, and 20 were found in the same tumor (case 1). Case 2 exhibited gains of chromosomes 12, 13, 16, and 17; chromosome 21 was monosomic and chromosome 7 was disomic.

No VHL gene abnormalities including mutations, hypermethylation of VHL promoter, and loss of heterozygosity of 3p locus were found in analyzable cases (Table 3).

4. Discussion

It has been evident since the so-called Heidelberg classification in 1997 that renal tumors represent a highly heterogeneous group of neoplasms not only morphologically but also from molecular-genetic perspectives [5]. In the 2004 World Health Organization classification of genitourinary tumors, 4 new subtypes of renal tumors were introduced [6]. In the 2012 ISUP Vancouver Renal Tumor Classification, further 5 new renal tumors were included and 3 more were recognized as “emerging” renal tumors [6]. The recent 2016 World Health Organization classification fully accepts the proposals of the 2012 ISUP Vancouver classification and one of the “emerging entities,” succinate dehydrogenase deficient renal cell carcinoma (RCC), has been added as a new entity [7]. It is evident from these ever-evolving classifications that the morphologic and genetic variability of renal tumors are enormous and that one can reasonably anticipate different clinical outcomes in particular tumor types. Therefore, prognostic criteria and predictor factors can play a crucial role in providing individual risk profiles with a suitable aftercare conception [8]. It would be challenging to apply prognostic morphologic criteria to RCCs owing to vast tumor heterogeneity and the diverse biological pathways that exist in various tumors [8,9].

Type 1 PRCC is currently considered a distinct entity with relative uniform gross, histologic, and immunohistochemical features as well as similar molecular-genetic profile. Our cohort is constituted of a homogenous subset of type 1 PRCC presenting with large unilocular cystic necrotic tumors.

Papillary renal cell carcinoma, the second most common RCCs, was initially classified as 2 morphologic groups of so-called type 1 and type 2 by Delahunt and Eble [2]. Papillary renal cell carcinomas are generally immunoreactive for vimentin, cytokeratins AE1-AE3, CAM5.2, high-molecular-weight cytokeratins, EMA, CD10, and AMACR. Type 1 PRCC is more frequently positive for CK7. Genetic abnormalities in PRCC most commonly include trisomy/polysomy of chromosomes 7, 12, 16, 17, and 20 and loss of the Y chromosome. Several studies have

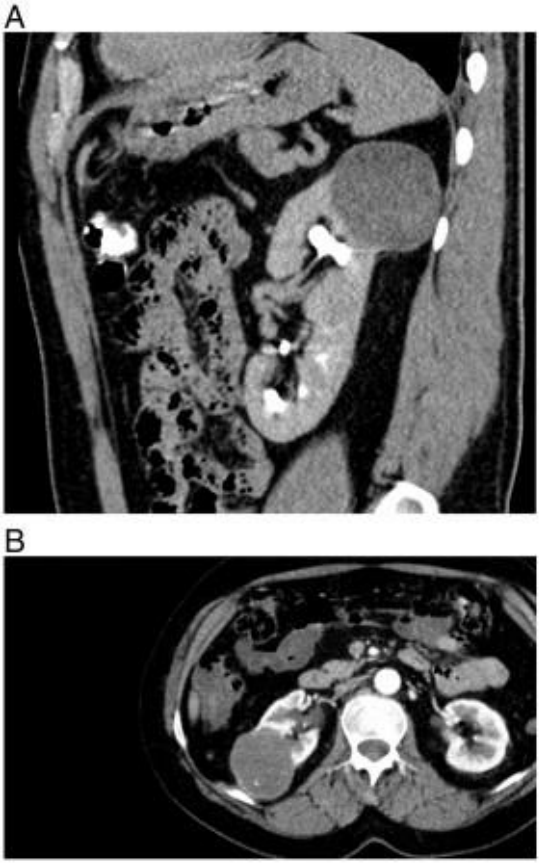

Fig. 1. (A) Case 2. Postcontrast computed tomography (CT), excretory phase, sagittal section. A round-shape tumor of the upper pole of the left kidney. Postcontrast density 17-61 HU. Necrotic center of the tumor is clearly visible. (B) Case 3. Postcontrast CT, arterial phase, axial section. Tumor of the right kidney, round shape with large central necrosis, postcontrast density 25-68 HU.

Fig. 2. Thick-walled cyst with thin, mostly necrotic rim of neoplastic tissue on the inner surface.

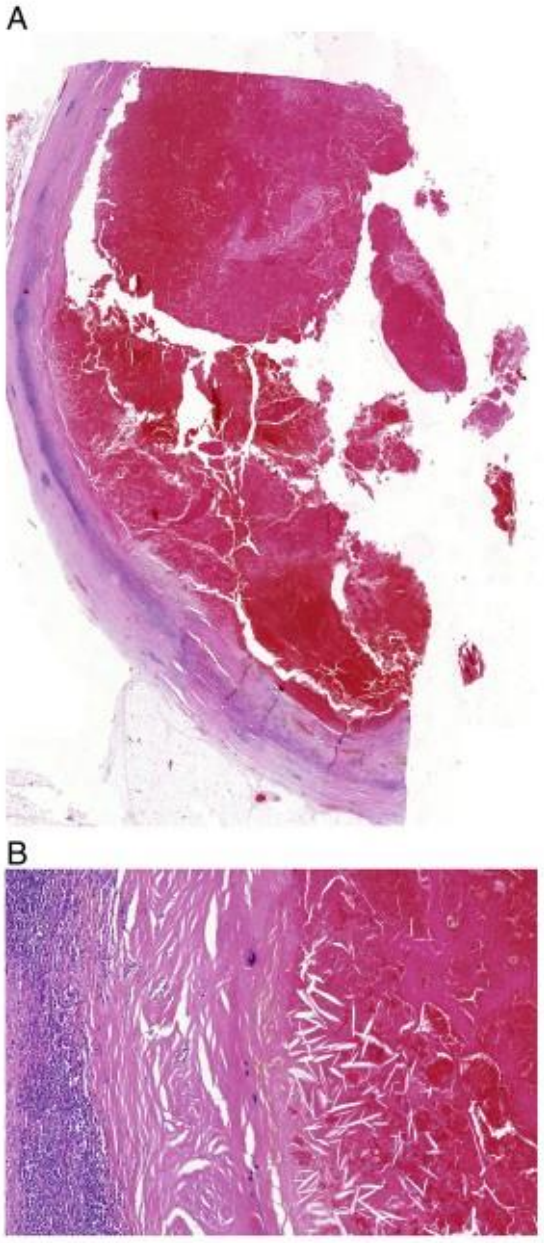

Fig. 3. (A + B) A limited amount of the vital neoplastic tissue lined the inner wall of the cyst. (A) Scanning magnification showing a large portion of thick-walled cyst. (B) Large areas of inner surface of the cyst were covered by necrotic material only.

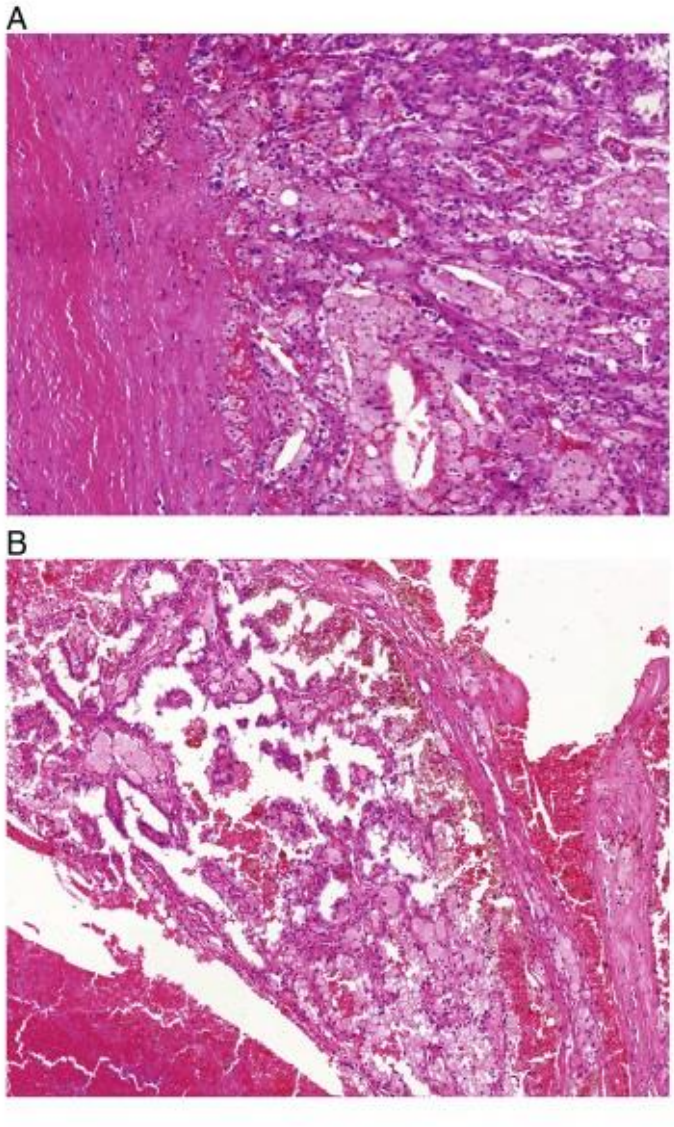

Fig. 4. Viable neoplastic tissue focally formed tubulopapillary (A) or short papillary (B) structures mostly lined by single-cuboidal or low-columnar epithelial cells with scant cytoplasm and uniform nuclei.

suggested genetic differences between type 1 (morphologically basophilic) and type 2 (morphologically eosinophilic) subtypes [6].

The increasing number of reported cases and the development of new diagnostic techniques have demonstrated that PRCC, as a group, is more diverse morphologically and genetically than previously thought.

Papillary renal cell carcinomas sometimes display overlapping morphologic features of type 1 and type 2, which can pose significant diagnostic difficulties in differentiating between the 2 types [10]. Several distinct variants of PRCC that are different from type 1 and type 2 have been described in the literature [11-14]. It should be noted that types 1 and 2 PRCCs are shown to be clinically and biologically distinct. Alterations in the MET pathway are associated with type 1, and activation of the NRF2-ARE pathway is described with type 2 [15]. Type 1 tumors often harbor gains of chromosomes 7p and 17p, whereas type 2 tumors contain an allelic imbalance of one or more chromosomes, namely, chromosomes 1p, 3p, 5, 6, 8, 9p, 10, 11, 15, 18, and 22 [6,15].

In our study, we attempted to assemble a uniform cohort of PRCC tumors that were consisted of large cystic necrotic/hemorrhagic tumors encapsulated by thick fibrous tissue. Morphologically and immunohistochemically, all lesions corresponded with type 1 PRCC. We noted that the tumors contained only scarce amounts of viable neoplastic tissue, mainly in the inner surface of the cyst wall, with most of tumor volume consisting of necrotic sanguinolent material.

The molecular-genetic profile was also expectedly consistent with type 1 PRCC (in 5/9 analyzable cases). Two of our cases demonstrated disomy in chromosomes 7 and 17, but also showed additional chromosomal abnormalities. Gains of chromosomes 9, 12, and 20 were found in 1 case (case 1), with a second case (case 6) exhibiting normal chromosome 7 and 17 status as well as disomy of all other chromosomes.

The prognosis of RCCs in general is attributed to several clinical and pathological factors such as symptomatic cancer, TNM classification, histologic grade, and presence/absence of a sarcomatoid differentiation [22]. The presence of TN has also been proposed repeatedly as an independent prognostic factor. Tumor necrosis appears to represent an interesting parameter in prognostic assessment owing to its easy and reproducible identification in routine histopathologic examination. However, there are several conflicting aspects that challenge the notion

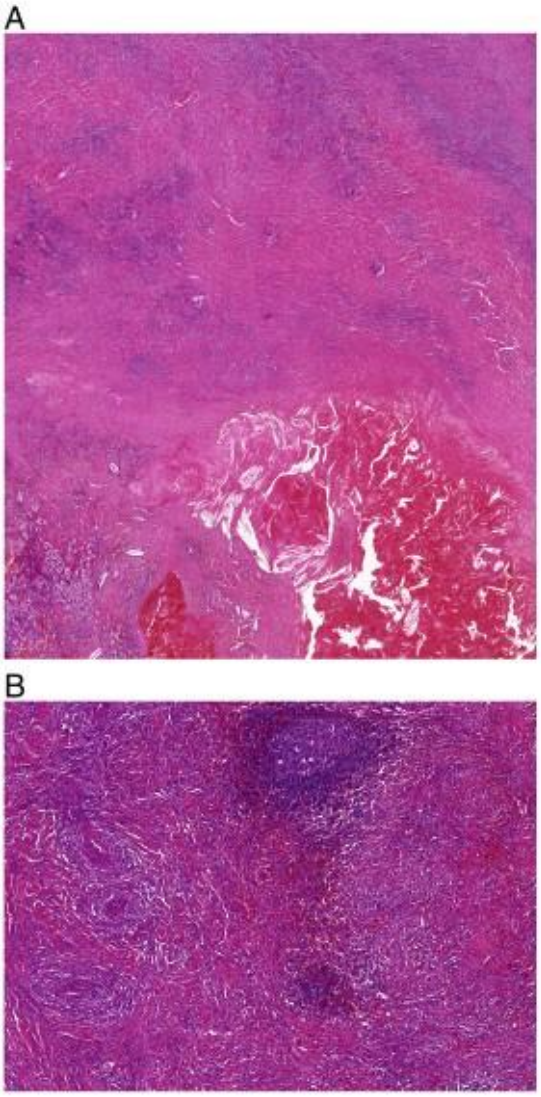

Fig. 5. Thick capsule resembling inflammatory pseudotumor was present in 2 cases. Scanning magnification (A) and detailed view (B).

of TN as a prognostic parameter. First, the prognostic significance of necrosis in RCCs remains controversial because the studies published to date have shown conflicting results [9,16,17]. This may be explained by the fact that no uniform consensus on assessing TN exists. Some researchers evaluate necrosis from gross specimens only [16,18], whereas others use radiologic or microscopic findings [9,17,19]. Klatte et al suggested that classification based solely on the presence or absence of necrosis is unsatisfactory. Conversely, they recommended a scoring system based on the extent of necrosis as a part of every pathological examination [33]. However, this concept is not currently accepted as part of standard reporting.

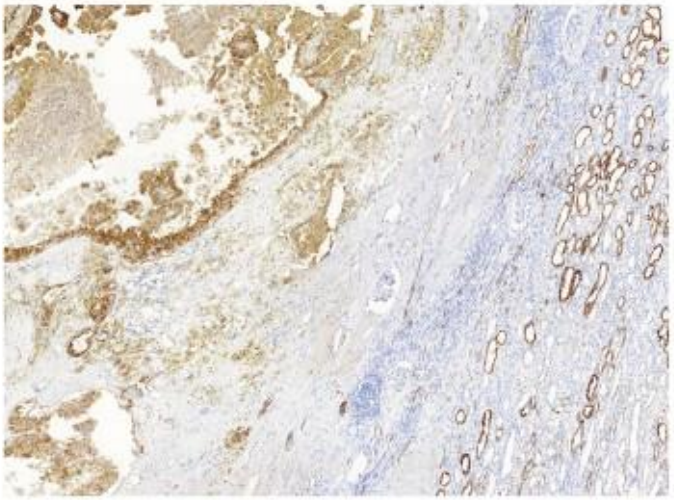

Fig. 6. All tumors were positive for AMACR.

Although TN is often reported as an adverse prognostic factor, its significance is only well established in clear cell RCC [6,20-22]. Furthermore, according to a recently proposed grading system for clear cell RCC, only coagulative-type necrosis is considered as a significant prognostic marker. It should be noted that no such criteria have been established for PRCC. Coagulative-type necrosis is characterized by preserved architecture of dead tissues and firm texture, with neoplastic cells showing no nuclei with limited structural damage, giving the appearance of so-called “ghost cells.”

On the other hand, liquefactive necrosis is characterized by digestion of the dead cells resulting in transformation of the tissue into a liquid viscous mass [23]. We consider the necrosis within our cohort to be liquefactive type, as a substantial part of the tumor was transformed into a liquid viscous, largely hemorrhagic mass in all cases.

Considering that PRCCs are composed of a diverse and heterogeneous group of tumors, the determination of prognostic factors would even be more difficult to ascertain. The situation is further complicated by the fact that the incidence of PRCC is much lower than that of clear cell RCC, and a relatively limited number of studies dealing with prognostic factors in PRCC have been published [24]. One of the strengths of our series is that all the cases were uniformly and exclusively composed of type 1 PRCC according to Delahunt classification. It is worth noting that studies assessing clinical outcomes in PRCC may have generated inconsistent conclusions simply due to heterogeneous nature of PRCCs. Hence, numerous researchers have made an effort to determine the most useful method of histologic assessment in establishing meaningful prognostic factors. Onishi et al [25] studied clinicopathologic features of 42 PRCCs and their influence on prognosis. They suggested that the presence or absence of foam cells, pseudocapsule, solid architecture, cytologic appearance, stage, and nuclear grade were meaningful prognostic factors. In addition, they observed that the prognosis of patients with PRCC was similar to those with clear cell RCC. They did not include TN among the list of prognostic parameters, assuming that TN simply indicates poor tumor vascularization and that would be clinically irrelevant. However, because PRCC refers to a rather diverse heterogenous group of tumors and no further subclassifications of PRCC were provided by the authors, it would be difficult to determine which prognostic factors would have been attributed to different types of PRCC. Several other studies also reached a similar conclusion to that of Onishi et al, not considering TN to be an adverse prognostic parameter in PRCC [9,25-28]. In contrast, a number of studies reported TN to be associated with an adverse clinical course. In this regard, it is thus understandable that some researchers have designated TN as an adverse prognostic factor for PRCC [24,29-32].

However, it is of note that the subclassifying of PRCC into the type 1 and type 2 was not taken into consideration in some of these studies [8,26,28,33,34], whereas it was included in others [9,16,29,31]. For this reason, it is unclear whether it would be possible to compare the results from studies dealing with such a heterogeneous cohort of tumors. For instance, some PRCCs (ie, familiar leiomyomatosis associated [papillary] RCC) are clinically aggressive tumors, and that it would be inappropriate to objectively assess the prognostic value of TN in PRCCs without further subtyping.

This study is one of its kind to address this issue in an objective fashion. In our series of 10 largely necrotic type 1 PRCCs, none of the tumors demonstrated an aggressive or metastatic behavior. However, we would like to point out that our study has no ambition to establish prognostic criteria for type 1 PRCC or to evaluate presence/absence of

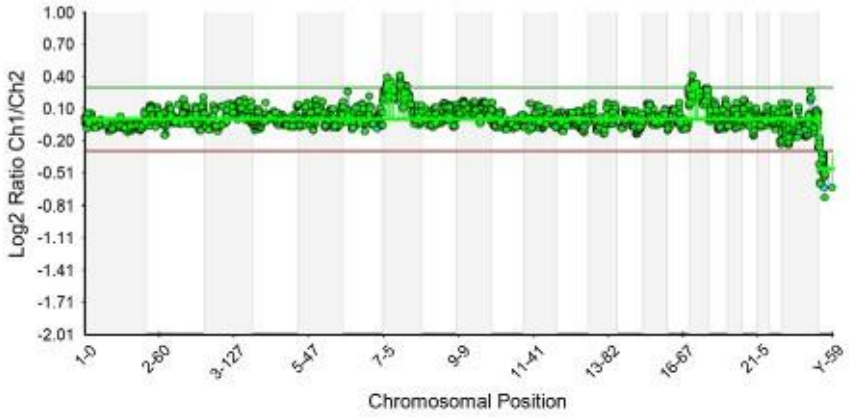

Fig. 7. Array CGH profile of case 7 revealing gains on chromosomes 7 (7pter-7q22.1) and 17, and a loss of chromosome Y.

necrosis as an adverse/ambivalent prognostic feature. The aim of this study was to describe a subpopulation of type 1 PRCC characterized by uniform, albeit unusual gross and histologic features.

An interesting phenomenon was documented in cases 9 and 10 of our series where the tumor capsule was composed of fibrous tissue, indistinguishable from inflammatory pseudotumor histologically. Therefore, it is very important to carefully examine the capsule and to distinguish myofibroblastic proliferation from sarcomatoid differentiation or even from sarcoma arising in an inflammatory pseudotumor. Inflammatory pseudotumors may express ALK-1 and cytokeratin immunostains, which can be helpful in differentiating ambiguous entities [33,34]. Neither ALK-1 nor cytokeratins showed a positive reaction in any tumor capsule in our series including the above-mentioned 2 cases. The capsules reminiscent of inflammatory pseudotumor in the above-mentioned cases exhibited identical immunohistochemical reaction against ALK-1 and cytokeratins as tumors with a “simple” fibrous capsule.

According to some authors, the presence of a fibromuscular pseudocapsule is rather characteristic of and more prominent in clear cell RCC, less frequently present in chromophobe RCC, and rarely in PRCC [34]. Fibromuscular pseudocapsules are characterized by a complex architecture including both connective tissue and smooth muscle fibers with thicker capsules sometimes containing vasculopathy. The presence of a pseudocapsule may be helpful to resolve diagnostic difficulties in challenging cases. The core biopsy specimen from patients with a high Bosniak type might be composed predominantly of fibromuscular tissue and only scant tumor fragments [34]. This kind of biopsy finding should lead to recommend additional tissue sampling. The designation of such a specimen as a nonrepresentative or even nonneoplastic biopsy should be considered with caution. According to some authors, radiologic and/or pathologic presence of a pseudocapsule/fibromuscular tissue may raise suspicion for RCC, with a higher probability of clear cell type [34]. The cases described in our study clearly show that a thick pseudocapsule can also be found in low-grade PRCC type 1.

5. Conclusions

Type 1 PRCC can present as a large unicystic lesion with necrotic/hemorrhagic content and surrounded by thick fibroleiomyomatous capsule. Most of our cases contained a chromosomal numerical aberration pattern characteristic of PRCC. All tumors followed a nonaggressive clinical course. Large liquefactive necrosis should not necessarily be considered an adverse prognostic feature, at least in a subset of type 1 PRCC with unilocular necrotic cystic presentation. Adequate tissue sampling in such tumors is crucial to arrive at accurate diagnosis, because most of these tumors contain limited viable neoplastic tissue lining the inner cyst wall.

Abbreviations: CEP, centromeric enumeration probe; F, female; LOH 3p, loss of heterozygosity of chromosome 3p; M, male; NA, not analyzable; Neg, negative; NP, not performed; P, polysomy; VHL, mutation analysis of VHL; VHLM, methylation of VHL; X-, loss of chromosome Y

References

[1] Moch H, Humphrey PA, Ulbright TM, Reuter VE. WHO classification of tumours of the urinary system and male genital organs; 2016.
[2] Delahunt B, Eble JN. Papillary renal cell carcinoma: a clinicopathologic and immunohistochemical study of 105 tumors. Mod Pathol 1997;10:537–44.
[3] Hes O, Hora M, Havlicek F, Chudacek Z, Klecka J, Michal M. Papillary renal cell carcinoma surrounded by unusual fibrotic reaction resembling inflammatory pseudotumour—a case report. Cesk Patol 2004;40:112–6.
[4] Herman JG, Graff JR, Myohanen S, Nelkin BD, Baylin SB. Methylation-specific PCR: a novel PCR assay for methylation status of CpG islands. Proc Natl Acad Sci U S A 1996;93:9821–6.
[5] Kovacs G, Akhtar M, Beckwith BJ, Bugert P, Cooper CS, Delahunt B, et al. The Heidelberg classification of renal cell tumours. J Pathol 1997;183:131–3.
[6] Srigley JR, Delahunt B, Eble JN, Egevad L, Epstein JI, Grignon D, et al. The International Society of Urological Pathology (ISUP) Vancouver classification of renal neoplasia. Am J Surg Pathol 2013;37:1469–89.
[7] Agaimy A. Succinate dehydrogenase (SDH)–deficient renal cell carcinoma. Pathologe 2016;37:144–52.
[8] Pflanz S, Brookman-Amissah S, Roigas J, Kendel F, Hoschke B, May M. Impact of macroscopic tumour necrosis to predict survival of patients with surgically resected renal cell carcinoma. Scand J Urol Nephrol 2008;42:507–13.
[9] Sengupta S, Lohse CM, Leibovich BC, Frank I, Thompson RH, Webster WS, et al. Histologic coagulative tumor necrosis as a prognostic indicator of renal cell carcinoma aggressiveness. Cancer 2005;104:511–20.
[10] Allory Y, Ouazana D, Boucher E, Thiounn N, Vieillefond A. Papillary renal cell carcinoma. Prognostic value of morphological subtypes in a clinicopathologic study of 43 cases. Virchows Arch 2003;442:336–42.
[11] Argani P, Netto GJ, Parwani AV. Papillary renal cell carcinoma with low-grade spindle cell foci: a mimic of mucinous tubular and spindle cell carcinoma. Am J Surg Pathol 2008;32:1353–9.
[12] Cantley R, Gattuso P, Cimbaluk D. Solid variant of papillary renal cell carcinoma with spindle cell and tubular components. Arch Pathol Lab Med 2010;134:1210–4.
[13] Hes O, Brunelli M, Michal M, Cossu Rocca P, Hora M, Chilosi M, et al. Oncocytic papillary renal cell carcinoma: a clinicopathologic, immunohistochemical, ultrastructural, and interphase cytogenetic study of 12 cases. Ann Diagn Pathol 2006;10:133–9.
[14] Val-Bernal JF, Gomez-Roman JJ, Vallina T, Villoria F, Mayorga M, Garcia-Arranz P. Papillary (chromophil) renal cell carcinoma with mucinous secretion. Pathol Res Pract 1999;195:11–7.
[15] Linehan WM, Spellman PT, Ricketts CJ, Creighton CJ, Fei SS, Davis C, et al. Comprehensive molecular characterization of papillary renal-cell carcinoma. N Engl J Med 2016;374:135–45.
[16] Leibovitch I, Lev R, Mor Y, Golomb J, Dotan ZA, Ramon J. Extensive necrosis in renal cell carcinoma specimens: potential clinical and prognostic implications. Isr Med Assoc J 2001;3:563–5.
[17] Zubac DP, Bostad L, Gestblom C, Kihl B, Seidal T, Wentzel-Larsen T, et al. Renal cell carcinoma: a clinicopathological follow-up study after radical nephrectomy. Scand J Urol Nephrol 2007;41:191–7.
[18] Sabo E, Boltenko A, Sova Y, Stein A, Kleinhaus S, Resnick MB. Microscopic analysis and significance of vascular architectural complexity in renal cell carcinoma. Clin Cancer Res 2001;7:533–7.
[19] Tollefson MK, Thompson RH, Sheinin Y, Lohse CM, Cheville JC, Leibovich BC, et al. Ki-67 and coagulative tumor necrosis are independent predictors of poor outcome for patients with clear cell renal cell carcinoma and not surrogates for each other. Cancer 2007;110:783–90.

[20] Delahunt B. Advances and controversies in grading and staging of renal cell carcinoma. Mod Pathol 2009;22(Suppl. 2):S24–36.
[21] Delahunt B, Bethwaite PB, Nacey JN. Outcome prediction for renal cell carcinoma: evaluation of prognostic factors for tumours divided according to histological subtype. Pathology 2007;39:459–65.
[22] Delahunt B, Bethwaite PB, Miller RJ, Sika-Paotonu D, Srigley JR. Re: Fuhrman grade provides higher prognostic accuracy than nucleolar grade for papillary renal cell carcinoma: T. Klatte, C. Anterasian, J. W. Said, M. de Martino, F. F. Kabbinavar, A. S. Belldegrun and A. J. Pantuck. J Urol 2010;183:2143-2147. J Urol 2011;185:356–7 [author reply 357-358].
[23] Kumar V, Abbas AK, Fausto N, Aster JC. Robbins and Cotran pathologic basis of diseases. , 3-42 Philadelpia: Saunders Elsevier; 2010.
[24] Sukov WR, Lohse CM, Leibovich BC, Thompson RH, Cheville JC. Clinical and pathological features associated with prognosis in patients with papillary renal cell carcinoma. J Urol 2012;187:54–9.
[25] Onishi T, Ohishi Y, Goto H, Suzuki M, Miyazawa Y. Papillary renal cell carcinoma: clinicopathological characteristics and evaluation of prognosis in 42 patients. BJU Int 1999;83:937–43.
[26] Moch H, Gasser T, Amin MB, Torhorst J, Sauter G, Mihatsch MJ. Prognostic utility of the recently recommended histologic classification and revised TNM staging system of renal cell carcinoma: a Swiss experience with 588 tumors. Cancer 2000;89:604–14.
[27] Kim H, Cho NH, Kim DS, Kwon YM, Kim EK, Rha SH, et al. Renal cell carcinoma in South Korea: a multicenter study. Hum Pathol 2004;35:1556–63.
[28] Cheville JC, Lohse CM, Zincke H, Weaver AL, Blute ML. Comparisons of outcome and prognostic features among histologic subtypes of renal cell carcinoma. Am J Surg Pathol 2003;27:612–24.
[29] Fu Z, Sun L, Huang Y, Zhang J, Zhang Z, Wang L, et al. A type 2 papillary renal cell carcinoma presenting as an intracystic necrotic lesion: a case report. Mol Clin Oncol 2013;1:318–20.
[30] Pichler M, Hutterer GC, Chromecki TF, Pummer K, Mannweiler S, Zigeuner R. Presence and extent of histological tumour necrosis is an adverse prognostic factor in papillary type 1 but not in papillary type 2 renal cell carcinoma. Histopathology 2013;62:219–28.
[31] Pichler M, Hutterer GC, Chromecki TF, Jesche J, Kampel-Kettner K, Rehak P, et al. Histologic tumor necrosis is an independent prognostic indicator for clear cell and papillary renal cell carcinoma. Am J Clin Pathol 2012;137:283–9.
[32] Klatte T, Remzi M, Zigeuner RE, Mannweiler S, Said JW, Kabbinavar FF, et al. Development and external validation of a nomogram predicting disease specific survival after nephrectomy for papillary renal cell carcinoma. J Urol 2010;184:53–8.
[33] Chan JK, Cheuk W, Shimizu M. Anaplastic lymphoma kinase expression in inflammatory pseudotumors. Am J Surg Pathol 2001;25:761–8.
[34] Roquero L, Kryvenko ON, Gupta NS, Lee MW. Characterization of fibromuscular pseudocapsule in renal cell carcinoma. Int J Surg Pathol 2015;23:359–63.

3.6 Molecular-genetic analysis is essential for accurate classification of renal carcinoma resembling Xp11.2 translocation carcinoma

Xp11.2 TRCC se prioritně vyskytuje u mladých pacientů a bývá popisován v souvislosti s předchozí expozicí chemoterapii.

U vybrané skupiny 20 případů (z celkem 17 500 renálních neoplásií v Plzeňském registru nádorů), u nichž vyvstalo na podkladě morfologického vzhledu podezření na diagnózu TRCC (tzv. TRCC-like), byla za účelem stanovení přesné diagnózy provedena další vyšetření pomocí imunohistochemie a molekulárně genetických metod. U devíti případů byla potvrzena translokace TFE3 (pomocí FISH), tyto nádory byly na základě výsledků molekulárně genetických metod označeny za Xp11.2 TRCC. Ze zbylých 11 TRCC-like nádorů (7 mužů, 4 ženy, věkové rozmezí pacientů 22-84 let), pouze u devíti případů byl k dispozici materiál pro další studii. Morfologické spektrum lézí bylo velmi různorodé, u šesti tumorů s přítomností buněk s eosinofilní či jasnou cytoplasmou v tubulárním, acinárním a papilárním uspořádání. Jeden z nádorů obsahoval epiteloidní vřetenité buňky a sarkomatoidní okrsky, celkově tak nádor působil high-grade morfologií. Další nádor se prezentoval okrsky s tubulární, solidní a papilární architektonikou a okrsky vřetenitých buněk, což celkově dávalo nádoru vzhled připomínající MTSRCC. Poslední z nádorů vykazoval na pozadí denzního lymfoplazmocytárního infiltrátu dyskohezivně rozprostřená hnízda velkých epitheloidních a histiocytárních buněk. Exprese cytokeratinových markerů byla vyjádřena ve třech případech za použití cytokeratinu AE1/AE3, cytokeratin CK7 reagoval silně u jednoho případu a u jednoho z tumorů byl exprimován pouze slabě fokálně. Imunohistochemický průkaz CD10 a PAX8 byl pozitivní v osmi případech, AMARC a vimentin vykazovaly pozitivitu u sedmi tumorů, exprese CA-IX byla zastižena ve čtyřech případech a dva případy byly pozitvní při imunohistochemickém průkazu TFE3 a kathepsinu K. Molekulárně genetické vyšetření pak u jednoho z TFE3 imunohistochemicky pozitivních případů ukázalo polysomii chromosomu 7, druhý TFE3 imunohistochemicky pozitivní tumor vykazoval polysomii chromosomu 17, oba tyto tumory nevykazovaly VHL abnormality a finálně byly klasifikovány jako RCC NOS. Ze sedmi TFE3 imunohistochemicky negativních případů byly tři klasifikovány jako kombinovaný CCRCC a PRCC (u nádorů prokázána polysomie chromosomů 7/17 a *VHL* abnormality), jeden tumor byl označen jako CCRCC (normální status chromozomů 7/17 avšak při přítomnosti *VHL* abnormality – LOH 3p), jeden případ vykazoval změny typické pro PRCC (polysomie 7/17, normální *VHL* status) a byl tedy jako PRCC klasifikován a dva případy (normální statut chromosomů 7/17, bez *VHL* abnormalit) byly zařazeny do kategorie RCC NOS.

Ve výsledku, při své morfologické a imunohistochemické heterogenitě, je přesná klasifikace a odlišení TRCC a TRCC-like nádorů možné pouze na základě posouzení morfologie a zejména provedením molekulárně-genetické analýzy, imunohistochemické vyšetření má jen relativně omezený význam. TRCC jsou tedy jednotkou diagnostikovanou na základě morfologických a molekulárně genetických metod. Je evidentní, že v minulosti řada nádorů označených jako TRCC byly renální karcinomy, které skutečné translokační karcinomy pouze napodobovaly.

Virchows Arch (2015) 466:313–322
DOI 10.1007/s00428-014-1702-7

ORIGINAL ARTICLE

Molecular-genetic analysis is essential for accurate classification of renal carcinoma resembling Xp11.2 translocation carcinoma

Malcolm Hayes & Kvetoslava Peckova & Petr Martinek & Milan Hora & Kristyna Kalusova & Lubomir Straka & Ondrej Daum & Bohuslava Kokoskova & Pavla Rotterova & Kristyna Pivovarčikova & Jindrich Branzovsky & Magdalena Dubova & Pavla Vesela & Michal Michal & Ondrej Hes

Received: 21 August 2014 / Revised: 26 October 2014 / Accepted: 1 December 2014 / Published online: 28 December 2014

Abstract Xp11.2-translocation renal carcinoma (TRCC) is suspected when a renal carcinoma occurs in young patients, patients with a prior history of exposure to chemotherapy and when the neoplasm has morphological features suggestive of that entity. We retrieved 20 renal tumours (from 17,500 archival cases) of which morphology arose suspicion for TRCC. In nine cases, TFE3 translocation was confirmed by fluorescence in situ hybridisation analysis. In 9 of the remaining 11 TRCC-like cases (7 male, 4 female, aged 22–84 years), material was available for further study. The morphological spectrum was diverse. Six tumours showed a mixture of cells with eosinophilic or clear cytoplasm in tubular, acinar and papillary architecture. One case was high grade with epithelioid, spindle cell and sarcomatoid areas. Another showed tubular, solid, and papillary areas and foci containing spindle cells reminiscent of mucinous tubular and spindle cell carcinoma. The third showed dyscohesive nests of large epithelioid and histiocytoid cells in a background of dense lymphoplasmacytic infiltrate. By immunohistochemistry, keratin AE1/AE3 was diffusely positive in three tumours, while CK7 strongly stained one tumour and another focally and weakly. CD10 and Pax8 were expressed by eight, AMACR and vimentin by seven, CA-IX by four and TFE3 and cathepsin K by two tumours. Of the two TFE3-positive tumours, one showed polysomy of chromosome 7 and the other of 17; they were VHL normal and diagnosed as unclassifiable RCC. Of the seven TFE3-negative tumours, three showed polysomy of 7/17 and VHL abnormality and were diagnosed as combined clear cell RCC/papillary RCC. One TFE3-negative tumour with normal 7/17 but LOH 3p (VHL abnormality) was diagnosed as clear cell RCC. One TFE3-negative tumour with polysomy 7/17 but normal VHL was diagnosed as papillary RCC, and two with normal chromosomes 7/17 and VHL gene were considered unclassifiable. As morphological features and IHC are heterogeneous, TRCC-like renal tumours can only be sub-classified accurately by multi-parameter molecular-genetic analysis.

Keywords Translocation . Renal cell carcinoma . TFE3 . Xp11 . FISH . Molecular genetics . MiTF . Immunohistochemistry

M. Hayes
Department of Pathology, BC Cancer Agency and Clinical Professor of Pathology, University of British Columbia, Vancouver, Canada

K. Peckova : P. Martinek : O. Daum : B. Kokoskova : P. Rotterova : K. Pivovarčikova : J. Branzovsky : M. Dubova : P. Vesela : M. Michal : O. Hes (*)
Department of Pathology, Medical Faculty, Charles University and Charles University Hospital Plzen, Alej Svobody 80, 304 60 Plzen, Czech Republic
e-mail: hes@medima.cz

M. Hora : K. Kalusova
Department of Urology, Medical Faculty, Charles University and Charles University Hospital Plzen, Plzen, Czech Republic

L. Straka
Klinicka Patologia Presov, Presov, Slovak Republic

Introduction

Translocation-associated renal cell carcinoma (TRCC) resulting from Xp11.2 (TFE3) translocation was recognised first in paediatric and young adult patients [30, 41]. Subsequently TRCC was documented in older adults, and its frequency in the adult population is probably underestimated [8, 13, 20, 25, 48]. While TRCC has a favourable prognosis in children, these neoplasms may be aggressive in adults [24, 27, 31, 40].

Several variants of TRCC with translocation of TFE3 to different partner genes are now described [1, 2, 6, 7, 17, 42,

43]. The more common partners are ASPL and PRCC genes. TFE3 translocation also occurs in other neoplasms including alveolar soft-part sarcoma and some forms of PEComa [3, 22, 47]. TRCC involving the closely related TFEB gene, which is also part of the MiTF gene family, is rarer than TFE3-TRCC but has a similar clinical presentation and may have overlapping morphology [4, 9, 18, 38]. The two variants of MiTF-TRCC lack a familial history and are not multifocal, in contrast to renal cancers of the hereditary CCRCC syndrome associated with chromosome 3 translocations, and the hereditary PRCC associated with c-MET mutations [46].

Renal carcinoma occurring in a child, or in a patient exposed to chemotherapy for an earlier cancer, suggests the possibility of TRCC. Morphological studies of TRCC delineated an association with histological features that include a mixed papillary and alveolar architecture, a mixture of cells with clear and eosinophilic cytoplasm and clear cells with abundant voluminous cytoplasm. Presence of blood lakes, psammoma bodies, stromal hyaline globules and eosinophilic cytoplasmic inclusions are additional features described in TRCC. None of these morphological features is specific for TRCC, and some of the features depend on the precise translocation partner of the TFE3 gene fusion. Demonstration of the TFE3 translocation is the defining characteristic of TRCC. This is best demonstrated by break-apart fluorescence in situ hybridisation (FISH) [32]. Over-expression of the TFE3 protein can be shown by immunohistochemistry, but the test requires careful calibration and adherence to strict standards of fixation and controls to avoid false results. Furthermore, TRCC has relatively specific immunohistochemical and gene expression profiles that assist in its distinction from CRCC and PRCC [5, 14, 38].

The present study was performed on a group of 20 renal neoplasms selected for their unusual morphology or clinical presentation, which were considered suspicious for TRCC. Having excluded the bona fide cases of TFE3-TRCC by FISH testing, the remaining nine TRCC-like cases with adequate material were studied further in an attempt to classify them in terms of the currently accepted Vancouver classification. This exercise entailed the development of an investigative algorithm for future recommendation.

Materials and methods

Twenty tumours suspect for TRCC based mostly on morphological features were identified in the Plzen archive of 17,500 renal neoplasms. Haematoxylin and eosin-stained (H&E) glass slides and formalin-fixed paraffin embedded blocks were retrieved, and the pathology reports and clinical records were studied to obtain demographic and follow-up data of the patients and for gross descriptions of the tumours. In addition to the original archival slides, standard 4-μm sections were cut from formalin-fixed, paraffin-embedded blocks selected from the tumours. These were stained with H&E for light microscopic examination using standard methodology and spare sections were cut for IHC. The number of blocks per case ranged from 3 to 30.

All H&E-stained sections and IHC stains were reviewed by three authors of this paper (MH, KP and OH).

The immunohistochemical study was performed using a Ventana Benchmark XT automated stainer (Ventana Medical System, Inc., Tucson, AZ, USA). Antibodies against CK7 (monoclonal, OV-TL 12/30, 1:200, Dako, Glostrup, Denmark), pan keratin (polyclonal, AE1-AE3/PCK26, RTU, Ventana-Roche), CD10 (monoclonal, 56C6, 1:20, Novocastra, Burlingame, CA, USA), AMACR (monoclonal, 13H4, 1:200, Dako), TFE3 (polyclonal, Abcam, 1:100, Cambridge, UK), vimentin (D9, monoclonal, Neomarkers, Westinghouse, CA, USA, 1:1000), CA-IX (monoclonal, 303123, 1:100, RD systems, Minneapolis, MN, USA), cathepsin K (monoclonal, 3F9, Abcam, 1:100), PAX-8 (polyclonal, Abcam, Cambridge, UK, 1:100) and anti-melanosome (monoclonal, HMB45, DakoCytomation, 1:200) were applied to all cases. Selected cases were also stained for S-100 protein (polyclonal, DakoCytomation, 1:400), wide spectrum keratin (OSCAR, monoclonal, Covance, Princetown, NJ, 1:2000), cytokeratin 20 (M7019, monoclonal, DakoCytomation, 1:100) and cytokeratin (CAM 5,2 monoclonal, Becton-Dickinson, San Jose, CA, USA, 1:200) as part of their initial diagnostic work-up.

For each case, 3–30 blocks were available; for immunohistochemical study, 1–2 selected blocks were used per case.

Molecular genetic study

FISH analysis was performed for TFE3 break and for enumeration of chromosomes X, Y, 7 and 17. The FISH procedure using centromeric probes for chromosomes 7 and 17 was described in paper of Petersson et al. [34]. The same technique of analysis and cut-off setting was used with probes CEP X/CEP Y (VYSIS/Abbott Molecular, Des Plaines, IL, USA) and ZytoLight® SPEC TFE3 Dual Color Break Apart Probe (ZytoVision GmbH, Bremerhaven, Germany). Monosomy and polysomy for chromosomes X and Y was defined as the presence of one signal per cell in >45 % and three and more signals in >10 % of cells, respectively. The cut-off value for TFE3 break was set to more than 10 % of nuclei with break signals. Mutation analysis of the VHL gene and loss of heterozygosity for chromosome 3p region (LOH3p) were studied by PCR and sequencing and fragmentation analysis, respectively. Methylation of the promoter of the VHL gene was analysed by methylation-specific PCR. All these methods were thoroughly described in paper of Petersson et al. [34].

Results

Clinical and gross findings

The patients, six male and three female, ranged in age from 43 to 84 years, 7 exceeding 50 years of age (Table 1). Tumour size ranged from 2.6 to 13 cm with six cases equal to or exceeding 5 cm in greatest dimension. Six cases were stage pT1 according TNM 09, two cases pT2 and one pT3. Four were from the left kidney and five from the right kidney. Most tumours were tan coloured with areas of brown, yellow to tan (Fig. 1a), white or grey with occasional, grossly visible necroses (Fig. 1b).

Follow-up was available in six cases. This ranged from 1 to 3 years. One patient died 1 year after diagnosis, and the other five patients are alive and well.

Histological findings

Three tumours had a prominent tubulopapillary architecture admixed with some solid nests of cells (Fig. 2a, b). Two tumours had a predominantly nested and alveolar pattern with alveolar spaces filled with eosinophilic secretions reminiscent of thyroid follicles (Fig. 3). One of these tumours contained small foci with a papillary architecture. Blood lakes were prominent in these two tumours and were seen focally in six other tumours. These two tumours and one of the neoplasms with a tubulopapillary architecture contained abundant clear cells with voluminous cytoplasm, prominent lateral cell borders and irregular apical cytoplasmic borders (so-called “blister” cells; Fig. 4). Such cells were seen focally in three other tumours. A population of cells with abundant eosinophilic (oncocyte-like) cytoplasm was also present in four of these tumours and predominated in two of the neoplasms (Fig. 5). One tumour with a nested and alveolar architecture mostly resembled CCRCC but had focal papillary architecture and some cells with eosinophilic granular cytoplasm (Fig. 6).

Three of the above tumours contained varying numbers of psammoma bodies and one demonstrated prominent eosinophilic hyaline cytoplasmic inclusion bodies. None showed extracellular hyaline nodules of the type descried in some cases of TRCC. These six tumours were within the classically described morphological spectrum of TFE3-TRCC. Nuclei were Fuhrman grade 2 in three tumours and grade 3 in the other 3 tumours. Necrosis was seen in four of the six tumours.

Three tumours had unusual morphology. One unusual tumour exhibited a mixture of compressed tubules, papillary structures and spindle cells associated with a myxoid stroma that in places resembled the mucinous tubular and spindle cell renal carcinoma. Other areas had a so-called “solid papillary” pattern. The spindle cells in this neoplasm had eosinophilic cytoplasm imparting a myoid appearance. Nuclei were predominantly grade 2, but focally nuclei were highly pleomorphic; grade 3–4 and necrosis was identified in several foci (Fig. 7). Mitoses were scanty and not atypical. Therefore, in our opinion, this tumour did not represent sarcomatoid carcinoma but was too atypical to be considered mucinous tubular and spindle cell renal carcinoma. The second showed poorly cohesive nests of large plump polygonal cells some with abundant eosinophilic cytoplasm imparting a histiocytoid and rhabdoid appearance. Some cells showed peripheral clearing and vacuolation of their cytoplasm resembling that seen in Touton giant cells. In many areas, the neoplastic cells were overrun by numerous lymphocytes and plasma cells simulating a lymphoepithelial carcinoma or recalling the morphology of Hashimoto’s thyroiditis. The third unusual tumour was composed predominantly of markedly atypical spindle cells arranged in poorly cohesive nests lying within a background of myxoid collagen imparting a sarcomatoid appearance. Focally, the spindle cell component was associated with intercellular eosinophilic matrix resembling osteoid. Elsewhere, this neoplasm showed poorly cohesive nests of large epithelioid cells with large vesicular nuclei containing macronucleoli suggesting melanoma or alveolar soft-part sarcoma. This

Table 1 Clinicopathologic data

Case	Sex	Age	Site	Size (cm)	pT TNM09	Color	Follow-up
1	M	51	Left	13	pT2	Yellowish	NA
2	M	80	Left	10×6×3	pT3a	Tan to brown	DOD 1 year after dg
3	F	60	Right	6×4×3	pT1b	Whitish	3 years AW
4	F	75	Right	2.6×2×2	pT1a	Gray to tan	1 year AW
5	F	84	Left	Diam. 5	pT1b	Gray to tan	NA
6	M	57	Right	2.5×2.7×2.9	pT1a	Yellowish	2 years AW
7	M	48	Right	9×8×7	pT2	Brownish-yellow	NA
8	M	72	Left	5×4.5×3.5	pT1b	Tan to brow	1 year AW, CRI, HT
9	M	43	Right	5.5×4.5×3	pT1b	Tan	1 year AW

M male, F female, NA not available, DOD dead of disease, AW alive and well, CRI chronic renal insufficiency, HT hypertension, dg diagnosis

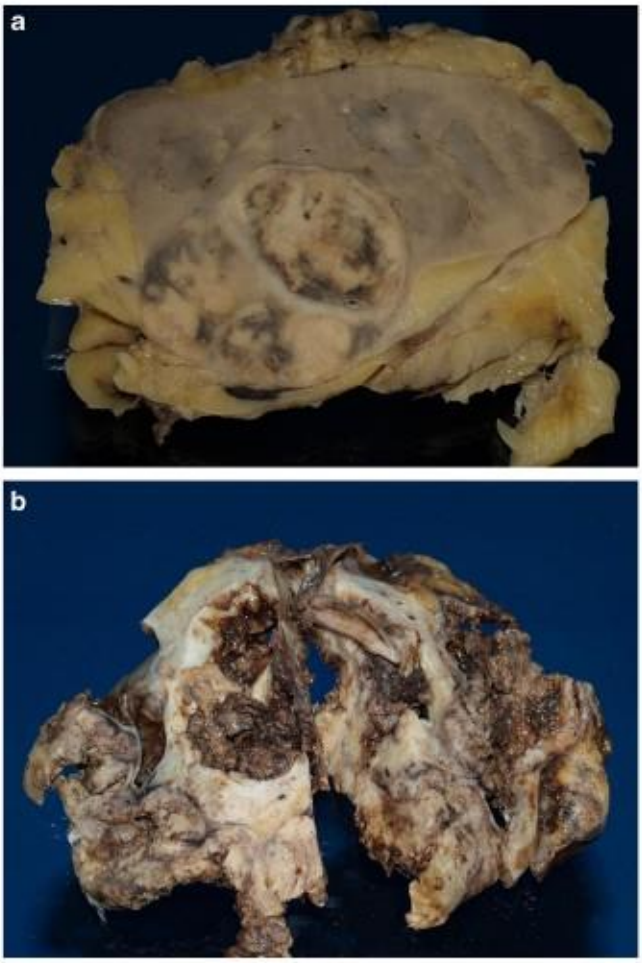

Fig. 1 Tumours were mostly yellow to tan on gross section (a) with foci of grossly visible necrosis (b)

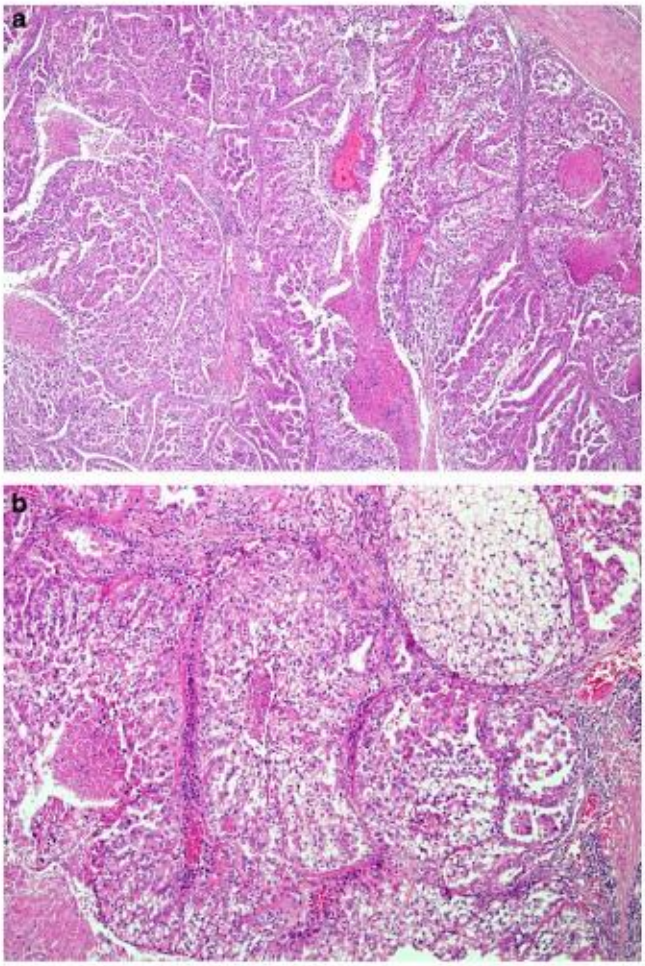

Fig. 2 Some tumours had a prominent tubulopapillary architecture admixed with solid nests of cells admixed with solid nests of cells(a, b)

tumour contained extensive necrosis, numerous mitoses and some atypical mitoses. It was invasive into perinephric fat and exhibited extensive lymphovascular invasion. This tumour was initially considered to potentially fall within the spectrum of ASPL-TFE3 or TFEB-TRCC and required exclusion of metastatic melanoma.

Immunohistochemical analysis

Results of the immunohistochemical analysis are listed in Table 2. None of the tumours showed an immunoprofile diagnostic of any particular type of RCC. Importantly, TFE3 was positive in two tumours neither of which was strongly positive for cathepsin K. A third tumour was initially interpreted as positive for TFE3 but presence of staining in adjacent benign tissues prompted repeat of the stain, which was negative. None of the tumours was positive for HMB45. Cathepsin K was positive in two tumours but one showed only weak focal staining. The latter tumour was positive for TFE3 by IHC but not FISH (Fig. 8). All but one of the nine TRCC-like tumours were positive for CD10, seven were positive for vimentin and four for carbonic anhydrase-IX (CA-IX). Seven were positive for AMACR. Keratin AE1/AE3 was diffusely positive in three tumours and was negative in six. CK7

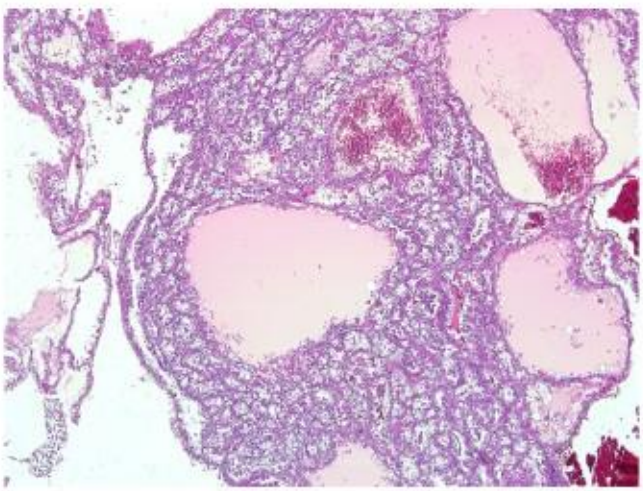

Fig. 3 Two tumours had a predominantly nested and alveolar pattern with alveolar spaces filled with eosinophilic secretions reminiscent of thyroid follicles

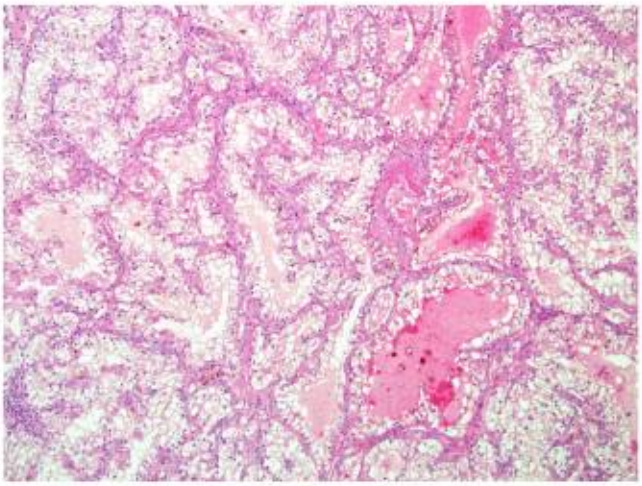

Fig. 4 Tumours with tubulopapillary architecture contained abundant clear cells with voluminous cytoplasm, prominent lateral cell borders and irregular apical cytoplasmic borders (so-called “blister” cells)

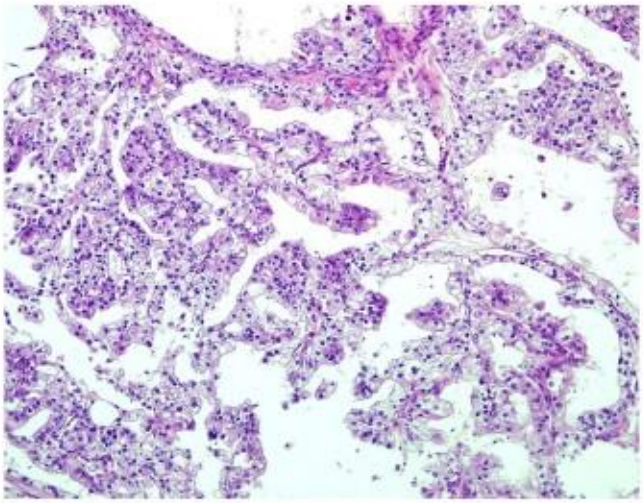

Fig. 6 One tumour with a nested and alveolar architecture mostly resembled CCRCC but had focal papillary architecture and some cells with eosinophilic granular cytoplasm

strongly stained one tumour, was weakly and focally positive in 1 and was negative in six cases. Pax 8 was positive in all but one case.

Molecular and cytogenetic analysis

One TFE3-negative tumour (case 8) showed normal copy numbers of 7,17 and LOH 3p (VHL abnormality) (Table 3). This tumour was diagnosed as clear cell RCC (CCRCC). One TFE3-negative tumour (case 1) with polysomy 7 and 17 but normal VHL status was diagnosed as papillary RCC (PRCC). Two TFE3-negative tumours (cases 4 and 6) had a normal complement of chromosomes 7 and 17 and no abnormality of the VHL gene. These tumours were considered unclassifiable. Three TFE3-negative tumours (cases 5, 7 and 9) that showed both polysomy of 7 and 17 and VHL abnormality were regarded as composite or combined CRCC/PRCC (unclassifiable). One of the two TFE3-IHC positive tumours (cases 2 and 3) showed only polysomy 7 and the other only polysomy 17, and both were negative for VHL gene abnormalities. These were also regarded as unclassifiable RCC.

Discussion

RCCs associated with TFE3 gene fusions are relatively rare tumours in adults but comprise approximately 30–50 % of renal cell carcinomas in children. There is an established association between TRCC and prior exposure to chemotherapy [14, 39]. The rarity of TRCC cases in our archive could be explained by the fact that a large majority of the renal neoplasms in the archive were obtained from hospitals concentrating on adult clinical practice (age of the patients is over 18 years). TFE3 translocation can occur to several different

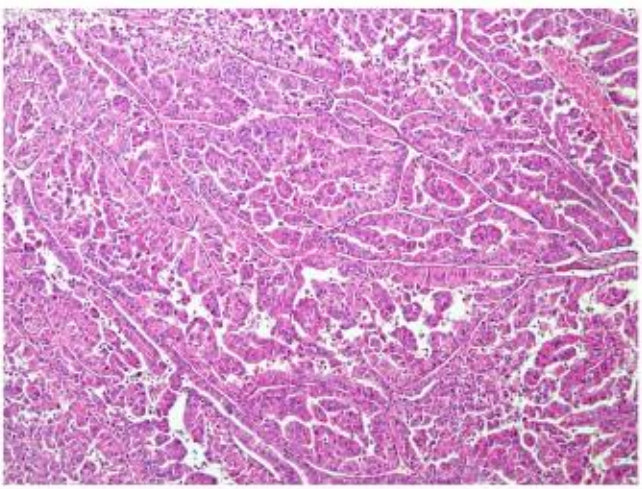

Fig. 5 A population of cells with abundant eosinophilic cytoplasm was also present in four of these tumours

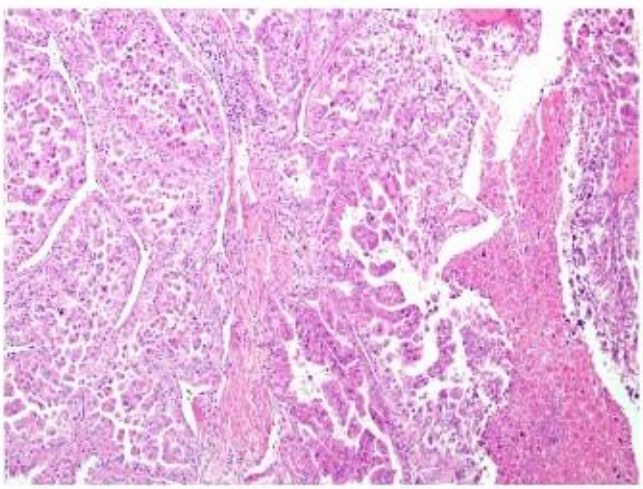

Fig. 7 Areas of necrosis were noted in the vicinity of papillary and micropapillary structures

Table 2 Immunohistochemical examination

Case:	TFE3	CANH9	CD10	Vim	AMACR	Cathep.	HMB45	AE1–AE3	CK7	Pax8
1	−	−	+++	+++	++	−	−	−	−	++
2	+++	−	++ foc	+++	−	−	−	−	+ foc	−
3	+++	−	+++ foc	+++	−	+ foc	−	−	−	+
4	−	−	++ foc	−	+++	+++	−	−	−	+
5	−	−	−	+++	+++	−	−	++	−	+
6	−	++ foc	+++	+++	+++	−	−	−	−	++
7	−	++ foc	+++	−	+++ foc	−	−	+++	−	++
8	−	++ foc	+++	+++	+++	−	−	++	+++	+
9	−	+++	+++	+++	+++ foc	−	−	−	−	+

foc=<25 % cells staining

CANH9 carbonic anhydrase IX, Vim Vimentin, AMACR alpha-methylacyl-CoA racemase, Cathep. cathepsin K, (−) negative, (+) weak, (++) moderate, (+++) strong

partner genes including ASPL, PRCC, PSF, CLTC, NonO, and others not yet fully clarified [7, 8, 10, 11, 19]. Prior to the recognition of translocation carcinomas of the kidney, most of these tumours were classified in the categories of clear cell renal cell carcinoma and papillary renal cell carcinoma [15, 35, 37]. Young age at presentation is one of the main indicators of a possible translocation-associated renal carcinoma and prompts the pathologist to consider such a diagnosis. However, since classical CCRCC and PRCC comprise the most common renal neoplasms in adults, the possibility of TRCC is seldom considered in that age group so the incidence of TFE3 translocation carcinomas in adults aged >50 years is not known but is likely underestimated. Recent studies have shown that TRCC occurs in younger adults who typically present a higher clinical stage than in paediatric patients. The more aggressive behaviour of TRCC in adults may also be explained by the progressive acquisition of chromosomal copy number alterations [33]. The importance of recognising TRCC is increasing in the era of potential targeted therapy [23, 28].

At the time of initial description, TRCC was noted to have mostly papillary architecture and to be composed of cells with voluminous clear cytoplasm. Additional histological pointers to possible TRCC include an admixture of cells with clear and eosinophilic cytoplasm, presence of psammoma bodies and hyaline stromal globules [2, 44]. However, larger studies have expanded the histological profile to include mixed solid, nested, alveolar and papillary patterns such that accurate distinction from CCRCC and PRCC is impossible based only on morphology [1, 45]. The cells may have clear or eosinophilic cytoplasm, which may or may not be voluminous. Rare cases of TRCC contain melanin, express melanocytic markers by immunohistochemistry and exhibit a morphology that overlaps with PEComa, melanoma and even alveolar soft part sarcoma [3]. Different variants of TFE3 translocation were thought to result in different morphological appearances, but cases with overlapping morphological features were described later. Furthermore, a closely related form of TRCC involving the TFEB gene, another member of the MiTF gene family, was likewise initially thought to have a distinctive morphology but more experience with larger numbers of cases has shown morphological overlap with the more common TFE3 neoplasms and the more usual variants of renal carcinoma [8, 14, 18].

Immunohistochemical analysis may be helpful in differentiating TRCC from PRCC in that TRCC is negative or only weakly and focally positive for keratins and EMA, and is negative for racemase (AMACR) [1, 2, 12, 14]. Similar to clear cell carcinoma, TRCC is positive with the antibody to vimentin and strongly positive with CD10. However, vimentin staining is patchy in TRCC but diffuse in CCRCC, and TRCC is negative for carbonic anhydrase-9 (CA-IX). Positive nuclear staining for TFE3 protein and cytoplasmic staining for cathepsin K have been regarded as specific for

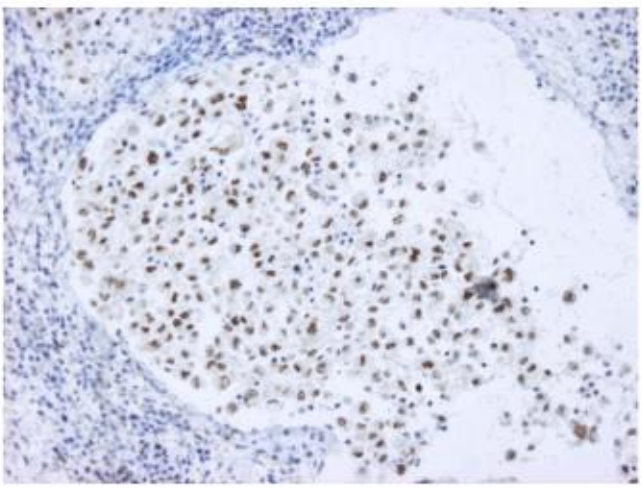

Fig. 8 Strong nuclear TFE3 positivity was noted in two tumours

Table 3 Results of molecular and cytogenetic analyses

Case	TFE3 ba	CEP 7	CEP 17	X/Y	LOH3p	Mut VHL	Methyl VHL	Diag
1	Neg	Polysomy[a]	Polysomy[a]	4~5X/0Y; 2X/1Y[b]	Neg	Neg	Neg	PRCC
2	Neg	Polysomy	Disomy	NA	NA	Neg	NA	UNC
3	Neg	Disomy	Polysomy[a]	NP	Neg	Neg	Neg	UNC
4	Neg	Disomy	Disomy	NP	Neg	Neg	Neg	UNC
5	Neg	Polysomy[a]	Polysomy[a]	NP	Pos	Neg	Neg	CRCC/PRCC
6	Neg	Disomy	Disomy	2X/1Y	Neg	Neg	Neg	UNC
7	Neg	Polysomy	Polysomy	2X/2Y	Pos	Pos[c]	Neg	CRCC/PRCC
8	Neg	Disomy	Disomy	2X/0Y	Pos	Neg	Neg	CCRCC
9	Neg	Polysomy[a]	Polysomy[a]	Neg	Pos	Pos[d]	Neg	CRCC/PRCC

Pos positive, Neg negative, NA not analysable, NP not performed, PRCC papillary renal cell carcinoma, UNC unclassified renal cell carcinoma, CRCC clear cell renal cell carcinoma, Mut VHL mutation of VHL gene, Methyl VHL methylation status of VHL gene, Diag diagnosis

[a] Polysomy in large nuclei only

[b] Gain X, loss Y (4~5X/0Y) in large nuclei; gain X (2X/1Y) in small nuclei

[c] Somatic mutation c.504_508del/p.Leu168GlnfsTer3

[d] Somatic mutation c.393C>G/p.Asn131Lys

TRCC [5, 29, 38], but false positive and negative results have been reported in several studies not all of which have been explained on the basis of technical problems [21]. Indeed, it seems that over-expression of wild-typeTFE3 protein transcript may occur as a result of up-regulation of the normal gene, or as the result of increased gene copy number due to polysomy or amplification particularly in high grade CCRCC and in carcinomas with sarcomatoid and cystic features [26, 48]. Similarly, positive immunostains for melanocytic markers such as HMB45 may be seen in some variants of TFE3-TRCC, in the TFEB-TRCC and in PEComas [14, 16].

In the present study of 20 cases of RCC in which there was a suspicion of TRCC, nine cases were confirmed as X11.2-TRCC by break-apart FISH analysis. The remaining TRCC-like carcinomas showed a diverse morphology that precluded definite classification of these tumours on morphological grounds. Thus, many showed a mixture of papillary and CCRCC patterns. Seven cases contained clear cells with voluminous cytoplasm, so-called “blister” cells, a well-known feature of TRCC. IHC was also contradictory to the morphology in many cases, again suggesting possible TRCC. Of five cases exhibiting a predominantly papillary architecture, only one was strongly positive for CK7 and that tumour was also positive for CA-IX, a marker of CCRCC. Those tumours with morphology similar to CCRCC were all positive for AMACR, a marker of PRCC. The sarcomatoid tumour with morphology suggestive of melanoma or APSL-TFE3 TRCC posed a diagnostic challenge. It was positive for TFE3 by IHC, negative for HMB45 and showed only focal weak staining for cathepsin K. Although the stain for Pax-8 was negative, there was no clinical history of prior cutaneous melanoma or other visceral malignancy. Furthermore, metastatic melanoma was excluded by negative immunostaining for S-100 protein and diffusely positive staining for wide spectrum keratin (OSCAR). Positive immunostaining for TFE3 in the absence of the translocation has been described previously in sarcomatoid and other high-grade RCCs sometimes explained by gene polysomy or amplification [26]. Because of the contradictory morphological and immunohistochemical profiles of these TRCC-like neoplasms, we conclude that molecular/genetic analysis is the most reliable method extant to classify this group of unusual renal tumours.

The final molecular/genetic diagnosis did not correlate exactly with the histomorphology and immunoprofile in some cases (Table 4). In the case diagnosed as CCRCC on the basis of isolated abnormality of the VHL locus, the histology showed a prominent papillary architecture and alveolar nests with a micropapillary pattern within them. Immunostains for CK7 and AMACR were strongly positive. However, CA-IX was also positive. The case diagnosed as PRCC on the basis of polysomy of chromosomes 7 and 17 in the absence of VHL abnormality had prominent papillary architecture but showed a predominance of clear cells with voluminous vacuolated cytoplasm suggesting TRCC. On IHC, the tumour was negative for CK7 and positive for CD10 and vimentin. However, the stain for AMACR was positive. One of the three tumours diagnosed as combined PRCC–CCRCC on the basis of morphology, immunohistochemical examination and polysomy of chromosomes 7 and 17 and VHL abnormality showed a combined papillary, tubular and nested architecture and a predominance of cells with eosinophilic cytoplasm and scanty clear cells. One PRCC–CCRCC did not contain papillary structures and had a morphology most consistent with CCRCC but with clear cells showing voluminous cytoplasm suggesting TRCC. The third PRCC–CCRCC was the unusual tumour with a solid papillary pattern and areas of spindle cells in a mucinous

Table 4 Summary of unusual features

Molecular category	Case	Unusual features
CRCC	8	Papillary architecture AMACR and CK 7 strongly positive
PRCC	1	Clear cells with voluminous cytoplasm Glassy hyaline intra-cytoplasmic globules CK 7 negative
Combined PRCC-CCRCC	5, 7, 9	Spindle cell component and myxoid stroma and no alveolar or solid nest patterns in 1 case Papillary pattern absent in 1 case Very scanty clear cell component in 2 cases CK 7 negative in all AMACR positive in all CA-IX positive in 2 cases
Unclassifiable NOS	4, 6 2 3	2 cases had mixed PRCC and CCRCC morphology. Both contained clear cells with voluminous cytoplasm CK 7 negative but AMACR and cathepsin K positive Strong TFE3 positivity (by IHC), not confirmed by FISH

CRCC clear cell renal cell carcinoma, PRCC papillary renal cell carcinoma, NOS not otherwise specified, IHC Immunohistochemistry

stroma described above. By IHC, all three tumours were negative for CK7, positive for AMACR, and two were positive for CA-IX.

The study reported herein confirms the conclusion of other workers [36] that cytogenetic analysis is preferable to morphology and immunostains for TFE3 and cathepsin K in the diagnosis of TRCC. Furthermore, when TRCC-like tumours are selected on the basis of histological changes that do not conform to those classically described for other subtypes of RCC, immunohistochemistry is shown to be especially unreliable in further classifying these unusual renal neoplasms.

In conclusion, the molecular/genetic algorithm used herein is recommended for tumours with a TRCC-like morphology. This algorithm could also be applied in the investigation of unclassifiable RCC. Firstly, break-apart FISH analysis for TFE3 is performed and true cases of X11.2 translocation separated out. Next, numerical analysis of chromosomes 7 and 17 is performed together with thorough investigation of the status of the VHL gene on chromosome 3p using PCR for mutation analysis and LOH and methylation-specific PCR for the methylation analysis of the promoter region of the VHL gene. This enables true CCRCC and PRCC to be separated from the tumours that have combined features of CCRCC–PRCC. The remainder of unclassifiable RCCs may contain rare cases of TFEB–TRCC. These tumours are usually positive for cathepsin K and melanocytic markers on immunohistochemistry and can be confirmed by break-apart FISH analysis for the t(6;11) TFEB translocation [9]. Further, such unclassifiable cases may benefit from whole genome sequencing studies. Molecular features are indeed one of the characteristics useful for classification of unusual renal tumours. However, in group of TRCC and TRCC-like cases, it seems that they play a key role in the differential diagnostic process.

Acknowledgements The study was supported by the Charles University Research Fund (project number P36), by the project by the project CZ.1.05/2.1.00/03.0076 from European Regional Development Fund and by Ministry of Health, Czech Republic—conceptual development of research organization (Faculty Hospital in Pilsen—FNPl, 00669806).

Conflict of interest All authors declare no conflict of interest.

References

1. Argani P, Antonescu CR, Couturier J, Fournet JC, Sciot R, Debiec-Rychter M, Hutchinson B, Reuter VE, Boccon-Gibod L, Timmons C, Hafez N, Ladanyi M (2002) PRCC-TFE3 renal carcinomas: morphologic, immunohistochemical, ultrastructural, and molecular analysis of an entity associated with the t(X;1)(p11.2;q21). Am J Surg Pathol 26:1553–1566
2. Argani P, Antonescu CR, Illei PB, Lui MY, Timmons CF, Newbury R, Reuter VE, Garvin AJ, Perez-Atayde AR, Fletcher JA, Beckwith JB, Bridge JA, Ladanyi M (2001) Primary renal neoplasms with the ASPL-TFE3 gene fusion of alveolar soft part sarcoma: a distinctive tumor entity previously included among renal cell carcinomas of children and adolescents. Am J Pathol 159:179–192. doi:10.1016/S0002-9440(10)61684-7
3. Argani P, Aulmann S, Illei PB, Netto GJ, Ro J, Cho HY, Dogan S, Ladanyi M, Martignoni G, Goldblum JR, Weiss SW (2010) A distinctive subset of PEComas harbors TFE3 gene fusions. Am J Surg Pathol 34:1395–1406. doi:10.1097/PAS.0b013e3181f17ac0

4. Argani P, Hawkins A, Griffin CA, Goldstein JD, Haas M, Beckwith JB, Mankinen CB, Perlman EJ (2001) A distinctive pediatric renal neoplasm characterized by epithelioid morphology, basement membrane production, focal HMB45 immunoreactivity, and t(6;11)(p21.1;q12) chromosome translocation. Am J Pathol 158:2089–2096. doi:10.1016/S0002-9440(10)64680-9
5. Argani P, Hicks J, De Marzo AM, Albadine R, Illei PB, Ladanyi M, Reuter VE, Netto GJ (2010) Xp11 translocation renal cell carcinoma (RCC): extended immunohistochemical profile emphasizing novel RCC markers. Am J Surg Pathol 34:1295–1303. doi:10.1097/PAS.0b013e3181e8ce5b
6. Argani P, Ladanyi M (2005) Translocation carcinomas of the kidney. Clin Lab Med 25:363–378. doi:10.1016/j.cll.2005.01.008
7. Argani P, Lui MY, Couturier J, Bouvier R, Fournet JC, Ladanyi M (2003) A novel CLTC-TFE3 gene fusion in pediatric renal adenocarcinoma with t(X;17)(p11.2;q23). Oncogene 22:5374–5378. doi:10.1038/sj.onc.1206686
8. Argani P, Olgac S, Tickoo SK, Goldfischer M, Moch H, Chan DY, Eble JN, Bonsib SM, Jimeno M, Lloreta J, Billis A, Hicks J, De Marzo AM, Reuter VE, Ladanyi M (2007) Xp11 translocation renal cell carcinoma in adults: expanded clinical, pathologic, and genetic spectrum. Am J Surg Pathol 31:1149–1160. doi:10.1097/PAS.0b013e318031ffff
9. Argani P, Yonescu R, Morsberger L, Morris K, Netto GJ, Smith N, Gonzalez N, Illei PB, Ladanyi M, Griffin CA (2012) Molecular confirmation of t(6;11)(p21;q12) renal cell carcinoma in archival paraffin-embedded material using a break-apart TFEB FISH assay expands its clinicopathologic spectrum. Am J Surg Pathol 36:1516–1526. doi:10.1097/PAS.0b013e3182613d8f
10. Armah HB, Parwani AV (2010) Xp11.2 translocation renal cell carcinoma. Arch Pathol Lab Med 134:124–129. doi:10.1043/2008-0391-RSR.1
11. Armah HB, Parwani AV, Surti U, Bastacky SI (2009) Xp11.2 translocation renal cell carcinoma occurring during pregnancy with a novel translocation involving chromosome 19: a case report with review of the literature. Diagn Pathol 4:15. doi:10.1186/1746-1596-4-15
12. Bazille C, Allory Y, Molinie V, Vieillefond A, Cochand-Priollet B, Cussenot O, Callard P, Sibony M (2004) Immunohistochemical characterisation of the main histologic subtypes of epithelial renal tumours on tissue-microarrays. Study of 310 cases. Ann Pathol 24:395–406
13. Bruder E, Moch H (2004) [Pediatric renal cell carcinoma] Der Pathologe 25:324–327. doi:10.1007/s00292-004-0699-0
14. Camparo P, Vasiliu V, Molinie V, Couturier J, Dykema KJ, Petillo D, Furge KA, Comperat EM, Lae M, Bouvier R, Boccon-Gibod L, Denoux Y, Ferlicot S, Forest E, Fromont G, Hintzy MC, Laghouati M, Sibony M, Tucker ML, Weber N, Teh BT, Vieillefond A (2008) Renal translocation carcinomas: clinicopathologic, immunohistochemical, and gene expression profiling analysis of 31 cases with a review of the literature. Am J Surg Pathol 32:656–670. doi:10.1097/PAS.0b013e3181609914
15. Cao Y, Paner GP, Perry KT, Flanigan RC, Campbell SC, Picken MM (2005) Renal neoplasms in younger adults: analysis of 112 tumors from a single institution according to the new 2004 World Health Organization classification and 2002 American Joint Committee on Cancer Staging System. Arch Pathol Lab Med 129:487–491. doi:10.1043/1543-2165(2005)129<487:RNIYAA>2.0.CO;2
16. Chang IW, Huang HY, Sung MT (2009) Melanotic Xp11 translocation renal cancer: a case with PSF-TFE3 gene fusion and up-regulation of melanogenetic transcripts. Am J Surg Pathol 33:1894–1901. doi:10.1097/PAS.0b013e3181ba7a5f
17. Clark J, Lu YJ, Sidhar SK, Parker C, Gill S, Smedley D, Hamoudi R, Linehan WM, Shipley J, Cooper CS (1997) Fusion of splicing factor genes PSF and NonO (p54nrb) to the TFE3 gene in papillary renal cell carcinoma. Oncogene 15:2233–2239. doi:10.1038/sj.onc.1201394
18. Davis IJ, Hsi BL, Arroyo JD, Vargas SO, Yeh YA, Motyckova G, Valencia P, Perez-Atayde AR, Argani P, Ladanyi M, Fletcher JA, Fisher DE (2003) Cloning of an Alpha-TFEB fusion in renal tumors harboring the t(6;11)(p21;q13) chromosome translocation. Proc Natl Acad Sci U S A 100:6051–6056. doi:10.1073/pnas.0931430100
19. Dijkhuizen T, van den Berg E, Wilbrink M, Weterman M, GeurtsvanKessel A, Storkel S, Folkers RP, Braam A, de Jong B (1995) Distinct Xp11.2 breakpoints in two renal cell carcinomas exhibiting X;autosome translocations. Gene Chromosome Cancer 14:43–50
20. Eble JN, Sauter G, Epstein JI, Sesterhenn I, WHO Classification of Tumours (2004) Tumours of the urinary system and male genital organs. Pathology and genetics. IARC Press, Lyon
21. Gaillot-Durand L, Chevallier M, Colombel M, Couturier J, Pierron G, Scoazec JY, Mege-Lechevallier F (2013) Diagnosis of Xp11 translocation renal cell carcinomas in adult patients under 50 years: interest and pitfalls of automated immunohistochemical detection of TFE3 protein. Pathol Res Pract 209:83–89. doi:10.1016/j.prp.2012.10.013
22. Hodge JC, Pearce KE, Wang X, Wiktor AE, Oliveira AM, Greipp PT (2014) Molecular cytogenetic analysis for TFE3 rearrangement in Xp11.2 renal cell carcinoma and alveolar soft part sarcoma: validation and clinical experience with 75 cases. Mod Pathol 27:113–127. doi:10.1038/modpathol.2013.83
23. Hora M, Urge T, Travnicek I, Ferda J, Chudacek Z, Vanecek T, Michal M, Petersson F, Kuroda N, Hes O (2014) MiT translocation renal cell carcinomas: two subgroups of tumours with translocations involving 6p21 [t (6; 11)] and Xp11.2 [t (X;1 or X or 17)]. SpringerPlus 3:245. doi:10.1186/2193-1801-3-245
24. Klatte T, Streubel B, Wrba F, Remzi M, Krammer B, de Martino M, Waldert M, Marberger M, Susani M, Haitel A (2012) Renal cell carcinoma associated with transcription factor E3 expression and Xp11.2 translocation: incidence, characteristics, and prognosis. Am J Clin Pathol 137:761–768. doi:10.1309/AJCPQ6LLFMC4OXGC
25. Komai Y, Fujiwara M, Fujii Y, Mukai H, Yonese J, Kawakami S, Yamamoto S, Migita T, Ishikawa Y, Kurata M, Nakamura T, Fukui I (2009) Adult Xp11 translocation renal cell carcinoma diagnosed by cytogenetics and immunohistochemistry. Clin Cancer Res: Off J Am Assoc Cancer Res 15:1170–1176. doi:10.1158/1078-0432.CCR-08-1183
26. Macher-Goeppinger S, Roth W, Wagener N, Hohenfellner M, Penzel R, Haferkamp A, Schirmacher P, Aulmann S (2012) Molecular heterogeneity of TFE3 activation in renal cell carcinomas. Mod Pathol: Off J U S Can Acad Pathol Inc 25:308–315. doi:10.1038/modpathol.2011.169
27. Malouf GG, Camparo P, Molinie V, Dedet G, Oudard S, Schleiermacher G, Theodore C, Dutcher J, Billemont B, Bompas E, Guillot A, Boccon-Gibod L, Couturier J, Escudier B (2011) Transcription factor E3 and transcription factor EB renal cell carcinomas: clinical features, biological behavior and prognostic factors. J Urol 185:24–29. doi:10.1016/j.juro.2010.08.092
28. Malouf GG, Camparo P, Oudard S, Schleiermacher G, Theodore C, Rustine A, Dutcher J, Billemont B, Rixe O, Bompas E, Guillot A, Boccon-Gibod L, Couturier J, Molinie V, Escudier B (2010) Targeted agents in metastatic Xp11 translocation/TFE3 gene fusion renal cell carcinoma (RCC): a report from the Juvenile RCC Network. Ann Oncol: Off J Eur Soc Med Oncol / ESMO 21:1834–1838. doi:10.1093/annonc/mdq029
29. Martignoni G, Pea M, Gobbo S, Brunelli M, Bonetti F, Segala D, Pan CC, Netto G, Doglioni C, Hes O, Argani P, Chilosi M (2009) Cathepsin-K immunoreactivity distinguishes MiTF/TFE family renal translocation carcinomas from other renal carcinomas. Mod Pathol: Off J U S Can Acad Pathol Inc 22:1016–1022. doi:10.1038/modpathol.2009.58

30. Meloni AM, Sandberg AA, Pontes JE, Dobbs RM Jr (1992) Translocation (X;1)(p11.2;q21). A subtype of renal adenocarcinomas. Cancer Genet Cytogenet 63:100–101
31. Meyer PN, Clark JI, Flanigan RC, Picken MM (2007) Xp11.2 translocation renal cell carcinoma with very aggressive course in five adults. Am J Clin Pathol 128:70–79. doi:10.1309/LR5G1VMXPY3G0CUK
32. Mosquera JM, Dal Cin P, Mertz KD, Perner S, Davis IJ, Fisher DE, Rubin MA, Hirsch MS (2011) Validation of a TFE3 break-apart FISH assay for Xp11.2 translocation renal cell carcinomas. Diagn Mol Pathol: Am J Surg Pathol B 20:129–137. doi:10.1097/PDM.0b013e31820e9c67
33. Pan CC, Sung MT, Huang HY, Yeh KT (2013) High chromosomal copy number alterations in Xp11 translocation renal cell carcinomas detected by array comparative genomic hybridization are associated with aggressive behavior. Am J Surg Pathol 37:1116–1119. doi:10.1097/PAS.0b013e318293d872
34. Petersson F, Grossmann P, Hora M, Sperga M, Montiel DP, Martinek P, Gutierrez ME, Bulimbasic S, Michal M, Branzovsky J, Hes O (2013) Renal cell carcinoma with areas mimicking renal angiomyoadenomatous tumor/clear cell papillary renal cell carcinoma. Hum Pathol. doi:10.1016/j.humpath.2012.11.019
35. Ramphal R, Pappo A, Zielenska M, Grant R, Ngan BY (2006) Pediatric renal cell carcinoma: clinical, pathologic, and molecular abnormalities associated with the members of the mit transcription factor family. Am J Clin Pathol 126:349–364. doi:10.1309/98YE9E442AR7LX2X
36. Rao Q, Williamson SR, Zhang S, Eble JN, Grignon DJ, Wang M, Zhou XJ, Huang W, Tan PH, Maclennan GT, Cheng L (2013) TFE3 break-apart FISH has a higher sensitivity for Xp11.2 translocation-associated renal cell carcinoma compared with TFE3 or cathepsin K immunohistochemical staining alone: expanding the morphologic spectrum. Am J Surg Pathol 37:804–815. doi:10.1097/PAS.0b013e31827e17cb
37. Renshaw AA, Zhang H, Corless CL, Fletcher JA, Pins MR (1997) Solid variants of papillary (chromophil) renal cell carcinoma: clinicopathologic and genetic features. Am J Surg Pathol 21:1203–1209
38. Smith NE, Illei PB, Allaf M, Gonzalez N, Morris K, Hicks J, Demarzo A, Reuter VE, Amin MB, Epstein JI, Netto GJ, Argani P (2014) t(6;11) renal cell carcinoma (RCC): expanded immunohistochemical profile emphasizing novel RCC markers and report of 10 new genetically confirmed cases. Am J Surg Pathol 38:604–614. doi:10.1097/PAS.0000000000000203
39. Srigley JR, Delahunt B, Eble JN, Egevad L, Epstein JI, Grignon D, Hes O, Moch H, Montironi R, Tickoo SK, Zhou M, Argani P, Panel IRT (2013) The International Society of Urological Pathology (ISUP) Vancouver classification of renal neoplasia. Am J Surg Pathol 37:1469–1489. doi:10.1097/PAS.0b013e318299f2d1
40. Sukov WR, Hodge JC, Lohse CM, Leibovich BC, Thompson RH, Pearce KE, Wiktor AE, Cheville JC (2012) TFE3 rearrangements in adult renal cell carcinoma: clinical and pathologic features with outcome in a large series of consecutively treated patients. Am J Surg Pathol 36:663–670. doi:10.1097/PAS.0b013e31824dd972
41. Tomlinson DC, L'Hote CG, Kennedy W, Pitt E, Knowles MA (2005) Alternative splicing of fibroblast growth factor receptor 3 produces a secreted isoform that inhibits fibroblast growth factor-induced proliferation and is repressed in urothelial carcinoma cell lines. Cancer Res 65:10441–10449. doi:10.1158/0008-5472.CAN-05-1718
42. Tonk V, Wilson KS, Timmons CF, Schneider NR, Tomlinson GE (1995) Renal cell carcinoma with translocation (X;1). Further evidence for a cytogenetically defined subtype. Cancer Genet Cytogenet 81:72–75
43. Weterman MA, Wilbrink M, Geurts van Kessel A (1996) Fusion of the transcription factor TFE3 gene to a novel gene, PRCC, in t(X;1)(p11;q21)-positive papillary renal cell carcinomas. Proc Natl Acad Sci U S A 93:15294–15298
44. Winarti NW, Argani P, De Marzo AM, Hicks J, Mulyadi K (2008) Pediatric renal cell carcinoma associated with Xp11.2 translocation/TFE3 gene fusion. Int J Surg Pathol 16:66–72. doi:10.1177/1066896907304994
45. Wu A, Kunju LP, Cheng L, Shah RB (2008) Renal cell carcinoma in children and young adults: analysis of clinicopathological, immunohistochemical and molecular characteristics with an emphasis on the spectrum of Xp11.2 translocation-associated and unusual clear cell subtypes. Histopathology 53:533–544. doi:10.1111/j.1365-2559.2008.03151.x
46. Yan BC, Mackinnon AC, Al-Ahmadie HA (2009) Recent developments in the pathology of renal tumors: morphology and molecular characteristics of select entities. Arch Pathol Lab Med 133:1026–1032. doi:10.1043/1543-2165-133.7.1026
47. Zhong M, De Angelo P, Osborne L, Keane-Tarchichi M, Goldfischer M, Edelmann L, Yang Y, Linehan WM, Merino MJ, Aisner S, Hameed M (2010) Dual-color, break-apart FISH assay on paraffin-embedded tissues as an adjunct to diagnosis of Xp11 translocation renal cell carcinoma and alveolar soft part sarcoma. Am J Surg Pathol 34:757–766. doi:10.1097/PAS.0b013e3181dd577e
Zhong M, De Angelo P, Osborne L, Paniz-Mondolfi AE, Geller M, Yang Y, Linehan WM, Merino MJ, Cordon-Cardo C, Cai D (2012) Translocation renal cell carcinomas in adults: a single-institution experience. Am J Surg Pathol 36:654–662. doi:10.1097/PAS.0b013e31824f24a6

3.7 TFE3-fusion variant analysis defines specific clinicopathologic associations among Xp11 translocation cancers (letter to the editor)

Argani a kol. publikovali v červenci 2016 v periodiku „American Journal of Surgical Pathology“ práci s názvem “TFE3-Fusion variant analysis defines specific clinicopathologic associations among Xp11 translocation cancers”. V této studii bylo analyzováno celkem 60 případů Xp11 translokačního karcinomu (za použití FISH) ve snaze stanovit spektrum fúzních partnerů genu *TFE3* u těchto lézí.

Z 60 případů zařazených do této studie se v 47 případech jednalo o Xp11 TRCC. Autoři v této práci popsali široké spektrum fúzních partnerů, mimo jiné byl u pěti tumorů detekovaným fúzním partnerem gen *NONO* (také nazývaný *p54nrb*). U těchto pěti *NONO-TFE3* TRCC byl dále nově popsán i typický morfologický vzhled (zastižený u všech pěti lézí). *NONO-TFE3* RCCs byly charakterizovány predominantně papilární architektonikou, buňkami s jasnou až slabě eosinofilní cytoplasmou a nápadnými subnukleárními vakuolami, vedoucími k efektu tzv. jaderného palisádování (zešikování jader).

V Plzeňském registru nádorů je zařazeno 41 Xp11.2 translokačních RCC, z nichž u tří případů byla molekulárně geneticky potvrzena přítomnost *NONO-TFE3* genové fúze. Pacienty byli dva muži a jedna žena s věkovým rozmezím 34-66 let (průměr 49,7 let). Dva z těchto případů se manifestovaly lokalizovanou, na ledvinu omezenou lézí, velikosti 0,8 cm a 6 cm (v největším rozměru). Histologicky oba nádory vykazovaly papilární architektoniku s papilami krytými neoplastickými buňkami se světlou až mírně eosinofilní cytoplasmou. Subnukleární vakuolizace a jaderné palisádování popisované Arganim a kol. byly v nádorech zastiženy alespoň fokálně. V obou případech byly dále zastiženy psammoma a dystrofické kalcifikace. Třetí případ byl lehce odlišný. Tumor měřil 2,3 cm (v největším rozměru) a byl léčen parciální nefrektomií. Histologicky tumor vykazoval tubulopapilární architektoniku s drobnými okrsky nekrózy. Neoplastické buňky byly spíše eosinofilní, s menším množstvím cytoplasmy, s protáhlými jádry (příležitostně i s nukleárními zářezy). Buňky tvořili pseudotubulární a papilární struktury, na periferii s uspořádáním připomínajícím palisádování. V materiálu byly zastiženy dystrofické kalcifikace. S odstupem čtyř měsíců byla u pacienta detekována rekurence onemocnění (nádor byl lokalizován v oblasti dolní renální dřeně a protrudoval do renální pánvičky). Tumor vykazoval stejné morfologické rysy jako primární léze s mírnou akcentací palisádování a to až do té míry, že léze až vágně připomínala uroteliální karcinom. Imunohistochemicky byly všechny léze positivní v barvení racemázou (AMACR), PAX8 a CD10, naopak negativní byla CA-IX. Diagnóza Xp11 translokačního renálního karcinomu byla ověřena FISH vyšetřením, FISH analýza detekovala zlom genu *NONO* a zlom genu *TFE3* ve všech třech primárních i v rekurentním tumoru.

Navzdory velkému množství rozličných morfologických variant Xp11 translokačního RCC popsaných v literatuře věříme, že morfologické spektrum těchto lézí je i tak ještě mnohem komplexnější. Touto malou sérií čítající tři případy *NONO-TFE3* TRCC jsme obohatili známé morfologické spektrum, což ukazuje, že i tyto léze si zaslouží další větší studie.

TFE3-Fusion Variant Analysis Defines Specific Clinicopathologic Associations Among Xp11 Translocation CancersJanuary

To the Editor:

We read with great interest the article by Argani and colleagues "TFE3-Fusion variant analysis defines specific clinicopathologic associations among Xp11 translocation cancers" published in June 2016 volume of American Journal of Surgical Pathology. The authors studied 60 Xp11 translocation carcinomas using fluorescence in situ hybridization (FISH) to establish their TFE3 fusion partner. Of 60 cases, 47 were Xp11 translocation renal cell carcinomas (RCCs). They identified, among others, 5 cases with NONO-TFE3 RCC and described theirs morphologic features. Tumors were characterized mostly by papillary architecture, with clear to weakly eosinophilic cytoplasm with subnuclear vacuoles leading to distinctive nuclear palisading.

Among 41 Xp11.2 (TFE3) translocation RCCs in our registry, we identified 3 cases of NONO-TFE3 RCC. Patients included 2 men and 1 woman, with an age range of 34 to 66 years (mean 49.7 y).

Two of our cases presented grossly as localized lesions, with a tumor size of 0.8 and 6 cm in greatest dimension. Histologically, they demonstrated papillary architecture, covered mostly by clear to eosinophilic neoplastic cells. Subnuclear vacuolization described by Argani and colleagues was at least focally noted in both cases. Both tumors had psammoma bodies and dystrophic calcifications (Fig. 1). The diagnosis of Xp11.2 translocation RCC was confirmed using FISH.

Our third case was particularly interesting with a tumor size of 2.3 cm in greatest dimension showing soft gray cut-surface (partial nephrectomy

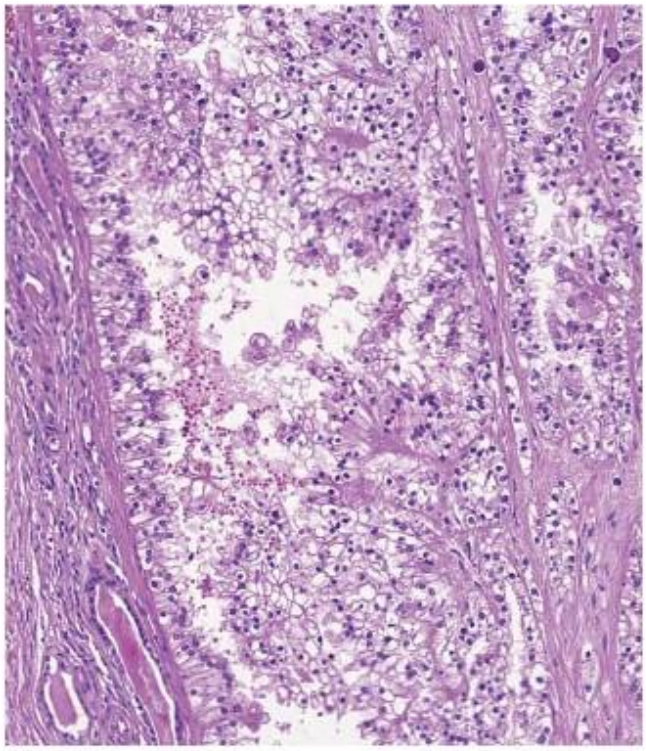

FIGURE 1. NONO-TFE3 translocation RCC (case 1) resembling cases described by Argani et al.[1]

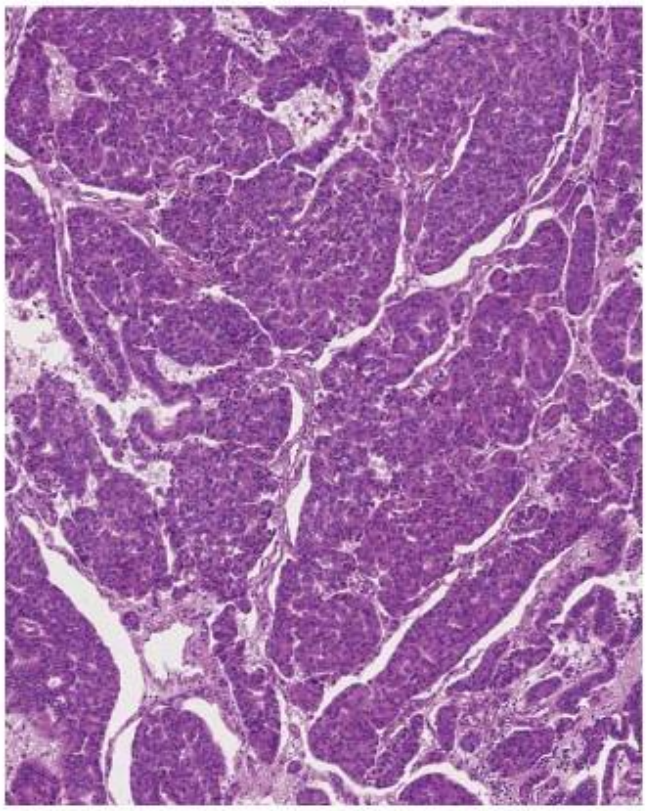

FIGURE 2. Overview of primary renal tumor (case 3) composed of eosinophilic cells with elongated polymorphic nuclei.

TABLE 1. Results of Immunohistochemical Examination of 3 NONO-TFE3 Cases

Case	Vim	AMARC	CANH9	PAX 8	TFE3	CK 7	CD 10	HMB45	GATA 3	Cathepsin K
Case 1	Foc. +	+	À	+	+	À	+	+	À	+
Case 2	À	+	À	+	À	À	+	+	À	À
Case 3	À	+	À	+	+	+	+	À	À	+
Case 3—recurrent lesion	À	+	À	+	À	+	+	À	À	À

À indicates negative; +, weak positivity; AMACR, racemase; CANH9, carbonic anhydrase IX; Foc. <50% cells staining; Vim, vimentin.

of the upper pole tumor with a pathologic stage of pT1a). Histologically, the tumor exhibited tubulopapillary architecture with small foci of necrosis. Neoplastic cells were eosinophilic and formed structures resembling a palisading pattern at the periphery of pseudotubular and papillary structures (Fig. 2). Nuclei were elongated with occasional nuclear grooves. Foci of dystrophic calcifications were also noted. Recurrent tumor (located within the lower portion of the renal medulla and protruding into the renal pelvis) was identified 4 months after resection by ultrasound examination during regular check-up. The tumor showed a similar architectural pattern to that seen in the primary lesion, with more pronounced palisading vaguely resembling urothelial carcinoma (UC).

Resultsofimmunohistochemical examination of our 3 NONO-TFE3 cases are summarized in Table 1. All cases were positive for racemase, PAX 8, and CD10, while negative for carbonic anhydrase IX. Interestingly, 2 tumors were positive for HMB45. Vimentin was positive focally in 1 case, and TFE3 was positive in 2 cases as well as cathepsin K.

FISH analysis showed the break of NONO gene (using probe SureFISH Xq13.1 NONO BA) and the break of TFE3 gene (using ZytoLight R SPEC TFE3 Dual-color Break-apart Probe) in all 3 primary tumors as well as the recurrent one. We also tested normal “nontumorous” tissue of the patient with recurrence, which showed no break of the NONO gene or the TFE3 gene.

First 2 cases from our small series were very similar to the description provided by Argani and colleagues. They all were arranged in a predominantly papillary pattern. The neoplastic cells mostly showed voluminous clear to weakly eosinophilic cytoplasm. Subnuclear vacuolization resembled similar changes known from clear cell papillary RCC, which should be considered in the differential diagnosis. Both tumors had psammoma bodies and/or dystrophic calcifications. Results of FISH analyses were close to the results reported by Argani et al[1] and Clark et al.[2]

The third case was particularly interesting for several reasons. First, the architecture was more tubular than papillary. Second, the neoplastic cells were eosinophilic with relative scant cytoplasm (in comparison with previous cases), making an overall resemblance to UC. The early detection of the recurrent tumor in the renal medulla and pelvis was highly surprising in this case. It should be noted that we were unable to fully rule out the possibility that the tumor may have been initially present within the renal pelvis during the first surgery. Coincidence of RCC and UC has repeatedly been described in the literature; however, we are not aware of any UC harboring NONO-TFE3 translocation. On the basis of morphology and immunohistochemical examination, it was evident that recurrent tumor was of renal cell origin, despite its morphologic resemblance to UC. Of note, the recurrent lesion was located deep within the renal medulla, with no connection to the surface urothelium of the renal pelvis. Further, no urothelial dysplasia or UC was identified. Nontumorous tissue in this patient did not show genetic changes, that is, no break NONO gene or TFE3 gene, and was used as a negative control. Similar case has been reported by Green et al[3] in 2013. Authors described Xp11 translocation RCC, which involved renal pelvis and simulated UC in several aspects.

Xp11 translocation RCCs are the most common translocation RCCs in adult population. In addition to typical Xp11.2 RCC with papillary architecture, mostly clear cells and frequent psammoma bodies, there are several other morphologic variants as well as tumors with different TFE3 fusion partners.[3–5] However many different morphologic variants of Xp11.2 translocation RCCs were described in the literature, we believe pathologic features of Xp11.2 translocation RCCs are much more complex than what is currently known. In our small series of 3 NONO-TFE3 RCCs, we enriched morphologic spectrum, which requires further investigations.

Kristyna Pivovarcikova, MD*
Petr Grossmann, PhD*
Reza Alaghehbandan, MDw
Maris Sperga, MDz
Michal Michal, MD*
Ondrej Hes, MD, PhD*

*Department of Pathology, Medical Faculty, Charles University, Charles University Hospital Plzen, Plzen Czech Republic
wDepartment of Pathology, Faculty of Medicine, University of British Columbia Royal Columbian Hospital, Vancouver BC, Canada
zDepartment of Pathology, East University, Riga, Latvia

Conflicts of Interest and Source of Funding: Supported by the Charles University Research Fund (project number P36) and by Institutional Research Fund FN 00669806. The authors have disclosed that they have no significant relationships with, or financial interest in, any commercial companies pertaining to this article.

REFERENCES

1. Argani P, Zhong M, Reuter VE, et al. TFE3-fusion variant analysis defines specific

clinicopathologic associations among Xp11 translocation cancers. Am J Surg Pathol. 2016;40:723–737.
2. Clark J, Lu YJ, Sidhar SK, et al. Fusion of splicing factor genes PSF and NonO (p54nrb) to the TFE3 gene in papillary renal cellcarcinoma.Oncogene.1997;15: 2233–2239.
3. Green WM, Yonescu R, Morsberger L, et al. Utilization of a TFE3 break-apart FISH assay in a renal tumor consultation service. Am J Surg Pathol. 2013;37: 1150–1163.
4. Argani P, Antonescu CR, Illei PB, et al. Primary renal neoplasms with the ASPL-TFE3 gene fusion of alveolar soft part sarcoma: a distinctive tumor entity previously included among renal cell carcinomas of children and adolescents. Am J Pathol. 2001;159:179–192.
5. Malouf GG, Monzon FA, Couturier J, et al. Genomic heterogeneity of translocation renal cell carcinoma. Clin Cancer Res. 2013;19: 4673–4684.

Nuclear Bubbles (Nuclear Pseudo-Pseudoinclusions): A Pitfall in the Interpretation of Microscopic Sections From the Thyroid and Other Human Organs

To the Editor:

An intriguing artifact in histopathology consists of the presence of single or multiple nuclear vacuoles (referred herein as bubbles) resulting in a bubbly appearance of the nucleus. We have referred to them, tongue-in-cheek, as “pseudo-pseudoinclusions” to distinguish them from the bonafide nuclear “pseudoinclusions” resulting from an invagination of the nuclear membrane and regarded as a pretty reliable marker of papillary thyroid carcinoma.[1–3] The bubbles that are the subject of this communication are variously sized, colorless or pale grayish, and sometimes coalescent and multiple, resulting in an empty-like appearance of the nucleus, with loss of chromatin texture and margination of nucleoli. They may severely interfere with the identification of cell types and grading assessment, especially in lymphoid neoplasms,[1] and also in epithelial and mesenchymal tumors.[2–5]

These nuclear bubbles have been thought to be caused by incomplete fixation, dehydration, or clearing during tissue processing, or by an excessively high temperature during tissue processing, water bath, or sections drying.[1–3,6] We noted the occurrence of this artifact sporadically on slides routinely prepared in

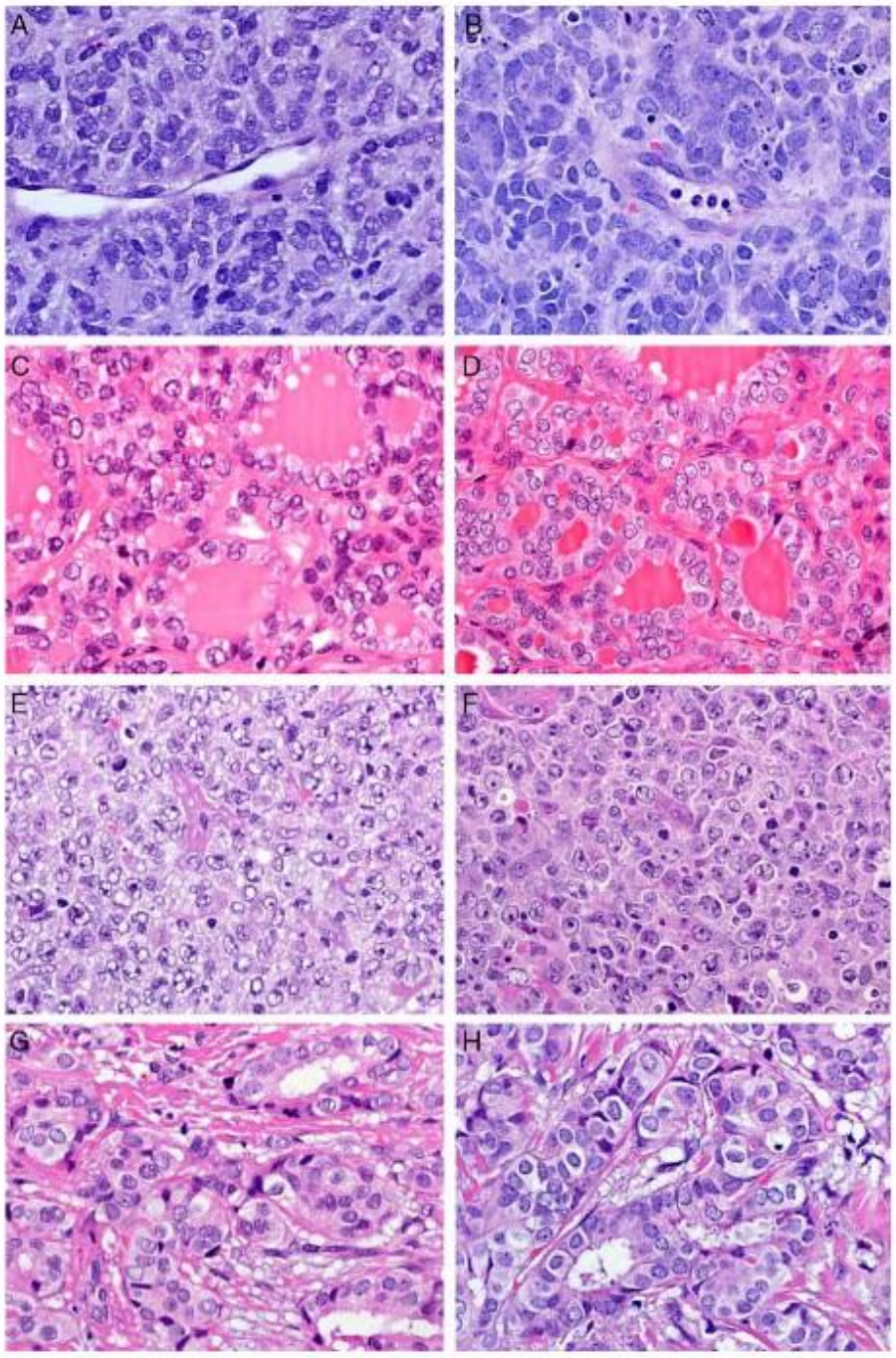

FIGURE 1. Pairs of images taken from the same tumor area on sections routinely dried (left) and dried following the fan procedure (right). A and B, Undifferentiated neoplasm. C and D, Thyroid papillary carcinoma, follicular variant (note that some “facts” are artifacts). E and F, Diffuse large B-cell lymphoma. G and H, Breast invasive ductal carcinoma (hematoxylin and eosin).

4 Závěr

Klasifikace nádorů ledvin se stává velmi komplikovanou. V posledních letech je popisováno velké množství zcela nových morfologických jednotek i variant dobře známých renálních neoplásií, kdy některé z těchto tumorů jsou diagnostikovány čistě na podkladě molekulárně genetických znaků (např. Xp11.2 TRCC, HLRCC). Molekulárně genetická analýza tak začíná být součástí rutinní diagnostické praxe a je společně s imunohistochemií hojně využívána jako jedna z diagnostických modalit u obtížně klasifikovatelných renálních neoplásií.

I v rámci renálních tumorů s papilární morfologií má genetika své místo v diagnostické rozvaze. Léze s papilární architektonikou mohou být za jistých okolností diferenciálně diagnosticky obtížnou kategorií, kde přesné odlišení a správná diagnóza má klinický význam, neboť se často jedná o léze s velmi odlišným biologickým chováním (indolentní průběh u CCPRCC, naopak vysoká agresivita u HLRCC či Xp11 TRCC).

Za molekulární genetikou však nelze upozaďovat morfologický obraz. Histologický nález stále zůstává nejdůležitějším diagnostickým parametrem, který rozhoduje o dalším diagnostickém postupu. Stejně tak důležité je nezapomínat na základní pravidla při zpracování vzorku, jako je dostatečně rozsáhlé zpracování materiálu (sampling), jež často může významně zjednodušit diagnostiku (některé typické znaky mohou být vyjádřeny jen fokálně, což lze někdy zastihnout právě pouze při dostatečném až excesivním zablokování materiálu).

Nově se mění i pohled na molekulárně genetické znaky klasicky přisuzované PRCC (trisomie/polysomie chromosomů 7 a 17 a ztráta chromosomu Y u mužských případů), kdy po pečlivé revizi doposud publikované literatury, velké množství publikovaných prací zabývajících se molekulárně genetickými změnami u PRCC ukazuje často relativně různorodé výsledky. To jen potvrzuje domněnku, že molekulárně genetickou analýzu nelze v běžné praxi užívat jako univerzální diagnostický nástroj, a že společně s imunohistochemickým barvením by měla být molekulárně genetická vyšetření užívána pouze jako součást diagnostického algoritmu, s vědomím, že výsledky vyšetření nutno brát vždy jistou rezervou a tyto metody neřeší diagnostické dilema ve 100% případů.

Dalším velmi aktuálním tématem je otázka Xp11 TRCC, kdy XP11 TRCC jakožto nádorová jednotka definovaná čistě na podkladě cytogenetické a molekulárně genetické analýzy celkem logicky vyžaduje pro stanovení diagnózy provedení molekulárně genetického vyšetření (klasicky užívaná FISH s break apart sondou). Snahy uvést do klinické praxe imunohistochemickou protilátku detekující protein TFE3 byly neúspěšné, imunohistochemický průkaz TFE3 je nekonstantní, velmi ovlivnitelný fixací materiálu a má jen omezený význam. FISH vyšetření tedy zůstává „zlatým standardem“ při diagnostice Xp11 TRCC. Recentně se však ukazuje, že i tento přístup má svá úskalí. Někteří z fúzní partnerů (např. *RBM10-TFE3*) mohou vykazovat jasnou pozitivitu imunohistochemického barvení na TFE3, avšak vést k falešné negativitě FISH vyšetření za použití klasických break apart sond. Je tedy evidentní, že molekulárně genetické a imunohistochemické metody se vzájemně doplňují, při diskrepanci výsledků těchto dvou vyšetření je třeba pomyslet i na možnost některého z vzácnějších fúzních partnerů a provést další vyšetření k potvrzení diagnózy (např. RNA sekvenování) (64, 65). Kromě vlivu fúzních genů na molekulárně genetickou detekci se do popředí dostává i snaha blíže definovat a popsat celé široké morfologické spektrum Xp11 TRCC. Od minulého roku se Xp11 TRCC vrátil do centra pozornosti urogenitálních patologů a v literatuře nyní vychází četné práce korelující jednotlivé specifické fúzní partnery genu

TFE3 s histologickým obrazem a imunohistochemickým profilem lézí (63-66), přičemž obdobné práce budou jistě i nadále přibývat.

Ačkoliv výše popsaná expanze morfologického a molekulárně genetického spektra renálních neoplásií zůstává prozatím bez přímého klinického dopadu, kdy léčebný algoritmus se u různých renálních nádorů zásadně neliší, v budoucnu, s rozvojem cílené léčby, by toto mělo nabýt na významu a mít klinické opodstatnění. Z pohledu patologa je pak znalost morfologického spektra, a především opora v literatuře, neodmyslitelnou součástí každodenní praxe a snad i zárukou správné diagnózy.

Molekulárně genetické metody (i imunohistochemická barvení) jsou do jisté míry závislé na dobré fixaci, kvalitním zpracování materiálu a dobré kvalitě DNA, což např. v konzultační praxi prakticky nelze ovlivnit. Morfologie tedy i nadále zůstává základním a hlavním diagnostickým kritériem, avšak v ideálních případech je molekulární genetika společně s imunohistochemií nemalou a velmi cennou pomocnou modalitou výrazně usnadňující diagnostiku renálních lézí.

5 Seznam použité literatury

1. Dušek L, Mužík J, Kubásek M, Koptíková J, Žaloudík J, Vyzula R. Epidemiologie zhoubných nádorů v České republice [online]. Masarykova univerzita.2005 [cited 2017-11-05]. Available from: http://svod.cz/.

2. Moch H, Humphrey PA, Ulbright TM, Reuter VE. WHO classification of tumours of the urinary system and male genital organs. Lyon: IARC; 2016.

3. Kovacs G, Akhtar M, Beckwith BJ, Bugert P, Cooper CS, Delahunt B, et al. The Heidelberg classification of renal cell tumours. The Journal of pathology. 1997;183(2):131-3.

4. Srigley JR, Delahunt B, Eble JN, Egevad L, Epstein JI, Grignon D, et al. The International Society of Urological Pathology (ISUP) Vancouver Classification of Renal Neoplasia. The American journal of surgical pathology. 2013;37(10):1469-89.

5. Delahunt B, Eble JN. Papillary renal cell carcinoma: a clinicopathologic and immunohistochemical study of 105 tumors. Modern pathology : an official journal of the United States and Canadian Academy of Pathology, Inc. 1997;10(6):537-44.

6. Delahunt B, Eble JN, McCredie MR, Bethwaite PB, Stewart JH, Bilous AM. Morphologic typing of papillary renal cell carcinoma: comparison of growth kinetics and patient survival in 66 cases. Human pathology. 2001;32(6):590-5.

7. Langner C, Wegscheider BJ, Ratschek M, Schips L, Zigeuner R. Keratin immunohistochemistry in renal cell carcinoma subtypes and renal oncocytomas: a systematic analysis of 233 tumors. Virchows Archiv : an international journal of pathology. 2004;444(2):127-34.

8. Jiang F, Richter J, Schraml P, Bubendorf L, Gasser T, Sauter G, et al. Chromosomal imbalances in papillary renal cell carcinoma: genetic differences between histological subtypes. The American journal of pathology. 1998;153(5):1467-73.

9. Kovac M, Navas C, Horswell S, Salm M, Bardella C, Rowan A, et al. Recurrent chromosomal gains and heterogeneous driver mutations characterise papillary renal cancer evolution. Nature communications. 2015;6:6336.

10. Yu W, Zhang W, Jiang Y, Wang Y, Li Y, Wang J, et al. Clinicopathological, genetic, ultrastructural characterizations and prognostic factors of papillary renal cell carcinoma: new diagnostic and prognostic information. Acta histochemica. 2013;115(5):452-9.

11. Marsaud A, Dadone B, Ambrosetti D, Baudoin C, Chamorey E, Rouleau E, et al. Dismantling papillary renal cell carcinoma classification: The heterogeneity of genetic profiles suggests several independent diseases. Genes, chromosomes & cancer. 2015;54(6):369-82.

12. Gunawan B, von Heydebreck A, Fritsch T, Huber W, Ringert RH, Jakse G, et al. Cytogenetic and morphologic typing of 58 papillary renal cell carcinomas: evidence for a cytogenetic evolution of type 2 from type 1 tumors. Cancer research. 2003;63(19):6200-5.

13. Antonelli A, Tardanico R, Balzarini P, Arrighi N, Perucchini L, Zanotelli T, et al. Cytogenetic features, clinical significance and prognostic impact of type 1 and type 2 papillary renal cell carcinoma. Cancer genetics and cytogenetics. 2010;199(2):128-33.

14. Saleeb RM, Brimo F, Farag M, Rompre-Brodeur A, Rotondo F, Beharry V, et al. Toward Biological Subtyping of Papillary Renal Cell Carcinoma With Clinical Implications Through Histologic, Immunohistochemical, and Molecular Analysis. The American journal of surgical pathology. 2017.

15. Bigot P, Bernhard JC, Gill IS, Vuong NS, Verhoest G, Flamand V, et al. The subclassification of papillary renal cell carcinoma does not affect oncological outcomes after nephron sparing surgery. World journal of urology. 2016;34(3):347-52.

16. Ledezma RA, Negron E, Paner GP, Rjepaj C, Lascano D, Haseebuddin M, et al. Clinically localized type 1 and 2 papillary renal cell carcinomas have similar survival outcomes following surgery. World journal of urology. 2016;34(5):687-93.

17. Ha YS, Chung JW, Choi SH, Lee JN, Kim HT, Kim TH, et al. Clinical Significance of Subclassification of Papillary Renal Cell Carcinoma: Comparison of Clinicopathologic Parameters and Oncologic Outcomes Between Papillary Histologic Subtypes 1 and 2 Using the Korean Renal Cell Carcinoma Database. Clinical genitourinary cancer. 2017;15(2):e181-e6.

18. Hes O, Brunelli M, Michal M, Cossu Rocca P, Hora M, Chilosi M, et al. Oncocytic papillary renal cell carcinoma: a clinicopathologic, immunohistochemical, ultrastructural, and interphase cytogenetic study of 12 cases. Annals of diagnostic pathology. 2006;10(3):133-9.

19. Xia QY, Rao Q, Shen Q, Shi SS, Li L, Liu B, et al. Oncocytic papillary renal cell carcinoma: a clinicopathological study emphasizing distinct morphology, extended immunohistochemical profile and cytogenetic features. International journal of clinical and experimental pathology. 2013;6(7):1392-9.

20. Park BH, Ro JY, Park WS, Jee KJ, Kim K, Gong G, et al. Oncocytic papillary renal cell carcinoma with inverted nuclear pattern: distinct subtype with an indolent clinical course. Pathology international. 2009;59(3):137-46.

21. Lefevre M, Couturier J, Sibony M, Bazille C, Boyer K, Callard P, et al. Adult papillary renal tumor with oncocytic cells: clinicopathologic, immunohistochemical, and cytogenetic features of 10 cases. The American journal of surgical pathology. 2005;29(12):1576-81.

22. Han G, Yu W, Chu J, Liu Y, Jiang Y, Li Y, et al. Oncocytic papillary renal cell carcinoma: A clinicopathological and genetic analysis and indolent clinical course in 14 cases. Pathology, research and practice. 2017;213(1):1-6.

23. Kunju LP, Wojno K, Wolf JS, Jr., Cheng L, Shah RB. Papillary renal cell carcinoma with oncocytic cells and nonoverlapping low grade nuclei: expanding the morphologic spectrum with emphasis on clinicopathologic, immunohistochemical and molecular features. Human pathology. 2008;39(1):96-101.

24. Michalova K, Steiner P, Montiel DP, Sperga M, Suster S, Alaghehbandan R, et al. Chromosomal Aberration Pattern in Oncocytic Papillary Renal Cell Carcinoma: Analysis of 28 Cases. United States & Canadian Academy of Pathology 106th Annual Meeting; San Antonio: Mod Pathol; 2017. p. 243 A.

25. Argani P, Netto GJ, Parwani AV. Papillary renal cell carcinoma with low-grade spindle cell foci: a mimic of mucinous tubular and spindle cell carcinoma. The American journal of surgical pathology. 2008;32(9):1353-9.

26. Foster EA, Levine, A.J. Mucin production in metastatic carcinomas. Cancer. 1963;16:506-9.

27. Grignon DJ, Ro JY, Ayala AG. Primary mucin-secreting adenocarcinoma of the kidney. Archives of pathology & laboratory medicine. 1988;112(8):847-9.

28. Val-Bernal JF, Mayorga M, Garcia-Arranz P, Gomez-Roman JJ. Mucin secretion in papillary (chromophil) renal cell carcinoma. The American journal of surgical pathology. 1998;22(8):1037-40.

29. Val-Bernal JF, Gomez-Roman JJ, Vallina T, Villoria F, Mayorga M, Garcia-Arranz P. Papillary (chromophil) renal cell carcinoma with mucinous secretion. Pathology, research and practice. 1999;195(1):11-7.

30. Pivovarcikova K, Peckova K, Martinek P, Montiel DP, Kalusova K, Pitra T, et al. "Mucin"-secreting papillary renal cell carcinoma: clinicopathological, immunohistochemical, and molecular genetic analysis of seven cases. Virchows Archiv : an international journal of pathology. 2016;469(1):71-80.

31. Skenderi F, Ulamec M, Vanecek T, Martinek P, Alaghehbandan R, Foix MP, et al. Warthin-like papillary renal cell carcinoma: Clinicopathologic, morphologic, immunohistochemical and molecular genetic analysis of 11 cases. Annals of diagnostic pathology. 2017;27:48-56.

32. Fuzesi L, Gunawan B, Bergmann F, Tack S, Braun S, Jakse G. Papillary renal cell carcinoma with clear cell cytomorphology and chromosomal loss of 3p. Histopathology. 1999;35(2):157-61.

33. Salama ME, Worsham MJ, DePeralta-Venturina M. Malignant papillary renal tumors with extensive clear cell change: a molecular analysis by microsatellite analysis and fluorescence in situ hybridization. Archives of pathology & laboratory medicine. 2003;127(9):1176-81.

34. Gobbo S, Eble JN, Grignon DJ, Martignoni G, MacLennan GT, Shah RB, et al. Clear cell papillary renal cell carcinoma: a distinct histopathologic and molecular genetic entity. The American journal of surgical pathology. 2008;32(8):1239-45.

35. Petersson F, Bulimbasic S, Hes O, Slavik P, Martinek P, Michal M, et al. Biphasic alveolosquamoid renal carcinoma: a histomorphological, immunohistochemical, molecular genetic, and ultrastructural study of a distinctive morphologic variant of renal cell carcinoma. Annals of diagnostic pathology. 2012;16(6):459-69.

36. Hes O, Condom Mundo E, Peckova K, Lopez JI, Martinek P, Vanecek T, et al. Biphasic Squamoid Alveolar Renal Cell Carcinoma: A Distinctive Subtype of Papillary Renal Cell Carcinoma? The American journal of surgical pathology. 2016;40(5):664-75.

37. Lopez JI. Case Report: Multifocal biphasic squamoid alveolar renal cell carcinoma. F1000Research. 2016;5:607.

38. Trpkov K, Athanazio D, Magi-Galluzzi C, Yilmaz H, Clouston D, Agaimy A, et al. Biphasic Papillary Renal Cell Carcinoma Is a Rare and Distinct Morphologic Variant – Clinicopathologic Study of 24 Novel Cases. United States & Canadian Academy of Pathology 106th Annual Meeting; San Antonio: Mod Pathol 2017. p. 264 A.

39. Chartier S, Mejean A, Richard S, Thiounn N, Vasiliu V, Verkarre V. Biphasic Squamoid Alveolar Renal Cell Carcinoma: 2 Cases in a Family Supporting a Continuous Spectrum With Papillary Type I Renal Cell Carcinoma. The American journal of surgical pathology. 2017.

40. Troxell ML, Higgins JP. Renal cell carcinoma in kidney allografts: histologic types, including biphasic papillary carcinoma. Human pathology. 2016;57:28-36.

41. Renshaw AA, Zhang H, Corless CL, Fletcher JA, Pins MR. Solid variants of papillary (chromophil) renal cell carcinoma: clinicopathologic and genetic features. The American journal of surgical pathology. 1997;21(10):1203-9.

42. Ulamec M, Skenderi F, Trpkov K, Kruslin B, Vranic S, Bulimbasic S, et al. Solid papillary renal cell carcinoma: clinicopathologic, morphologic, and immunohistochemical analysis of 10 cases and review of the literature. Annals of diagnostic pathology. 2016;23:51-7.

43. Mantoan Padilha M, Billis A, Allende D, Zhou M, Magi-Galluzzi C. Metanephric adenoma and solid variant of papillary renal cell carcinoma: common and distinctive features. Histopathology. 2013;62(6):941-53.

44. Zhang Y, Yong X, Wu Q, Wang X, Zhang Q, Wu S, et al. Mucinous tubular and spindle cell carcinoma and solid variant papillary renal cell carcinoma: a clinicopathologic comparative analysis of four cases with similar molecular genetics datum. Diagnostic pathology. 2014;9:194.

45. Launonen V, Vierimaa O, Kiuru M, Isola J, Roth S, Pukkala E, et al. Inherited susceptibility to uterine leiomyomas and renal cell cancer. Proceedings of the National Academy of Sciences of the United States of America. 2001;98(6):3387-92.

46. Eble J.N. SG, Epstein J.I., Sesterhenn I.A. . World Health Organization Classification of Tumours Pathology and Genetics Tumours of the Urinary System and Male Genital Organs. IARC Press Lyon. 2004.

47. Toro JR, Nickerson ML, Wei MH, Warren MB, Glenn GM, Turner ML, et al. Mutations in the fumarate hydratase gene cause hereditary leiomyomatosis and renal cell cancer in families in North America. American journal of human genetics. 2003;73(1):95-106.

48. Merino MJ, Torres-Cabala C, Pinto P, Linehan WM. The morphologic spectrum of kidney tumors in hereditary leiomyomatosis and renal cell carcinoma (HLRCC) syndrome. The American journal of surgical pathology. 2007;31(10):1578-85.

49. Trpkov K, Hes O, Agaimy A, Bonert M, Martinek P, Magi-Galluzzi C, et al. Fumarate Hydratase-deficient Renal Cell Carcinoma Is Strongly Correlated With Fumarate Hydratase Mutation and Hereditary Leiomyomatosis and Renal Cell Carcinoma Syndrome. The American journal of surgical pathology. 2016;40(7):865-75.

50. Grubb RL, 3rd, Franks ME, Toro J, Middelton L, Choyke L, Fowler S, et al. Hereditary leiomyomatosis and renal cell cancer: a syndrome associated with an aggressive form of inherited renal cancer. The Journal of urology. 2007;177(6):2074-9; discussion 9-80.

51. Tomlinson IP, Alam NA, Rowan AJ, Barclay E, Jaeger EE, Kelsell D, et al. Germline mutations in FH predispose to dominantly inherited uterine fibroids, skin leiomyomata and papillary renal cell cancer. Nature genetics. 2002;30(4):406-10.

52. Wei MH, Toure O, Glenn GM, Pithukpakorn M, Neckers L, Stolle C, et al. Novel mutations in FH and expansion of the spectrum of phenotypes expressed in families with hereditary leiomyomatosis and renal cell cancer. Journal of medical genetics. 2006;43(1):18-27.

53. Bardella C, El-Bahrawy M, Frizzell N, Adam J, Ternette N, Hatipoglu E, et al. Aberrant succination of proteins in fumarate hydratase-deficient mice and HLRCC patients is a robust biomarker of mutation status. The Journal of pathology. 2011;225(1):4-11.

54. Chen YB, Brannon AR, Toubaji A, Dudas ME, Won HH, Al-Ahmadie HA, et al. Hereditary leiomyomatosis and renal cell carcinoma syndrome-associated renal cancer: recognition of the syndrome by pathologic features and the utility of detecting aberrant succination by immunohistochemistry. The American journal of surgical pathology. 2014;38(5):627-37.

55. Michal M, Hes O, Havlicek F. Benign renal angiomyoadenomatous tumor: a previously unreported renal tumor. Annals of diagnostic pathology. 2000;4(5):311-5.

56. Tickoo SK, dePeralta-Venturina MN, Harik LR, Worcester HD, Salama ME, Young AN, et al. Spectrum of epithelial neoplasms in end-stage renal disease: an experience from 66 tumor-bearing kidneys with emphasis on histologic patterns distinct from those in sporadic adult renal neoplasia. The American journal of surgical pathology. 2006;30(2):141-53.

57. Aron M, Chang E, Herrera L, Hes O, Hirsch MS, Comperat E, et al. Clear cell-papillary renal cell carcinoma of the kidney not associated with end-stage renal disease: clinicopathologic correlation with expanded immunophenotypic and molecular characterization of a large cohort with emphasis on relationship with renal angiomyoadenomatous tumor. The American journal of surgical pathology. 2015;39(7):873-88.

58. Deml KF, Schildhaus HU, Comperat E, von Teichman A, Storz M, Schraml P, et al. Clear cell papillary renal cell carcinoma and renal angiomyoadenomatous tumor: two variants of a morphologic, immunohistochemical, and genetic distinct entity of renal cell carcinoma. The American journal of surgical pathology. 2015;39(7):889-901.

59. Hes O, Comperat EM, Rioux-Leclercq N. Clear cell papillary renal cell carcinoma, renal angiomyoadenomatous tumor, and renal cell carcinoma with leiomyomatous stroma relationship of 3 types of renal tumors: a review. Annals of diagnostic pathology. 2016;21:59-64.

60. Kuroda N, Ohe C, Kawakami F, Mikami S, Furuya M, Matsuura K, et al. Clear cell papillary renal cell carcinoma: a review. International journal of clinical and experimental pathology. 2014;7(11):7312-8.

61. Argani P, Lae M, Ballard ET, Amin M, Manivel C, Hutchinson B, et al. Translocation carcinomas of the kidney after chemotherapy in childhood. Journal of clinical oncology : official journal of the American Society of Clinical Oncology. 2006;24(10):1529-34.

62. Argani P, Antonescu CR, Illei PB, Lui MY, Timmons CF, Newbury R, et al. Primary renal neoplasms with the ASPL-TFE3 gene fusion of alveolar soft part sarcoma: a distinctive tumor entity previously included among renal cell carcinomas of children and adolescents. The American journal of pathology. 2001;159(1):179-92.

63. Argani P, Zhong M, Reuter VE, Fallon JT, Epstein JI, Netto GJ, et al. TFE3-Fusion Variant Analysis Defines Specific Clinicopathologic Associations Among Xp11 Translocation Cancers. The American journal of surgical pathology. 2016;40(6):723-37.

64. Argani P, Zhang L, Reuter VE, Tickoo SK, Antonescu CR. RBM10-TFE3 Renal Cell Carcinoma: A Potential Diagnostic Pitfall Due to Cryptic Intrachromosomal Xp11.2 Inversion Resulting in False-negative TFE3 FISH. The American journal of surgical pathology. 2017;41(5):655-62.

65. Xia QY, Wang XT, Zhan XM, Tan X, Chen H, Liu Y, et al. Xp11 Translocation Renal Cell Carcinomas (RCCs) With RBM10-TFE3 Gene Fusion Demonstrating Melanotic Features and Overlapping Morphology With t(6;11) RCC: Interest and Diagnostic Pitfall in Detecting a Paracentric Inversion of TFE3. The American journal of surgical pathology. 2017;41(5):663-76.

66. Wang XT, Xia QY, Ni H, Ye SB, Li R, Wang X, et al. SFPQ/PSF-TFE3 renal cell carcinoma: a clinicopathologic study emphasizing extended morphology and reviewing the differences between SFPQ-TFE3 RCC and the corresponding mesenchymal neoplasm despite an identical gene fusion. Human pathology. 2017;63:190-200.

67. Pflueger D, Sboner A, Storz M, Roth J, Comperat E, Bruder E, et al. Identification of molecular tumor markers in renal cell carcinomas with TFE3 protein expression by RNA sequencing. Neoplasia. 2013;15(11):1231-40.

6 Publikace

6.1 Publikace autorky, které jsou podkladem dizertační práce

1. **Pivovarcikova K**, Peckova K, Martinek P, Montiel DP, Kalusova K, Pitra T, Hora M, Skenderi F, Ulamec M, Daum O, Rotterova P, Ondic O, Dubova M, Curik R, Dunatov A, Svoboda T, Michal M, Hes O. "Mucin"-secreting papillary renal cell carcinoma: clinicopathological, immunohistochemical, and molecular genetic analysis of seven cases. Virchows Arch. 2016 Jul;469(1):71-80. IF 2.848

2. Skenderi F, Ulamec M, Vanecek T, Martinek P, Alaghehbandan R, Foix MP, Babankova I, Montiel DP, Alvarado-Cabrero I, Svajdler M, Dubinský P, Cempirkova D, Pavlovsky M, Vranic S, Daum O, Ondic O, **Pivovarcikova K**, Michalova K, Hora M, Rotterova P, Stehlikova A, Dusek M, Michal M, Hes O. Warthin-like papillary renal cell carcinoma: Clinicopathologic, morphologic, immunohistochemical and molecular genetic analysis of 11 cases. Ann Diagn Pathol. 2017 Apr;27:48-56. IF 1.734

3. Hes O, Condom Mundo E, Peckova K, Lopez JI, Martinek P, Vanecek T, Falconieri G, Agaimy A, Davidson W, Petersson F, Bulimbasic S, Damjanov I,Jimeno M, Ulamec M, Podhola M, Sperga M, Pane Foix M, Shelekhova K, Kalusova K, Hora M, Rotterova P, Daum O, **Pivovarcikova K**, Michal M. Biphasic Squamoid Alveolar Renal Cell Carcinoma: A Distinctive Subtype of Papillary Renal Cell Carcinoma? Am J Surg Pathol. 2016 May;40(5):664-75. IF 5.363

4. Ulamec M, Skenderi F, Trpkov K, Kruslin B, Vranic S, Bulimbasic S, Trivunic S, Montiel DP, Peckova K, **Pivovarcikova K**, Ondic O, Daum O,Rotterova P, Dusek M, Hora M, Michal M, Hes O. Solid papillary renal cell carcinoma: clinicopathologic, morphologic, and immunohistochemical analysis of 10 cases and review of the literature. Ann Diagn Pathol. 2016 Aug;23:51-7. IF 1.734

5. Peckova K, Martinek P, **Pivovarcikova K**, Vanecek T, Alaghehbandan R, Prochazkova K, Montiel DP, Hora M, Skenderi F, Ulamec M, Rotterova P, Daum O, Ferda J, Davidson W, Ondic O, Dubova M, Michal M, Hes O. Cystic and necrotic papillary renal cell carcinoma: prognosis, morphology, immunohistochemical, and molecular-genetic profile of 10 cases. Ann Diagn Pathol. 2017 Feb;26:23-30. IF 1.734

6. Hayes M, Peckova K, Martinek P, Hora M, Kalusova K, Straka L, Daum O, Kokoskova B, Rotterova P, **Pivovarčikova K**, Branzovsky J, Dubova M, Vesela P, Michal M, Hes O. Molecular-genetic analysis is essential for accurate classification of renal carcinoma resembling Xp11.2 translocation carcinoma. Virchows Arch. 2015 Mar;466(3):313-22. IF 2.613

7. **Pivovarcikova K**, Grossmann P, Alaghehbandan R, Sperga M, Michal M, Hes O. TFE3-Fusion Variant Analysis Defines Specific Clinicopathologic Associations Amog Xp11 Translocation Cancers. Am J Surg Pathol. 2017 Jan;41(1):138-140. IF 5.363

6.2 Další publikace autorky se vztahem k tématu dizertační práce

8. Hes O, de Souza TG, **Pivovarcikova K**, Grossmann P, Martinek P, Kuroda N, Kacerovska D, Svajdler M, Straka L, Petersson F, Hora M, Michal M. Distinctive renal cell tumor simulating atrophic kidney with 2 types of microcalcifications. Report of 3 cases. Ann Diagn Pathol. 2014 Apr;18(2):82-8. IF1.117

9. Hes O, **Pivovarcikova K**, Stehlik J, Martinek P, Vanecek T, Bauleth K, Dolejsova O, Petersson F, Hora M, Perez Montiel D, Peckova K, Branzovsky J, Slouka D, Vodicka J, Kokoskova B, Matej R, Michal M. Choriogonadotropin positive seminoma-a clinicopathological and molecular genetic study of 15 cases. Ann Diagn Pathol. 2014 Apr;18(2):89-94. IF1.117

10. Petersson F, Branzovsky J, Martinek P, Korabecna M, Kruslin B, Hora M, Peckova K, Bauleth K, **Pivovarcikova K**, Michal M, Svajdler M, Sperga M, Bulimbasic S, Leroy X, Rychly B, Trivunic S, Kokoskova B, Rotterova P, Podhola M, Suster S, Hes O. The leiomyomatous stroma in renal cell carcinomas is polyclonal and not part of the neoplastic process. Virchows Arch. 2014 Jul;465(1):89-96. IF 2.651

11. Petersson F, Sperga M, Bulimbasic S, Martinek P, Svajdler M, Kuroda N, Hora M, Simpson R, Tichy T, Peckova K, Branzovsky J, **Pivovarcikova K**, Rotterova P, Kokoskova B, Bauleth K, Martincok D, Nagy V, Michal M, Hes O. Foamy cell (hibernoma-like) change is a rare histopathological feature in renal cell carcinoma. Virchows Arch. 2014 Aug;465(2):215-24. IF 2.651

12. Peckova K, Grossmann P, Bulimbasic S, Sperga M, Perez Montiel D, Daum O, Rotterova P, Kokoskova B, Vesela P, **Pivovarcikova K**, Bauleth K, Branzovsky J, Dubova M, Hora M, Michal M, Hes O. Renal cell carcinoma with leiomyomatous stroma--further immunohistochemical and molecular genetic characteristics of unusual entity. Ann Diagn Pathol. 2014 Oct;18(5):291-6. IF1.117

13. Peckova K, Vanecek T, Martinek P, Spagnolo D, Kuroda N, Brunelli M, Vranic S, Djuricic S, Rotterova P, Daum O, Kokoskova B, Vesela P, **Pivovarcikova K**, Bauleth K, Dubova M, Kalusova K, Hora M, Michal M, Hes O. Aggressive and nonaggressive translocation t(6;11) renal cell carcinoma: comparative study of 6 cases and review of the literature. Ann Diagn Pathol. 2014 Dec;18(6):351-7. IF1.117

14. Peckova K, Martinek P, Sperga M, Montiel DP, Daum O, Rotterova P, Kalusová K, Hora M, **Pivovarcikova K**, Rychly B, Vranic S, Davidson W, Vodicka J, Dubová M, Michal M, Hes O. Mucinous spindle and tubular renal cell carcinoma: analysis of chromosomal aberration pattern of low-grade, high-grade, and overlapping morphologic variant with papillary renal cell carcinoma. Ann Diagn Pathol. 2015 Aug;19(4):226-31. IF 1.022

15. Peckova K, Martinek P, Ohe C, Kuroda N, Bulimbasic S, Condom Mundo E, Perez Montiel D, Lopez JI, Daum O, Rotterova P, Kokoskova B, Dubova M, **Pivovarcikova K**, Bauleth K, Grossmann P, Hora M, Kalusova K, Davidson W, Slouka D, Miroslav S, Buzrla P, Hynek M, Michal M, Hes O. Chromophobe renal cell

carcinoma with neuroendocrine and neuroendocrine-like features. Morphologic, immunohistochemical, ultrastructural, and array comparative genomic hybridization analysis of 18 cases and review of the literature. Ann Diagn Pathol. 2015 Aug;19(4):261-8. IF 1.022

16. Vanecek T, **Pivovarcikova K**, Pitra T, Peckova K, Rotterova P, Daum O, Davidson W, Montiel DP, Kalusova K, Hora M, Ondic O, Dubova M, Michal M, Hes O.Mixed Epithelial and Stromal Tumor of the Kidney: Mutation Analysis of the DICER 1 Gene in 29 Cases. Appl Immunohistochem Mol Morphol. 2015 Oct 27. 2017 Feb;25(2):117-121. IF 1.553

17. **Pivovarcikova K**, Pitra T, Vanecek T, Alaghehbandan R, Barbora Gomolcakova, Ondic O, Peckova K, Rotterova P, Hora M, Dusek M, Michal M, Hes O. Comparative study of *TERT* gene mutation analysis on voided liquid-based urine cytology and paraffin-embedded tumorous tissue. Ann Diagn Pathol. 2016 Oct; 24:7-10. IF 1.734

18. Foix MP, Dunatov A, Martinek P, Mundó EC, Suster S, Sperga M, Lopez JI, Ulamec M, Bulimbasic S, Montiel DP, Alaghehbandan R, Peckova K, **Pivovarcikova K**, Ondrej D, Rotterova P, Skenderi F, Prochazkova K, Dusek M, Hora M, Michal M, Hes O. Morphological, immunohistochemical, and chromosomal analysis of multicystic chromophobe renal cell carcinoma, an architecturally unusual challenging variant. Virchows Arch. 2016 Dec;469(6):669-678. IF 2.848

19. Alaghehbandan R, Stehlik J, Trpkov K, Magi-Galluzzi C, Condom Mundo E, Pane Foix M, Berney D, Sibony M, Suster S, Agaimy A, Montiel DP, **Pivovarcikova K**, Michalova K, Daum O, Ondic O, Rotterova P, Dusek M, Hora M, Michal M, Hes O. Programmed death-1 (PD-1) receptor/PD-1 ligand (PD-L1) expression in fumarate hydratase-deficient renal cell carcinoma. Ann Diagn Pathol. 2017 Aug;29:17-22. IF 1.734

20. Rotterova P, Martinek P, Alaghehbandan R, Prochazkova K, Damjanov I, Rogala J, Suster S, Perez-Montiel D, Alvarado-Cabrero I, Sperga M, Svajdler M, Michalova K, **Pivovarcikova K**, Daum O, Hora M, Dusek M, Ondic O, Stehlikova A, Michal M, Hes O. High-grade renal cell carcinoma with emperipolesis: Clinicopathological, immunohistochemical and molecular-genetic analysis of 14 cases. Histol Histopathol. 2017 Sep 1 [Epub ahead of print].

6.3 Publikace autorky bez vztahu k tématu dizertační práce

1. **Pivovarčíková K**, Branžovský J, Bauleth K, Trávníček I, Dolejšová O, Šobrová A, Eret V, Ferda J, Hora M, Hes O. Radikální prostatektomie - analýza 191 případů vyšetřovaných metodikou celoplošných řezů (Whole-Mount Section). Ces Urol 2014, 18(1):26-32.

2. Šobrová A, Eret V, Dolejšová O, Ferda J, Kastner J, Hes O, **Pivovarčíková K**, Hora M. Komparace multiparametrické magnetické rezonance se silou magnetického pole 3 Tesla s transrektální sonografií naváděnou biopsií prostaty. Ces Urol 2014, 18(3):225-233.

3. Kalusová K, Trávníček I, Eberlová L, **Pivovarčíková K**, Hes O, Eret V, Pitra T, Hora M. Komplikace po lokální aplikaci cizorodého materiálu do podkoží penisu. Ces Urol 2015, 19(1):64-68.

4. Pitra T, **Pivovarčíková K**, Trávníček I, Procházková K, Hes O, Mírka H, Tupý R, Hora M. Cystické tumory ledvin. Ces Urol 2016, 20(3):204-213.

5. Polivka J Jr, Polivka J, Holubec L, Kubikova T, Priban V, Hes O, **Pivovarcikova K**, Treskova I. Advances in Experimental Targeted Therapy and Immunotherapy for Patients with Glioblastoma Multiforme. Anticancer Res. 2017 Jan;37(1):21-33. Review. IF 1.937

6.4 Prezentace na vědeckých konferencích

103rd Annual Meeting of the United States & **Canadian Academy of Pathology, 1.-7.3. 2014, San Diego Convention Center, San Diego, CA, USA**

Poster: Hes O, **Pivovarcikova K**, Stehlik J, Hora M, Michal M. Choriogonadotropin Positive Seminomas-Clinicopathological and Molecular Genetic Analysis of 15 Cases.

105th Annual Meeting of the United States & **Canadian Academy of Pathology,12.-18.3.2016 Washington State Convention Center, Seattle, WA, USA**

Poster**:** Foix MP, Dunatov A, Martinek P, Condom-Mundo E, Suster S, Sperga M, Lopez JI, Ulamec M, Bulimbasic S, Michal M, Peckova K, **Pivovarcikova K**, Daum O, Rotterova P, Kalusova K, Hora M, Hes O.Multicystic Chromophobe Renal Cell Carcinoma: A Challenging Unusual Architectural Variant. Morphological, Immunohistochemical and arrayCGH Analysis of 11 Cases.

Poster: Rotterova P, Martinek P, Kalusova K, Damjanov I, Suster S, Alvarado-Cabrero I, Sperga M, Svajdler M, Peckova K, **Pivovarcikova K**, Daum O, Hora M, Michal M, Hes O.High Grade Renal Cell Carcinoma with Emperipolesis. Clinicopathological, Immunohistochemical and Molecular-Genetic Analysis of 14 Cases.

EAU 16th Central European Meeting, 7.-8.10.2016, Vienna, Austria

Poster: Pitra T, **Pivovarcikova K**, Vanecek T, Alaghehbandan R, Gomolcakova B, Ondic O, Peckova K, Rotterova P, Hora M, Michal M, Hes O. Comparative study of TERT gene mutation analysis on voided liquid-based urine cytology and paraffin-embedded tumorous tissue.

106th Annual Meeting of the United States & **Canadian Academy of Pathology,4.-10.3.2017 Henry B. Gonzalez Convention Center, San Antonio, TX, USA**

Poster**:** Alaghehbandan R, Stehlik J, Trpkov K, Magi-Galluzzi C, Foix MP, Berney D, Sibony M, Suster S, Agaimy A, Montiel DP, **Pivovarcikova K**, Michalova K, Daum O, Ondic O, Rotterova P, Michal M, Hes O. Programmed Death-1 (PD-1) Receptor/PD-1 Ligand (PD-L1) Expression in Fumarate Hydratase-Deficient Renal Cell Carcinoma.

Poster: Michalova K, Steiner P, Perez Montiel D, Sperga M, Suster S, Alaghehbandan R, **Pivovarcikova K**, Daum O, Ondic O, Rotterova P, Hora M, Michal M, Hes O. Chromosomal Aberration Pattern in Oncocytic Papillary Renal Cell Carcinoma: Analysis of 28 Cases.

Poster: Isikci OT, He H, Grossmann P, Alaghehbandan R, Ulamec M, Petersson F, Perez Montiel D, Michalova K, **Pivovarcikova K**, Ondic O, Saskova B, Rotterova P, Hora M, Michal M, Hes O. Low-Grade Spindle Cell Proliferation in Clear Cell Renal Cell Carcinoma Is Unlikely an Initial Step in Sarcomatoid Differentiation

7.edukační symposium České nefrologické společnosti – Brodovy dny 2017, 6.-7.4.2017, Ústí nad Labem, Czech Republic

Prezentace kazuistik v bloku „Závažné akutní tubulointersticiální léze za hranicí pyelonefritidy či sepse“
Kazuistika: Kačer M, Pivovarčíková K. Zhoršení funkce ledvin a hmotnostní úbytek u diabetika 2. typu
Kazuistika: Kielberger L, Pivovarčíková K. Anurie po návštěvě několika non-stop barů
Kazuistika: Machová J, Pivovarčíková K. Selhání ledvin jako suvenýr z dovolené?

Komplexní novinky v onkourologii (KNOU), 19. - 20. 5. 2017, Hotel Angelo, Praha, Czech Republic

Přednáška: Aktuální pohled na histologickou klasifikaci uroteliálních nádorů - co by měl urolog a onkolog vědět?

EAU 17th Central European Meeting, 19.-20.10.2017, Plzeň, Czech Republic

Poster: Pitra T, **Pivovarcikova K**, Tupy R, Alaghehbandan R, Travnicek I, Prochazkova K, Klatte T, Chlosta P, Hes O, Hora M. Impact of MRI on Clasification of Cystic Renal Lesions: Is MRI Helpful in Bosniak IIF and Bosniak III Categories?.

29th European Congress of Pathology, 2.-6.9.2017, RAI Amsterdam, Amsterdam, The Netherlands

Poster: **Pivovarcikova K**, Sperga M, Saskova B, Grossmann P, Hes O. Xp11 Translocation Renal Cell Carcinoma with *NONO* Fusion Partner: Analysis of 4 Cases. In: Poster.

Poster: Saskova B, **Pivovarcikova K**, Hes O. Morphologic Variability in t(6;11) Translocation Renal Cell Carcinoma: Analysis of 9 Cases.

107th Annual Meeting of the United States & Canadian Academy of Pathology,17.-23.3.2018 Vancouver Convention Centre, Vancouver, BC, Canada

Poster: **Pivovarcikova K**, Martinek P, Alaghehbandan R, Perez Montiel MD, Alvarado-Cabrero I, Rogala J, Kuroda N, Rychly B, Gasparov S, Michalova K, Saskova B, Michal M, Hes O. Primary Renal Well-differentiated Neuroendocrine Tumor (Carcinoid): Next-Generation Sequencing Study of 12 Cases. *(accepted for presentation)*

Poster: **Pivovarcikova K**, Martinek P, Trpkov K, Alaghehbandan R, Magi-Galluzzi C, Condom Mundo E, Comperat EM, Suster S, Michalova K, Saskova B, Michal M, Hes o. Fumarate-Hydratase Deficient Renal Cell Carcinoma Does not Demonstrate a Distinct Chromosomal Numerical Aberration Pattern. *(accepted for presentation)*

Poster: Pires-Luís A, Martinek P, Filipovic J, Alaghehbandan R, Comperat EM, Perez Montiel MD, Bulimbasic S, Henrique RM, Vanecek T, **Pivovarcikova K**, Michalova K, Saskova B, Michal M, Hes O. Primary Adenocarcinoma of the Urinary Bladder: Next-Generation Sequencing (NGS) of Non-urachal Enteric-type Adenocarcinomas, Urachal Adenocarcinomas, Mucinous Adenocarcinomas, and Colonic Metaplasias/Adenomas. *(accepted for presentation)*